5-HYDROXYTRYPTAMINE MODULATION OF CALCIUM CURRENTS RECORDED FROM MAMMALIAN CENTRAL SEROTONERGIC NEURONES

by

R.H. McAllister-Williams

Thesis presented for the degree of

Doctor of Philosophy

University of Edinburgh

1993

DEDICATION

To Alison, with love.

In accordance with the requirements of the University of Edinburgh regulation 3.4.7 this thesis has been composed by myself and the work presented herein is my own.

R.H. McAllister-Williams

ACKNOWLEDGEMENTS

There are so many people that deserve to be acknowledged, it would be easy to say that they could not be all named individually. However, this would simply belittle my gratitude to them. I therefore will try to name everybody, with the danger that I forget somebody. If this occurs, then I offer my profound apologies.

I would like to thank Dr Nick Penington for initially teaching me the technique of acutely isolating neurones, Dr Ian Forsythe for supplying the circuit diagram for the temperature controller, and helping getting it to work, and Dr Reg Docherty for letting me have a copy of a calcium chelator calculation programme. Professor P. Cohen provided the okadaic acid and inhibitor-1 peptide used in this study, together with advice as to their use. Thanks must also go to Drs Phil Larkman and Joe Hodgkiss who were always willing to have their ears bent allowing me to talk over problems, as has Dr Jamieson Walker.

There have been several people in the Department of Pharmacology who have provided technical support and I am grateful to all of them, particularly Mr John Lisimore, and Mr Murray Dippie who has always been happy to help with day to day computing problems. Professor I.M.L. Donaldson deserves special thanks for writing the initial curve fitting programmes that were subsequently adapted for use in this study, and helping in my early attempts at programming.

Obviously special thanks must go to my supervisor, Professor J.S. Kelly, for firstly providing me with the opportunity to obtain a research training, and secondly for his guidance during the project. Funding for the work, and my salary, was by means of a Clinical Research Fellowship from the Wellcome Trust. Clearly the Trust have my grateful thanks for their support.

A mention must be made of the involvement of Professor Bernard Ginsborg. It was his interest and enthusiasm for neuroscience, when teaching me during my intercalated Honours year, that developed my own passion. This was furthered by our frequent chats over lunch in the last few years, prior to his departure from the Department of Pharmacology. I would like to wish him all the very best in his retirement, and give him my thanks for helping to direct me down the path that I have taken.

I would like to give my very special thanks to my parents. They were always prepared to go without for many years to provide me with opportunities. Without their support, love and encouragement, I am sure that I would never have achieved what I have. Lastly, I would like to give my love to my wife, Alison. She has put up with a great deal over the last four years, especially when things were not going well, and I thank her from my heart.

ABSTRACT

It has previously been shown that 5-hydroxytryptamine (5-HT; serotonin), is able to inhibit high threshold voltage dependent (HVA) calcium currents in 5-HT containing dorsal raphé (DR) neurones via 5-HT_{1A} receptors (Penington & Kelly, 1990, Neuron, 4,751). This inhibition involves a retardation of current activation, and a partial reduction in amplitude. These calcium currents, and the action of 5-HT, have been further characterised using the whole cell patch clamp method in acutely isolated adult rat DR cells.

The effect of temperature on HVA currents has been studied in considerable detail. Results of the temperature dependency are in keeping with the presumed heterogeneous nature of HVA current in neuronal cells. In addition, it was found that a fast inactivating component is uncovered by increases in temperature to 25°C or above, and this component is voltage sensitive, decreasing in prominence with increasing sizes of test pulses. This is in keeping with at least three HVA components. While the temperature coefficient (Q_{10}) of current amplitude and inactivation rate was found to be in the expected 2-3 range, the activation rate was discovered to be much more sensitive, being between 10 and 12.

Stimulation of 5-HT_{1A} receptors, or direct G-protein activation had no effect on HVA calcium current amplitude Q_{10}'s, but led to a dramatic reduction in the activation rate Q_{10} down to 2-3. This could be reversed by the prior application of large depolarising prepulses prior to the test pulse. The possible involvement of phosphorylation in the maintenance of HVA calcium currents and the action of 5-HT was investigated using phosphatase inhibitors. It was found that phosphatase inhibition tended to lead to a gradual increase in current amplitude over a period of some minutes, but then had no clear effect on the subsequent rate of time dependent decrease in current amplitude ('rundown'). With the single dose of inhibitor used, it was found that 5-HT_{1A} receptor stimulation, while still causing some reduction in current amplitude, was unable to lead to a reduction in activation rate Q_{10}. Likewise currents recorded with direct G-protein stimulation, together with a phosphatase inhibitor, had current activation rates with a Q_{10} of the same order as controls.

It is hypothesised that 5-HT_{1A} receptor stimulation causes an alteration in the mechanisms underlying current activation, to account for the reduction in Q_{10} value observed. In addition, it appears that the phosphorylation state of HVA channels is involved in their ability to pass current on depolarisation, together with the action of 5-HT on channel activation. The phosphorylation connected with the action of 5-HT would appear to be voltage dependent, to explain the finding that the 5-HT mediated reduction in activation rate Q_{10}, is reversed by large depolarisations. A model is presented to explain the above hypotheses.

CONTENTS

Chapter 1 Introduction

The aim of this study was to investigate calcium currents, and particularly their modulation by 5-hydroxytryptamine (5-HT) in dorsal raphé (DR) neurones. In this introductory chapter, it is intended to give an outline of the classification of voltage-activated calcium current in vertebrate neuronal cells. This is discussed on the basis of voltage sensitivity, kinetics, unitary conductance (section 1), and channel blocking and activating drugs (section 2). Section 3 includes information as to postulated roles for the various classes of current. Calcium channel structure is outlined in section 4, as a background to hypotheses that are formulated, when discussing possible mechanisms of channel modulation by transmitters (chapter 7). A summary of the actions of a variety of different transmitters in various vertebrate neuronal or closely related preparations is given in section 5, and table 1.1. This includes current hypotheses as to the transduction pathway between receptor and channel. Previous work has been conducted into the action of 5-HT in DR on both potassium and calcium conductances. This is detailed in section 6, along with brief ideas as to the relevance of this to 5-HT and DR function. Since much of the work reported here has involved an investigation of temperature sensitivity, the effect of temperature on ionic conductances is reviewed in section 7. In addition, since phosphotase inhibitors have been used in this study, a brief review of protein phosphotases is given (section 8). Finally, an outline of the direction of the investigation and a synopsis of the results is presented (section 9).

Calcium ions (Ca^{2+}) have been known to be involved in membrane excitability for many years. In 1953 Fatt & Katz found that normally inexcitable crab muscle fibres produced prolonged action potentials

when Na^+ was replaced by quaternary ammonium ions such as tetraethyl-ammonium (TEA) or tetrabutylammonium (TBA) in the external solution. In crayfish, Fatt & Ginsborg (1958) showed that a similar action potential was independent of Na^+ and Mg^{2+} and suggested that the action potential was based on the inflow of Ca^{2+}, rather than Na^+, during the up stroke. These 'calcium spikes' were induced by TEA and TBA, and required Ca^{2+}, Sr^{2+} or Ba^{2+} ions to be present in the external medium. It is now known that TEA and TBA act by blocking the repolarising action of K^+, and allowing weak inward calcium currents to depolarise the cell via voltage-dependent calcium channels. Reduction of internal free Ca^{2+} concentration using the divalent cation chelator ethylene-diaminotetraacetic acid (EDTA), also enhances the latent calcium spikes in crustacean muscle fibres (Hagiwara & Nakajima, 1966a & b). Work on Aplysia neurones and *paramecium* has suggested that this may be because during a depolarising pulse, the inflow of Ca^{2+} leads to a local rise in intracellular free Ca^{2+} that causes inactivation of the calcium channels (Brehm & Eckert, 1978, Tillotson, 1979, Brown et al. 1981). Calcium channels seem to be present in every excitable cell so far studied (Hagiwara & Byerly, 1981, Reuter,1983, Tsien, 1983, Deitmer, 1984, Hille, 1984, Bean, 1989a, Hosey & Lazdunski, 1989, Hess, 1990). They appear to be members of the voltage-dependent channel family, that includes sodium channels and the delayed rectifier potassium channel. As such they open with a delay on depolarisation, shut rapidly on repolarisation, and undergo a variable amount of inactivation during sustained depolarisation. They are at least moderately ion selective and are blocked by various hydrophobic and quaternary agents acting on the intracellular side of the membrane. However, unlike sodium and

potassium channels, calcium channels have a unique role. Not only are they involved in membrane excitability, such as pacemaker depolarisations and full blown calcium spikes, but by controlling the influx of Ca^{2+} into cells, they are able to regulate many Ca^{2+} sensitive intracellular mechanisms that may include ion channel gating, transmitter release, enzyme activation, metabolism, gene expression, and neurite activity (Miller, 1987, Tsien et al. 1988). This is made possible by the fact that the intracellular Ca^{2+} concentration can vary as much as 100 fold or more (Janis & Triggle, 1983, Hosey & Lazdunski, 1989). While the calcium transport systems out of cells have been extensively studied (see Carafoli, 1987), the routes of Ca^{2+} entry, that include voltage-dependent calcium channels, have only relatively recently been investigated in detail, particularly in vertebrate neurones. This has been, to a large extent, because of the problems of isolating calcium currents from the net currents seen in cells. This has only become simpler since the advent of the patch-clamp technique that allows close control of both the intracellular and extracellular mediums, together with accurate control of membrane potential (Hamill et al. 1981).

Calcium channels have now been extensively studied in many cell types. However, only voltage-dependent calcium channels in vertebrate neurones will be discussed here, though non neuronal and invertebrate examples will be used where appropriate.

1. Multiple Voltage-Dependent Calcium Channels in Neuronal Membranes

For some years there has been increasing evidence of the existence of multiple calcium channels within given cell types (Hagiwara &

Byerly, 1981). This has been shown in invertebrate and non-neuronal vertebrate cells such as eggs (Hagiwara et al. 1975), ciliates (Deitmer, 1984), pituitary tumour cells (Armstrong & Matteson, 1985) and cardiac cells (Bean, 1985). In vertebrate neurones, one of the first demonstrations of the co-existence of at least two types of calcium channels was by Llinás and Yarom in 1981. Using extra- and intracellular recording techniques, in guinea-pig brain stem slices, these workers found high and low threshold calcium spikes in inferior olivary neurones. The low threshold calcium spike was initiated by membrane depolarisations from -70 mV or more negative, and hyper-polarisation removed a voltage dependent calcium inactivation, which was present at normal resting membrane potentials (-65 mV). The high threshold calcium spike showed lack of refractoriness, and Llinás and Yarom believed it to be dendritically distributed. Similar work in cerebellar Purkinje cell dendrites, demonstrated this high threshold calcium current was activated at around 10 mV and showed little or no inactivation (Llinás & Sugimori, 1980). Similar types of calcium spikes have also been demonstrated in immature rat dorsal horn cells (Murase & Randic, 1983). Corresponding low voltage-activated (LVA) and high voltage-activated (HVA) calcium currents have been observed in chick and rat dorsal root ganglion (DRG) neurones (Carbone & Lux, 1984a, Fedulova et al. 1985, Nowychy et al. 1985). Carbone and Lux (1984a), found the previously identified large inward calcium current that activated between -15 and 0 mV, existed along with a rapidly inactivating component that activated between -50 and -40 mV. Further work showed that these components often occurred together in the same patch of membrane, the HVA passing a unitary current of 0.86 pA while the LVA passed 0.45 pA (Gross & MacDonald, 1988a).

Single Channel work in chick DRG neurones has suggested the presence of not two, but three types of calcium channel. In addition to the LVA (or T-type) channel with a conductance (with 110 mM Ba^{2+} in the patch pipette) of around 8 pS that is activated positive to -70 mV, inactivates rapidly (τ_i = 20-50 ms), and is deinactivated between -60 and -100 mV, and the HVA long lasting component (or L-type) that has a single channel conductance of 25 pS, τ_i greater than 500 ms, activates positive to -10 mV, and is deinactivated between -60 and -10 mV, there is a third channel. This channel (named N-type) passes part of the previously defined HVA current. However unlike L-type channels it inactivates much faster (τ_i = 50-80 ms), requires more negative potentials to completely remove inactivation (-30 to -120 mV), and has a smaller unitary conductance (13 pS, Nowycky et al. 1985, Fox et al. 1987a, Fox et al. 1987b). Single channel recordings in mouse and rat DRG cells have also revealed three types of calcium channels with conductances of 8, 13 and 23 pS (in 110 mM Ba^{2+}) that have activation and inactivation characteristics very similar to those seen in chick (Green & Cottrell, 1988). This is also the case in rat hippocampal neurones (Mogul & Fox, 1991), rabbit sensory neurones (McCarthy & TanPiengco, 1992), and mouse cerebellar granule cells (Slesinger & Lansman, 1991b). This clear difference in unitary conductance is, however, somewhat clouded by the reports of N-type channels also exhibiting openings with a 22 pS conductance (Plummer et al. 1989), and also the possibility of multiple conductance states for L-type channels with some substates having values similar to N-type openings (Kunze & Ritchie, 1990). In frog sensory neurones there is a virtual lack of T-type channel activity, however N and L-types are present with slope conductances of 15 and 28 pS respectively (Lipscombe et al.

1988). In addition their voltage dependence is also similar to that seen in chick DRG neurones, such that the open probability of L-type channels opened by pulses to 20 mV from -100 mV is virtually unchanged when the holding potential is increased to -40 mV. In contrast, the open probability of N-type channels decreases significantly within 10-20 ms of changing the holding potential from -100 to -40 mV (Lipscombe et al. 1988, Kongsamut et al. 1989).

Not withstanding the apparent difference in the rate of inactivation, as an approximation, 'steady state' current at the end of a voltage test pulse of 150 - 200 ms, has often been equated with L-type, and the peak current, a mixture of L- and N-types. However, the rate of inactivation seen in whole cell recordings can be altered by various means that leads to further scepticism of this idea. For example, Bossu et al. (1989), have shown that the inactivation of HVA current in chick sensory neurones is drastically reduced when internal calcium is buffered at 1 nM. Similar results have also been shown in hippocampal cells (Myers & Barker, 1989), and dihydropyridine (DHP) sensitive current (see below) in GH3 cells is also inhibited by procedures that increase intracellular calcium (Kalman et al. 1988). Using Ca^{2+} as the charge carrier, large depolarising prepulses prior to test pulses, cause an inhibition of HVA but not LVA current in rat pituitary cells (Williams et al. 1991). This effect is reduced substantially by the addition of 5 mM 1,2-bis(2-aminophenoxy)ethane N,N,N',N'-tetraacetic acid (BAPTA) to the internal solution, suggesting that the inhibition is mediated by an elevation of intracellular calcium. In addition, while T and L-type currents seem to be fairly well preserved between different cell types in vertebrates (Tsien et al. 1988, Bean, 1989a), N-type have seemed a rather heterogeneous

group. For example the inactivation time constant ranges from 50 to 80 ms in chick DRG neurones (Fox et al. 1987a) to over 500 ms in rat sympathetic neurones (Hirning et al. 1988a), and around 800 ms in neuroblastoma cells (Docherty, 1988). There even appears to be diversity of inactivation time constants of N-type current within a single cell type. In frog sympathetic neurones, N-type channels can be seen that rapidly inactivate ($\tau_i \approx 50$ ms) with depolarisations to -10 mV in some patches, while in others there appears to be little or no inactivation during a 320 ms test pulse (Kongsamut et al. 1989). However in other respects (unitary conductance and sensitivity to organic blockers) they appear to be identical and distinct from L-type channels. Similar results have been obtained in chick DRGs (Aosaki & Kasai, 1989), PC12 phaeochromocytoma cells (Plummer et al. 1989), and rat sympathetic neurones (Hirning et al. 1988a). In single human neuroblastoma cells N-type current (defined on the basis of *Conus geographicus* GVIA ω-toxin fraction sensitivity - see below), shows two clear inactivating components with time constants of 75 and 750 ms (Seward & Henderson, 1990). Single channel recordings of N-type openings in rat superior cervical ganglia (SCG) neurones has suggested that not only can different types of N-type current inactivation be seen in a single cell, but individual channels may be able to switch between slow and fast inactivating states (Plummer & Hess, 1991). This has also been hypothesised to occur with L-type current in cerebellar granule cells (Slesinger & Lansman, 1991a & b). It is clearly difficult, therefore, in whole cell recordings to separate slowly inactivating N and L-type components. However, although there is diversity in vertebrate neurones, it is far less than that seen in vertebrate muscle and invertebrate cells (e.g. see Garcia & Stefani,

1987, Nerbonne & Gurney, 1987, Strong et al. 1987, Charlton & Augustine, 1990).

It appears that HVA current in most neuronal membranes is a variable mixture of at least N and L-type currents, but is universally present. This is not always the case for LVA. For example single channel recordings fail to show a T-type channel in rat myenteric plexus neurones (Hirning et al. 1990), which is also the case in SCG cells (Hirning et al. 1988a). Whole cell recordings in hippocampal cells from neonatal rats, demonstrate the presence of a T-type component in around 66% of cells, and this percentage decreases with postnatal development (Yaari et al. 1987, Ozawa et al. 1989, O'Dell & Alger, 1991, Thompson & Wong, 1991). The increase in the proportion of HVA current with development has also been observed in chick sensory and autonomic neuronal precursor cells (Gottman et al. 1988). The density of T-type current in DRG has also been shown to vary between cells of different sizes, in that it is more prominent in small rather than large diameter neurones (Scroggs & Fox, 1991 & 1992a). These observations may account for some groups not observing LVA current (e.g. Wanke et al. 1987) though they have been observed in adult preparations (e.g. Ikeda & Schofield, 1989, Kostyuk & Shirokov, 1989, Penington and Kelly, 1990, Williams et al. 1990a, Mogul & Fox, 1991). However, T-type current has been identified in many different cell types. In addition to chick (Carbone & Lux, 1984a & b, Carbone & Lux 1987a & b, Fox et al. 1987a & b, Swandulla & Armstrong, 1988), rat (Bossu et al. 1985, Fedulova et al. 1985, Bossu & Feltz, 1986, Carbone & Lux, 1987a & b) and mouse DRG neurones (Kostyuk & Shirokov, 1989), T-type current has also been identified in mammalian hippocampus (Bley et al. 1987, Yarri et al. 1987), neocortex (Sutor & Zieglgansberger,

1987), neostriatum (Bargas et al. 1991), cerebellar Purkinje cells (Regan, 1987), amygdala (Kaneda & Akaike, 1989), DR (Penington & Kelly, 1990), and neuroblastoma cells (Narahashi et al. 1987, Tang et al. 1988). It appears that T current is never found in the absence of HVA current.

T, N and L-type channels seen in vertebrate neurones can be further characterised by their ion selectivity and sensitivity to inorganic blockers, though there are variations between cell types. While N and L-type channels are more permeable to Ba^{2+} than Ca^{2+}, T channels show equal selectivity for these two divalent cations in sensory, hippocampal, cerebellar granule neurones and neuroblastoma cells (Fox et al. 1987a, Yaari et al. 1987, Kostyuk et al. 1989, Marchetti et al. 1991, Slesinger & Lansman, 1991a, Kasai & Neher, 1992), though it has been reported that in rat hypothalamic neurones, substituting Ba^{2+} for Ca^{2+} decreases a LVA component by 30-50% (Akaike et al. 1989). This was suggested to possibly be due to a different effect of Ba^{2+} on calcium channel gating rather than a difference in the 'selectivity filter' of the various classes of channel. This would be supported by the observation that less inactivation of HVA current is observed with Ba^{2+} rather than Ca^{2+} (Eckert & Tillotson, 1981, Kass & Sanguinetti, 1984, Leung et al. 1991). L and N also differ from T-type channels in chick DRG neurones in that 20-50 μM Cd^{2+} blocks the L and N components by more than 90%, yet reduces T-type current by less than 50% (Fox et al. 1987a), a finding that is also seen in rat hippocampal neurones (Ozawa et al. 1989), and by some in mouse DRGs (Gross & MacDonald, 1987), but not by others (Kostyuk et al. 1989). 100 μM Cd^{2+} has been shown to completely suppress both the LVA and HVA current seen in rat hippocampal cells (Yarri et al. 1987).

In cerebellar granule cells, Cd^{2+} at as low a dose as 1 μM completely abolishes all calcium currents (De Waard et al. 1991). Ni^{2+} on the other hand at 100 μM strongly reduces T current but leaves HVA little changed (Fox et al. 1987a). Similar findings have been made in neuroblastoma cells (Narahashi et al. 1987), and hippocampal neurones (Ozawa et al. 1989, Mogul & Fox, 1991). By contrast, the LVA component in hypothalamic neurones is more sensitive to Cd^{2+} than Ni^{2+}, where it is also found to be sensitive to Zn^{2+} (Akaike et al. 1989). Sensitivity of the LVA current to Zn^{2+} has also been demonstrated in amygdaloid neurones, where these currents are more sensitive to Ni^{2+} than Cd^{2+}, as in DRGs (Kaneda & Akaike, 1989). The trivalent cation, La^{3+}, appears to be remarkably non-selective in its block. It is able to block all three components of calcium current seen in mouse DRG (Kostyuk et al. 1989), rat hippocampal (Ozawa et al. 1989), hypothalamic (Akaike et al. 1989), and amygdaloid neurones (Kaneda & Akaike, 1989), in addition to neuroblastoma cells (Narahashi et al. 1987, Kasai & Neher, 1992). Another lanthanide, Gd^{3+}, has also been found to block calcium currents, but this has been reported to relatively specifically block N-type current in neuroblastoma cells (Docherty, 1988, Brown et al. 1989), though this has been challenged both in rat DRG (Boland et al. 1991b), and neuroblastoma cells (Kasai & Neher, 1992). Interestingly, Pb^{2+} has been found to preferentially block HVA current in human neuroblastoma cells, with a K_i of around 1 μM (Reuveny & Narahashi, 1991).

Other blockers that are to some extent selective have been suggested. For example, diphenylhydantoin (Narahashi et al. 1987, Yarri et al. 1987), octanol (Llinás & Yarom, 1986), tetramethrin (Hagiwara et al. 1988),and amiloride (Tang et al. 1988, Mogul & Fox,

1991, Thompson & Wong, 1991, Scroggs & Fox, 1991 & 1992a) have been claimed to selectively block T-type current. Endothelin (Yanagisawa et al. 1988) and antibodies (Morton et al. 1988) have been used to block L current. However this latter component has been most closely studied with the dihydropyridines (DHP), and related groups of drugs, that are known as calcium channel blockers, though interestingly, some DHP drugs are actually capable of increasing L-type currents (see section below).

2. Neuronal Calcium Channel Ligands

Many drugs that have been shown to affect calcium conductances are thought to bind to calcium channels themselves. They are generally referred to as calcium antagonists or channel blockers, and calcium agonists or channel activators. Collectively they can be referred to as channel ligands.

The pharmacology of calcium channel blocking drugs has been extensively investigated, particularly in the cardiovascular system. This is due to their ability to interfere with uptake of Ca^{2+} into myocardial cells and prevent necrotization arising from intracellular Ca^{2+} overload. In addition they block excitation-contraction coupling of vascular smooth muscle, and hence lower calcium-dependent coronary vascular tone (Fleckenstein, 1983, Triggle & Janis, 1987). These actions have obvious clinical significance with regard to angina and hypertension. The most widely studied, and clinically used, drugs fall into three classes on the basis of their chemical structure. These are 1) the 1,4-dihydropyridine (DHP) derivatives, that include nitrendipine, nimodipine, nifedipine, and BayK 8644; 2) the phenyl-

alkylamines including verapamil, D-600, and D-888; and 3) the benzothiazepines, for example diltiazem. However, there are many other drugs which can probably also directly affect L-type channels and fall into the broad terminology of calcium channel blockers. These include 4) bepridil; 5) the diphenylbutylpiperidines including pimozide and fluspirilene; and 6) the diphenylpiperazines including cinnarizine and flunarizine. These drugs have been extensively reviewed (e.g. Janis & Triggle, 1983, Miller & Freedman, 1984, Miller, 1985, Godfraind et al. 1986, Triggle & Janis, 1987, Hosey & Lazdunski, 1989). Recently diazepam has been shown to inhibit calcium currents in phaeochromocytoma cells (Nakazawa et al. 1991). It seems that the same component of whole-cell current is blocked as occurs with nicardipine, a DHP, though different binding sites are proposed. Binding studies in skeletal muscle have suggested that there may be multiple binding sites for the main classes of channel blockers on L channels as well. There appear to be independent sites for at least DHPs, phenylalkylamines and bepridil, benzothiazepines, and diphenylbutylpiperidines in a 1:1:1:1 stoichiometry, that are capable of allosterically interacting (Galizzi et al. 1986, Barhanin et al. 1987, Catterall & Striessnig, 1992), though it is not known if this can be extrapolated to neuronal L channels.

DHP analogues have not been shown to be effective in all cell types. At concentrations of 10 μM or more they do not modify calcium spikes in a variety of cells including rat pars intermedia (Douglas & Tarashevich, 1982), guinea-pig olfactory cortex (Kuan et al. 1985), rat synaptosomes and cortical slices (Ogura & Takahashi, 1984), and hippocampus (Taube & Schwartzkroin, 1984). 10 μM nifedipine also has been shown to have no effect on calcium currents in rat SCG cells

(Gurney & Nerbonne, 1984). Usually phenylalkylamines and benzothiazepines block calcium currents or calcium spikes only at rather high concentrations (10-100 μM), such as has been found in rabbit nodose ganglion cells (Ito et al. 1984). This has led some to suggest that their action is rather non specific (Miller & Freedman, 1984). However, calcium channel blockers, and in particular DHP analogues, have been shown to reduce the L-type component of calcium currents in many cell types, and are now generally accepted for defining this component (Mogul & Fox, 1991, Plummer et al. 1991, Cox & Dunlap, 1992, McCarthy & TanPiengco, 1992).

Calcium channel blockers of the DHP series have been shown to act with significantly higher affinity on depolarised compared to polarised membranes in rat adrenal medullary tumour cells (Kanze et al. 1987), guinea-pig ventricular cells (Hamilton et al. 1987) as well as rat hippocampal cells (Ozawa et al. 1989) and DRG neurones (Scroggs & Fox, 1991, McCarthy & TanPiengco, 1992). This has been interpreted by some as indicating that DHPs bind with higher affinity to the inactivated form of the channel rather than the non-inactivated closed form (Hosey & Lazdunski, 1989). However, even when inhibition is maximised by eliciting current from depolarised holding potentials, the block by DHPs in vertebrate neurones, is usually less than 50% (Fox et al. 1987a, Rane et al. 1987, Ozawa et al. 1989), at concentrations that would completely abolish L current in cardiac cells (Sanguinetti & Kass, 1984). This lack of effect could be due to the difficulty of separating L current from the non-inactivating N-type component, or the fact that there is another type of HVA calcium channel that is neither L nor N (see below). Studies aimed at more accurately determining the potency of DHPs have found values of an

EC_{50} for nifedipine in frog sympathetic neurones of 300 nM (Jones & Jacobs, 1990), and a K_i for nimodipine in rabbit DRG of 5.3 nM (McCarthy & TanPiengco, 1992). These results suggest that DHPs are in fact just as potent in neurones as in cardiac myocytes. However it should be noted that in frog sympathetic neurones, when the dose of nifedipine is increased to 10 μM, there appears to be a non specific block of HVA channels (Jones & Jacobs, 1990). A partial block of N-type current and possibly a third type of HVA current (see below) by 10 μM nitrendipine has also been shown in a variety of neuronal preparations (Regan et al. 1991). Therefore the use of DHPs to define L-type current has to be interpreted with care.

The action of DHP drugs appears to be complex. In neuroblastoma and DRG cells, nimodipine decreases maximal calcium current, but in addition also shifts the whole current-voltage relationship in the hyperpolarising direction, in such a way that small depolarisations can actually lead to a larger inward current than in the absence of the blocker (Fox et al. 1987a, Taylor, 1988, Brown et al, 1989, Meyers & Barker, 1989, Marchetti et al. 1991, Mogul & Fox, 1991, Scroggs & Fox, 1991, Huang & McArdle, 1992). Single channel recordings in chick DRG neurones suggest that nifedipine produces its effect by decreasing L channel opening probability (Fox et al. 1987b), which is also the case in mouse sensory neurones (Kostyuk et al. 1989), and rabbit DRG cells (McCarthy & TanPiengco, 1992), where DHPs are clearly selective for L- rather than N-type channel currents. This modification of channel gating has been suggested to occur some distance from the DHP receptor site(s) (Catterall & Striessnig, 1992). Thus it seems that DHP's are probably allosteric modulators of L-type channels, rather than simple channel blockers.

While calcium channel antagonists have in the past been shown to be solely effective on HVA, and in particular L-type current, there have been reports that a whole range of blocking drugs decrease LVA current in a use dependent fashion, in rat hypothalamic (Akaike et al. 1989), and amygdaloid neurones (Kaneda & Akaike, 1989). In both of these cell types flunarizine was by far the most potent blocker, and interestingly, the L channel activator, BayK 8644, was found to act as a blocker of LVA current in hypothalamic neurones (Akaike et al. 1989).

Some DHP analogues, rather than blocking L-type current, actually cause an increase in current, and are known as activators or calcium channel agonists. The drug BayK 8644 potently increases calcium current in a variety of cell types including neuroblastoma (Docherty & McFadzean, 1989), and DRGs (Fox et al. 1987a & b). Interestingly, it has been found that the sterioisomers of these particular drugs, for example (-)BayK 8644 and (+)202-791 are activators, while (+)BayK 8644 and (-)202-791 are blockers (Franckowiak et al. 1985, Hamilton et al. 1987). This was originally proposed to explain the observed anomaly of these drugs causing increased currents at low concentrations, and inhibition at high concentrations (Hof et al. 1985, Kongsamut et al. 1985). However, even pure enantiomers are capable of both stimulation and inhibition (Franckowiak et al. 1985, Williams et al. 1985), raising the possibility that there may be multiple DHP binding sites with one mediating activation, and the other inhibition. This may explain the rather unusual findings that when rat DRG cells are pretreated with pertussis toxin (PTx), BayK 8644 causes a decrease in calcium current rather than an increase (Dolphin & Scott, 1988, 1989a). It therefore appears that BayK 8644 requires a PTx sensitive

G-protein to be able to elicit activation of calcium currents. When the G-protein is inactivated, than only inhibition is seen. The involvement of a G-protein in the activation mediated by BayK 8644 is further suggested by the fact that this action is enhanced by internally applied guanosine 5'-O-3-thiotriphosphate (GTPγS), a non-hydrolysable analogue of GTP that irreversible activates G-proteins (Dolphin & Scott, 1988, 1989a). This potentiation is also seen with 202-791 (Dolphin & Scott, 1989b). In addition, when GTPγS is applied to rat DRGs, nifedipine, D600, and diltiazem, representing the three main groups of channel blockers, no longer inhibit current, but rather enhance it (Scott & Dolphin, 1987, Dolphin & Scott, 1989b). These findings, though, could not be replicated in a phaeochromocytoma PC12 cell line (Plummer et al. 1989). The exact role of G-proteins in the action of calcium channel ligands, and their interaction with possible multiple binding sites is still far from clear.

Tail currents following repolarisation are greatly prolonged by DHP agonists (Plummer et al. 1989, Jones & Jacobs, 1990, Marchetti et al. 1991), and studies of these currents have found that BayK 8644 causes a considerable increase in a slow exponential component of HVA current in mouse DRG neurones (Kostyuk & Shirokov, 1989). In rat, mouse, rabbit, and chick DRGs, and rat hippocampal cells, single channel studies have suggested that while nifedipine causes fewer L-type channel openings, the application of BayK 8644 leads to the channels remaining in the open state for longer (Hess et al. 1984, Fox et al. 1987b, Green & Cottrell, 1988, Kostyuk et al. 1989, Mogul & Fox, 1991, O'Dell & Alger, 1991, McCarthy & TanPiengco, 1992).

One of the most potent calcium channel blockers is the ω-toxin fraction GVIA from the venom of the marine snail *Conus geographicus*

(ω-CgTx). This peptide binds with high affinity and specificity to presynaptic calcium channels (Cruz & Olivera, 1986, McCleskey et al. 1987) and produces a long lasting block of somatic HVA current. There has been some dispute over how selective this block is. Some have claimed that ω-CgTx blocks both L- and N-type currents but leaves T-type unaffected, such as in chick DRGs (McClesky et al. 1987, Fox et al. 1987a, Yawo, 1990), frog DRGs (Oyama et al. 1987), rat sympathetic neurones (Hirning et al. 1988a), and rat cerebellar granule cells (De Waard et al. 1991). In rat neurohypophysis nerve terminals, ω-CgTx blocks N-type currents with an IC_{50} of 50 nM. It is also able to block L-type current but the IC_{50} is 10 times higher (513 nM, Wang et al. 1992). However in neurone-like rat phaeochromocytoma PC12 cells, L-type channels appear insensitive, but ω-CgTx reveals two pharmacologically distinct components of N-type current. One is blocked irreversibly, and the other reversibly (Plummer et al. 1989). There are several studies that have shown that DHP sensitive current is insensitive to ω-CgTx (Toselli & Taglietti, 1990, Bossu et al. 1991a & b, Mogul & Fox, 1991, Regan et al. 1991, Scroggs & Fox, 1991, Cox & Dunlap, 1992, Kasai & Neher, 1992, McCarthy & TanPiengco, 1992, Scroggs & Fox, 1992a & b). Single channel studies to clarify this issue are hampered by the fact that ω-CgTx binding seems to be depressed by the high divalent cation concentrations needed to perform them (McClesky et al. 1987, Oyama et al. 1987). However single channel recordings from chick DRG cells do suggest that ω-CgTx has no persistent action on L-type channels (Aosaki & Kasai, 1989), though this may not be the case in neurone related chromaffin cells (Bossu et al. 1991b). As a result there does now seem to be general acceptance that ω-CgTx can be used to define the N-type component of calcium

currents (Bean, 1989a, Hess, 1990, Scroggs & Fox, 1991, Cox & Dunlap, 1992). This would be supported by the fact that ω-CgTx has little or no effect on currents in cardiac, smooth, or skeletal muscle (McCleskey et al. 1987) that do not contain N-type channels (Tsien et al. 1988, Bean, 1989a, Hess, 1990), though human neuronal DHP sensitive calcium channels expressed in *Xenopus* oocytes do show some, but reversible, sensitivity to ω-CgTx (Williams et al. 1992).

Acceptance of the N-type channel selectivity of ω-CgTx does throw up other anomalies in the classical classification of HVA current. In chick DRG cells (Cox & Dunlap, 1992), and bovine chromaffin cells (Artalejo et al. 1992a), a significant fraction of ω-CgTx sensitive current remains even with depolarised holding potentials that would normally be expected to inactivate N-type current. This has not been accounted for in many previous works that have used holding potential to differentiate HVA current. In rat neuroblastoma cells the situation may be even more extreme, with there being no difference in the kinetics or voltage sensitivity between DHP and ω-CgTx sensitive current (Boland & Dingledine, 1990, Caulfield et al. 1992).

There has been growing interest in the possibility of a class of calcium channel carrying HVA current that is insensitive to both DHPs and ω-CgTx. Llinás et al. (1989) have described such a channel found in cerebellar Purkinje cells, which they studied reconstituted in bilayers. This channel has recently been cloned and the lack of DHP and ω-CgTx sensitivity confirmed (Mori et al. 1991). The unitary properties of this channel are thought to differ from those of other neuronal calcium channels, and it has tentatively been named 'P-type'. This ω-CgTx and DHP insensitive calcium current has been further investigated in acutely dissociated rat Purkinje cells. In this

preparation, DHPs block less than 10% of HVA current, and ω-CgTx has little or no effect (Regan, 1991, Regan et al. 1991). The majority of HVA current (90%) shows extremely slow rates of inactivation with only a small fall in amplitude during a 2 second test pulse, and thus is like "classical" L-type current. However, the current is inactivated by holding potentials between -60 and -20 mV, with a potential of -34 mV for half maximal inactivation (Regan, 1991). This is considerably more negative than one would expect for L-type current in DRG cells (Fox et al. 1987a). By contrast, in line with other HVA currents, that in Purkinje cells was nearly twice the amplitude when Ca^{2+} was replaced by Ba^{2+} (Regan, 1991). Conversely, unlike DRG cells, both LVA and HVA current show little sensitivity to 100 μM Ni^{2+}.

While a combination of ω-CgTx and DHP has been shown to virtually iradicate HVA current in neuroblastoma cells (Kasai & Neher, 1992), this is certainly not universally the case. If ω-CgTx is accepted as N-type and DHPs as L-type channel selective, then there appears to be a third class of HVA calcium current in many cell types including rat phaeocromocytoma cells (Plummer et al. 1989), DRG neurones (Regan et al. 1991, Scroggs & Fox, 1991 & 1992a), hippocampal cells (Regan et al. 1991, Mogul & Fox, 1991), SCG, spinal cord, visual cortex, as well as cerebellar Purkinji cells (Regan et al. 1991). However, single channel recordings in hippocampal cells, where a third type of HVA current is defined on pharmacological grounds, are only able to identify two HVA unitary conductance levels (Mogul & Fox, 1991). Therefore if a third distinct HVA channel exists, then its unitary conductance may be rather similar to L- or N-type channels.

It has been shown that venom of the funnel web spider *Agelenopsis aperta* can block HVA calcium current (Llinás et al. 1989, Mori et al.

1991). One component of this venom is ω-aga-toxin IVA (ω-Aga-IVA), a 48 amino acid peptide, which potently blocks both K^+ stimulated Ca^{2+} into rat brain synaptosomes and calcium currents in rat cerebellar Purkinje neurones (Mintz et al. 1992a). Recently it has been shown that ω-Aga-IVA, in a variety of rat cell types including hippocampal CA1 and CA3, visual cortex, spinal cord, and DRG neurones, had no effect on LVA or DHP- or ω-CgTx-sensitive HVA, but did block a component of HVA like that of P-type channels in Purkinje neurones (Mintz et al. 1992b). In these cell types, the proportion of HVA that appears to be P-type is less than in Purkinje cells (`90%), ranging from 45% in spinal cord to 14% in hippocampal CA3 neurones. It should also be noted that some types of neurones, such as sympathetic neurones, appear to have little or no P-type current. In addition, not all calcium current resistant to N and L-type channel blockers can be attributed to P-type channels (Mintz et al. 1992b). Another toxin fraction that has been suggested to block P-type channels in Purkinje cells is the MVIIC fraction (rather than the GVIA fraction which blocks N-type channels) from the venom of *Conus magnus*, a close relative of *Conus geographicus* (Hillyard et al. 1992). This illustrates the importance of high quality purification of peptide fractions from venoms, prior to their use to characterise channel types.

The acceptance of at least another channel type contributing to HVA current may possibly be the explanation of many of the apparent anomalies previously noted, such as the supposed lack of potency of DHPs in neurones reported by some.

3. Functions of Calcium Channels

The different classes of calcium channel may serve different functions such as pacemaker activity, transmitter release and gene expression (Miller, 1987, Tsien et al. 1988), however more information is required to establish the precise role of each type in different cells with any certainty.

With their activation with relatively weak depolarisations, there have been suggestions that T-type current may be involved in pacemaker activity in spontaneously active neurones (Llinás & Yarom, 1981, Burlhis & Aghajanian, 1987). In addition to this, T-type current may also influence calcium influx through other calcium channels. Using action potential waveform commands in voltage clamp, it has been shown that calcium entry through HVA channels is highly dependent on the duration of the currents elicited (McCobb & Beam, 1991). In a similar way, Scroggs and Fox (1992b) have shown that in rat DRG cells, the duration of the resultant calcium currents depends on the cells proportion of T-type current. The more T-type current present, the longer the duration, and thus the greater the calcium entry. Application of amiloride (which is thought to block T-type channels) leads to a decreased duration and a smaller rise in intracellular calcium. It may therefore be that the effects mediated by HVA currents are potentiated by LVA current. If T-type channels are particularly prevalent in immature cells, then this may be particularly relevant to the actions of L-type current on gene expression (see below).

Transmitter release upon depolarisation at synapses, is thought to normally be as a result of calcium entry (Miller, 1987, Smith &

Augustine, 1988, Knight et al. 1989), rather than simply the change in membrane potential (Zucker & Haydon, 1988). In addition, release is normally triggered by a large brief, and sharply localised rise in intracellular calcium, rather than a diffuse cellular increase (Swandulla et al. 1991a). It therefore seems likely that voltage-dependent calcium channels may be involved in the mechanism of this rise in calcium. Calcium entry through both L and N-type channels has been suggested to be involved. For example, the involvement of L channels in substance P release from chick and rat DRG neurones is implicated by this being DHP sensitive (Perney et al. 1986, Rane et al. 1987), while noradrenaline (NA) release from sympathetic nerve cell bodies is ω-CgTx and Cd^{2+}, but not DHP, sensitive, suggesting N-type involvement (Hirning et al. 1988a, Kongsamut et al. 1989). This is also the case for NA release from hippocampus (Dooley et al. 1988), and transmitter release at the mouse neuromuscular junction (Protti et al. 1991). Using microdialysis techniques, it has been shown that 5-HT release in hippocampus on electrical stimulation of the DR, is Cd^{2+}, but not DHP, sensitive (Sharp et al. 1990). Glutamate release from cerebellar granule cells has been suggested to be DHP sensitive by some (Huston & Dolphin, 1990), but not by others (Barnes & Davies, 1988). In rat neurohypophysis, a good model for the study of presynaptic control of neuropeptide secretion, the class of calcium channel responsible for controlling vasopressin release seems complex. While ω-CgTx substantially decreases both electrically and high K^+ stimulated release, DHPs have no effect. However, verapamil and diltiazem also have a small but significant effect on release, which is additive to the ω-CgTx effect (von Spreckelsen et al. 1990). This suggests that both ω-CgTx sensitive (probably N-type) channels, and a

channel that is ω-CgTx and DHP insensitive, but sensitive to phenylalkylamines and benzothiazepines, are involved. The identity of this second channel is far from clear. This may reflect a difference in calcium channels presynaptically compared to those of the cell soma, where virtually all investigations have been conducted. Recently reports have been published where the presynaptic terminal of cholinergic fibres in chick ciliary ganglion have been voltage-clamped (Yawo, 1990, Stanley & Goping, 1991). These groups have shown that there does appear to be an HVA calcium current presynaptically that resembles N-type current seen in cell bodies. In addition, this has been shown to have a unitary conductance of 11 - 14 pS with 110 mM Ba^{2+} (Stanley, 1991), again like somatic N-type channels. However there are differences in the characteristics of the HVA current, and further work is required to completely clarify the situation.

With the balance of evidence pointing toward the involvement of N-type current in transmitter release in the majority of synapses, a role for L-type channels is not clear, though recent work may have uncovered one possibility. It is known that synaptic stimulation is able to rapidly activate several transcription factor genes such as *c-fos* (reviewed by Sheng & Greenberg, 1990). This gene is believed to be involved in orchestrating changes in gene expression that underlie neuronal plasticity (Morgan & Curran, 1989). The question arises as to how synaptic signals are able to regulate gene expression. In rat cerebral cortex, L-type current only contributes a small fraction of HVA current. However, the basal expression of several transcription factor genes, such as *c-fos, jun-B*, and *fos-b*, are all rapidly suppressed by exposure of the cells to DHP antagonists, while BayK 8644 leads to an increased expression (Murphy et al. 1991). Effects

of L-type current on gene expression may help to explain another recent observation. Franklin et al. (1992) have shown that if rat myenteric neurones are grown in culture with high levels of K^+, causing them to be depolarised and so have high levels of intracellular calcium, the density of HVA current is reduced substantially. Both transient and sustained components are affected. The reduction in the sustained current is attenuated by inhibitors of RNA and protein synthesis, as well as inclusion of DHP antagonists in the culture medium. It may well be, therefore, that one of the targets for the transcription factor genes that are L-type current dependent, is the expression of L-type channels themselves. Clearly this potential long term negative feedback system, is an interesting avenue for research.

4. Calcium Channel Structure

Due to the high density of DHP binding calcium channels in skeletal muscle, these are the most extensively studied. Initial solubilization and purification of DHP receptors suggested that they consisted of one large (150 - 200 kDa) and several smaller (30 - 50 kDa) subunits (Glossmann & Ferry, 1983, Curtis & Catterall, 1984, Borsotto et al. 1985). However, it now appears that two, rather than one, large subunits copurify with equimolar stoichiometry and these are termed α_1 and α_2 (Leung et al. 1987, Takahashi et al. 1987, Tanabe et al. 1987). These two can be distinguished by the fact that disulfide reducing agents have no effect on α_1 but decrease the mass of α_2 to 140 - 150 kDa, and lead to the appearance of a small peptide of 24 - 30 kDa, termed δ (Takahashi et al. 1987). Thus the α_2 and δ

subunits appear to be linked by disulfide bonds. The α_1 subunit is generally accepted as containing the DHP binding site (Hosey & Lazdunski, 1989, Hess, 1990). In addition to the α_1, α_2 and δ subunits, there are two others, referred to as β ($\approx$ 55 kDa) and γ ($\approx$ 30 kDa, Glossmann & Ferry, 1983, Curtis & Catterall, 1984, Borsotto et al. 1985, Leung et al. 1987). α_1 and β subunits can be phosphorylated by cAMP-dependent kinase (AK, Curtis & Catterall, 1985, Hosey et al. 1986, Takahashi et al. 1987), calcium/calmodulin-dependent kinase (Hosey et al. 1986), and by protein kinase C (PKC, Campbell et al. 1988). Studies have suggested that the α_2, γ, and δ subunits are glycosylated while the other two are not (Takahashi et al. 1987). Takahashi et al. (1987) proposed a model for the quaternary structure of the DHP sensitive calcium channel, in which the α_1 subunit forms the channel, and is surrounded by the α_2 and γ subunits. The β subunit, because of its phosphorylation sites and lack of hydrophobicity, is proposed to attach non-covalently to the cytoplasmic side of α_1, whereas the δ subunit is disulfide linked to the α_2 subunit and extends to the external surface because of its glycosylation sites. This model seems fairly well accepted at present (Catterall, 1988, Campbell et al. 1988, Hosey & Lazdunski, 1989).

The amino acid sequence of the α_1 subunit demonstrates a high degree of homology with voltage-activated sodium and potassium channels. Sodium α and calcium α_1 subunits appear to have four repeated homologous domains (I - IV), while potassium channels seem to have just one of these domains (Catterall, 1988). Each domain is believed to have six transmembrane segments (S1 - S6), with S4 containing 5 or 6 Arg or Lys residues (Tanabe et al. 1987). This S4 segment is a good candidate for the voltage-sensing region of the

channel, and is particularly well conserved between calcium, sodium (Noda et al. 1984), and potassium channels (Pongs et al. 1988). The DHP binding site on calcium channels appears to be located at the interface between domains III and IV, and may affect domain-domain interactions that are important determinants of activation gating (Catterall & Striessnig, 1992). Recently it has been shown in skeletal muscle that immature α_1 subunits are 2 kb shorter than adult ones, due to the deletion of domains II and III (Malouf et al. 1992), though the significance of this is unclear.

Unlike the α_1 subunit, the α_2 shows no significant homology to any other membrane bound protein (Ellis et al. 1988). It is more hydrophobic than the α_1 subunit, and only has two transmembrane domains. This is also the case for the δ subunit which has one transmembrane segment, while the β and γ subunits have four each (Catterall & Striessnig, 1992).

How similar other calcium channels are to skeletal DHP sensitive channels is not clear. There are certainly indications that there are differences between DHP sensitive channels in different regions. For example dysgenic mice that lack DHP receptors in muscle still have normal levels of DHP binding sites in heart and sensory neurones (Beam et al. 1983), suggesting that different genes may code for the channels in different regions. In addition, the unitary conductance of skeletal DHP channels is lower and they activate around ten times slower than DHP channels elsewhere (Rosenberg et al. 1986). However, there are also indications of similarities. For example, antibodies raised against the S3 - S4 loop of the α_1 subunit of DHP sensitive skeletal muscle channels, cross react with DHP insensitive channels in neuroblastoma cells (Wilson et al. 1991).

One of the "dangers" of molecular biological techniques is that they often uncover greater complexity than had previously been envisaged, as witnessed with receptor classification. This may also be the case with calcium channels as well (Snutch et al. 1990). There are reports that there are at least five distinct genes in a family that encode α_1 subunits (Ellis et al. 1988). One of these, expressed in rabbit brain, directs the synthesis of calcium channels that are insensitive to both DHPs and ω-CgTx, when coexpressed with rabbit skeletal muscle α_2 and β subunits in *Xenopus* oocytes (Mori et al. 1991). As such it may represent the α_1 subunit of the putative P-type channel. Recent characterisation of a human neuronal L-type channel has shown that it possesses many of the voltage and pharmacological properties expected (Williams et al. 1992). However unlike skeletal muscle L-channels, the α_1 subunit is unable to pass current normally in the absence of the β subunit. In addition, at least two splice variants of this subunit have been identified. Cloning of the α_1 subunits from rat brain also suggest multiple isoforms that have around 75% homology with skeletal muscle versions (Hui et al. 1991).

5. Transmitter Modulation of Voltage-Dependent Calcium Channels

Many different drugs have been shown to modulate calcium currents. These fall into broadly two categories, those that act by presumably binding to calcium channels, and those that bind to sites distal to the channel, whose action may be mediated via a G-protein and possibly an intracellular second messenger. The former group has already been discussed in section 2, while the latter, for simplicity, will be referred to as transmitter modulation of calcium channels, and will be discussed here. The actions of drugs such as the barbiturates (Gross & MacDonald, 1988b), menthol (Carbone & Lux, 1989), halothane (Takenoshita & Steinbach, 1991), and ethanol (Wang et al. 1991), which appear to have an effect on calcium currents, but whose sites of action have not been clearly elucidated, will not be discussed.

One of the first observations, in vertebrate neurones, of the modulation of calcium currents by transmitters, presumably acting at receptors distal to the channels, was by Dunlap and Fischbach in 1978. These workers found that a number of transmitters, GABA, NA, 5-HT, DA, enkephalin and somatostatin, but not acetylcholine or glycine, were capable of reducing the calcium spike duration in cultured chick DRG cells. The actions of NA and GABA in particular were thought to be receptor specific, involving α-adrenergic and $GABA_B$ receptors respectively. This action of NA has also been confirmed in rat SCG cells (Horn & McAfee, 1980), and with enkephalin in mouse DRG neurones (Werz & MacDonald, 1982). Using tetrodotoxin (TTX) to block sodium channels and TEA and 4-aminopyridine (4-AP) to block potassium channels and voltage-clamping the cells, Dunlap and Fischbach were able to isolate the calcium current underlying the calcium spikes they had studied

earlier. They found that GABA, NA and 5-HT reduce the maximal calcium current, with no change in its threshold or voltage dependence (Dunlap & Fischbach, 1981), though a slowing of the activation rate was seen. These findings have been replicated in many tissues, with many different transmitters, and a far from exhaustive list is given in table 1.1.

There have been reports of transmitters decreasing the LVA current, with uniform proportional effects throughout the time course of this current (Marchetti et al. 1986, Bean, 1989c, Carbone & Lux, 1989, Schroeder et al. 1991). This may involve the action of PKC, since activation of this kinase with phorbol esters, has been reported to selectively inhibit T-type current in rat DRG cells (Schroeder et al. 1990). LVA currents have also been observed to be increased by neurotransmitters in spinal motoneurones (Berger & Takahashi, 1990) and hippocampal interneurones (Fraser & MacVicar, 1991). Little work has been conducted in this area, and in particular with regard to signal transduction. In DRG neurones GTPγS normally mimics the action of transmitters, such as GABA, in inhibiting HVA (see table 1.1). In addition, using caged GTPγS, Scott et al. (1990) have demonstrated that at low levels of GTPγS, before inhibition of HVA is seen, LVA is enhanced. Further evidence for a G-protein involvement comes from work with the protein product of the proto-oncogene *ras*. This protein, $p21^{ras}$ shows close homology to the α subunit of G-proteins, binds GTP, and has intrinsic GTPase activity, while the oncogenic $p21^{ras}$ has reduced GTPase activity, and thus shows persistent activation (Dolphin, 1988). Oncogenic $p21^{ras}$ has no effect on HVA current in chick DRG cells, but leads to an increased T-type channel density (Hahnel et al. 1992). C-terminal-truncated $p21^{ras}$ with GTP is

able to enhance LVA current amplitude within minutes. In view of the nature of the *c-ras* gene, and the fact that LVA current is particularly prevalent in neonatal neurones, this finding may well have important implications with regard to calcium channel and cell differentiation.

More commonly in cells, the effect of transmitters is seen primarily on HVA current, with an apparent slowing of activation, and a decrease in the 'steady state' amplitude after 100-150 ms of depolarisation (for references see table 1.1), though this latter feature is not always observed (Marchetti et al. 1986, Hescheler et al. 1987, Carbone & Lux, 1989, Dolphin et al. 1989). Slowed activation is not always seen, for example NA has been reported as only slowing the activation of calcium currents in 14% of NG108-15 neuroblastoma cells, with the remained showing a uniform effect on the current amplitude (McFadzean & Docerty, 1989). However, when Ba^{2+} was substituted for Ca^{2+} as the charge carrier, although NA was only 2/3 as effective at reducing current amplitude, more slowed activation occurred. Also in NG108-15 cells, leu-enkephalin slows the activation and decreases the 'steady state' current elicited by depolarisations to -10 or 0 mV. However if larger depolarisations are used, then the current towards the end of the test pulse (135 ms) approaches the control levels (Tsunoo et al. 1986), an effect seen by several other groups (Marchetti et al. 1986, Wanke et al. 1987, Akaike et al. 1989). Since the block seems to be removed by sustained depolarisations, it raises the possibility that the channels are kept shut in their non-inactivated closed state by receptor activation. The kinetics of this have been studied by Kasai & Aosaki (1989), looking at the action of an adenosine analogue, 2-chloroadenosine, on HVA current in chick

DRGs. They suggested that the modulation of calcium channels can be explained by an activated G-protein revealing an additional activation gating state of the calcium channel.

The slowing of activation with an apparent loss of the more rapidly inactivating component of HVA current has led many to suggest a preferential action of transmitters on N-type current (Gross & MacDonald, 1987, Lipscombe & Tsien, 1987, Madison et al. 1987, Wanke et al. 1987, Hirning et al. 1988b, Wiley et al. 1988, Bean, 1989b, Brown et al. 1989, Gross et al. 1989, Kongsamut et al. 1989, Akasu et al. 1990, Chernevskaya et al. 1991, Plummer et al. 1991, Seward et al. 1991, Cox & Dunlap, 1992), though an action on L-type current is not ruled out (Bley & Tsien, 1988, Ewald et al. 1988a, Green & Cottrell, 1988, Ikeda & Schofield, 1989, Penington & Kelly, 1990, Scholz & Miller, 1991), especially since some workers do not find a classical inactivating N-type component (e.g. Tsunoo et al. 1986). In NG108-15 cells, while the percentage reduction in current amplitude is reduced in the presence of BayK 8644, the absolute amount is not (Docherty & McFadzean, 1989). Since BayK 8644 is thought to act primarily on L-type current, then this finding is consistent with the transmitter having an effect on HVA current that is distinct from L-type. There are also reports of transmitters only affecting DHP insensitive HVA current (e.g. Chernevskaya et al. 1991, Plummer et al. 1991, Cox & Dunlap, 1992, Kasai, 1992, Mathie et al. 1992), or no action being seen in the presence of ω-CgTx (e.g. Caulfield et al. 1992), though this is not clear cut, with some seeing effects of transmitters on both ω-CgTx and DHP sensitive current (Scholz & Miller, 1991, Schroeder et al. 1991). However it does seem that the slowing of activation seen with transmitters is not merely due to block of N-type

current, since kinetic changes are seen even in pure ω-CgTx sensitive current (Kasai, 1992), suggesting an action on channel gating mechanisms.

While there are an increasing number of groups claiming that transmitters have an effect only on DHP insensitive or ω-CgTx sensitive HVA current, to be certain that the effect is on N-type current, single channel recordings are necessary, of which there have been relatively few. Following on from whole-cell recordings in frog sympathetic neurones, where NA reduces a component of the calcium current that has a time course of inactivation and voltage dependence consistent with the N component, Kongsamut and colleagues have performed single channel recordings (Kongsamut et al. 1989). Using various voltage protocols, they were able to isolate either N (holding at -80 and depolarising to -10 mV), or L (holding at -40 and depolarising to 20 mV) current (note that holding at -40 and depolarising to -10 mV elicited few openings). 100 μM NA in the patch pipette produced a dramatic reduction in N channel openings, with no alteration in the unitary conductance. No effect was seen on L channel openings. In this case, NA reduced both the sustained and inactivating components of N-like current. Hirning et al. (1990) have also performed single channel studies on myenteric plexus neurones, investigating the action of neuropeptide Y. They also find that the transmitter appears to only affect channels with a conductance and voltage sensitivity compatible with N-type. If this is the case universally, then it is interesting to note that transmitters appear to inhibit the class of calcium current thought most likely to be involved in transmitter release (see above). Certainly the pharmacology of $GABA_B$ mediated inhibition of glutamate release in

cerebellar granule cells, and inhibition of calcium currents in DRG neurones, is similar (Huston et al. 1990).

The emerging consensus of transmitters acting on N-type channels has recently been thrown up in the air again. Mathie et al. (1992) have investigated the actions of NA on α-adrenoceptors, and oxotremorine-M on muscarinic receptors in rat SCG. Activation of both receptors causes an inhibition of HVA calcium currents that occurs relatively rapidly (< 1 s). However, while NA has no effect on (+)202-791 (a DHP agonist) augmented tail currents (as would be expected), oxotremorine-M causes a dramatic reduction. This suggests an action of muscarinic receptors on L-type channels, which has been confirmed at the single channel level, where the open probability of L-type channels is decreased (Mathie et al. 1992). The rate of inhibition of L-type current occurs at a slower rate than that of N-type (> 4 s), suggesting the possible involvement of a diffusible second messenger (Beech et al. 1991, Bernheim et al. 1991). The L-type current modulation is found to be PTx insensitive unlike the N-type inhibition (Beech et al. 1992). In addition, the L-type current modulation has been shown to be calcium dependent since it is abolished when the internal BAPTA concentration is increased from 0.1 to 20 mM (Beech et al. 1991, Bernheim et al. 1991). With the higher level of BAPTA, only the more conventional effect on N-type current is seen, with both NA and oxotremorine-M (Mathie et al. 1992). It therefore appears that the activation of muscarinic receptors in sympathetic neurones causes a reduction of both L- and N-type current, with the former being mediated by a rise in intracellular calcium. This mechanism of action may also be involved in the action of thyroid releasing hormone (TRH) mediated inhibition of HVA current in GH3

cells (Kramer et al. 1991), and kainate in hippocampal neurones (Nistri & Cherubini, 1991). It is possible that this action on L-type channels is widespread since it may have been undetected in virtually all previous studies on calcium currents, since these invariably have used concentrations of Ca^{2+} chelators vastly in excess of the 0.1 mM BAPTA that was necessary to reveal it in SCG.

The effect of transmitters has been stated by many as to not appear to influence the voltage dependence of calcium currents, for the entire range of inward current from -70 to +30 to +50 mV (Dolphin et al. 1986, Dolphin & Scott, 1986, MacDonald et al. 1986, Gross et al. 1989, Ikeda & Schofield, 1989, McFadzean & Docerty, 1989, Akasu et al. 1990, Lester & Jahr, 1990, Penington & Kelly, 1990). However Bean (1989b) has shown that in frog DRGs, NA's effects of reducing HVA current is not apparent when large depolarisations are used, beyond the reversal potential, to elicit outward current. This is also the case in rat SCG with NA (Plummer et al. 1991). Combined with analysis of the current tails, Bean (1989b) has suggested that calcium current modulation is by means of shifting the activation curve towards more positive values. Thus at any given test potential, a modulated channel would be less likely to open in response to a depolarisation. This hypothesis has been supported by some (e.g. Ikeda & Schofield, 1989, Beech et al. 1992), but has been challenged since $GABA_B$ agonists have been shown to inhibit both inward and outward currents in rat DRG cells (Dolphin & Scott, 1990), and spinal neurones (Sah, 1990), as does NA in submucosal neurones (Surprenant et al. 1990). In addition, others have challenged the experimental basis of Bean's experiments, in that it has been argued that the shift in voltage dependence was overestimated due to the voltage jumps being of too short a duration

(Kasai, 1992).

Interestingly there have been reports of noradrenaline increasing rather than decreasing HVA current in hippocampal CA3 neurones that are patched onto in guinea-pig brain slices (Gray & Johnston, 1987). In this instance, single channel recordings demonstrated an enhancement of an inactivating 14 pS channel by the β agonist, isoproterenol (Fisher et al. 1988), and isoprenaline also was found to increase N channel open times (Gray & Johnston, 1987). The fact that this effect of NA is mediated by β-adrenoceptors is at variance with reduction of N-type current which seems to be α_2-adrenoceptor related (Brown et al. 1989, MacFadzean & Docerty, 1989). In addition the enhancement of N-type current appears to involve cAMP (Gray & Johnston, 1987) rather than a tight linkage between G-protein and channel that seems to be the case for inhibition (see below). Therefore the enhancement may be analogous to the β-adrenoceptor increase in L current well studied in heart cells, that probably involves cAMP-dependent phosphorylation of L-type channels (Cachelin et al. 1983, Bean, 1985, Hagiwara et al. 1988, Hess, 1990).

The subject of receptor signal transduction with regard to calcium current modulation in neuronal cells, has often been portrayed as being extremely complex (e.g. Tsien et al. 1988). However, there are a few clear patterns that are apparent. PTx leads to the ADP-ribosylation of the α subunit of the G-proteins G_i and G_o and their uncoupling from receptors (Katada & Ui, 1980). Pretreatment of cells, in many preparations, with PTx, blocks the action of transmitters (see table 1.1), suggesting the involvement of a G-protein such as G_{oA}, G_{oB}, G_{i1}, G_{i2}, and G_{i3} (Sternweis & Robishaw, 1984, Gilman, 1987). This does not though seem to be the case universally since while PTx

prevents the actions of leu-enkephalin, NA and somatostatin in neuroblastoma cells, the action of bradykinin is not prevented (Taussig et al. 1992). However, the action of bradykinin may be far from typical for additional reasons (Boland et al. 1991a, and see below). Differential actions of PTx, though, are also seen in rat SCG where the action of acetylcholine is completely abolished, but NA inhibition is only partially reduced (Song et al. 1991). If a G-protein is involved, then the application of a non-hydrolysable analogue of GTP, such as GTPγS, should mimic the action of the transmitter, or lead to the transmitters action being irreversible, and a non-hydrolysable analogue of GDP, such as guanosine 5'-O-2-thiodiphosphate (GDPβS), should block the action of a transmitter. This again has been demonstrated in several cell types (see table 1.1). In submucosal neurones, intracellular application of purified G_i and G_o were both able to reverse the effect of PTx blocking calcium current inhibition by NA, somatostatin and enkephalin (Surprenant et al. 1990). In PTx treated neuroblastoma cells, intracellular application of purified G-protein also leads to a partial recovery of the response to enkephalin, with G_o being ten times more potent than G_i (Hescheler et al. 1987), and α_o, the active subunit of G_o, being the most potent of all (Hescheler et al. 1987, Ewald et al. 1988a). Likewise antibodies to G_o block the action of NA in NG108-15 cells (McFadzean et al. 1989), and baclofen in DRG neurones (Menon-Johansson & Dolphin, 1992). The situation is however complicated by the occurrence of two splice variants of G_o, G_{oA}, and G_{oB} (Strathmann et al. 1989). A role for G_{oA} has been proposed for the action of DA in rat pituitary cells (Lledo et al. 1992). In NG108-15 cells containing a PTx resistant mutant of G_{oA}, PTx blocks the action of somatostatin,

but not leu-enkephalin or NA (Taussig et al. 1992). Thus while NA and leu-enkephalin's actions are probably mediated via G_{oA}, somatostatin appears to act through another PTx sensitive G protein. Different G-proteins mediating the action of different transmitters has also been proposed in frog sympathetic neurones, on the basis of variable effects of PTx and GTPγS (Elmslie, 1992). Such a situation would allow the possible differential regulation of the action of different transmitters on single cell types.

The question of whether a freely diffusible second messenger is concerned is much more controversial. Many workers have suggested a tight coupling between the G-protein and calcium channel, since when transmitter is applied to the extrapatch membrane, there is little or no decrease in calcium current (Forscher et al. 1986, Anderson & Dunlap, 1988, Green & Cottrell, 1988, Hirning et al. 1990). This would be analogous to the coupling of muscarinic receptors to potassium channels in cardiac atrial myocytes (Breitweiser & Szabo, 1985, Pfaffinger et al. 1985, Yatani et al. 1987). In addition, there have been reports that non selective kinase inhibitors (Lester & Jahr, 1990), PKC activators (Wanke et al. 1987, Dolphin et al. 1989), phorbol esters which down regulate PKC (Akaike et al. 1989, Brown et al. 1989, Kongsamut et al. 1989, Kasai, 1992), PKC inhibitors (Dolphin et al. 1989, Plummer et al. 1991, Trombley & Westbrook, 1992), cAMP or its analogues (Forscher & Oxford, 1985, Dolphin & Scott, 1987, Wanke et al. 1987, Brown et al. 1989, Dolphin et al. 1989, Gross et al. 1989, Ikeda & Schofield, 1989, McFadzean & Docherty, 1989, Song et al. 1989, Lester & Jahr, 1990, Wang et al. 1990), phosphodiesterase inhibitors for example isobutylmethylxanthine (IBMX, Brown et al. 1989, McFadzean & Docherty, 1989), forskolin (Forscher et al. 1986,

Dolphin & Scott, 1987, Akaike et al. 1989, Dolphin et al. 1989, McFadzean & Docerty, 1989, Song et al. 1989), cGMP (Lester & Jahr, 1990), or arachadonic acid (Penington et al. 1991, Kasai, 1992), all have no effect on transmitter mediated reduction of calcium currents. However there have been reports of PKC activators being able to mimic the action of transmitters in a few instances, for example in chick DRG neurones (Holz et al. 1986, Rane & Dunlap, 1986). The action of bradykinin in a clonal rat DRG cell line can also be mimicked by 1-oleoyl-2-acetylglycerol (OAG, Boland et al. 1991), however it should be noted that in this example, the actions of bradykinin and OAG are not typical, in that no slowing of activation is seen. In addition, down regulation of PKC with phorbol esters has been shown to decrease the inhibition of calcium currents by NPY (Ewald et al. 1988a). These seemingly contradictory findings may not be inconsistent with the idea of a G-protein tightly coupled to N-type calcium channels. In chick DRG neurones, it has been demonstrated that some PKC activators may act directly on the external surface of the membrane to decrease calcium currents (Hockberger et al. 1989), while in rat SCG, OAG depresses both DHP sensitive and insensitive HVA current, and could not be blocked by PTx (unlike NA, Plummer et al. 1991). Thus the examples of the actions of transmitters being mimicked by PKC activators cited above may have to be reinterpreted in this light. Another complication with phorbol esters is that they have been reported by some to only have an effect on calcium currents at temperatures of 29°C or above (Schroeder et al. 1990), while most studies have been conducted at room temperature. Phorbol esters have also been shown to increase an L-type current in hippocampal neurones, an effect blocked by a kinase inhibitor (H7, O'Dell & Alger, 1991),

though this has not been found in any other vertebrate neuronal preparation to date.

6. 5-HT and Calcium Currents in Dorsal Raphé Neurones

The DR nucleus is a large distinct cell mass situated in the tegmentum of the mesencephalon and pons, that has been shown to contain numerous serotonin-synthesizing cells (Dahlstrom & Fuxe, 1964). These give rise to both ascending and descending fibres. The ascending fibres constitute two sections known as the dorsal and ventral serotoninergic bundles. The fibres of the dorsal bundle terminate mainly in the caudate-putamen complex, whereas those of the ventral bundle innervate a considerable number of other telencephalic and diencephalic centres. The descending fibres of the DR are distributed to the cerebellum, the lower brain stem and spinal cord (Steinbusch et al. 1981, Steinbusch, 1981). However the cells of the DR nucleus do show a fair degree of heterogeneity of cytoarchitecture, and indeed they are not exclusively serotonergic (Steinbusch et al. 1981). Only the serotonergic cells will be discussed here, and steps were taken to maximise the chances of recording from these cells during this investigation (see chapter 2).

In vivo, the serotonergic neurones of the DR exhibit a pattern of repetitive firing at a rate that is affected by external stimuli, such as the ambient light level, and the general level of arousal of the animal (Aghajanian et al. 1968, Bramwell, 1974, Mosko & Jacobs, 1974, Trulson & Jacobs, 1979). Since this repetitive activity is present spontaneously when DR neurones are recorded from in vitro (Mosko & Jacobs, 1976, Crunelli et al. 1983, Williams et al. 1988, Penington et

al. 1991) it suggests that the cells have intrinsic tonic pacemaker properties. Intracellular recordings demonstrate that the cells undergo a pronounced postspike hyperpolarisation (AHP) followed by a gradual interspike depolarisation leading to the succeeding spike (Aghajanian & VanderMaelen, 1982, Crunelli et al. 1983, VanderMaelen & Aghajanian, 1983a, Williams et al. 1988). A calcium-activated potassium current underlies the AHP (Crunelli et al. 1983, VanderMaelen & Aghajanian, 1983b). Serotoninergic neurones also possess a pronounced voltage-dependent transient outward potassium conductance (I_A) that slows the rate of depolarisation, and suppression of which, by α_1-adrenoceptor agonists, causes acceleration of the firing rate (Aghajanian, 1985). The pacemaker potential is consistent with a LVA calcium current that enables the membrane potential to rebound to action potential threshold from the AHP, and it has been reported to be insensitive to both 5-HT and α_1-agonists (Burlhis & Aghajanian, 1987).

While 5-HT has been shown to have no effect on the pacemaker potential in DR neurones, it has been known for some time that 5-HT or D-lysergic acid diethylamide (LSD, a 5-HT receptor agonist) have an inhibitory effect on the repetitive firing of DR cells, through a proposed 'somatodendritic autoreceptor' (Aghajanian et al, 1972, Trulson & Frederickson, 1987). Intracellular recordings in vivo (Aghajanian & VanderMaelen, 1982), and in brain slices (VanderMaelen & Aghajanian, 1983a) showed that 5-HT and LSD cause a hyperpolarisation of DR neurones. This is due to an increase in an inwardly rectifying potassium conductance (Aghajanian & Lakoski, 1984, Yoshimura & Higashi, 1985, Rainnie et al. 1987, Williams et al. 1988).

The somatodendritic autoreceptor present on DR neurones has been

characterised as of the 5-HT_{1A} subtype. Tritiated 8-hydroxy-2-(di-n-propylamino)tetraline (8-OH-DPAT), a 5-HT_{1A} selective ligand (Tricklebank et al. 1985), labels cells in the DR nucleus (Marcinkiewicz et al. 1984). This labelling decreases dramatically following 5,7-dihydroxytryptamine induced degeneration of serotoninergic cell bodies (Verge et al. 1985). Further confirmation has been gained by a demonstration of a close correlation between [^{3}H]8-OH-DPAT binding and 5-HT_{1A} mRNA in situ hybridisation histochemistry in DR (Chalmers & Watson, 1991). Electrophysiologically, 8-OH-DPAT exerts a similar depressant effect on DR firing rate as LSD and 5-HT (De Montigny et al. 1984, Sinton & Fallon, 1988, McCall & Clement, 1989), as does ipsapirone (Sprouse & Aghajanian, 1985), another highly selective 5-HT_{1A} ligand (Glaser et al. 1985). The actions of ipsapirone and 8-OH-DPAT have also been shown to increase a potassium conductance identical to that mediated by 5-HT (Sprouse & Aghajanian, 1987 & 1988, Rainnie et al. 1987, Williams et al. 1988). In addition the increase in potassium conductance mediated by 8-OH-DPAT is blocked by (-)-propranolol (Sprouse & Aghajanian, 1986), further indication that the receptor involved is of the 5-HT_{1A} subtype (Middlemiss, 1984).

It has been shown that intracerebral injection of PTx has no effect on the baseline firing rate of serotoninergic DR neurones, but blocks the action of 5-HT and ipsapirone in vivo (Innis & Aghajanian, 1987) and in vitro (Williams et al. 1988), suggesting the involvement of G_i or G_o in the signal transduction pathway. The involvement of a G-protein is further supported by the observation that GTPγS mimics the action of 5-HT in increasing the potassium conductance of DR neurones recorded in brain slices (Innis et al. 1988).

Recently a study has been performed on calcium currents recorded in adult rat DR neurones (Penington & Kelly, 1990, Penington et al. 1991). This was enabled by whole-cell patch-clamping acutely isolated cells, allowing control of both intra and extracellular media, to isolate current through calcium channels. Acute isolation has the additional advantage in that the proportions of the various components of calcium currents have been shown to alter in culture under various conditions (e.g. Doerner et al. 1988). Isolated cells have resting membrane potentials in the range -40 to -60 mV, and fire spontaneous action potentials of magnitudes of 80 - 100 mV, that can also be elicited by depolarisations from -60 mV (Penington et al. 1991). In the presence of TTX (0.2 μM) depolarisations lead to both low- and high-threshold calcium dependent spikes, with the low-threshold spike being inactivated by holding potentials positive to -50 mV (Penington et al. 1991). In voltage-clamp, depolarisations to -50 to -35 mV from a holding potential of -80 mV elicit small inward currents that completely inactivate during a 150 ms test pulse (Penington et al. 1991). These are similar to the T-type current seen in DRG cells (Fox et al. 1987a). Larger depolarisations cause a current that is maximal at -10 mV, from a holding potential of -100 mV, that are more reminiscent of HVA current. If the holding potential is changed to -50 mV, there is an approximate 60% reduction in the current amplitude, with the remaining current showing little or no inactivation (Penington et al. 1991). Single channel recordings show channel openings with a slope conductance of 8 pS with small depolarisations, that would be consistent with T-type channels. Larger depolarisations elicit openings with a large conductance of 23 pS, whose mean open time is prolonged by BayK 8644. These would be

consistent with L-type channels. A third, intermediate sized, channel is also seen with a conductance of 15 pS that could be of the N-type. No other sized opening have been reported (Penington et al. 1991).

Since at least three types of calcium channels are present, that are not inconsistent with the classical classification of T, L, and N, it is tempting to speculate that the current elicited by voltage steps from -100 to -10 mV is composed of L and N-types. When the holding potential is changed to -50 mV, the remaining current (40% of the total) would be L-type, and the component that is inactivated at this holding potential, N-type. Studies with DHPs and ω-CgTx have been performed to try to clarify this. These, however, found that 1 μM nimodipine decreased HVA current by around 4% (Penington et al. 1991), rather than the 40% that would be expected for a complete block of the proposed L-type current. 1 μM ω-CgTx decreased the HVA current by around 40%, again short of the 60% that would be expected for the block of the putative N-type current. To date the combined action of both nimodipine and ω-CgTx, the action of ω-CgTx with a holding potential of -50 mV, or the action of FTX, have not been studied, but it does appear that DR neurones possess an N-type current, a small L-type component, and a significant (50-60%) amount of HVA current that is both DHP and ω-CgTx insensitive.

The application of 10 μM 5-HT to isolated DR cells causes an approximate 50% reduction in the peak HVA current recorded at -10 mV, with a slowing of the activation rate, while LVA appears to be unaffected (Penington & Kelly, 1990). This action is mimicked by 8-OH-DPAT and blocked by 1-(2-meth-oxyphenyl)-4-[4-(2-phthalimmido-butyl]piperazine (NAN 190) that is reported to be a 5-HT_{1A} specific

antagonist (Glennon et al. 1988a & b). It therefore appears likely that the same somatodendritic autoreceptor causes both hyperpolarisation via an increase in potassium conductance, and inhibits HVA calcium current, and both of these actions have been shown to occur simultaneously in the same cell (Penington et al. 1992).

Similar to other neuronal preparations, inhibition of calcium currents in DR neurones can be made irreversible by the application of intracellular GTPγS (Penington et al. 1991), and it is also thought that PTx blocks the action of 5-HT (Penington - personal communication). Also similar to other preparations are the findings that phorbol esters, 8-Br-cAMP, the nonspecific kinase inhibitor H-7, and arachadonic acid, all have no effect on the 5-HT inhibition of HVA current (Penington et al. 1991). In addition, 5-HT applied to the extrapatch membrane has no effect on cell-attached single-channel recordings. It therefore appears that the inhibition of calcium currents by 5-HT in DR neurones is mediated via a 5-HT_{1A} receptor, a PTx sensitive G-protein, and no freely diffusable intracellular messenger. How a G-protein influences calcium channels, and whether or not the same G-protein is involved in both the calcium and potassium effects is unknown. Both responses are reported to be PTx sensitive (Penington - personal communication), though in other cells different PTx sensitive G-proteins are reported to link a receptor to calcium and potassium channels (Surprenant et al. 1990, Lledo et al. 1992).

The exact component of HVA calcium current inhibited by 5-HT is not clear. The percentage reduction of peak current by 5-HT is unaffected by a change in holding potential from -100 to -50 mV, but in the presence of ω-CgTx, the inhibition was reduced from 50% to

under 40% (Penington et al. 1991). While simply looking at the percentage reduction in peak current is a rather crude assessment of the action of 5-HT in the light of the altered kinetics, it seems that both ω-CgTx sensitive and insensitive calcium current is inhibited.

Interestingly, the inhibition of HVA calcium current by 5-HT in DR neurones is reversed to a large degree by the application of a voltage step to a large positive value (40 to 80 mV) just prior to the test pulse (Penington et al. 1991), as has been shown for the action of noradrenaline, luteinizing hormone-releasing hormone (LHRH, Elmslie et al. 1990), and GABA (Tatebayashi & Ogata, 1992) in DRG neurones. Such pulses have little or no effect on control currents.

Clearly the action of 5-HT on the autoreceptors of DR neurones is inhibitory. 5-HT applied to the DR causes a rapid inhibition of the release of 5-HT from axonal nerve endings at sites distant to the DR (Sharp et al. 1989, Becquet et al. 1990). This is highly significant since 5-HT can be synthesized and released in the DR nucleus itself (Héry et al. 1982). Since few axon terminals in the DR show 5-HT immunostaining (Baraban & Aghajanian, 1981, Descarries et al. 1982) it seems unlikely that the source of this 5-HT is from recurrent collateral axons, and so it may be that the source is from the somatodendritic compartment (Héry et al. 1986, Becquet et al. 1990). 5-HT mediated hyperpolarisation decreases DR firing rates, and so would be expected to reduce both local and distal release of 5-HT. The function of the additional inhibition of calcium currents by 5-HT is not clear. It is impossible to speculate whether this phenomena in the cell soma reflects events at the axon terminals. However, if 5-HT is released from the cell bodies and dendrites of DR neurones, reduction in calcium currents here may very well augment the reduction

in this 5-HT release that would occur with membrane hypopolarisation. Therefore a negative feedback system may be highly tuned to damp down the local release of 5-HT that itself acts on the somatodendritic autoreceptors. It is interesting to note that the presynaptic noradrenergic autoreceptor is of the α_2 subtype (e.g. Shen & Surprenant, 1990), and stimulation of this has been shown to cause hyperpolarisation via a potassium conductance (North & Yoshimura, 1984, Andrade & Aghajanian, 1985, Fukuda et al. 1987, Shen & Surprenant, 1990), in addition to inhibition of calcium currents (Docherty & McFadzean, 1989, Kongsamut et al. 1989, Surprenant et al. 1990, Akasu et al. 1990) in mammalian central neurones. In both cases a pertussis toxin sensitive G-protein appears to be involved in the signal transduction. Thus a combined hyperpolarisation and inhibition of calcium influx may be a common feature of inhibitory autoreceptors in neurones.

7. The Effect of Temperature on Ionic Conductances

Studies of the effect of temperature on ionic conductances have been performed for many years, initially primarily on sodium and potassium currents. It has often been argued that the temperature dependence of these currents reflects in some particular way, the underlying processes. This section describes some of the theory of temperature dependency measurements, the effect of temperature on sodium and potassium currents, and lastly, details some results from more recent work on calcium currents.

The two mathematical approaches which have been used most frequently to describe the relationship between the rate of a

biological process and temperature are the Arrhenius relationship and the van't Hoff rule. Both approaches were developed for simple chemical systems but have been widely applied to biology.

The Arrhenius relationship describes the relationship between the reaction rate (k) and absolute temperature (T):

$$k = A.e^{(-E_a/RT)} \qquad (1.1)$$

where R is the gas constant, A is a constant, and E_a is the Arrhenius activation energy. A plot of the natural logarithm of k against the reciprocal of T is therefore linear, with a slope of $-E_a/R$. This is an Arrhenius plot and is a standard way of estimating activation free energies in enzyme kinetics. The Arrhenius relationship was developed to describe the temperature dependence of the equilibrium constant and strictly assumes that the reaction involves only a single rate-limiting step.

The van't Hoff rule stemmed from the empirical observation that the rate of a chemical reaction often approximately doubled with a 10°C increase in temperature. This is quantified as the Q_{10} where

$$Q_{10} = \text{rate at } (T + 10)/\text{rate at } T \qquad (1.2)$$

with T being the temperature in °C. The Q_{10} can be calculated for any temperature interval as

$$Q_{10} = (k_1/k_2)^{10/(T_2 - T_1)} \qquad (1.3)$$

where k_1 and k_2 are the rate constants observed at T_1 and T_2

respectively (Belehradek, 1935).

The van't Hoff and Arrhenius relationships are not equivalent, though E_a and Q_{10} are related such that

$$\ln(Q_{10}) = 10.E_a/RT_1T_2 \qquad (1.4)$$

Thus while the Q_{10} is purely an empirical measurement, since its magnitude is proportional to the activation energy of a reaction, it is able to provide some rather circumstantial evidence as to possible mechanisms that might underlie the process under study (see Morris & Clarke, 1981). Physical processes which do not involve any modification of any kind of interatomic bonds have a Q_{10} near 1.03. Cellular biochemical processes which operate on covalent chemical bonds exhibit Q_{10}'s in the 2-3 range because enzymatic procedures lower the energy requirements. Higher Q_{10} values are indicative of more complex process like a multi-step biochemical pathway and/or translocation of a molecule through a high viscosity medium such as the lipid membrane. Changes in the viscosity of the lipids with temperature can affect the interaction of molecules embedded in cell membranes. This can lead to phase transitions and breaks in the linearity of the Arrhenius plot (Chapman, 1975). In such situations, the value of the Q_{10} can vary substantially depending on the temperature range in which it is measured (e.g. Fischbach & Lass, 1978, Schwarz, 1979, Kimura & Meves, 1979, Narahashi et al. 1987).

As far as ionic conductances through ion channels are concerned, several factors need to be considered when examining their temperature dependence, particularly of current amplitude. The conductance depends on the conditions of ionic displacement. Water has a

viscosity with a relatively high Q_{10} due to liquid water being a relatively ordered medium. Between 0 and 50°C, the viscosity Q_{10} varies between 1.2 and 1.4 (Franks, 1981). As a result, free water diffusion conductance of chloride salts, for example, show Q_{10}'s of about 1.2 - 1.3 (Benson & Gordon, 1945). With ions binding to molecules or sequestration in restricted stores (which particularly applies to Ca^{2+}), the Q_{10} for cytoplasmic conductance is higher at about 1.4 or more at room temperature (Hodgkin & Nakajima, 1972, Adrian & Marshall, 1977).

Many early estimations of the Q_{10} for the amplitude of currents flowing through voltage dependent potassium and sodium channels were in the 1.3 to 1.5 range (e.g. Hodgkin et al. 1952, Frankenhaeser & Moore, 1963, Schauf, 1973). These values were comparable to the conductance of electrolytes in free solution, and so the possible implication is that these channels, when opened by depolarisation, passively allow the passage of ions. This hypothesis fits with the finding that gramicidin, which constitutes an unspecified, unmodulated ionophore in membranes, has a temperature dependence of conductance close to that of free water, with Q_{10} values of 1.34 and 1.38 for Na^+ and K^+ respectively (Hladky & Haydon, 1972). However the idea of voltage dependent channels simply forming passive pores on depolarisation seems slightly at odds with their complex structure (particularly sodium and calcium channels), and their ability to be ion selective. It would be expected that the Q_{10} values would therefore be higher. This may in fact be the case. A diminution of the recorded current in voltage clamp experiments caused by a decrease in temperature can be partly masked by a parallel increase in the input resistance of the cell. Therefore the apparent Q_{10} for the current

amplitude must be multiplied by the Q_{10} of the series resistance (about 1.4, see above), to obtain the actual Q_{10} (Schwarz, 1986). This leads to an estimate of the actual Q_{10} being around 2. Many more recent reports do in fact quote Q_{10} values for sodium and potassium current amplitudes as being between 1.7 and 2.5 (Kukita, 1982, Sevcik, 1982, Magura et al. 1985). Thus these values for the amplitude Q_{10}s may reflect the possible involvement of more active processes, rather than simply diffusion of ions through passive pores.

Ion channel kinetic processes such as activation and inactivation, not surprisingly, have been shown to have Q_{10} values clearly in excess of that of simple diffusion in an aqueous medium. This presumably reflects possible alterations in the channels configuration. Generally speaking, kinetic parameters of both sodium and potassium channels, have consistently been shown, in several preparations, to have Q_{10}s of around 2.5 - 3 (e.g. Hodgkin et al. 1952, Moore, 1971, Schauf, 1973, Beam & Donaldson, 1983, Schwarz, 1986).

There is growing evidence that additional processes regulate the function of calcium channels, in addition to direct channel block or activation, and distal receptor modulation. Most evidence suggests that cAMP is not involved in the transduction of transmitter modulation of calcium conductances, however, in the presence of intracellular GTPγS, the adenylate cyclase stimulator forskolin, which normally has no effect, is able to enhance calcium currents in DRG cells (Dolphin, 1991a). This suggests that under certain conditions, cAMP is able to regulate calcium flux through voltage sensitive calcium channels.

The possible involvement of complex multistage processes in the regulation of calcium channels may endow the currents with a

temperature sensitivity somewhat different to that seen for sodium and potassium channels. The temperature dependence of calcium currents has been studied in detail in several non-neuronal or invertebrate preparations. These have generally demonstrated that they are at least as sensitive as sodium and potassium currents, with increases in amplitude and particularly large accelerations of kinetic parameters with increases in temperature. For example in ventricular myocytes both the amplitude and activation rate of calcium currents have a Q_{10} in the order of 3 (Cavali et al. 1985). In molluscan neurones, current amplitude appears less sensitive with Q_{10}'s ranging from 1.2 to 2.3, but the Q_{10} for the rate of activation is higher (Kostyuk et al. 1981a, Brown et al. 1983, Byerly et al. 1984, Lux & Brown, 1984), and can be as high as 6.5 (Brown et al. 1983). The situation is similar in frog skeletal muscle (Cota et al. 1983). Single channel recordings in snail neurones suggests that the increase in amplitude is primarily due to an increase in open channel probability rather than an increase in unitary conductance (Lux & Brown, 1984), which would be expected if the Q_{10} simply reflected ion diffusion through a passive pore.

To date there have been relatively few studies conducted in vertebrate neuronal tissue. Interpretation of the data from the peripheral nervous system is complicated by the heterogeneous nature of calcium channels (Nowycky et al. 1985, Fox et al. 1987a) coupled with the different voltage protocols used and different temperature ranges studied. However there are certain similarities with the invertebrate data, in that the Q_{10}'s for current amplitude range from 2.6 (cat and chick DRG, Taylor, 1988, Nobile et al. 1990), to 3.0 (mouse neuroblastoma, Narahashi et al. 1987). The Q_{10} for the

activation rate (3.4 to 7.5) was found to be higher than that for the amplitude (Taylor, 1988, Nobile et al., 1990). The time constants of exponential curves fitted to tail currents, on the other hand, have lower Q_{10} values of 1.5 to 3.1 (Taylor, 1988, Swandulla & Armstrong, 1988, Nobile et al. 1990). Narahashi and workers (1987) found a clear transition temperature at around 20°C in neuroblastoma cells for all parameters studied, below which the Q_{10}'s increased dramatically. This has not been seen by any other group.

8. Protein Phosphatases

Phosphorylation of proteins is recognised as being of major importance in the regulation of intracellular processes. The phosphorylation or dephosphorylation of serine, threonine and tyrosine residues leads to conformational changes in the protein altering its biological properties, and the level of phosphorylation is governed by the relative activity of the protein kinase and phosphatase that catalyze the interconversion processes. The control of protein kinase activity by second messangers and phosphorylation is well understood (Cohen, 1988). Recently there has been growing interest in the study of the role of protein phosphatases (PPs) in the control of calcium channels (e.g. Lang et al. 1991, Swain et al. 1991, Artalejo et al. 1992b, Dolphin, 1992a, Yakel, 1992). It is known that certainly the L-type channel has a number of potential serine and threonine phosphorylation sites on various subunits (see section 4 above), therefore it is the serine and threonine specific PPs that are of particular interest.

These PPs can be divided into two groups depending on whether they

dephosphorylate the β subunit of phosphorylase kinase, and are inhibited by two small endogenous proteins termed inhibitor-1 and inhibitor-2 (PP1), or whether they dephosphorylate the α subunit of phosphorylase kinase and are insensitive to the 2 inhibitors (PP2). PP2 is also divided into PP2A which is cation independent, PP2B which is Ca^{2+} dependent, and PP2C which is Mg^{2+} dependent (Ingebritsen & Cohen, 1983a & b). All appear to occur in the brain (Ingebritsen et al. 1983a), though mostly they have been studied in non-neuronal cells. The active form of PP1 appears to be mostly particulate being associated with glycogen (Strålfors et al. 1985) and reticulocyte ribosomes (Foulkes et al. 1983), suggesting that it may participate in glycogen metabolism and protein synthesis. On the other hand, PP2A and PP2C are cytosolic and display their highest activity towards proteins involved in glycolysis, gluconeogenesis, fatty acid sythesis and aromatic amino acid breakdown (Ingebritsen et al. 1983b, Pelech et al. 1984). Although the precise roles of PPs *in vivo* have still to be defined, it seems certain that they each act on many phosphoproteins. Consequently anything that alters their activities is likely to change the phosphorylation states of numerous proteins. This in turn suggests that their activities should be closely controlled.

PP1 is inhibited by cAMP through the action of inhibitor-1 (Huang & Glinsmann, 1976), which is effective at nanomolar concentrations, provided that a specific threonine residue is phosphorylated by AK (Cohen, 1988). Because a number of substrates for PP1 are phosphorylated by AK, activation of inhibitor-1 should inhibit their dephosphorylation and thereby amplify the effects of cAMP. However PP1 also dephosphorylates several proteins that are phosphorylated by other protein kinases, and activation of inhibitor-1 presumably allows

the signals that act through cAMP to modulate the phosphorylation states of these substrates as well. A second form of inhibitor-1 has been detected in brain, where it is highly concentrated in neurones expressing D_1 dopamine receptors. This protein, termed DARPP (dopamine and cAMP regulated phosphoprotein) becomes phosphorylated in response to elevations in cAMP as a result of D_1 receptor activation (Williams et al. 1986). By contrast, inhibitor-1 is distributed much more widely and is present in numerous brain regions (Hemmings et al. 1984). It is thought that *in vivo* when AK is activated, this leads to phosphorylation not only of inhibitor-1, causing it to activate, but also the G-subunit of the glycogen-protein particles to which PP1 is bound, causing the PP1 to dissociate into the cytosol (Hiraga & Cohen, 1986). The release of PP1 is then able to be inhibited by inhibitor-1. The role of inhibitor-2 in the control of PP1 is not as clear. It appears that a variant of PP1 found in skeletal muscle can be activated *in vitro* by incubation with MgATP and a protein kinase that phosphorylates inhibitor-2 (Holmes et al. 1986). However, whether this mechanism functions *in vivo* is not known.

PP2B is composed of two subunits, A and B, with the B subunit being structurally similar to calmodulin, and binding Ca^{2+} (Aitken et al. 1984), and there is evidence that the binding of calcium to the B subunit is essential for the A subunit to interact with the protein substrates (Tonks & Cohen, 1983). In addition, in the presence of Ca^{2+}, the A subunit also interacts with calmodulin, increasing its activity around ten fold. PP2B has a much narrower specificity than the other PPs, and the most effective substrates so far identified are proteins that regulate other PPs and kinases, such as inhibitor-1 (Ingebritsen et al. 1983a), DARPP (Hemmings et al. 1984), and the

regulatory subunit of AK (Blumenthal et al. 1986). At micromolar concentrations of Ca^{2+}, PP2B is the most active inhibitor-1 phosphatase in skeletal muscle (Ingebritsen et al. 1983a), and in brain PP2B and DARPP appear to localise in the same neurones (Nestler et al. 1984). The dephosphorylation of inhibitor-1 by PP2B represents a mechanism by which Ca^{2+} can lead to the activation of PP1. This may allow signals that act through Ca^{2+} to override those that act through cAMP, and act in conjunction with calmodulin sensitive phosphodiesterases that should lower the concentration of cAMP, and hence the activity of AK, in the presence of Ca^{2+}. Increases in the activity of PP1 would lead to the dephosphorylation of substrates of AK, and dephosphorylation of the regulatory subunit of AK by PP2B further promotes the inactivation of AK. One area where these processes may be in action is in D_1 containing dopaminergic neurones. In these cells, dopamine (possibly acting by increasing levels of cAMP) prevents glutamate depolarisation (mediated by an increase in calcium conductance). It may be that dopamine's ability to decrease the firing rate of these neurones relatively slowly may involve the phosphorylation of DARPP. Conversely, the ability of glutamate to terminate the action of dopamine may be achieved through the activation of PP2B and cAMP phosphodiesterases (Nestler et al. 1984).

Much less is known about the regulation of PP2A and PP2C. It appears that PP2A is present in cells as a low activity. The only candidate, so far, for a physiological activator is the polyamine, spermine (Cohen, 1989). PP2C is dependent on Mg^{2+}, but this is unlikely to regulate its activity *in vivo*, since its free concentration does not fluctuate much (Cohen, 1989).

9. Investigational Aims and Synopsis of Thesis

As described in section 5, the action of the majority of transmitter substances on calcium currents in a whole range of neuronal preparations, is characterised by a partial inhibition, and a slowing of activation, with no apparent freely diffusable second messenger. To date there have been virtually no reports of detailed analysis of the action of transmitters on the activation rate, and in addition, there are few ideas as to how channel kinetics are affected to cause this slowing. This investigation was aimed at trying to answer these questions in DR, and also to further ideas concerning the transduction mechanism between receptor and channel. Following chapter 2, which details the methods used, there are four results chapters (3 - 6). The first of these records some initial results on the voltage dependency of calcium currents in DR, confirming the previous work in the preparation (Penington & Kelly, 1990, Penington et al. 1991), and to validate the procedures. The action of cadmium was studied, initially to confirm that all active current recorded was through calcium channels. The results obtained suggested that current could be differentiated by cadmium, in that LVA current appeared relatively insensitive, and this was to prove particularly useful concerning an observation made in chapter 5 of an action of 8-OH-DPAT and GTPγS. Chapter 3 also details an assessment of the decrease in current amplitude with time (or 'rundown'), so that subsequent results could be interpreted in the light of this. Finally, the pharmacology of the 5-HT action has been furthered from that of Penington & Kelly (1990). Additional evidence was gained that 5-HT acts via 5-HT_{1A} receptors to inhibit HVA current. Also additional work on possible

second messengers was performed, particularly by investigating the action of forskolin. This appeared to cause either decreased rundown or increased 'runup', but did not affect the actions of either 8-OH-DPAT or GTPγS. Most importantly, a detailed quantitative analysis of the action of 5-HT_{1A} agonists was made.

Previously it has been shown that calcium currents are extremely temperature sensitive (see section 7 above), and this may well reflect the complex nature of calcium channels. It was decided to investigate the temperature dependence of calcium currents in DR in the hope that this might give some ideas as to the nature of the processes underlying the currents seen, and in particular activation. This is reported in chapter 4. This work demonstrated that current amplitude had a similar temperature sensitivity to that seen in other preparations. However the activation rate had a Q_{10} in double figures. Analysis of the amplitude sensitivity suggested that the various components of HVA current have different temperature dependencies. Increases in temperature also revealed an additional fast inactivating HVA component, not present at room temperature.

Having obtained a some what surprising result that activation in DR is even more temperature sensitive than would have been predicted, it was clearly of interest to see if this was affected by 5-HT_{1A} agonists or GTPγS. Chapter 5 describes how receptor and G-protein activation not only slow the current activation rate, but also change its temperature sensitivity, decreasing the activation rate Q_{10} from over 10 to around 3. Interestingly, application of large depolarising pulses prior to the test pulse not only partially reversed the slowing of activation and reduction in amplitude, as previously observed, but also reversed the reduction in activation rate Q_{10} by both 8-OH-DPAT

and GTPγS. A novel action of 8-OH-DPAT and GTPγS in DR was also identified, that of a prolongation of current tails. Since these tails appeared to be relatively cadmium insensitive, it is postulated that this is as a result of an enhancement of LVA current.

Since calcium channels have multiple phosphorylation sites, then it may well be that the effects of transmitters are mediated by a change in the phosphorylation state. This is certainly the case in cardiac cells for the enhancement of calcium currents by β-adrenoceptor agonists (Dolphin, 1991b). Preliminary data using phosphatase inhibitors to investigate this possibility in DR neurones is presented in chapter 6. This suggests that by blocking an okadaic acid (OA) sensitive phosphatase, the extent of 'runup' was greatly enhanced. In addition, while 8-OH-DPAT still caused some reduction in current amplitude and slowing of activation, this was reduced. More dramatically, the reduction in activation rate Q_{10} was completely abolished. This was also the case for the prolongation of current tails by 8-OH-DPAT and GTPγS.

Chapter 7 discusses the results obtained with regard to the heterogeneous nature of the HVA current in DR, and the modulation of the currents by 5-HT. A model is presented to help explain 5-HT mediated modulation of HVA current in DR, and the role of phosphorylation in both this and current rundown. Conclusions drawn from the study are also presented in this chapter.

Table 1.1 - Inhibition of Vertebrate Neuronal HVA Calcium Currents

This table (see over) lists examples of the action of agonists at a number of different transmitter, or putative transmitter, receptors on HVA calcium currents in vertebrate neuronal preparations. One none neuronal, but similar preparation, pituitary cells, is also included. All have in common the observations that even at high doses only partial inhibition (usually 40 - 60%) of currents is seen, together with a variable degree of slowing of current activation. The first column lists the preparations, the second the transmitter, and the third lists the references that describe the inhibition. The fourth column lists reports of the effect being PTX sensitive, while the fifth those that describe it being mimicked or made irreversible by a non-hydrolysable analogue of GTP, such as GTPγS. The last column lists reports where the effect of the transmitter could be blocked by non-hydrolysable analogues of GDP, such as GDPβS. The abbreviations used are listed here, while the references are listed after the table.

5-HT = 5-Hydroxytryptamine
Ach = Acetylcholine
AD = Adenosine
ATP = Adenosine Triphosphate
BK = Bradykinin
CG = Ciliary Ganglion
CGC = Cerebellar Granule Cell
DA = Dopamine
DN = Dynorphine
DR = Dorsal Raphé
DRG = Dorsal Root Ganglion
Enk = Enkephalin
GABA = γ-Amminobutyric Acid
Glu = Glutamate
G-P = Guinea Pig
H = Hippocampus
LC = Locus Coeruleus
LHRH = Leutinising Hormone Releasing Hormone
MP = Myenteric Plexus
NA = Noradrenaline
Neurobla. = Neuroblastoma Cell Line
NC = Neocortex
NG = Nodose Ganglion
NPY = Neuropeptide Y
OB = Olfactory Bulb
PC = Pituitary Cell
PS = Parasympathetic Neurones
SC = Spinal Cord
SCG = Superior Cervical Ganglion
SM = Submucosa Neurones
SN = Sympathetic Neurones
SP = Substance P
SS = Somatostatin

Table 1.1 - Inhibition of Vertebrate Neuronal HVA Calcium Currents

Prep.	Trans.	Inhibition	PTX sens.	GTPγS	GDPβS
Frog SN	NA	2,18,36,38	18	18,36	
	LHRH	3,17,18		17,18	
	SP	3,18		18	
	Ach	18		18	
	ATP	18		18	
Chick DRG	GABA	9,10,16,24,31	31	31	31
	NA	2,3,16,36,47	31	31	31
	5-HT	16			
	DA	5,6,43			
	AD	34		34	
Chick CG	SS	15	15		
Mouse DRG	AD	26,40,52	26,52		
	DN	27,41			
	GABA	25			
Rat DRG	DN	2			
	SS	2,32	32	32	
	AD	12			
	NA	23,55	55		
	GABA	12,13,24		13,14	14
	NPY	19,20	19,20		
Rat SCG	Ach	45,51,55,56,62	51,55,56,62	51,55,56,62	62
	NA	45,51,56	51,56	51,56	
	NPY	51	51	51	
Rat MP	NPY	29,30	29,30		
Rat NG	NPY	63	63		
Rat SC	GABA	53	53	53	
	5-HT	53			
	NA	53			
	AD	53			
	SS	53			
	DN	53			
Rat OB	Glu	59	59	59	
Rat H	AD	42			
	Ach	22			
	GABA	54	54	54	
	Glu	8		8	
Rat LC	NA	65			
Rat DR	5-HT	49,50	48	49	49
Rat PC	SS	7,47	7		
	DA	35,39,64	39,64	35,64	
Rat NC	SS	61	61	61	
Rat CGC	GABA	44			
G-P SM	NA	57	57	57	
	SS	57	57	57	
	Enk	57	57	57	
Rabbit PS	NA	1			
Neurobla.	NA	4,6,11,33,46,58	4,33,46,58	4,46	
	Enk	4,11,28,33,40,58	4,28,33,58	4,28	28
	SS	58,60	58		
	DA	4			
	BK	58			
	Ach	6,33	33		

Table 1.1 - Inhibition of Vertebrate Neuronal HVA Calcium Currents

References

1. Akasu et al. 1990
2. Bean, 1989a
3. Bley & Tsien, 1988
4. Brown et al. 1989
5. Carbone & Lux, 1989
6. Caulfield et al. 1992
7. Chen et al. 1990
8. Chernevskaya et al. 1991
9. Cox & Dunlap, 1992
10. Deisz & Lux, 1985
11. Docherty & McFadzean, 1989
12. Dolphin et al. 1986
13. Dolphin & Scott, 1986
14. Dolphin & Scott, 1987
15. Dryer et al. 1991
16. Dunlap & Fischbach, 1981
17. Elmslie et al. 1990
18. Elmslie, 1992
19. Ewald et al. 1988a
20. Ewald et al. 1988b
21. Forscher & Oxford, 1985
22. Gahwiler & Brown, 1987
23. Galvan & Adams, 1982
24. Grassi & Lux, 1989
25. Green & Cottrell, 1988
26. Gross et al. 1989
27. Gross & MacDonald, 1987
28. Hescheler et al. 1987
29. Hirning et al. 1988a
30. Hirning et al. 1990
31. Holz et al. 1986
32. Ikeda & Schofield, 1989
33. Kasai, 1992
34. Kasai & Aosaki, 1989
35. Keja et al. 1992
36. Kongsamut et al. 1989
37. Lester & Jahr, 1990
38. Lipscombe & Tsien, 1987
39. Lledo et al. 1992
40. MacDonald et al. 1986
41. MacDonald & Werz, 1986
42. Madison et al. 1987
43. Marchetti et al. 1986
44. Marchetti et al. 1991
45. Mathie et al. 1992
46. McFadzean & Docherty, 1989
47. Nussinovitch, 1989
48. Penington - personal communication
49. Penington et al. 1991
50. Penington & Kelly, 1990
51. Plummer et al. 1991
52. Ryan-Jastrow et al. 1988
53. Sah, 1990
54. Scholz & Miller, 1991
55. Song et al. 1989
56. Song et al. 1991
57. Surprenant et al. 1990
58. Taussig et al. 1992
59. Trombley & Westbrook, 1992
60. Tsunoo et al. 1986
61. Wang et al. 1990
62. Wanke et al. 1987
63. Wiley et al. 1988
64. Williams et al. 1990b
65. Williams & North, 1985

Chapter 2 Methods

1. Tissue Preparation

Adult male Cob Wistar rats of around 200g were decapitated by guillotine without anaesthetic, and the occipital and parietal bones removed. The cranial nerves were severed by blunt dissection, and the brain rapidly removed and placed in pre-oxygenated ice cold artificial cerebrospinal fluid (aCSF - see Table 2.1). The tissue was then placed on aCSF moistened filter paper, the cerebral cortices reflected and removed, along with the cerebellum, using a razor blade. The rostral end was squared off with the blade to allow the tissue to be glued to a plastic mount using cyanoacrylate glue, with the caudal surface uppermost. A 4% agar block was used to support the ventral surface of the brain. The mounted brain was placed in the plexiglass chamber of a vibroslice (Campden Instruments), and surrounded by ice cold aCSF. Three 500 μm coronal slices were cut in the dorso-ventral direction through the brain stem at the level of the DR nucleus using the vibroslice. The slices were approximately taken from between 0 to 2 mm rostral to the interaural line, using the superior colliculus, the size of the aqueduct of Sylvius, and the decussation of the superior cerebellar peduncle as markers (see figure 2.1). Slices were placed on plates of 4% agar kept moist with aCSF, and the area of grey matter immediately ventral to the aqueduct and dorsal to the decussation, containing the DR nucleus, was cut from each using a razor blade (figure 2.1). This whole procedure, from guillotining, took on average about 10 minutes. Brains from two rats were dissected in quick succession, thus providing 6 pieces of tissue.

Cell isolation was by the method of Kay and Wong (1986). One of the main advantages of using acutely isolated cells is that it has

previously been shown that various culture conditions can affect the expression of calcium channels in neurones (Plummer et al. 1989, Boland & Dingledine, 1990, Eckert et al. 1990, Streit & Lux, 1990, Usowicz et al. 1990, Marchetti et al. 1991), in addition to alterations in the action of transmitter substances (Kasai, 1992). As soon as obtained, the pieces of grey matter were placed in 10 ml of a piperazine-N,N'-bis[2-ethane-sulfonic acid] (PIPES) buffered solution (see table 2.1) containing approximately 5000 units of trypsin per ml (Sigma, U.K. Type XI). This was stirred using a small magnetic flea at a rate sufficient to keep the pieces of tissue suspended above the bottom of the container, and incubated for ninety minutes at 33°C under pure oxygen. After this time 9 ml of the trypsin solution was removed and replaced by plain PIPES buffer twice, and the tissue cooled to room temperature (17-22°C). When required for use (1-6 hours later), two pieces of tissue at a time were removed and triturated with two fire polished Pasteur pipettes with decreasing sized tips of approximately 1 and 0.5 mm diameters, in Dulbecco's modified Eagle's medium (Gibco). Cells were then allowed to settle out in a plain perspex petri dish (Corning), for 15-20 minutes. The dish was placed in the temperature control chamber, mounted on the stage of an inverted phase contrast Nikon Diaphot microscope. It has been shown that cells isolated in this manor retain the basic electrophysiological characteristics of those studied in the brain slice preparation (Penington et al. 1991).

2. Electrophysiological Measurements

Cells were chosen that were phase-bright and had a soma with one

dimension of at least 20 μm (figure 2.2). It has been shown by Lawrence, Penington & Kelly (1989) that 90% of these cells contain 5-HT immunoreactivity. Electrodes were pulled from 1.6:1.0 mm (outside : inside diameter) pyrex tubing, with an internal filament, using a List-Medical L/M-3P-A puller. When filled with pipette solution (see table 2.1), their resistance ranged from 6-13 and averaged 9.5 ± 0.1 MΩ (mean ± SEM, n = 165). Occasionally electrodes were coated with Sylgard (Dow Corning) to reduce their capacitance, and fire polished. Electrodes were lowered through the gas/water interphase while positive pressure was applied, which was removed on entry into the solution. The Axoclamp-2A amplifier (Axon Instruments) used in this study, was turned on in bridge mode, the electrode resistance measured, and any tip potential occurring offset. Measured junction potentials of external solution containing cadmium, forskolin, or 8-OH-DPAT, differed by less than 2 mV. The tip of the electrode was advanced towards the chosen cell, using a Burleigh patch clamp micro-manipulator, until a small voltage deflection was seen in response to a 10 ms current pulse occurring at 10 Hz. Negative pressure was then applied by pulling the plunger of a 1 ml syringe back 0.1-0.2 ml. This led to the formation of a seal between the electrode glass and the cell membrane. Seal resistance, prior to going whole cell, ranged from 1-13 with an average of 6.4 ± 0.3 GΩ (n = 128), though the effect of breaking the membrane under the electrode on the seal is impossible to predict. If the resistance was less than 1 GΩ, then the cell was discarded. 37 (22.4%) of cells went spontaneously whole cell when the seal was formed. Seals were found to be best obtained in a solution containing calcium, so a calcium tyrode solution (see table 2.1) was used, which was then replaced by external recording medium once the

seal was obtained. Further positive pressure was applied by mouth suction to convert from cell attached to whole cell mode (Hamill et al. 1981), and a five minute equilibrium period allowed before recording began. Once whole cell mode had been achieved, hyperpolarising current was passed to hold the membrane potential around -100 mV. The reference bath electrode was a Ag/AgCl pellet at the bottom of a well filled with 3 M KCl (labelled 3 in figure 2.5). This well was connected to the recording dish containing external solution by means of bent glass electrode tubing filled with 4% agar made with 3 M KCl. These 'agar bridges' were kept submerged in 3 M KCl when not in use.

Recordings were all made using a high input impedance amplifier, the Axoclamp 2A. This amplifier was used in a switching mode for both current and voltage clamping, where a single electrode is used to both monitor potential and inject current by a system of multiplexing. This involves rapidly cycling the circuitry between voltage monitoring and current passing. Figure 2.3 illustrates a schematic circuit and timing diagram of the method used by the Axoclamp 2A. When switch S1 is in the voltage recording position, an electrode measures the sum of the membrane potential (V_m) and the potential drop (V_e) across the electrode itself due to the passage of current (I_o) across the electrode resistance (R_e). This voltage is buffered by a high speed amplifier (A1) and passed to a sample-and-hold amplifier (SH1) at the sample times marked (i.e. just prior to the onset of current injection). This occurs during the T_v section of the cycle. If switch S2 is set to discontinuous current clamp (DCC), when S1 moves to the current passing position, during time T_i, a current command voltage (V_I) is passed to a controlled current source (CCS) which

injects current (I_o) to change V_m. Switch S1 cycles between its two positions at a frequency of 1/T, where $T = T_i + T_v$. The average output of SH1 (V_{ms}(ave)) is a reliable measure of V_m if V_e has decayed to near zero by the time SH1 samples the output of A1. This decay, in simplistic terms, is a single exponential with time constant τ_e, which is determined by R_e and the capacitance of the electrode (C_e) and amplifier A1. Thus the cycle time (T) needs to be around 10 times τ_e. For a fast response time in voltage clamp mode, T needs to be as small as possible (explained below). Therefore certain steps were taken to reduce τ_e. These involved: 1. keeping R_e as low as possible, though generally the smaller R_e, the harder it was to obtain a high resistance seal; 2. having as low a level of solution in the dish as possible to reduce C_e and occasionally augmenting this with the use of Sylgard; 3. using the capacity compensation (CC) circuitry of the Axoclamp to compensate for residual C_e and other capacitance in the circuit. This involves passing negative current generated by a variable amplified output applied through a fixed capacitor to the input. Compensation was adjusted in DCC mode while monitoring the output of A1 in an attempt to maximise the rate at which V_e approached zero without causing an over shoot to below zero. The cycle frequency (1/T) was adjusted at the same time to as high a level as possible that still allowed V_e to decay fully, and was commensurate with a stable recording with no electrode oscillation. The range of frequencies used was 6-16 kHz with an average of 12.0 ± 0.2 kHz (n = 165). 78% of cells studied, mainly the later ones, had cycle frequencies in double figures.

Once T and CC had been set, the Axoclamp was switched to discontinuous single electrode voltage clamp mode (dSEVC), by means of

switch S2. In dSEVC, V_{ms} is compared to a voltage command (V_c) by a differential amplifier, A2. During time periods T_i the output from A2 is passed to CCS which injects a current (I_o) directly proportional to V_c-V_{ms}. Thus A2 acts in a negative feedback fashion to control V_{ms} to approximately V_c. If T and CC are set appropriately then $V_{ms} \approx V_m$ and so I_o is independent of R_e, unlike a non-switching SEVC, leading to, in theory, no voltage error in assumed V_m. However, in practice, the averaged V_{ms} (to reduce effects of extraneous noise) minus V_c is the steady state error of the clamp (ϵ_∞) due to residual V_e ($V_e(\infty)$) as a result of a non-finite gain (G_T) of CCS. It can be shown (Finkel & Redman, 1984) that if the 'equivalent electrode resistance'

$$R_a = V_e(\infty)/i(\infty) \qquad (2.1)$$

where $i(\infty)$ = the steady state current at the end of T_v, then

$$R_a = \frac{R_e(1-e^{-DT_1})e^{-(1-D)T_1}}{1-e^{-T_1}} \qquad (2.2)$$

where $T_1 = T/\tau_e$, and D = duty cycle such that $T_i = DT$. D is preset to 0.3 in the Axoclamp. Assuming that the CC and T have been set adequately, then T_1 will be at least 10. Putting this figure for T_1, the set value for D, and the average value of 9.5 MΩ for R_e into equation 2.2, gives a value for R_a of 8.2 KΩ. Finkel and Redman (1984) also show that if (a) R_a << the cells input resistance (R_N), and (b) T << the cells time constant ($\tau_m = R_N C_N$, where C_N is the cell capacitance), then

$$\epsilon(\infty) \rightarrow \frac{V_c}{1 + R_N G_T D} \qquad (2.3)$$

R_N was measured from small depolarising test pulses where no active current was induced. It was found to range from 0.4 to 10.4 GΩ with an average of 1.9 ± 0.1 GΩ (n = 165). Therefore it can be seen that criteria (a) is satisfied. C_N has not been measured for these cells. However it would be expected that they would have a fairly small capacitance due to the fact that the isolation method leads to considerable truncation of the dendritic tree, with many cells not being far from an approximate sphere. Reports of the value for membrane capacitance in neurones give values such as 1 $\mu F/cm^2$ in dorsal root ganglion cells (Brown et al. 1981a), and 4.5 $\mu F/cm^2$ in hippocampal neurones (Brown et al. 1981b). If one assumes the worst scenario of a 20 μm diameter sphere with a unit capacitance of 1 $\mu F/cm^2$, then this would give a value for C_N of 1.3×10^{-5} μF, and a τ_m of 25 ms. This is considerably larger than the average value for T of 83 μs, so criteria (b) also holds. A value for G_T that gives $\epsilon(\infty)$ of just 0.1% of V_c can then be calculated from equation 2.3, and this is 1.8 nA/mV. In practice values of between 3 and 8 nA/mV were achieved.

The values of G_T and T affect the speed of response of the voltage clamp to step perturbations in membrane potential. For a fast response time, T needs to be as small as possible, and G_T as large as possible. As already stated, T was set in DCC mode before the Axoclamp was switched to dSEVC. Once dSEVC mode was begun, G_T was adjusted so as to produce both a stable recording, and one with a fast settling time with as little over-shoot on voltage change as possible.

Finkel and Redman (1984) show that for stability

$$0 < \frac{G_T DT}{C_N} < 2 \qquad (2.4)$$

and for critical dampening were steady state is achieved 1-2 cycles following a change in V_c

$$\frac{G_T DT}{C_N} = 1 \qquad (2.5)$$

With T = 83 μs, and $C_N = 1.3 \times 10^{-5}$ μF, equation 2.5 gives a value for G_T of 52 nA/mV. This would imply that the gains used would lead to a slow settling, needing several cycles to achieve a steady state. This was the case, however the value for C_N used above is a minimum estimate, and if larger, this would lead to a lower G_T needed for critical dampening. In practice some over shoot was accepted if T had been reduced to such a level that the settling time was in the order of 0.6-1.0 ms.

Amplifier A2 (figure 2.3), as well as providing negative feedback control, is also able to modify the phase shift in the feedback path of the clamp circuit. It was found that the optimum setting for DR neurones was a phase lag of around 3.6 ms. This allowed a larger value of G_T to be obtained. The danger of using phase shift is that if the CC is under set, then τ_e is larger than one would want optimally, and so T/τ_e becomes smaller, resulting in R_a no longer being negligible in relation to R_N. In this situation, the SEVC in effect clamps the electrode artefact resistance rather than the cell, a condition known as a false clamp. This was guarded against by

ensuring adequate CC in DCC mode before entering dSEVC. In addition, a false clamp can be spotted by the fact that V_{ms} does not decay to the baseline during T_V, and that the step response of V_{ms} alters if T is increased. This was routinely checked for before recordings began with each cell. In addition, once the phase shift had been adjusted, the CC was not altered. No anti-alias filtering was used.

3. Temperature Manipulation

Temperature manipulation was by means of a perfusion dish to the design of Forsythe & Coates (1988, Medical Systems Corp., N.Y., USA). A 35 mm petri dish (2 on figure 2.4) is surrounded by heat sink 1 (6). This heat sink forms a sandwich with another (7) that have two peltier devices (5) between them. These peltiers are able to either heat or cool heat sink 1, and thus the petri dish. When cooling, heat is transferred to heat sink 2, and is further dissipated by the microscope stage, with which the dish is in thermal contact. However, if the ambient temperature was more than 7-8°C warmer than the set temperature, then heat dissipation was augmented by passing ice cold water through copper tubing (4) in tight contact with heat sink 2. External solution was pumped into the dish at 1-2 ml/min by a peristaltic pump, with a bubble trap in line to dampen out the pulsatile flow and electrically isolate the dish from the pump, through tubing (1) coiled on top of heat sink 1. The solution level was kept constant at around 1 mm by a suction device positioned on the opposite side of the petri dish from the solution input.

The input (7) and output (8) of the perfusion tubing are also shown in figure 2.5. The temperature of the dish is controlled by a

bipolar feedback mechanism with a temperature sensor (AD-590, see figure 2.6) on heat sink 1. The cells and solution in the petri dish are therefore heated or cooled directly by heat sink 1, along with the solution being pre warmed or cooled as it passes through the tubing coiled on top of the heat sink. In addition 100% oxygen is blown at 50-100 ml/min over the top of the petri dish via an inlet (4 in figure 2.5) that causes it to pass over the heat sink. This reduces heat loss from the open top of the dish. The temperature control dish is shown in situ on a Nikon diaphot microscope in the photograph in figure 2.6.

The temperature controller (circuit kindly designed by Dr I. Forsythe) was powered by dry cell batteries to eliminate the introduction of 50 Hz mains noise into the Faraday cage. In addition, the power source for the peltier devices was two commercial car batteries, to allow large DC current of up to 4 A to be passed, again without the problem of noise. The control circuit was calibrated using a bipolar thermometer (Comark) with the reference thermistor placed in boiling tetramethylsilene (26.8°C) and the test thermistor in the centre of the petri dish, with normal operating conditions. With a perfusion rate of 1.0 ml/min the central area of the dish can be kept at a fairly constant and predictable temperature. Figure 2.7 illustrates an isotherm map produced by Medical Systems Corp., and similar to one published by Forsythe and Coates (1988). In this example, with a set temperature nearly 20°C above the ambient, there would be a variation of no more than 1°C in the central area of the dish. In the experiments described in this thesis, the main bulk involved measurements between 15 and 25°C. The average ambient temperature was 22.1 ± 0.2°C (n = 165). Thus the difference from

ambient was never as extreme as that shown in figure 2.7, and all measurements, that were frequently done, suggested that the central area of the dish used to allow cells to settle on, was at temperatures that were controlled to ± 0.5°C of the desired level. Increases in temperature of 5°C (the normal magnitude of temperature jumps) could be performed in less than one minute, while cooling by 5°C took 1-3 minutes, depending on the relation of the desired temperature to ambient, and whether ice cold water was being passed through the copper tube in heat sink 2. Figure 2.8 illustrates the length of time taken for two parameters, amplitude and activation rate, to settle at a new temperature. The cell was originally held at 15°C, during the time shown by the horizontal bar. It can be seen that the heat sink temperature reached a level appropriate for the dish to be at 20°C after just 40 seconds. Both the activation rate and the amplitude settled to new values after a further 40 seconds, though it can be seen that the activation rate changed quicker than the amplitude. Recordings of all parameters were normally made two minutes after the temperature of the heat sink settled at a new level.

The effects of temperature have been studied in the range 15-30°C where the current kinetics could be clearly resolved, though most experiments were conducted between 15 and 25°C as explained in the results sections.

4. Solutions and Drug Application

Details of the solutions used are given in table 2.1, and the source of chemicals and drugs given in table 2.2. The aCSF used during the tissue dissection is of a fairly standard composition. The

solutions used for the dissociation of the cells are as originally described by Kay and Wong (1986), and used for DR dissociation by Penington and Kelly (1990). As mentioned above, it was found easier to obtain high quality seals in a calcium tyrode solution. This was then replaced by a standard recording medium in which sodium had been replaced by TEA and TTX was present to eliminate sodium currents. Potassium currents were also eliminated by the use of TEA and by adding 4-AP to ensure the blockade of the prominent A-current that these cells exhibit (Aghajanian, 1985). Barium was exchanged for calcium as the charge carrier for all experiments. This has several advantages in that barium contributes to the blockade of potassium conductances (Constanti & Galvan, 1983), does not activate calcium dependent processes, and leads to less severe 'rundown' than with calcium (Dolphin & Scott, 1989b). However, the exchange of barium for calcium may affect calcium current kinetics. Certainly in cardiac cells (Kass & Sanguinetti, 1984), smooth muscle cells (Lang et al. 1991), pituitary cells (Williams et al. 1991), and hippocampal neurones (Kay, 1991), inactivation of L-type channels is slowed by replacement of Ca^{2+} with Ba^{2+}, though this does not occur in mouse cerebellar neurones (Slesinger & Lansman, 1991a), or rat DRG cells (Tatebayashi & Ogata, 1992). In addition, tail currents are reported to be much faster with Ba^{2+} as opposed to Ca^{2+} (Akasu et al. 1990). Thus all measurements of kinetics need to be assessed in this light. It should be noted that where ever "calcium currents" are referred to in the results and discussion chapters of this thesis, in fact they were actually "barium currents".

Pipettes contained a solution where potassium was replaced by a large impermeant ion, trizma (Sigma, U.K.). This solution has been

found to be better in DR cells than a more conventional caesium based one in that it helps to minimise 'rundown' (Penington, N.J. - personal communication). The main anion used was phosphate rather than chloride. Chloride has several disadvantages in that it has a high lyotrophic number and so a tendency to interact with proteins that help stabilize plasma membranes (Inoue et al. 1976). With phosphate as the major anion, stable recordings could be made for up to one hour, presumably since this has a low lyotrophic number (Tasaki et al. 1965). TEA was added to the internal solution to ensure adequate blockade of potassium currents, and MgATP to help reduce rundown of current amplitude (Forscher & Oxford, 1985, De Waard et al. 1991, Kay, 1991). Intracellular calcium and barium was buffered by the inclusion of ethylene glycol-bis(β-aminoethyl ether)N,N,N',N'-tetraacetic acid (EGTA). This chelator has a rather slow on rate and is sensitive to pH (Neher, 1986), and in retrospect it would have been preferable to have used the faster and less sensitive newer buffer, 1,2-bis(2-aminophenoxy)ethane N,N,N',N'-tetraacetic acid (BAPTA). Since the pH will be fractionally altered by temperature changes, it could be that so will internal barium/calcium levels. This could lead to some temperature effects not being the direct result of temperature on the functioning of the channels. To exclude this possibility a programme to calculate free ionic concentrations was used that takes into account temperature, pH, ionic strengths, and chelator used (React version 2.01, G.L. Smith, Chelcom Software, 1986). Over a million fold range of total internal divalent cation concentrations (from 1 μM to 1 pM), for a change in temperature between 15 and 25°C there was never more than a 2% change in free ion concentration.

External solution was either made up fresh on the day of an experiment, of kept refrigerated at 4°C overnight for a couple of days. Internal solutions were aliquoted and frozen, and used for up to one month. No deterioration was noted. On the day of an experiment an aliquot was thawed, drawn up into a syringe, and kept on ice. The syringe was allowed to warm to room temperature for 10-15 minutes prior to use for each batch of cells, and then returned to the ice. Pipettes were filled via a 0.1 μm filter and a syringe that had been heated and pulled to produce a tube fine enough to insert into the pipette. The use of stainless steel needles was avoided in this way.

Initially both the internal and external solutions were pH'd to 7.2. However in later experiments the external was increased to 7.4. This helped to improve cell stability and had no effect on the currents recorded or on temperature sensitivity. Sucrose was used to adjust the osmolarity of the solutions so that the internal had a value of approximately 310 mOsm, and the external 320 mOsm. Having a hypo-osmotic intracellular solution tends to help cell viability and prevent cell swelling (Baker, 1984). However on occasions cells did swell. When this happened, it was spotted by the fact that the current amplitude usually increased, and the voltage clamp improved due to the cell becoming spherical, enabling a more perfect space clamp. This is illustrated in figure 2.9, where it can be seen that although there was a significant increase in current amplitude (from 1.15 to 1.57 nA at 20°C), there was no major alteration in the currents kinetics such as the activation rate (1.91 and 2.14 ms). Small degrees of swelling could not be excluded but if a cell clearly became spherical requiring the dSEVC parameters to be reset, then it

was usually lost or discarded. In the rare case of recordings becoming stable following swelling, then all measurements were exclusively either pre or post swelling. Such data showed no obvious qualitative or quantitative difference to data obtained from healthy cells.

Drugs such as GTPγS, GDPβS, OA and phosphatase inhibitor 1 (I1PP) were added to the internal solution at the time it was made up. GTPγS and GDPβS were added as solids. I1PP and OA were stored as 1.5 and 5 mM stock solutions, made up with dimethyl sulphoxide (DMSO), deep frozen, and then diluted to their final concentration with internal solution. With 1 μM I1PP this gave a concentration of just under 0.07% DMSO in the final internal solution. Control experiments showed no effects with 0.1% DMSO (n = 5). 5-HT, NA, DA, ipsapirone, cadmium, forskolin and 8-OH-DPAT were all applied externally. All except forskolin were made up as aqueous stock solutions at 10 mM and kept frozen. 1 mg/ml ascorbic acid was included with 5-HT, DA, and NA to help prevent oxidation. For each experiment that they were needed, drugs were diluted to their final concentrations with external solution. Forskolin was initially made up in DMSO so that with a final concentration of 10 μM forskolin there was 0.5% DMSO in the external solution. However, when this concentration of DMSO was applied to cells without forskolin, a large rapid increase in current amplitude was seen (figure 2.10) that was only partially reversible (n = 3). As a result forskolin was subsequently made up in ethanol at a concentration of 2 mg/ml. With 10 μM forskolin this gave a final ethanol concentration of under 0.2%, which in control experiments had no effect (n = 4).

Agonists, where short rapid application was required, were applied

by diffusion from a broken patch pipette with a tip diameter of 2-5 μm positioned around 50 μm away from the cell under study. Slight positive pressure was produced when the pipette was placed in the holder which aided diffusion. With this setup solution could clearly be seen flowing out of the pipette and around the investigated cell. Pipettes containing plain external solution were also positioned by most cells that had agonists applied, to check for artifacts produced by the rapid flow of solution over the cell. This was rarely seen, and if did occur then the cell was discarded. Forskolin and cadmium, where more prolonged application was required, were added to external solution and superfused into the dish instead of plain solution. Figure 2.11 illustrates the block of barium current seen with the application of 200 μM $CdCl_2$. It can be seen that it took 3.5 to 4 minutes from switching to cadmium containing solution to reach a steady level of inhibition. Presumably a fairly complete exchange of the solution in the dish occurred within this time, even in the absence of an assumption that the Cd^{2+} was acting on the external surface of the cell.

5. Data Analysis

Data was normally generated at a frequency of 0.05 Hz and stored, after filtering at 1 KHz, on a Sony SL-F30 video cassette recorder via a Sony PCM-701 digital audio processor (both modified by Fentronics Ltd, Cambridge, U.K.). Current and voltage traces were normally digitised at 5 kHz, though sometimes this was increased up to 20 kHz, and analysed on an IBM clone using CED (Cambridge, U.K.) 5.0 voltage clamp software. Leak and capacity subtraction was calculated from

small depolarising test pulses that elicited no active current, and then scaled linearly. Currents are illustrated leak and capacity subtracted unless otherwise stated. To eliminate residual capacity artifacts after leak subtraction, current data points 0.4-0.6 ms following a voltage step have been left blank in the figures. Due to incomplete capacitance subtraction, the first few tenths of milliseconds of tail currents are prone to considerable error. As a result, no attempt has been made to measure the amplitude of the tails either directly, or by retrograde extrapolation of tail current exponential curves. In addition, since the measured current immediately on repolarisation was large in comparison to the current recorded during test pulses, to improve the resolution of the figures illustrated in this thesis, the tail currents have been truncated. Voltage records are as recorded. If Leakage was more than 5% of the peak current amplitude then the cell was discarded.

Fitting of theoretical curves was by means of the iterative "Amoeba" algorithm (Press et al. 1986) utilising the downhill simplex method in multidimensions of Nelder & Mead (1965). This was written into a Borland Turbo Pascal (version 6.0) unit of a programme (Newfit4 - see Appendix B) designed to aid data analysis (Curves unit). The algorithm involves creating a multidimensional object with one more vertex than unknown constants, whose volume represent the sum of the squares of the difference of the data points from the estimated curve on that iteration. The procedure adjusts the vertices to minimise the volume. Once a minimum is reached, values for the constants are returned. To prevent the detection of false local minima, values obtained were multiplied by 0.1 and 10 and returned to the procedure as starting points for a re-run. This continued until the final sum

of the squares of the difference of the re-run varied from the previous one by less than 0.001%. This normally took 2-4 runs of the procedure, though occasionally no definite minimum could be found, and so a maximum of 8 runs was set to prevent the programme being stuck in endless calculations (see Curves unit, Appendix B).

Fitting of curves was either to raw data, or to data which had been forward averaged to reduce noise and computing time (see NewMak2 unit, Appendix B). This had little effect of the calculated parameters. For example, a piece of data, digitised at 5 kHz and with 728 points, was fitted by both single and double exponential functions. The calculated time constants were 32.8, 3.9, and 52.3 ms for the single, fast double, and slow double constants respectively. When the data was forward averaged every 5 points, giving 145, these values were returned as 32.7, 3.8 and 52.0 ms, thus no more than 0.8% error occurred for any. However, if there was any doubt that there may have been an effect of forward averaging, then raw data was fitted. All calculated curves were overlaid onto the data and checked by eye to exclude false minima.

Activating, inactivating, and deactivating portions of the current data were fitted by either single exponential functions of the form

$$I_m(t) = A + B.e^{(-t/\tau)} \qquad (2.6)$$

or double exponential equations of the form

$$I_m(t) = A + B.e^{(-t/\tau_f)} + C.e^{(-t/\tau_s)} \qquad (2.7)$$

where $I_m(t)$ is the membrane current at time t, A, B, and C are

constants, and τ, τ_f and τ_s are time constants. In addition, activation portions of current data was also fitted to the model developed by Hodgkin and Huxley (1952) to describe sodium and potassium conductances in squid giant axons using the equation

$$I_m(t) = I_{max} \cdot [I_\infty - (I_\infty - I_0) \cdot e^{(-t/\tau)}]^x \qquad (2.8)$$

where I_{max} is the maximum inward current, I_∞ and I_0 are the final and initial proportions of I_{max}, and x is an integer. Fits to this equation are referred to as m^1, m^2, m^3 or m^4, depending on the value of x. The voltage dependence of currents was assessed by fitting modified Boltzman equations to current-voltage data, using the Amoeba algorithm, of the form

$$I/I_{max} = \frac{1}{1 + e^{(\pm(V - V_h)/k)}} \qquad (2.9)$$

where I is the current amplitude elicited when the membrane potential is stepped to V, I_{max} is the maximum current amplitude observed, V_h is the voltage needed for half activation, and k is the slope constant. Curves fitted to the same piece of data were compared by calculating the variance ratio from the residual sum of squares of the fitted equations (see variance procedure, curves unit, in the appendix).

The temperature coefficient, Q_{10}, was calculated from the van't Hoff equation (see equation 1.3), and all are quoted for the temperature range 15 - 25°C, for reasons that are described in the results chapters. Arrhenius plots were always made to check that the value of the associated Q_{10} was approximately constant over this temperature range. These are all included in the results section. It

was found that Q_{10} values were clearly not normally distributed (figure 2.12). As a result, average Q_{10} values were calculated as geometric means. In addition due to this non symmetrical distribution of Q_{10} values, 95% confidence intervals (CI) are quoted. The sample size was taken into account with these calculations by using Student 't' tables to calculate the CI's. All other values are arithmetic means ± standard errors (SEM), including normalised values used in Arrhenius plots. As a result, the gradient of lines in Arrhenius plots reflect the magnitude of the given Q_{10} (according to the relationship defined in equation 1.4), but there is not exact numerical equivalence. Note also, that all Q_{10} values quoted are positive, irrespective of whether the measurement increased (e.g. amplitude) or decreased (e.g. activation time constant) with temperature. Arrhenius plots on the other hand reflect the direction of the change, such that a positive slope implies the parameter increased with temperature, and vice versa.

The number of experiments averaged for any given measurement, are given in parentheses. For Q_{10} values these are for the number of values averaged and the number of cells these had been obtained from. This was because in some stable cells, measurements could be made from 20°C to both 15 and 25°C, though no more than two Q_{10} values were calculated for any one cell. Statistical analysis was by means of the Mann-Whitney-Wilcox non-parametric test, and significance was adjudged if $p < 0.01$.

Table 2.1 - Composition of Solutions

	aCSF	PIPES	Ca Tyrode	External	Internal
NaCl	119	120	135		
KCl	2.5	5	1		
$MgSO_4$	1.3				
MgCl		1	1		
$CaCl_2$	2.5	1	5		
$BaCl_2$			5		
NaH_2PO_4	1				
$NaHCO_3$	26.3				
TEA Cl				138	40
Trizma PO_4					70
Trizma EGTA					28
PIPES		20			
HEPES			20	20	
Glucose	11	25	10	10	
Sucrose			10	15	30
TTX				0.0002	
4-AP				5	
MgATP					2
GTP					0.0003
pH	7.4	7.0	7.4	7.4	7.2
pH'd with	95% O_2/ 5% CO_2	NaOH	NaOH	TEA OH	Trizma base

PIPES = piperazine-N,N'-bis[2-ethane-sulfonic acid]

HEPES = N-2-hydroxyethylpiperazine-N'-2-ethanesulfonic acid

TEA = tetraethylammonium

TTX = tetrodotoxin

4-AP = 4-aminopyridine

Trizma = 2-amino-2-(hydroxymethyl)-1,3-propanediol

EGTA = ethylene glycol-bis(β-aminoethyl ether)N,N,N',N'-tetraacetic acid

Table 2.2 - Source of Drugs

PIPES	Sigma, U.K.
HEPES	Sigma, U.K.
TEA Cl	Aldrich, U.K.
TEA OH	Aldrich, U.K.
4-AP	Sigma, U.K.
TTX	Sigma, U.K.
Trizma PO_4	Sigma, U.K.
Trizma Base	Sigma, U.K.
EGTA	Sigma, U.K.
5-HT creatinine sulphate	Sigma, U.K.
Dopamine.HCl	Sigma, U.K.
Noradrenaline.HCl	Sigma, U.K.
8-OH-DPAT.HBr	Research Biochemicals Incorporated
Ipsapirone	Troponwerbe, Cologne
Forskolin	Research Biochemicals Incorporated
MgATP	Sigma, U.K.
GTP	Sigma, U.K.
GTPγS	Sigma, U.K.
GDPβS	Sigma, U.K.
Okadaic Acid	Professor P. Cohen, University of Dundee
I1PP-fragmnet	Professor P. Cohen, University of Dundee

I1PP-fragment = residues 9 - 14 of phosphatase inhibitor 1 peptide

Other abbreviations as in table 2.1

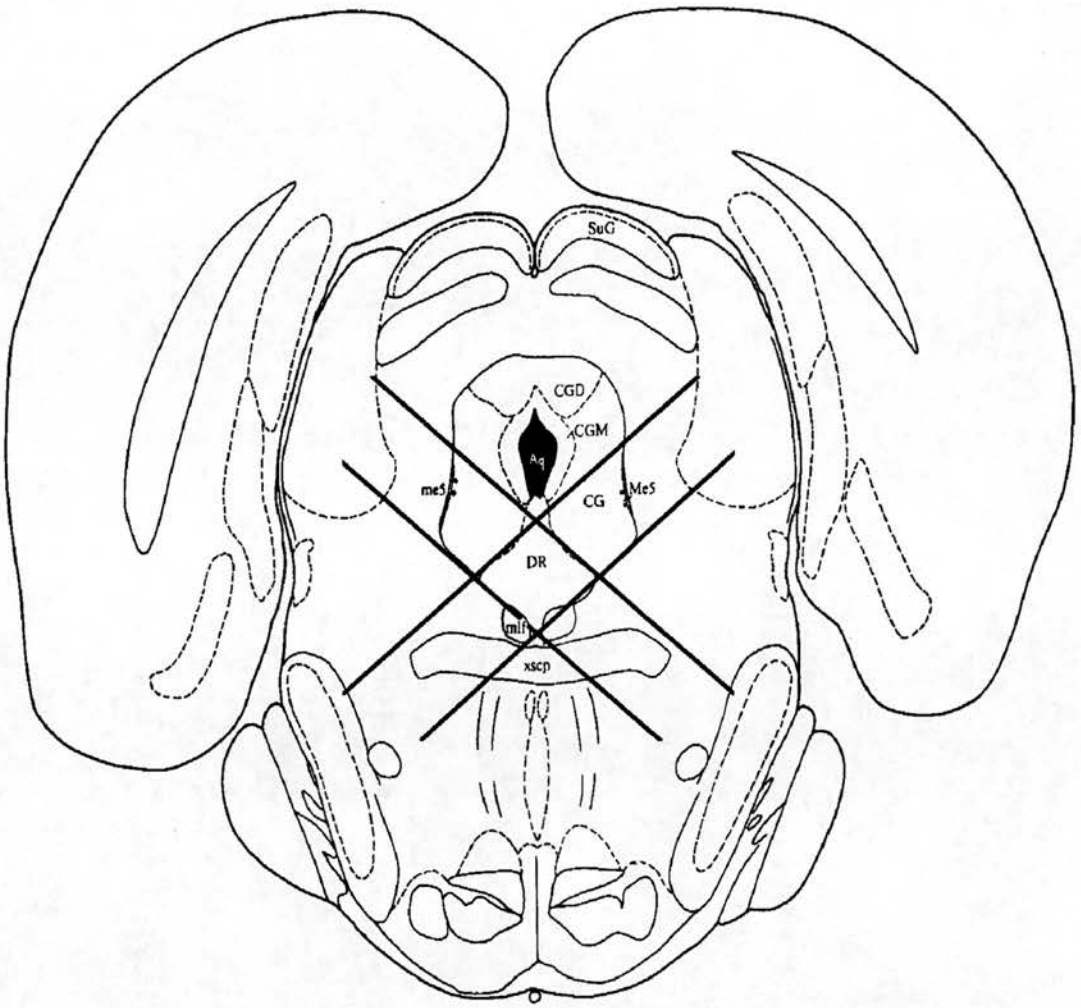

Figure 2.1: **Coronal line drawing of the location of the DR nucleus and surrounding structures in a rat brain, 1.2 mm rostral to the interaural line, adapted from Paxinos and Watson (1982).** Bold lines show the position of cuts made to remove the DR. Relevant abbreviations: DR - dorsal raphé nucleus; Aq - aqueduct; CG - central grey matter; CGD - dorsal central grey matter; CGM - medial central grey matter; me5 - mesencephalic trigeminal nerve; Me5 - mesencephalic trigeminal nucleus; mlf - medial longitudinal fasciculus; xsep - decussation of the superior cerebellar peduncle; SuG - superior colliculus grey matter.

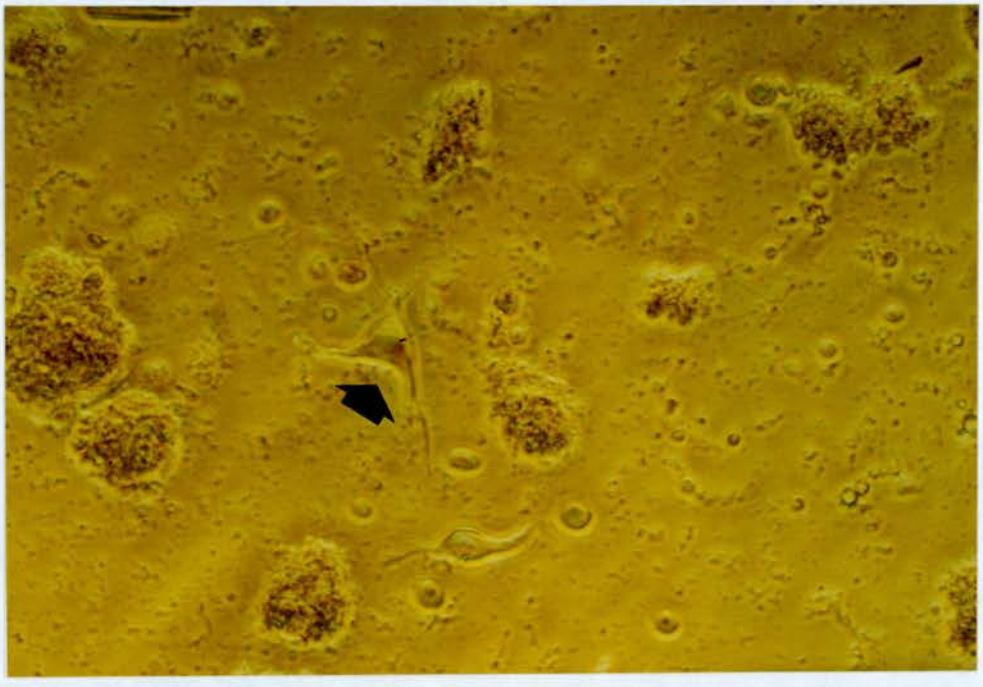

Figure 2.2: **Phase contrast photomicrograph of an acutely dissociated DR neurone.** The cell marked with an arrow is a typical triangular shaped DR neurone that would be chosen for patch clamping. Note the short dendrites that facilitate good space clamping, and that the cell is phase bright illustrating its health. This cell was approximately 35 μm across at its largest dimension. Photograph kindly supplied by Dr Jane Lawrence.

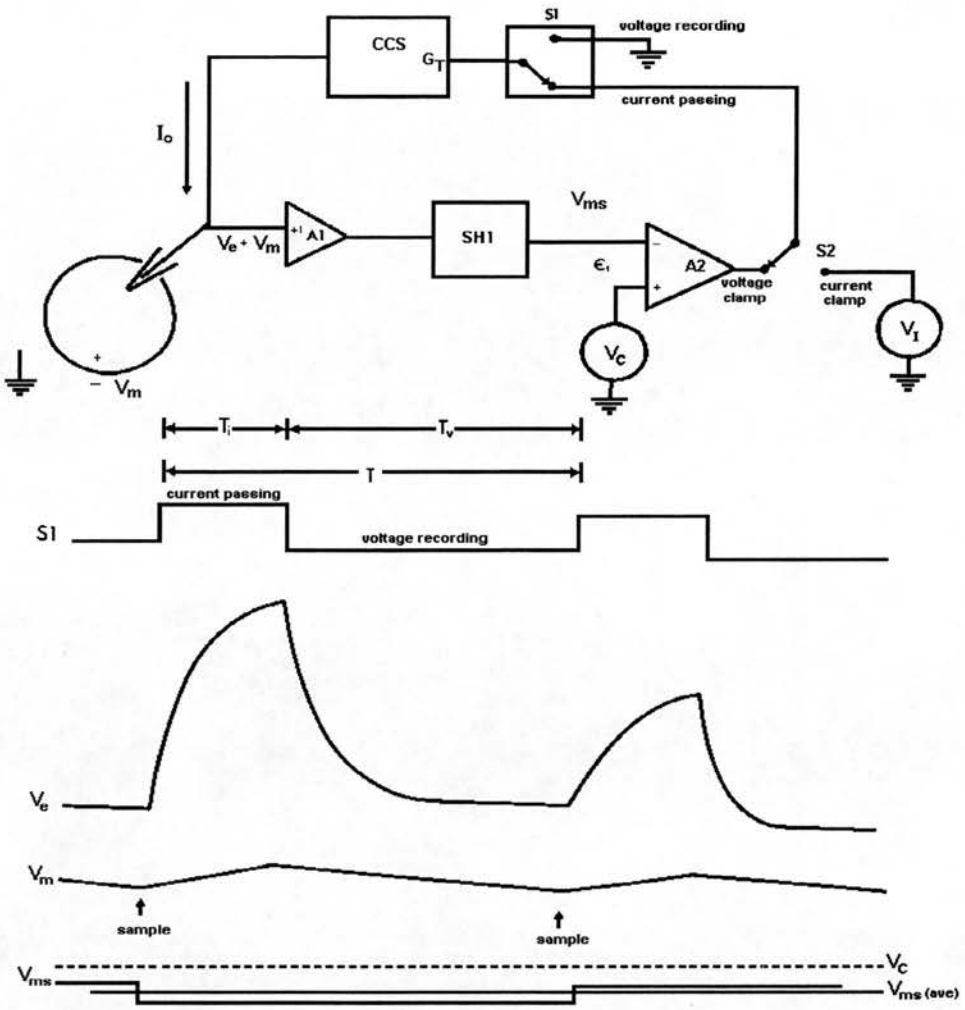

Figure 2.3: Schematic circuit and timing diagram of the discontinuous current clamp and single electrode voltage clamp of the Axoclamp 2A, taken from **Finkel and** Redman (1984). V_m - membrane potential; V_e - electrode voltage; A1 - high speed amplifier; SH1 - sample and hold amplifier; V_{ms} - output from SH1; V_c - command potential; A2 - differential amplifier; $\epsilon_1 = V_c - V_{ms}$; V_I - command potential in current clamp; S1 and S2 - switches; CCS - controlled current source; G_T - CCS gain; I_o current passed to cell; T - cycle period; T_i current passing phase; T_V voltage recording phase. Operation described in text.

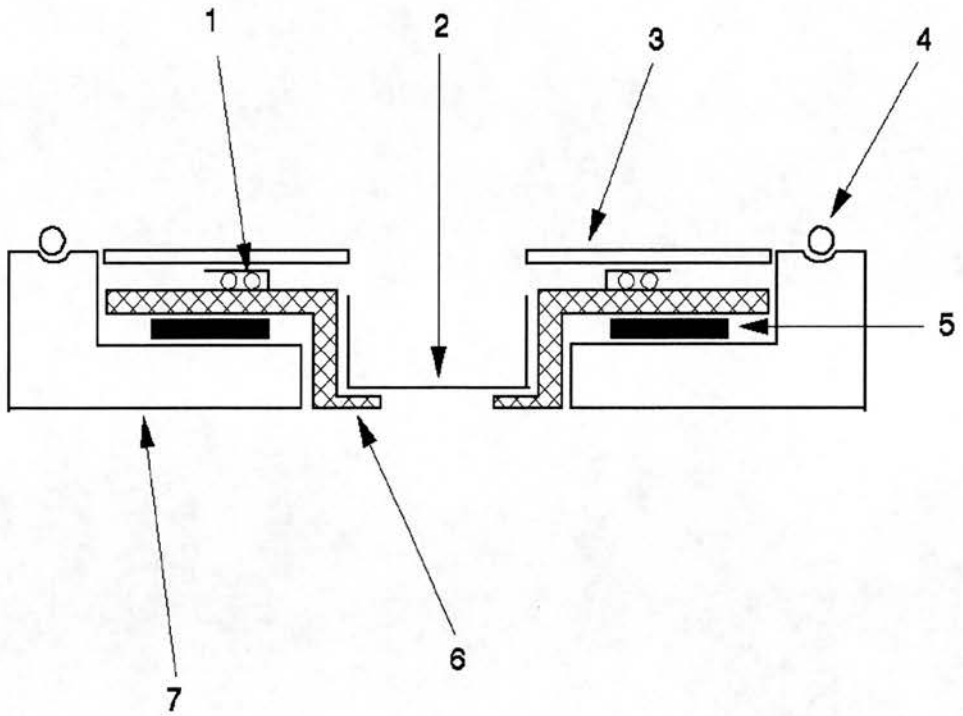

Figure 2.4: Schematic cross section of temperature control dish (Medical Systems Corp.). 1. perfusion tubes, 2. petri dish, 3. lid, 4. copper tubing, 5. peltier devices, 6. heat sink 1, 7. heat sink 2. Functioning described in the text.

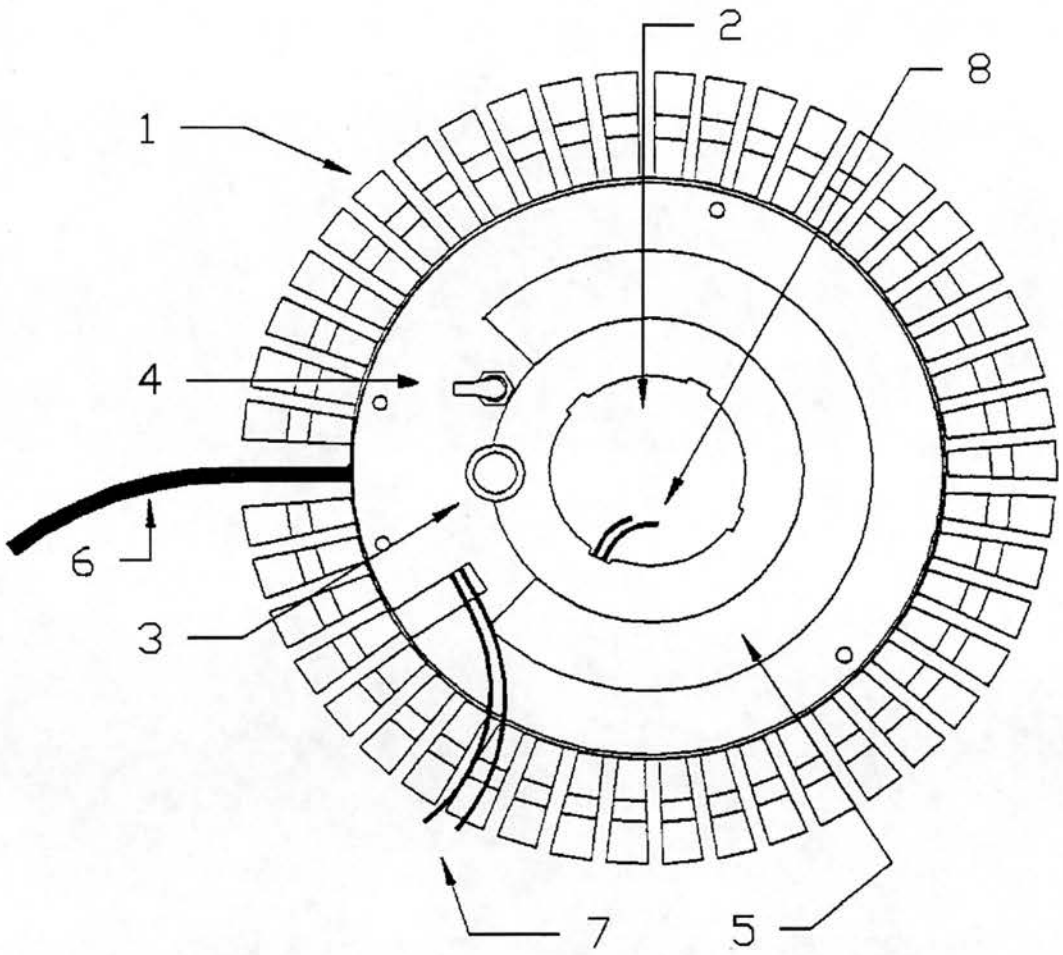

Figure 2.5: **Top view of temperature control dish.** 1. fins of heat sink 2, 2. petri dish, 3. Ag/AgCl well for earth connection, 4. gas inlet, 5. metal strip for attaching magnetic holders, 6. peltier power cable, 7 & 8. perfusion tubing. Dish described in detail in text.

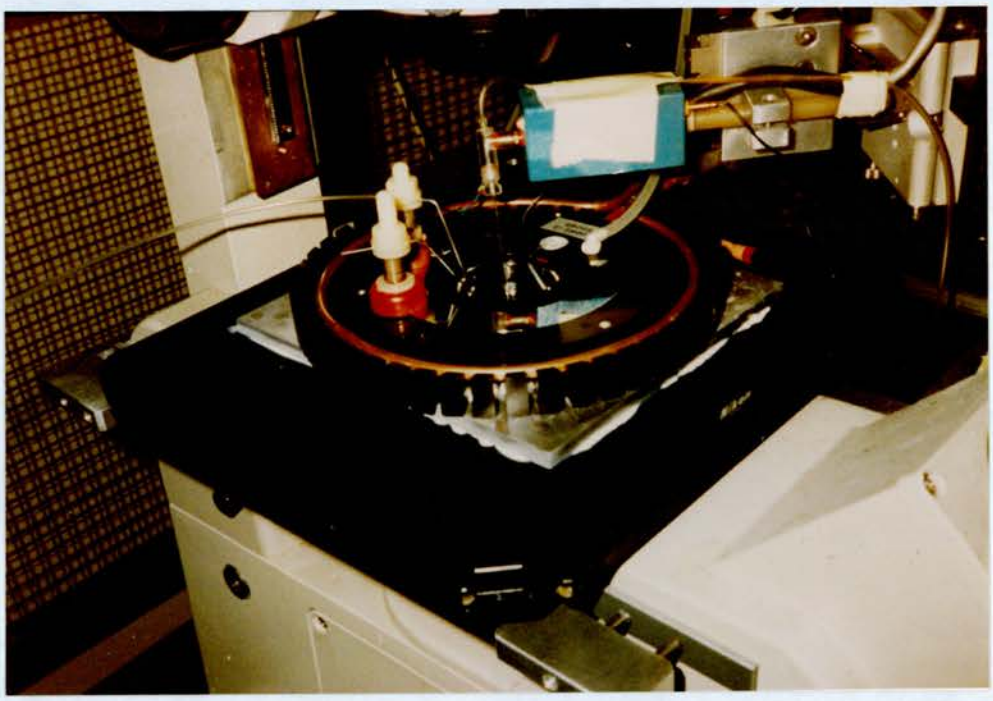

Figure 2.6: Photograph of the temperature control dish in situ on the stage of a Nikon Diaphot microscope. Note the AD-590 mounted through the lid of the black temperature control dish onto heat sink 1. One of the two supports with red magnetic bases holds the perfusion inlet tubes in place, and the other is the suction device.

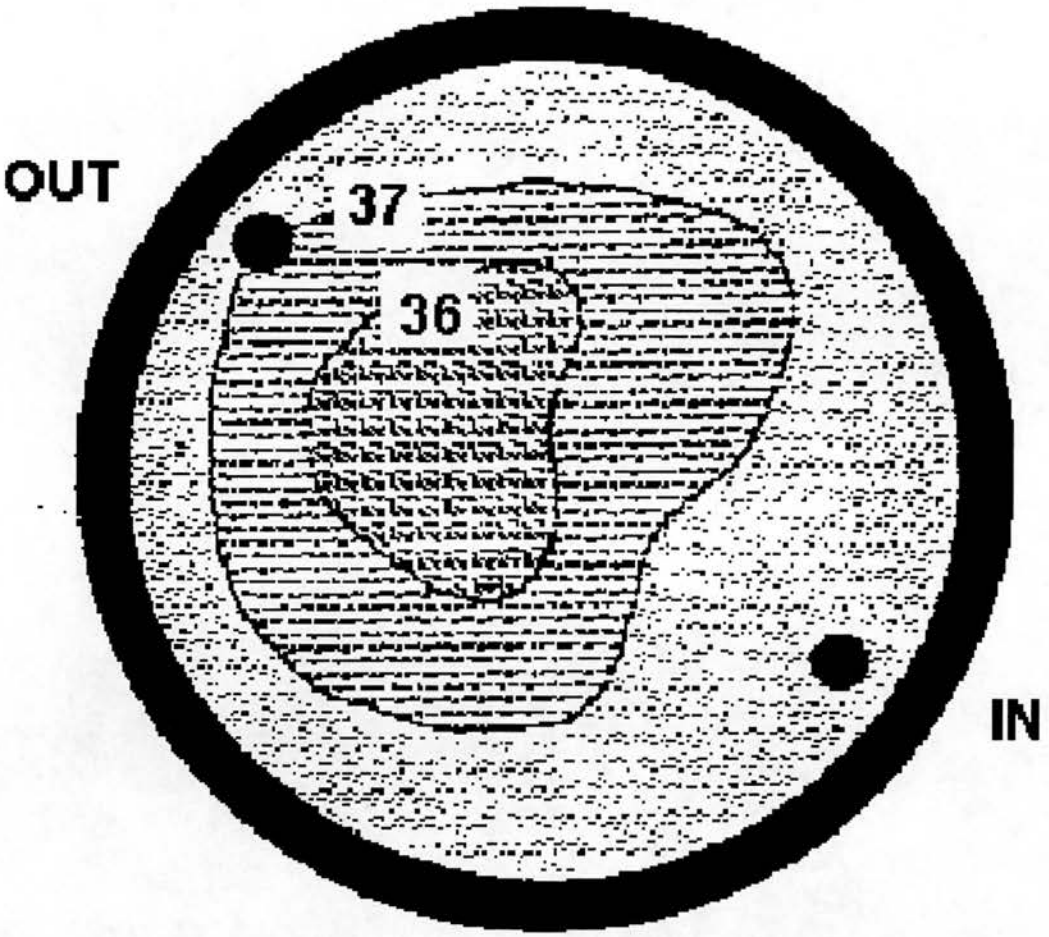

Figure 2.7: **Temperature isotherm map produced by Medical Systems for the temperature control dish used in this study.** The dish was perfused at a rate of 1.0 ml/min, with a bath volume of 1.5 ml. Set temperature was 37°C, while the ambient was 18.5°C. 'IN' and 'OUT' mark the in flow and out flow of the perfused solution. Gas was piped between the lid of the dish and heat sink 1 to reduce heat loss from the exposed upper surface of the fluid.

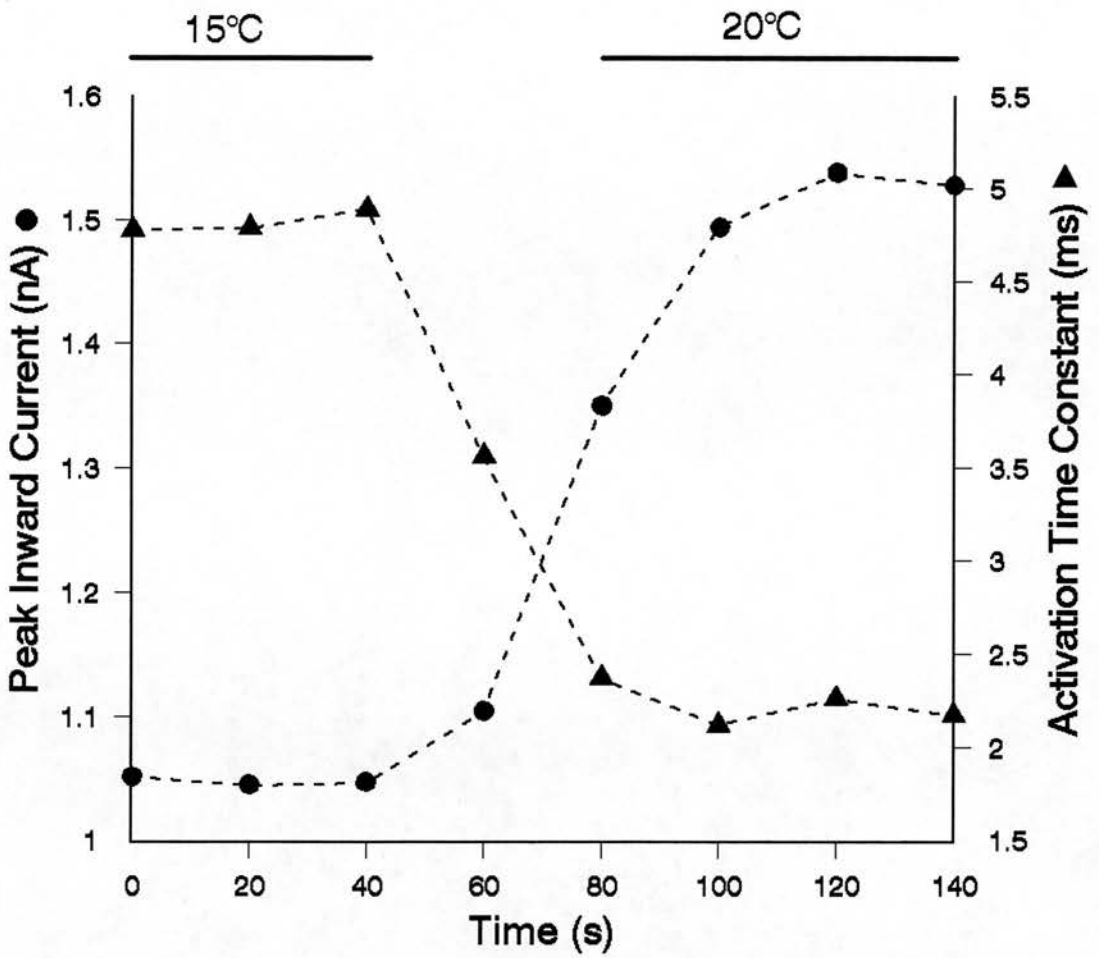

Figure 2.8: Example of the time taken to settle at a new temperature. The temperature was maintained at 15°C during the time indicated by the horizontal bar, and then rapidly increased to 20°C, where it was maintained during the time shown. Currents were elicited every 20 seconds by voltage steps from -100 to -10 mV. Peak current amplitude is plotted against time (circles), as is the activation time constant (triangles) calculated by fitting single exponentials to the activation portion of the current traces. Standard solutions. Cell 02109102.

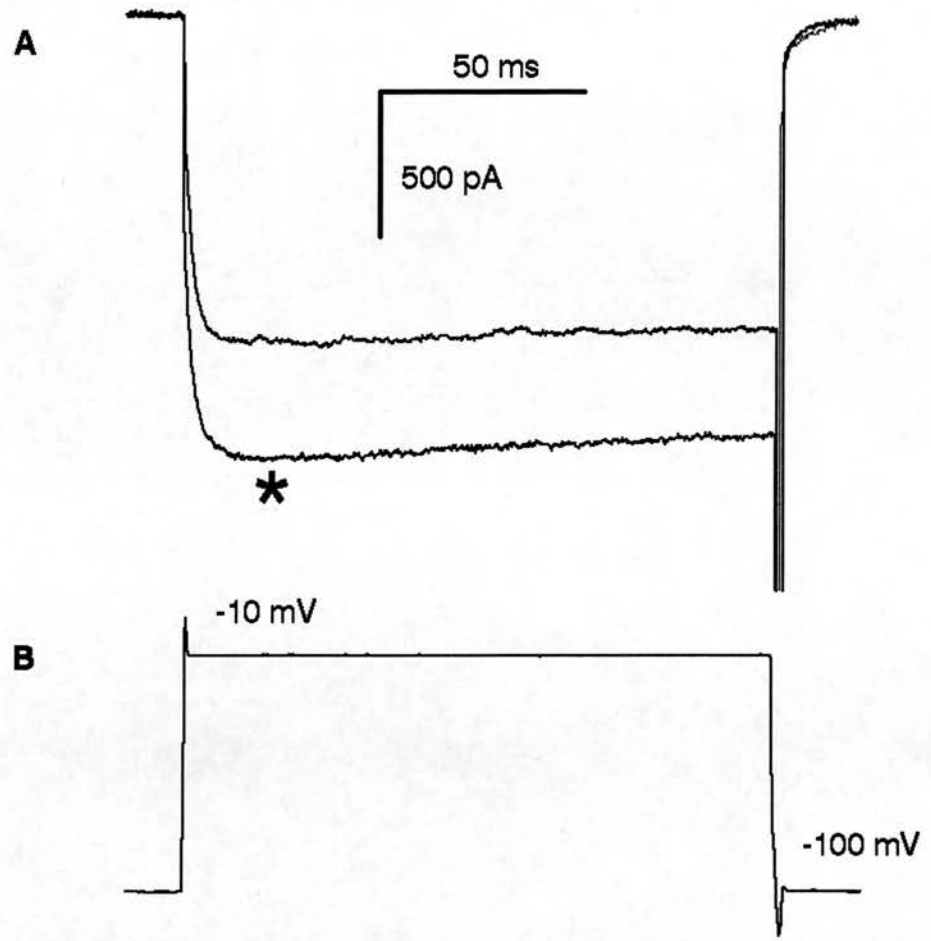

Figure 2.9: **High threshold currents (A) recorded from a DR neurone, before and after (*) the cell became spherical due to swelling.** Holding potential of the cell was -100 mV, with approximately 10 pA holding current. The currents were elicited by voltage steps (B) to -10 mV for 150 ms, at 20°C. The sampling rate was increased from 10.8 to 12.4 kHz between the two current recordings. Both the internal and external solutions were standard. Current data has been leak and capacity subtracted. Cell 02100901/2.

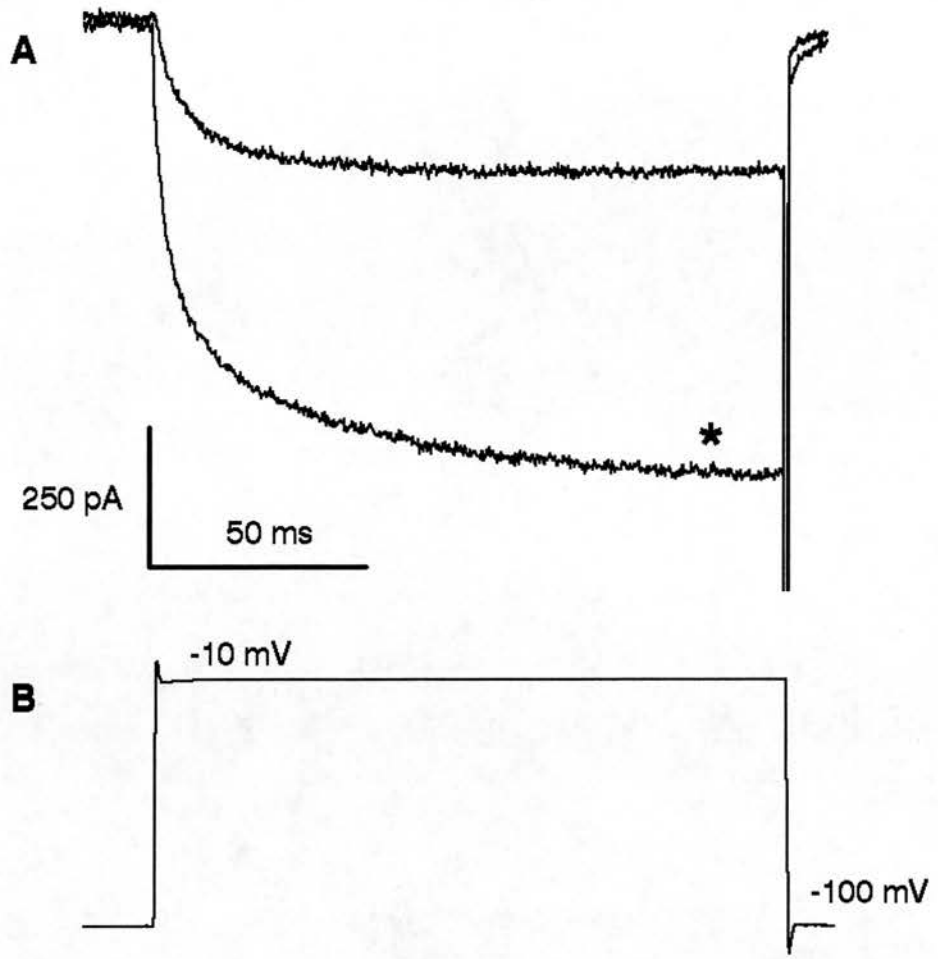

Figure 2.10: **Effect of DMSO.** High threshold calcium currents (A) were elicited by voltage steps from -100 mV to -10 mV (B). Application of external solution containing 0.5% DMSO from a broken patch pipette positioned around 50 μm from the cell led to a large increase in the current recorded (*). Note that DMSO also led to an increase in leakage, reflected by an increase in the current needed to hold the cell at -100 mV, from approximately 20 to 60 pA. To illustrate this, the currents have not been leak subtracted. Standard external solution, pipette solution contained 200 μM GTPγS. Cell 28109101.

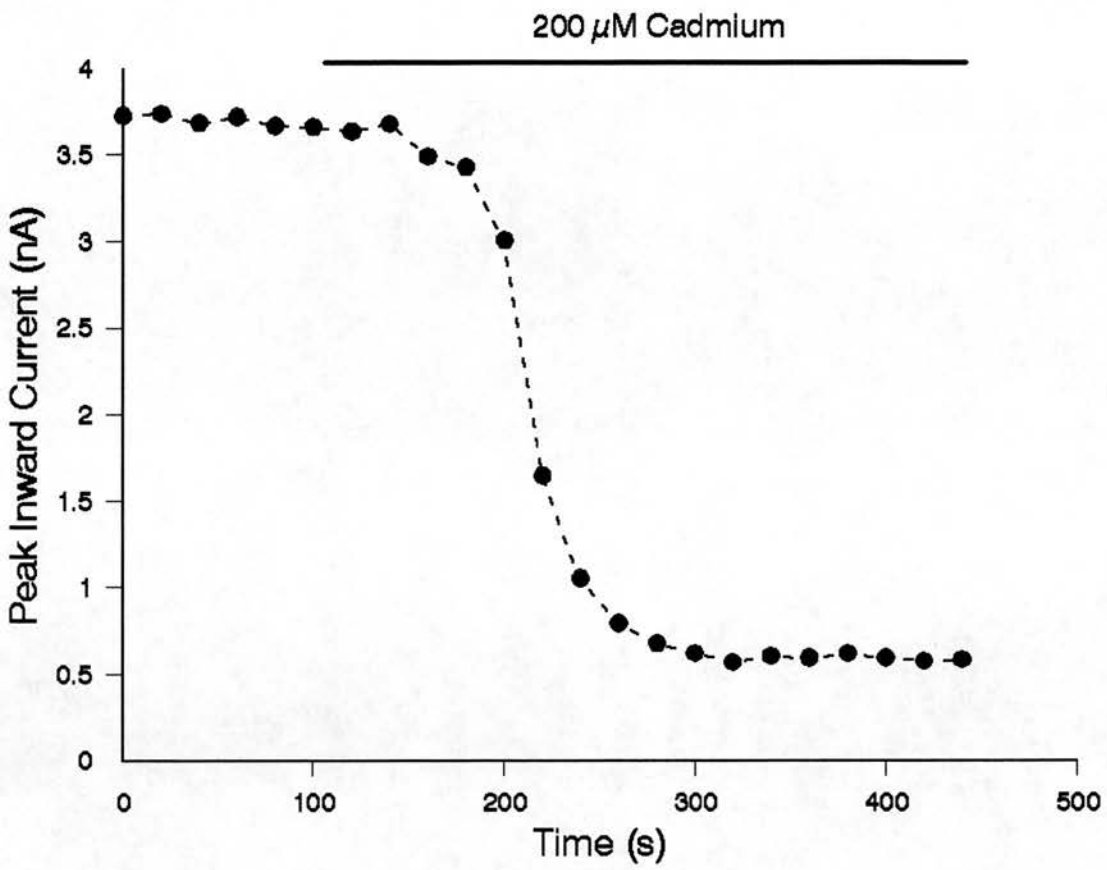

Figure 2.11: Time to exchange the external solution. The graph plots the peak inward calcium currents elicited by voltage steps from -100 mV to -10 mV occurring every 20 seconds. After just over 100 seconds, the bath solution was changed from a standard external solution, to one containing 200 μM Cd^{2+} (illustrated by the horizontal bar). It can be seen that the effect of the cadmium reached a steady level within a period of less than three minutes. Standard pipette solution. Cell 06029201.

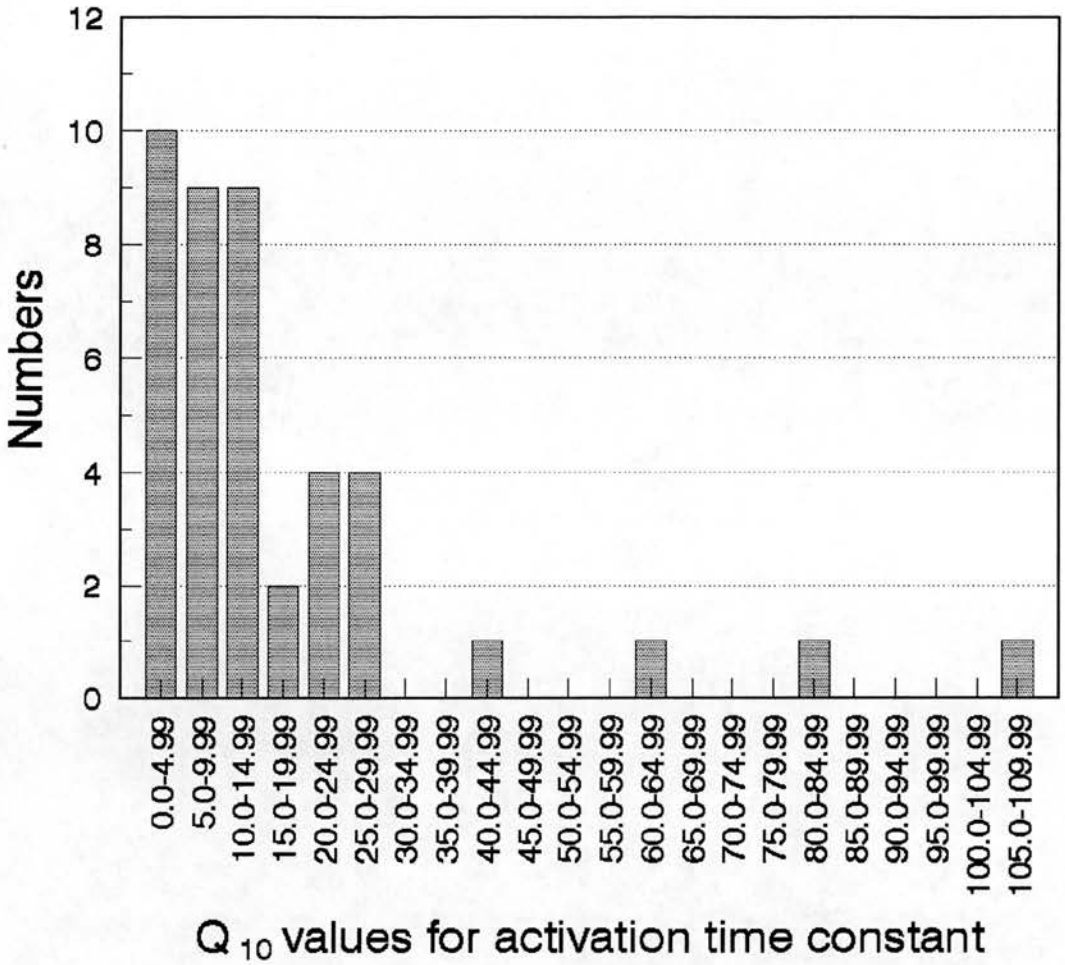

Figure 2.12: Skewed distribution of Q_{10} values. Histogram of the Q_{10} values derived from the time constants of single exponential functions fitted to the activation portion of current data for 42 measurements from 32 cells. Currents were elicited by voltage jumps from -100 to -10 mV. Standard solutions. The arithmetic mean of the values is 17.49 while the geometric mean is 10.20.

Chapter 3 Calcium Currents and their Modulation in Dorsal Raphé Neurones

Previously, the modulation by 5-HT of calcium currents in DR neurones has been characterised in some detail (Penington & Kelly, 1990, Penington et al. 1991). An extension of this work is reported here. Experiments described in this chapter were not done at a controlled temperature, unless otherwise stated.

In total 165 presumed DR cells were investigated. These had average input resistances of 1.9 ± 0.1 GΩ (range 0.4 - 10.4), and required currents of -17 ± 2 pA (range 1 - 90) to hold them at a potential of -100 mV.

1. Voltage Dependency of Calcium Currents

Figure 3.1A Illustrates currents elicited by 150 ms depolarising voltage steps from a holding potential of -100 mV (figure 3.1B). This was the standard holding potential used throughout, since at this level all available current is de-inactivated (Penington et al. 1991). Depolarisations to around -50 to -40 mV produced a small current of less than 0.2 nA that inactivated nearly completely by the end of the test pulse. These small 'low threshold' (LVA) currents were found to be extremely inconsistent between cells, but if present to a significant degree, they led to a notch on the IV curve (figure 3.1C). As such they are rather reminiscent of a similar, but larger, current seen in dorsal root ganglion (DRG) cells and termed 'T' current by Fox and his co-workers (1987a & b).

At depolarisations greater than -40 mV, the size of the currents increase dramatically as indicated by the steepness of the IV curve. These currents will be referred to as 'high threshold' (HVA). At around 20°C, using the trizma based internal solution, the maximum

current in most cells was seen with voltage steps to -10 mV. This is some what more negative than in many cell types, and may in part be due to the internal solution, since it is reported that the maximum current occurs at more positive values with a caesium based solution (Penington, personal communication). In addition, the use of Ba^{2+} rather than Ca^{2+} may also lead to more negative values. This is certainly the case with the putative P-type current recorded in cerebellar Purkinje cells (Regan, 1991). Peak current amplitude at this voltage was usually in the 1 - 3 nA range, and averaged 1.56 ± 0.09 nA (n = 42) at 20°C. The degree of inactivation of the high threshold current during a standard 150 ms test depolarisation was extremely variable. Normally, maximal inactivation was seen in currents elicited by voltage steps negative to, or around, -10 mV. Larger depolarisations tended to lead to a decreasing level of inactivation. In this respect, the cell illustrated in figure 3.1 is not typical in that there was less inactivation at -10 than at 0 mV. The variable degree of inactivation seen between cells depolarised to -10 mV is illustrated by currents recorded from two cells shown in figure 3.2.

Increasing depolarisations to levels beyond -10 mV leads to a decrease in current amplitude as the reversal potential is neared. As is discussed by Hille (1984), calcium currents tend to asymptote towards the current axis on an IV plot at potentials considerably less than their theoretical reversal potential (+40/50 compared to +175 mV). This is partly due to the excessive asymmetry of calcium (or barium) ions either side of the plasma membrane, so that the normal Nernst relationship does not hold, and possibly also as a result of the movement of other cations through calcium channels at larger

depolarisations. It was generally found that with the solutions used, the current tended to reverse at around 50 mV. However, it was also noted that applying depolarisations much in excess of this level often led to cell deterioration. This may be partly explained by the fact that the internal solution did not contain a major permeant cation. In experiments done with caesium in the internal solution, workers on other preparations are able to measure large outward currents beyond the reversal potential due to the movement of caesium ions (e.g. Bean, 1989b, Dolphin & Scott, 1990).

The voltage dependence of activation of the calcium currents was assessed by plotting peak current amplitude divided by the maximum peak current amplitude, against test potential, and fitting a modified Boltzman function (e.g. see figure 3.6). As will be shown later in this chapter, and in the next, the activation voltage shifts to the left with both time and temperature. However data obtained within the first five minutes of recording at 20°C gave a value for V_h (see equation 2.9, chapter 2) of -25.7 ± 1.1 mV (n = 16). This is the voltage at which a half maximal current was obtained. The steepness of the IV plots to the left of the maximum current is reflected by a low average value for k, the slope factor, of 5.1 ± 0.3 mV (for example see curve at time 0 in figure 3.6).

2. Effect of Cadmium on Calcium Currents

Cadmium is a relatively selective calcium current blocker, and is often used to define calcium current from leakage. In some tissues though, such as DRG neurones, cadmium blocks high threshold current at lower concentrations than low threshold (Fox et al. 1987a, Gross &

MacDonald, 1987), where 20-50 μM Cd^{2+} blocks HVA current by over 90%, while LVA is only reduced by around 50%. However, this is not always the case,for example 100 μM Cd^{2+} completely abolishes both HVA and LVA in rat hippocampal cells (Yarri et al. 1987).

To confirm that the internal and external solutions used in the current series of experiments did lead to the complete isolation of current through calcium channels, 200 μM cadmium chloride was superfused over DR cells, a dose that was expected to completely abolish the active currents. However, it was found that this dose only blocked the maximum peak amplitude by 82.7 ± 2.1% (n = 4, figure 3.2A). When the concentration was 2 mM, the block was more complete (94.7 ± 1.6%, n = 3, figure 3.2B). This suggests that either the cells were not seeing the total concentration of cadmium added to the perfusate, perhaps as a result of flow artifacts in the dish, or that DR neurones are less cadmium sensitive than DRG or hippocampal neurones.

The current remaining in the presence of 200 μM Cd^{2+} was further investigated. Figure 3.3 illustrates examples of this current elicited by voltage steps from a holding potential of -100 mV, and the IV relationship. The currents had slightly different characteristics than the control currents (figure 3.1). The rate of activation was generally slower, with a higher degree of inactivation at all voltages. Proportionately there was a much larger current at low voltages, than in the control situation (figure 3.3C), illustrated by the Boltzman activation function being shifted leftward (figure 3.4). This was reflected by a V_h value for the activation Boltzman of -32.6 ± 2.3 mV (n = 4), that was significantly more negative than the control ($p = 0.006$). However, there was no clear shift in the voltage

that elicited the maximum current amplitude (compare figures 3.1C and 3.3C). While it would appear that in the cell illustrated in figure 3.3C, the reversal potential was less positive than usually seen in controls (e.g. see figure 3.1C), with the solutions used it is difficult to make accurate measurements and thus conclusions in this regard. Taken together this would suggest that while there was probably some remnant of HVA left with 200 μM Cd^{2+}, LVA was relatively insensitive, as in DRG cells. Figure 3.4 also illustrates the inactivation Boltzman function of the relatively cadmium insensitive current. This was calculated by measuring the peak current amplitude elicited by voltage steps to -10 mV from various holding potentials. The abscissa in this case is holding potential, while the ordinate is the amplitude divided by the maximal current obtained. The V_h for half maximal inactivation of the cell illustrated here was -72.2 mV. Assuming a gross similarity between calcium currents recorded in DR and DRG, then from the observations of Fox and his co-workers (1987a), this would be suggestive of the idea that the cadmium insensitive current does not contain L-type current.

3. Rundown of Calcium Currents

In common with whole-cell recordings of calcium currents in other preparations (Forscher & Oxford, 1985, Carbone & Lux, 1987a, Fox et al. 1987a, Belles et al. 1988, Hagiwara et al. 1988, Ozawa et al. 1989, Bargas et al. 1991, De Waard et al. 1991), the amplitudes of HVA currents in DR were observed to decrease over time, or 'rundown'. Figure 3.5 illustrates the decrease in the peak amplitude of currents with time at 20°C. Rundown was assessed by performing voltage steps

from -100 mV to -10 mV for 150 ms at a frequency of 0.05 Hz. This was interrupted every 10 minutes to study the current-voltage relationship. At 20°C, cells remained relatively stable for periods of 30 - 60 minutes. During a period of 30 minutes, the average amount of rundown was 21.0 ± 5.8 % of the maximum, at a rate of 1.1 ± 0.6 %/min (n=6). Several cells initially showed a small amount of 'runup' over a period of up to 5 - 10 minutes which amounted to 0.5 ± 0.5 % at a rate of 0.06 ± 0.05 %/min (n = 6). Although the peak amplitude decreased considerably during the recording period, the kinetics did not alter significantly (see current inserts in figure 3.5). In this particular example, the activation time constant, τ_a, was 2.6 and 2.0 ms at the two times indicated, while the inactivation time constant, τ_i, was 206 and 216 ms. On the other hand, as has been observed in cardiac tissue (Belles et al. 1988), the voltage dependence of activation did change with time. Figure 3.6 illustrates modified Boltzman activation curves, whose data acquisition was at 0, 10, 20, and 30 minutes after the commencement of recording, for the cell shown in figure 3.5. The V_h was progressively shifted to the left, in this example from -22 to -26 mV. On average the V_h was shifted 0.26 ± 0.07 mV/min (n = 6), in the hyperpolarising direction, over the first 30 minutes of recording. Since the voltage protocol was constant throughout, this shift in voltage sensitivity will have accentuated the apparent rundown, because a voltage step to -10 mV after a period of time will no longer elicit a maximum current.

4. Transmitter Modulation of Calcium Currents

As has been previously shown (Penington & Kelly, 1990, Penington

et al. 1991), a supra-maximal dose of 5-HT (10 μM), produces a 57.1 ± 4.4 % decrease in the peak current amplitude (n = 7, figure 3.7A). However it is clear that the action of 5-HT is not simply to reduce current amplitude. While the average activation time constant, τ_a, of controls is 2.30 ± 0.18 ms at 20°C (n = 41), the average τ_a in the presence of 5-HT at room temperature (slightly above 20°C) was 28.4 ± 11.5 ms (n = 7). Comparing 5-HT τ_a with control τ_a from the same cells showed that 5-HT increased τ_a 17.8 ± 9.9 fold (n = 7). Possibly as a result of the slowing of the rate of activation, the proportionate reduction of the 'steady state' current at the end of the test pulse, was less than that of the peak, at 42.1 ± 9.7 %.

Penington and Kelly (1990) have shown that the action of 5-HT is probably mediated via 5-HT_{1A} receptors in that it is mimicked by the 5-HT_{1A} receptor agonist, 8-OH-DPAT, and blocked by the putative 5-HT_{1A} antagonist NAN 190 (Glennon et al. 1988a & b). In my hands, a supra-maximal dose of 8-OH-DPAT (50 μM) caused a 38.9 ± 4.1 % reduction in peak current, and slowed τ_a 4.77 ± 1.44 fold (n = 17, figure 3.7B). In addition, another 5-HT_{1A} agonist, ipsapirone, at 10 μM caused a 41.4 ± 2.3 % reduction in peak current, and slowed τ_a 2.51 ± 0.72 fold (n = 4, figure 3.7C). Although there is no significant difference between 5-HT, 8-OH-DPAT, and ipsapirone in their ability to decrease peak current, 8-OH-DPAT slows τ_a to a lesser (but non-significant, p = 0.07) degree, while ipsapirone's slowing ability is significantly less (p = 0.008). Certainly the doses of 5-HT and 8-OH-DPAT were maximal (see Penington & Kelly, 1990), but it is possible that 10 μM ipsapirone is not so. This could be the reason for the smaller effect seen with ipsapirone. However another possibility is that while 5-HT acts on 5-HT_{1A} receptors as a full agonist, ipsapirone, and possibly

also 8-OH-DPAT, are actually partial agonists. Lower efficacy of 8-OH-DPAT compared to 5-HT together with low receptor reserves, has certainly been postulated to explain why it appears to act as only a partial agonist at 5-HT_{1A} receptors in hippocampus (Andrade & Nicoll, 1987a), and this may also be the case for ipsapirone (Andrade & Nicoll, 1987b).

As previously reported (Penington & Kelly, 1990) not all cells exposed to agonists responded. 5 out of a total of 45 (11.1%) showed no response at all, and were not included in the figures quoted above. This finding may be due to the lack of expression of 5-HT_{1A} receptors occurring in all cells, the receptors being damaged or lost by the isolation or recording procedures, or the fact that not all cells tested were serotonergic neurones. This last possibility is probably most likely, in that only 90% of the type of cells selected in this study contain 5-HT immunoreactivity (Lawrence et al. 1989).

10 μM phenylephrine has previously been shown to have no effect on the calcium currents recorded from DR cells (Penington & Kelly, 1990). In addition in this study 10 μM NA also had no effect (n = 4). In 9 out of 10 cells 10 μM DA produced no response. However, in one cell DA caused a reversible increase in current amplitude and an acceleration of τ_a (figure 3.8). This cell was unusual in that in the control situation it had a very slow activation rate, rather similar in appearance to that seen with GTPγS treatment (see chapter 5). However in the same cell 10 μM 5-HT caused a reduction in current amplitude, though rather small. This cell was interesting in that the current, and the action of DA, was rather similar to that seen in bovine chromaffin cells (Artalejo et al. 1990, 1991), but since it was only seen in one cell out of ten, and this was not the main line of

investigation, it was not studied further.

The action of 5-HT has been shown to be transduced by a pertussis toxin sensitive G-protein, but not involve protein kinase A (AK), PKC, or cGMP-dependent kinase (Penington et al. 1991). One drug that has not previously been tested is the adenylate cyclase stimulator, forskolin. This is of especial interest in that recently it has been shown that in the presence of internal GTPγS, forskolin is able to enhance calcium currents in DRG cells (Dolphin, 1991a). Therefore forskolin was applied to cells in control conditions with and without 8-OH-DPAT, and to cells containing GTPγS. On some cells (3/5) 10 μM forskolin perfused into the dish caused a prolonged and extensive 'runup' of the peak current amplitude (figure 3.9), though this was not universal. When clear significant runup did not occur, there was an impression of reduced rundown, though this was not measured. Whether runup occurred or not, the action of 8-OH-DPAT was not significantly different in any respect from control 8-OH-DPAT responses, with a 40.1 ± 7.9 % reduction in peak current, and τ_a slowed 3.39 ± 2.12 fold (n = 4). When GTPγS was present in the cell, no significant effect was seen (n = 4), though again there was an impression of decreased rundown (compare figure 3.10 with 3.5). As explained in chapter 2, forskolin was made up with ethanol, rather than DMSO which is normally recommended for stimulation of adenylate cyclase (Laurenza et al. 1989). It is therefore possible that the lack of effect, particularly with GTPγS, may be due to this.

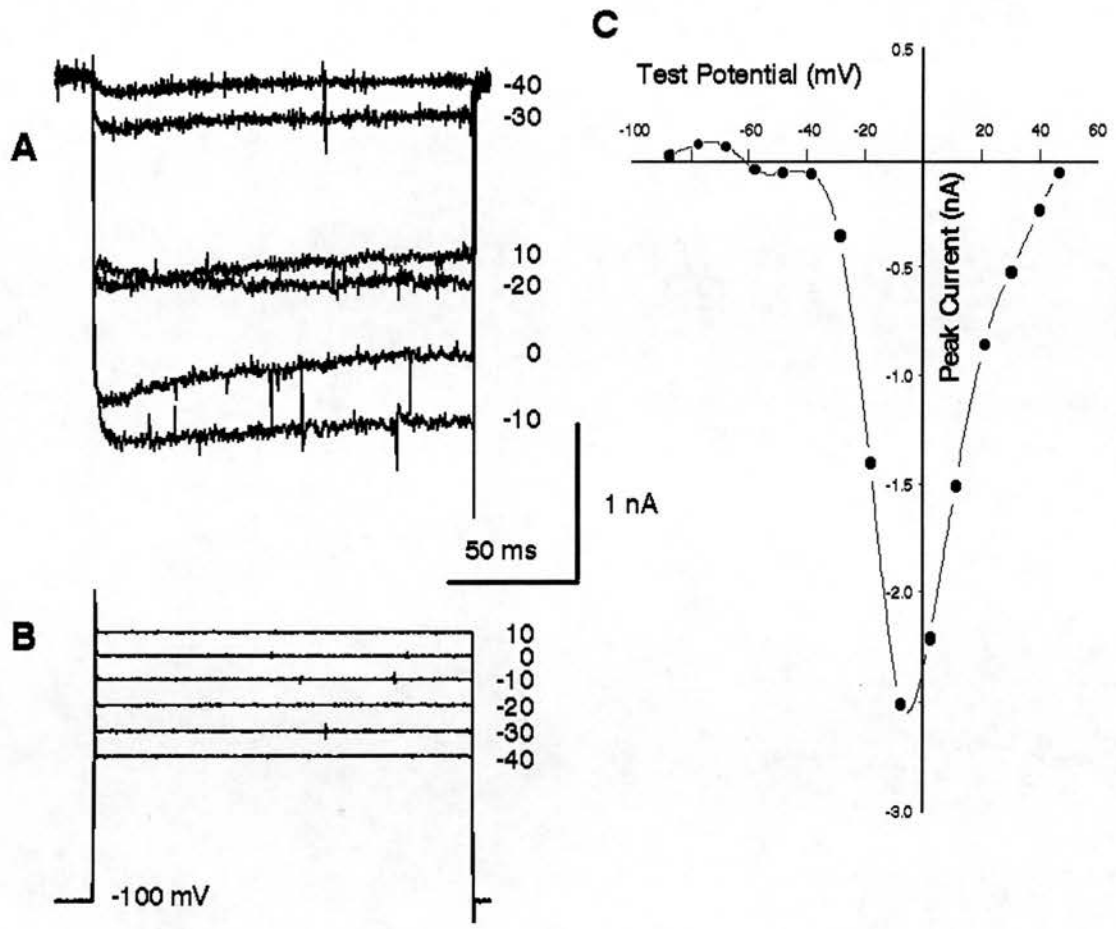

Figure 3.1: Current/voltage relationship of calcium currents recorded from DR neurones at approximately 20°C. Currents (A) were elicited by voltage jumps from -100 mV to a series of depolarised levels (B) for 150 ms. The nominal test potentials are annotated alongside the voltage and appropriate current traces. The relationship between the test potentials and peak current amplitude is shown in C. The curve was fitted using a cubic spline routine. Examples of currents are leak and capacity subtracted, but the raw data is plotted in C. Standard internal and external solutions. Cell held at -100 mV with approximately 30 pA. Cell 17088904.

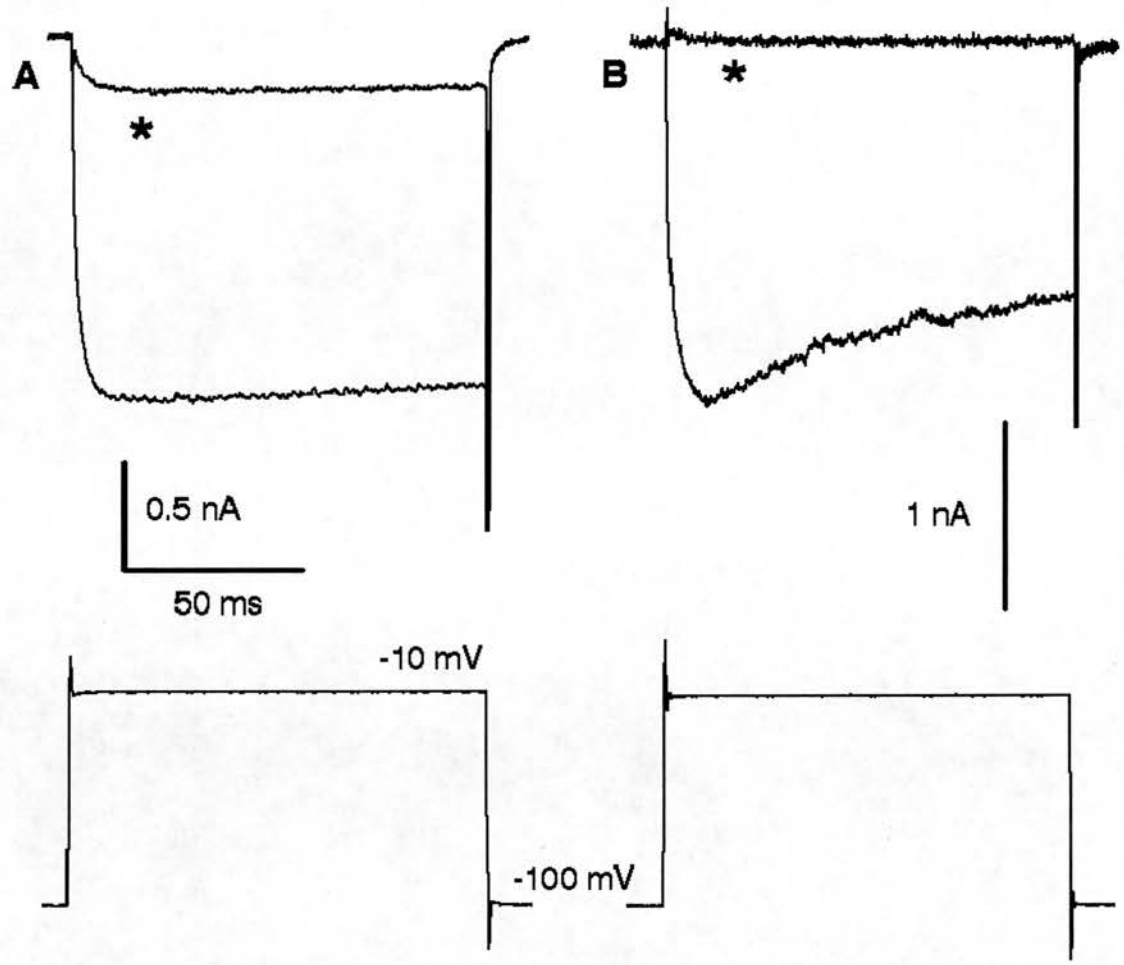

Figure 3.2: The effect of cadmium on high threshold calcium currents. Currents were elicited by voltage steps to -10 mV from holding potentials of -100 mV. 200 μM cadmium led to a large (83%) but incomplete reduction in high threshold current (A, *), while 2 mM cadmium led to a complete abolition of calcium current (B, *). Cadmium chloride was added to the standard external solution and perfused into the recording dish. Standard pipette solution. Note that two different cells are illustrated in this figure, and there is a current calibration bar for each. Currents leak and capacity subtracted. Cells 06029201 (A), 20029201 (B).

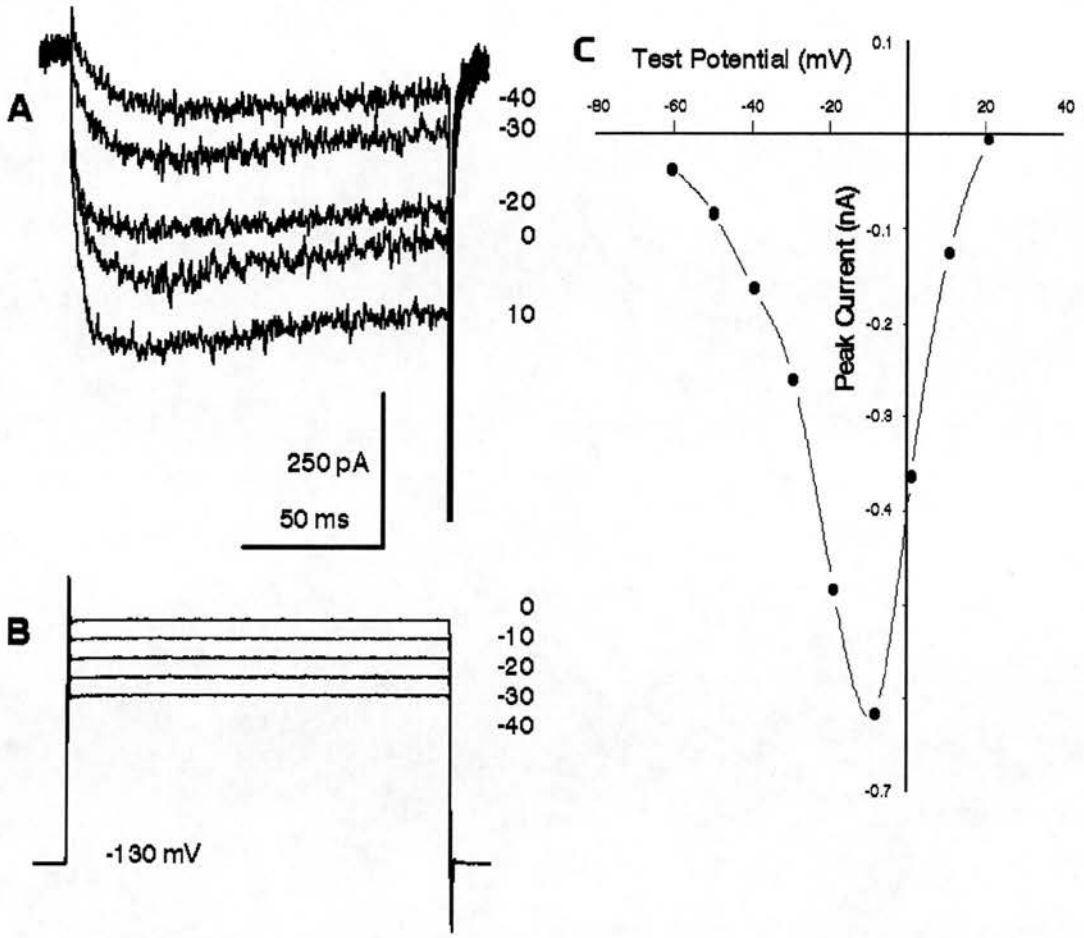

Figure 3.3: Current voltage relationship of calcium currents recorded in the presence of 200 μM cadmium. Currents (A) were elicited by voltage jumps from -130 mV to a series of depolarised levels (B) for 150 ms. The nominal test potentials are annotated alongside the voltage and appropriate current traces. The relationship between the test potentials and peak current amplitude is shown (C), fitted with a cubic spline. All data is leak and capacity subtracted. The external solution contained 200 μM cadmium chloride throughout. Standard pipette solution. Cell 06029201.

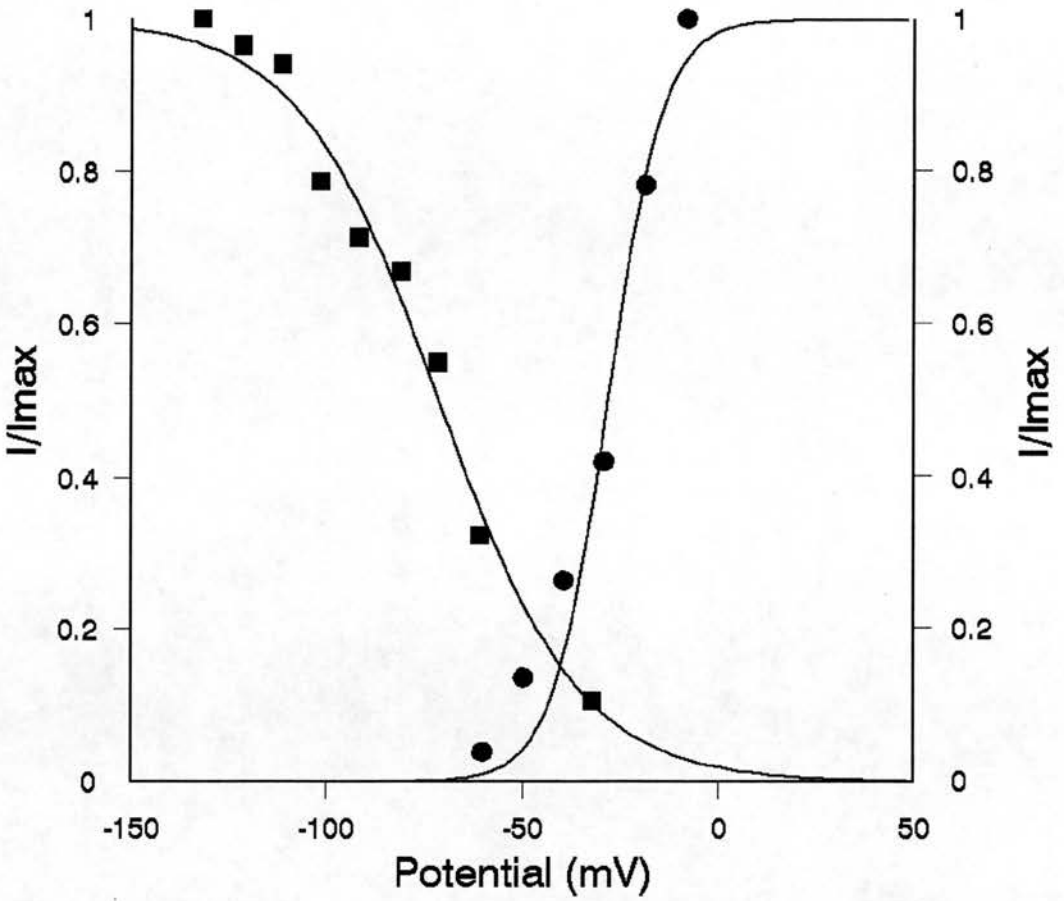

Figure 3.4: **Voltage dependence of activation and inactivation of calcium current in the presence of 200 μM cadmium.** Circles: Peak current amplitude, normalised to that obtained by a voltage jump from -130 mV to -10 mV, plotted against various levels of test potential (data as in figure 3.3). Squares: Peak current amplitude, normalised to that obtained by the same voltage jump as above, plotted against holding potential. Best fit modified Boltzman functions are also plotted for each set of data. These have V_h's of -28.1 and -71.2 mV, and k's of 6.9 and 18.0 mV respectively. Boltzman functions in the absence of cadmium are shown in figure 3.6. Same conditions as in figure 3.3. Cell 06029201.

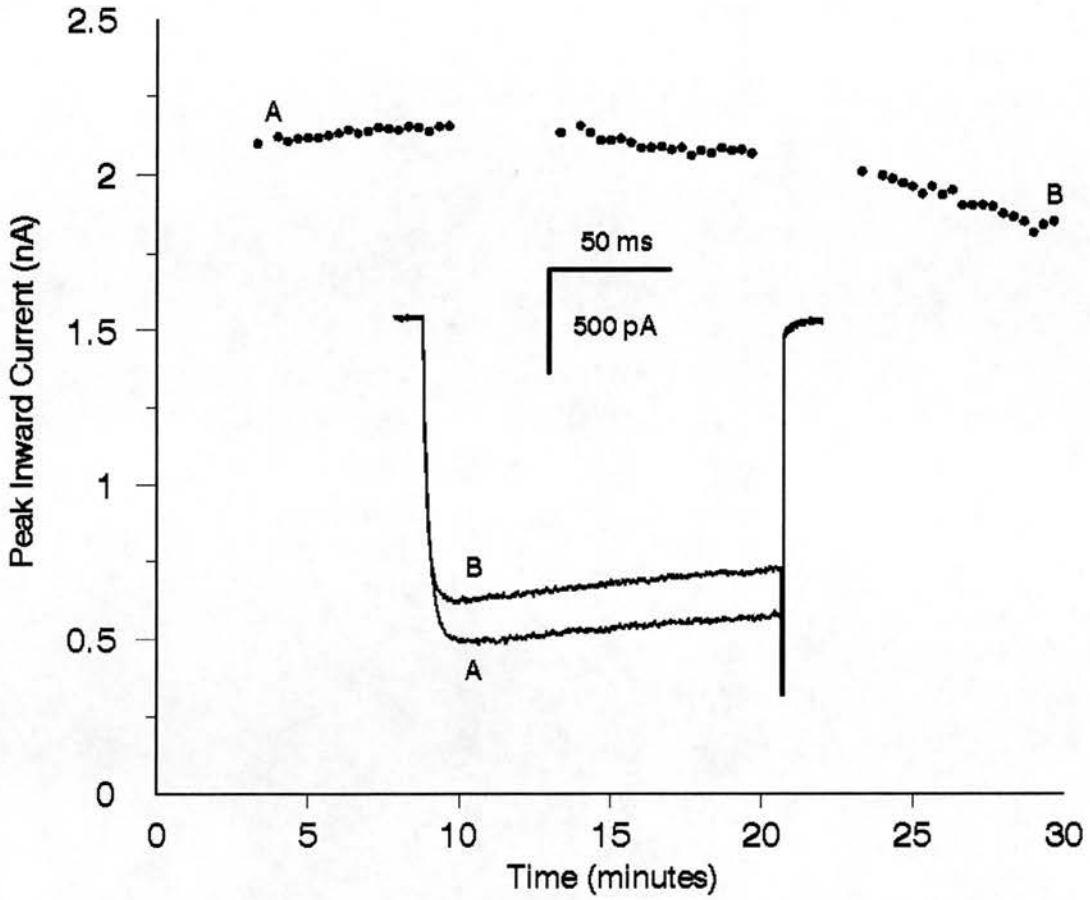

Figure 3.5: **Rundown of high threshold calcium current at 20°C.** Currents were elicited by voltage steps from -100 to -10 mV every 20 seconds. Peak current is plotted against time. Time 0 is 5 minutes after whole-cell mode was achieved and the bath solution was switched to the standard external solution. Standard pipette solution. The breaks in the data beginning at times 0, 10, 20 and 30 minutes, are when the current voltage relationship was determined, and is illustrated in figure 3.6. The insert illustrates currents recorded at the beginning (A) and end (B) of the experiment. All data leak and capacity subtracted. Cell 22019101.

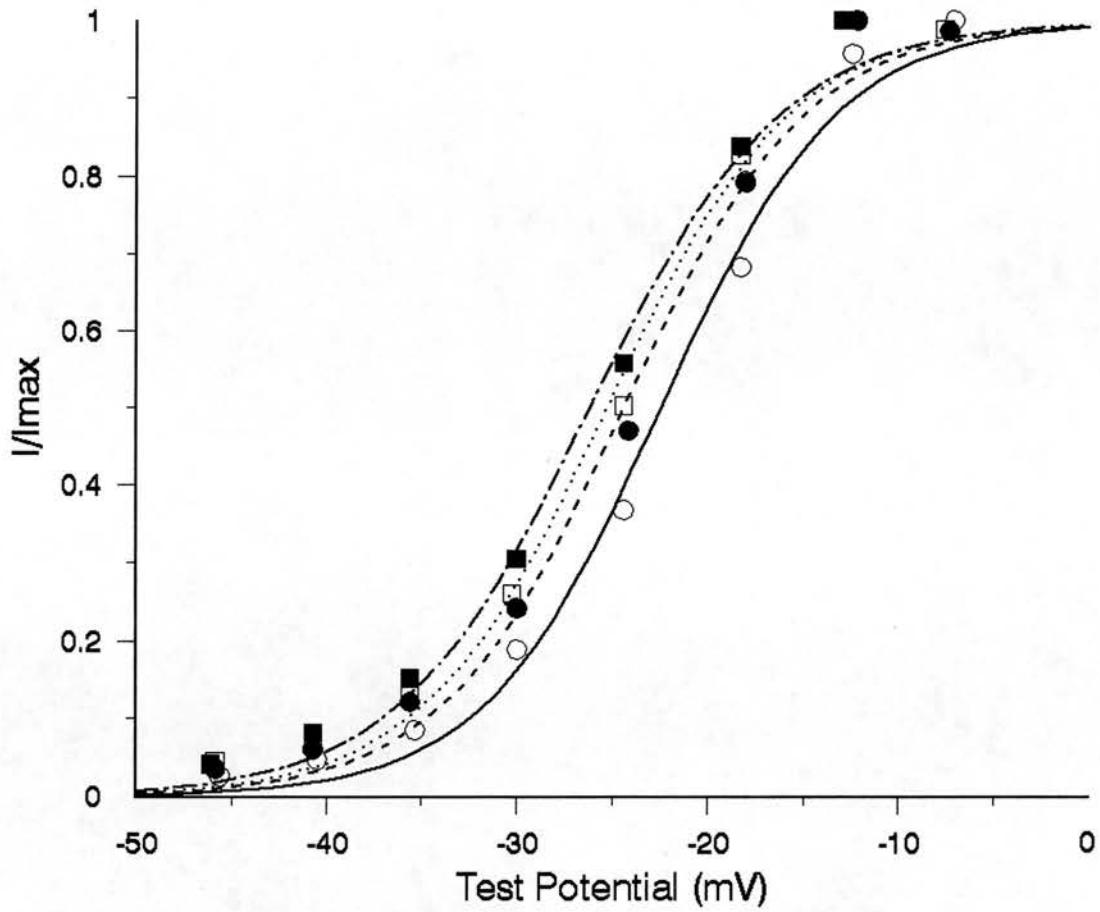

Figure 3.6: Voltage dependence of activation with time. Current-voltage data was obtained, and the peak I/I_{max} plotted against the test potential, at times 0 (open circles), 10 (filled circles), 20 (open squares), and 30 minutes (filled squares) after the commencement of recording. Data is fitted in each case by modified Boltzman curves whose V_h and k are -22.43 and 4.59 (solid line), -24.37 and 4.73 (dashed line), -25.27 and 4.76 (dotted line), and -26.15 mV and 4.97 mV (dots and dashes) for times 0, 10, 20 and 30 minutes respectively. Same cell and conditions as figure 3.5.

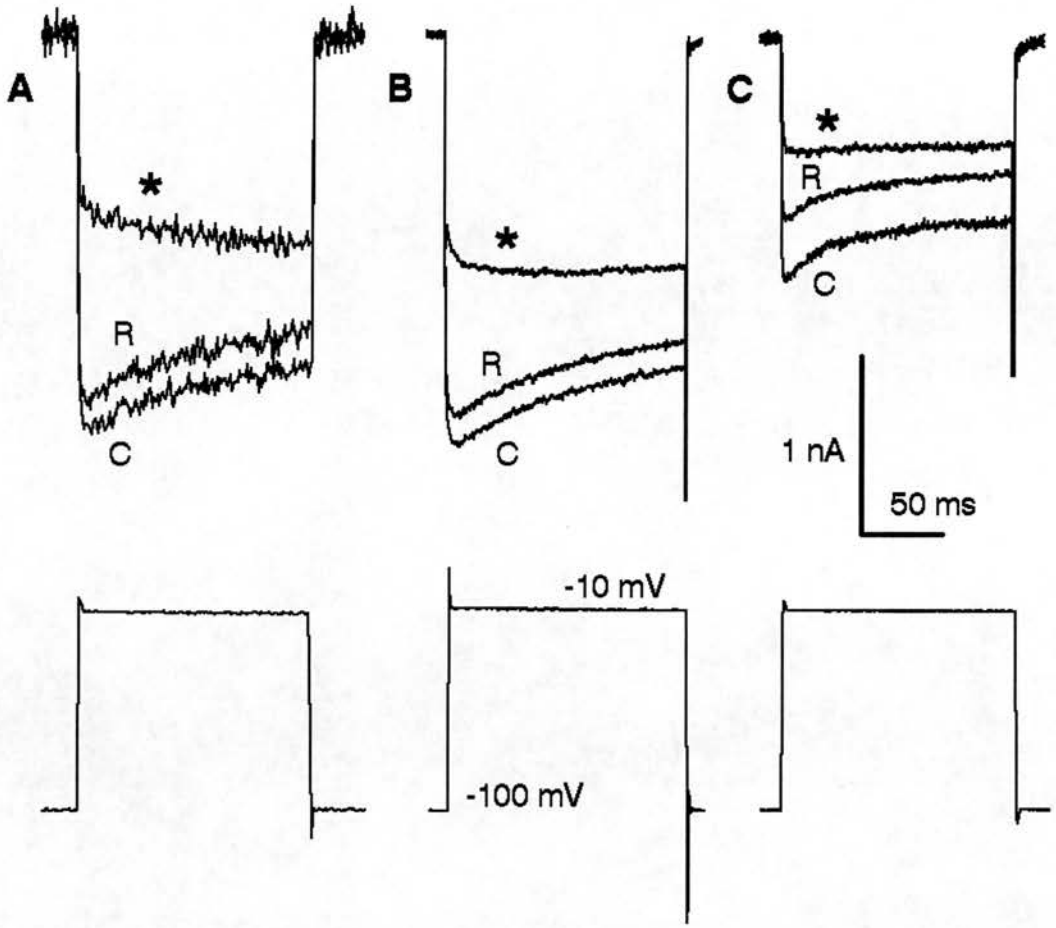

Figure 3.7: Effect of (A) 10 μM 5-HT, (B) 50 μM 8-OH-DPAT, and (C) 10 μM Ipsapirone on high threshold calcium currents. In all three cells, currents were elicited by voltage steps to -10 mV from holding potentials of -100 mV (illustrated for each cell below the current traces). Currents shown are control (C), in the presence of the drug (*), and on recovery (R). Currents are leak and capacity subtracted. Drugs applied from broken patch pipette, with tip diameters of 2 - 5 μm, positioned around 50 μm from the cell. Standard internal and external solutions. Cells 21088902 (A), 20099101 (B), 08128901 (C).

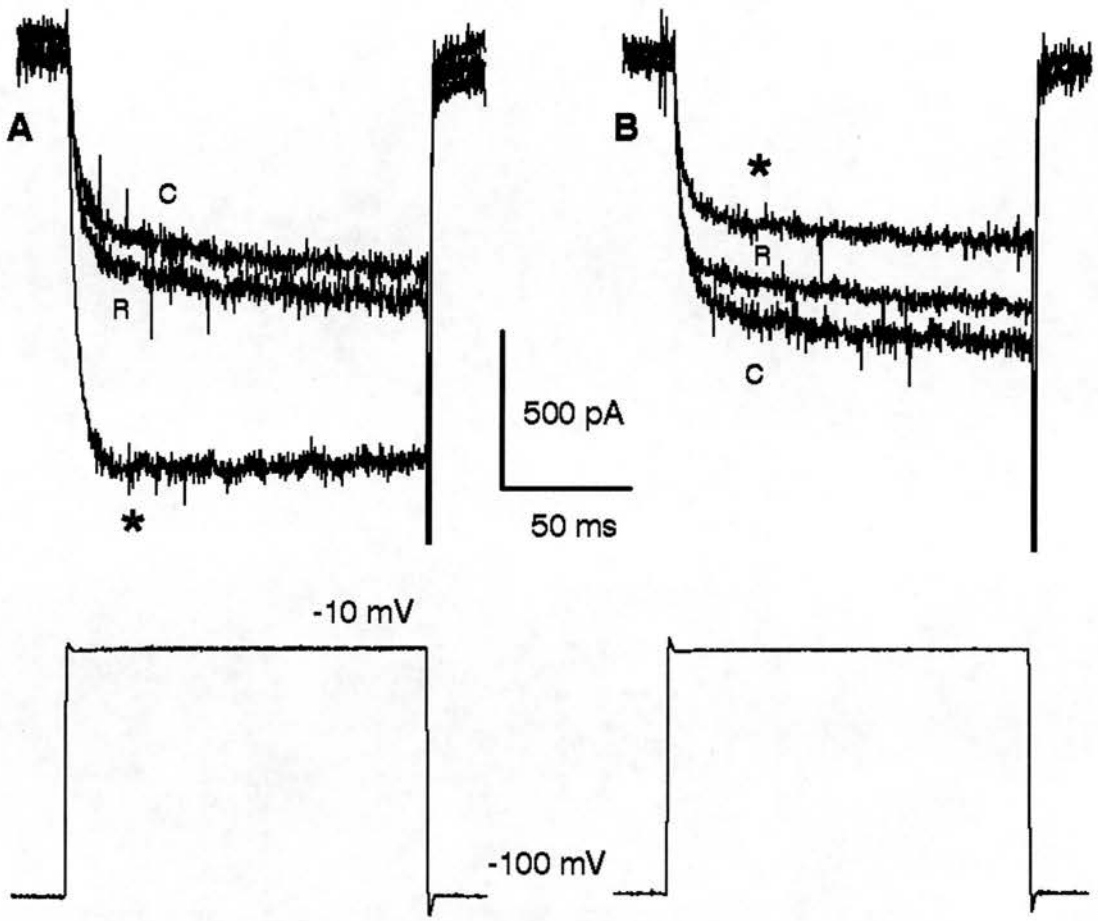

Figure 3.8: **Atypical dopamine effect on calcium currents in dorsal raphé neurone.** High threshold currents were elicited by voltage steps from -100 mV to -10 mV for 150 ms. In this atypical cell (see text), 10 μM dopamine (A) led to a large reversible increase in current amplitude, and acceleration of activation (*). 10 μM 5-HT (B) produced a small reduction of current amplitude, and a minimal effect on the activation kinetics (*). Current traces marked C and R are the control and recovery traces in each instance. Drugs were applied via a broken patch pipette, as in figure 3.7. Standard internal and external solutions. Currents leak and capacity subtracted. Cell 04108901.

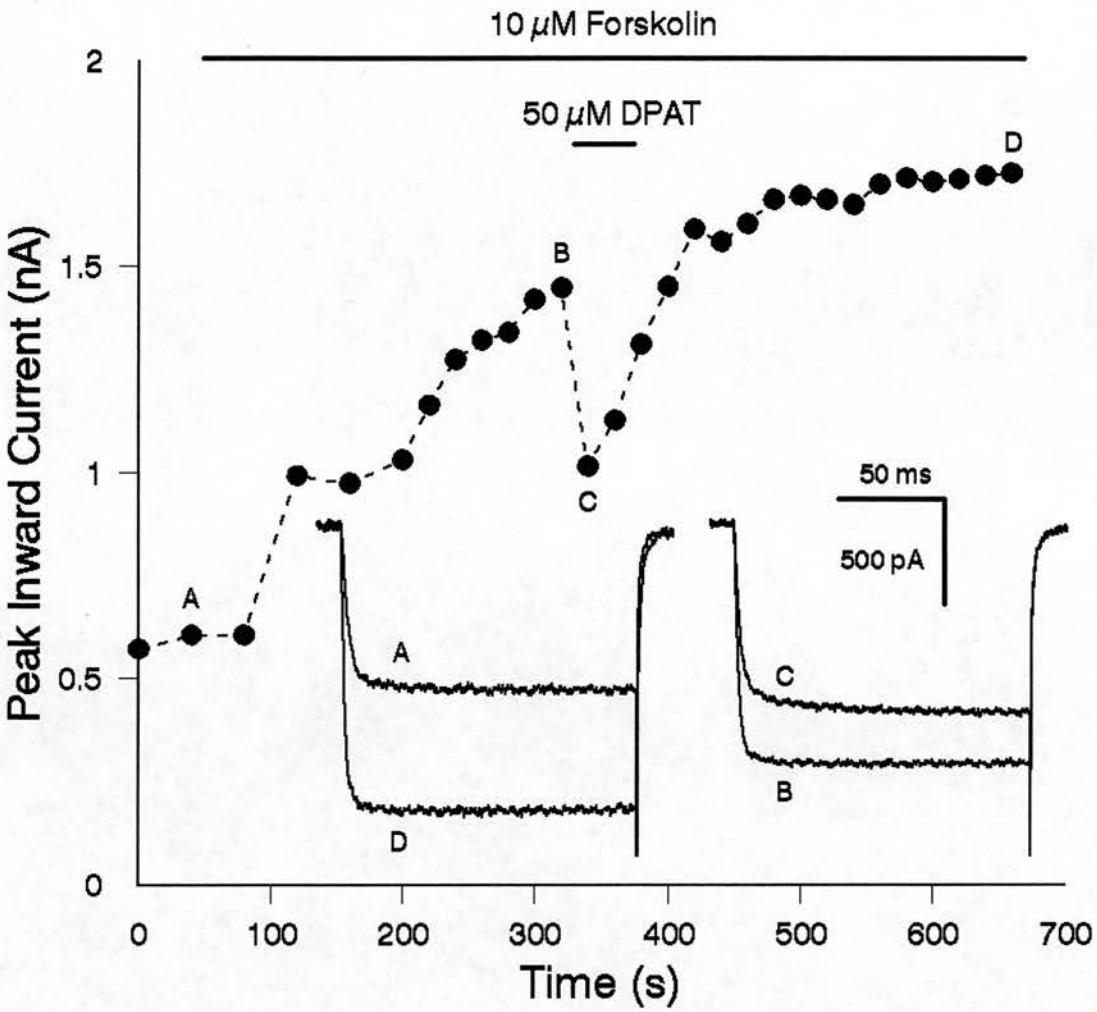

Figure 3.9: The effect of forskolin on peak HVA calcium current. Currents elicited by voltage steps from -100 to -10 mV. Peak current amplitude is plotted against time. 10 μM forskolin in standard external solution was perfused into the bath during the time indicated by the upper horizontal bar. This led to pronounced 'runup', but with little change in the kinetics of the currents, as illustrated by the current inserts A and D, recorded at the times indicated on the graph. 50 μM 8-OH-DPAT applied using a broken patch pipette led to a normal decrease in amplitude and slowing of activation, see inserts B and C. Standard pipette solution. Forskolin made up in ethanol and diluted with external solution. Currents leak subtracted. Cell 26029202.

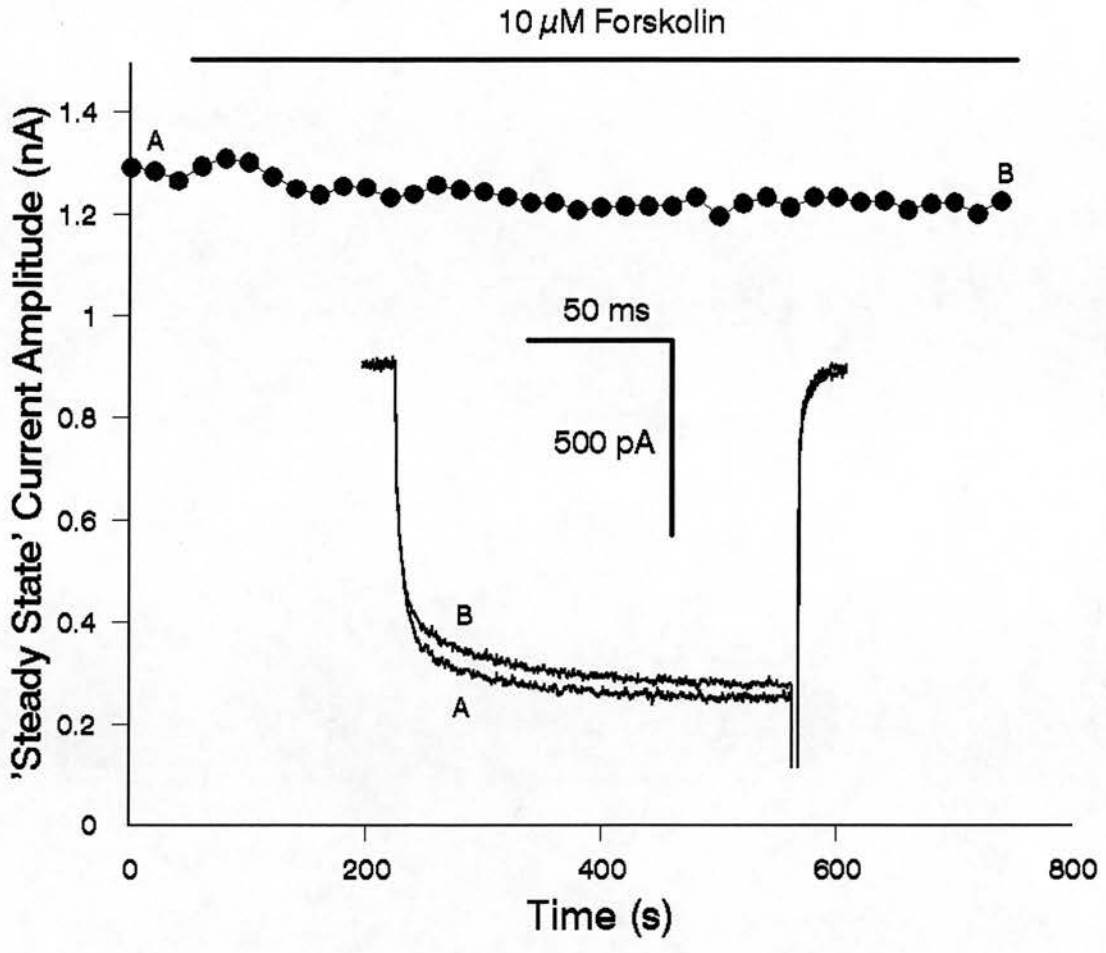

Figure 3.10: **Effect of forskolin on peak HVA calcium currents in the presence of GTPγS.** Currents were elicited by voltage steps from -100 mV to -10 mV. 'Steady state' current amplitude (i.e. at end of the 150 ms voltage step) is plotted against time. 10 μM forskolin in standard external solution was perfused into the bath during the time indicated by the horizontal bar. Examples of the current prior to application (A), and after over 10 minutes exposure to forskolin (B), are shown. Pipette solution contained 200 μM GTPγS. All data is leak and capacity subtracted. Cell 14119101.

Chapter 4 Effect of Temperature on Calcium Currents

1. Effect of Temperature on Current Amplitude

Compared to 20°C, cells were much less stable at 25°C, as has been noted by others (Schroeder et al. 1990), and recordings could only be made for 15-20 minutes. The rate of rundown and the shift in V_h were also greater being 1.58 +/- 0.72 %/min and 0.55 +/- 0.22 mV/min (n=3) respectively. As a result, all baseline measurements were made at 20°C, and short duration temperature jumps made to 15, 25 and 30°C. There are clearly inherent problems in assessing the effect of temperature on current amplitude in the presence of rundown. In an attempt to minimise these problems, cells were only used where the amplitude of the current on recovery from a temperature 'jump' was within 10% of the control value, see, for example, figure 4.1A.

The dramatic effect of temperature on high-threshold currents in DR neurones is illustrated in figures 4.1. Increases in temperature of 5°C caused a large and reversible increase in current amplitude. Analysis of the peak amplitude of currents elicited by voltage steps from -100 mV to -10 mV shows that the Arrhenius relationship between 15 and 25°C is linear (figure 4.2). Between these temperatures there was a Q_{10} of 2.47 (CI = 1.06 - 5.08, n = 42,32). This value is similar to that found in mouse neuroblastoma (3.0, 20-30°C, Narahashi et al. 1987), and cat (2.6, 10-20°C, Taylor, 1988), and chick DRG cells (2.6, 20-30°C, Nobile et al. 1990). No transition temperature was seen at around 20°C as observed in neuroblastoma cells (Narahashi et al. 1987). The temperature dependence is voltage sensitive, in that a change in the holding potential to -50 mV (figure 4.3), changes the Q_{10} of the peak amplitude to a significantly ($p< 0.001$) smaller value of 1.69 (CI = 1.07 - 2.66, n = 10,8). Calcium currents evoked

from the more depolarised level were smaller, and the amount of inactivation that occurred during the test pulse was less than when elicited from -100 mV (compare figures 4.1 and 4.3). This agrees with the disappearance of a presumably voltage dependent inactivating component, that could correspond to N-type current. When the holding potential is -100 mV, the Q_{10} for the 'steady state' amplitude at the end of the 150 ms test pulse (which again would classically be interpreted as having less N-type current involvement) is also significantly lower (2.08, CI = 1.00 - 4.30, n = 38,30, $p < 0.01$) than that for the peak (figure 4.2), but not significantly different from the peak value when the holding potential is -50. These findings may reflect the probable heterogeneous nature of HVA calcium current in these cells (Penington & Kelly, 1990).

Increasing the temperature from 20°C to 25°C was also observed to cause a shift in the IV plot of both peak and 'steady state' currents (figure 4.4), as observed in other neuronal tissue (Nobile et al. 1990), but not seen in ventricular myocytes (Cavalié et al. 1985). There was an average shift to the left of the V_h by 7.69 +/- 1.96 mV, when the temperature was increased from 20 to 25°C, from -26.80 ± 1.87 to -34.48 ± 1.27 mV (n = 6). Since these V_h values were calculated within 5-6 minutes of each other, it seems unlikely that an effect as large as this can be accounted for entirely by the leftward shift seen with time (see chapter 3). However, the shift was not reversible, since on return to 20°C the V_h was 35.55 ± 1.90 mV. However this does help to rule out the possibility that the initial shift was simply due to time since cooling took longer than heating. When the temperature was decreased from 20 to 15°C, there was a small leftward shift of 2.67 ± 1.42 mV from -23.46 ± 0.94 to -26.13 ± 1.44 mV (n = 4),

followed by a much larger shift on return to 20°C (V_h = -33.21 ± 2.09 mV). This suggests that the process of heating accelerates the leftward shift with time. The accompanying change in the IV plot may, at least in part, explain the apparent non-linearity of the Arrhenius plots for both peak and steady state amplitudes between 25 and 30°C (figure 4.2).

The current/voltage plots of both peak and 'steady state' currents at 20 and 25°C appeared remarkably similar in their gross appearance, baring the shift in the maximum to the left, with no change in the apparent reversal potential (figure 4.4). The increase in current amplitude with temperature, would seem to be greater with test potentials that are more negative than that which elicits the maximal current. However, this can be explained by the shift in the voltage dependency. While there is occasionally a small 'notch' on the calcium current IV plot due to LVA current (figure 3.1), this is not always the case (figure 4.4), due to the LVA current being small and inconsistent in DR cells. In addition, the shift in the voltage dependence of the calcium currents with increases in temperature made it impossible to identify changes in the T-type current using voltage criteria alone. As a result the temperature dependence of the low-threshold component has not been determined.

2. Effect of Temperature on Current Activation Rate

The most striking effect of temperature on DR neurones is the dramatic effect on the activation kinetics, as can be clearly seen in figure 4.1. In this particular cell, activation was some 4 fold faster at 25°C, compared to 20°C. However, to obtain clear

measurements of the effect of temperature, it was necessary to first of all examine the actual kinetics of activation. This was by means of attempting to fit single and double exponential, and Hodgkin and Huxley, functions to activation current data. This will be described prior to the actual temperature dependency of the activation rate.

Current activation data produced by depolarising voltage steps, from the instant the voltage stabilised to the peak current, was fitted by various functions (see equations 2.6, 2.7, and 2.8 in chapter 2). Figure 4.5 illustrates raw data points from the activation portion of current recorded at 15 and 20°C, from a typical cell. The data is shown overlaid with single and double exponentials. The single functions had activation time constants (τ_a) of 7.28 and 2.87 ms at 15 and 20°C, the double functions fast time constants ($\tau_{a,f}$) of 2.61 and 5.10, and slow time constants ($\tau_{a,s}$) of 5.59 and 12.05 ms. At 15°C the double exponential fitted significantly better ($p<0.001$) than the single, while at 20°C, the reverse was true. Table 4.1 details how the different fits compared for all cells studied. It can be seen that the majority of data (57/83) was best fitted by a single function. This apparent contradiction to the finding of others (Fenwick et al. 1982, Taylor, 1988), that calcium current activation kinetics are best fitted by the addition of fast and slow components, may be due to the relatively slow settling time of the voltage-clamp (0.5-1 ms) used in the present study, and a failure to resolve the fast component (with a time constant in the order of 0.1-0.2 ms at 20°C in cat DRG, Taylor, 1988). This would be supported by the fact that there was a preponderance of data best fitted by double functions at lower temperatures where the fast component presumably had been slowed enough to be resolved.

The same activation portion of current data as in figure 4.5 is shown in figure 4.6 fitted with Hodgkin and Huxley model equations m^1 to m^3. These had τ_a's of 7.28, 5.98, and 5.65 ms at 15°C, and 2.87, 2.51, and 2.41 ms at 20°C. In both cases, m^1 was the best fit ($p< 0.001$). Table 4.1 shows that this was almost universally the case with 67 out of 83 portions of activation data best fitted by m^1 functions. Again this is not entirely in line with the results of other workers, in that m^2 functions have been reported to fit data better than m^1 or m^3 (Kostyuk et al. 1977, Sala, 1991). Again this may be due to the fact that the voltage clamp employed by Sala was fast enough to detect a short (< 0.5 ms) delay in the current activation, making the data clearly sigmoidal in shape. The higher the value of x in an m^x function, the more 'sigmoidal' it is, with a longer 'delay' at the start. A delay was never detected in DR cells, but the duration of delay may well have been less than the settling time of the clamp. This may well explain why m^1 functions were usually the best fit Hodgkin and Huxley equation, and also why for most data (67/83), the best exponential function was better than the best Hodgkin & Huxley fit. It should also be noted that τ_a's derived from single exponentials and m^1 functions for the same piece of data are identical.

Using a voltage protocol of a step from a holding potential of -100 mV to -10 mV, at 20°C τ_a, derived from single exponential functions, averaged 2.30 ± 0.18 ms (n = 41). Increasing the temperature to 25°C caused an approximate 4-fold decrease in this time, with a 3-fold increase on cooling to 15°C. An Arrhenius plot for this parameter (figure 4.7B) was linear between 15 and 25°C with a Q_{10} much higher than that for current amplitude of 10.20 (CI = 1.19

- 87.56, n = 42,32). Others have reported Q_{10}'s for activation in vertebrate neuronal tissues higher than for other of the calcium current parameters (Taylor, 1988, Nobile et al. 1990), however, none have reported values as high as that seen in DR cells.

τ_a showed marked dependency on the voltage of the test pulse, decreasing in the region of 50-fold with increasing depolarisations from -45 to 40 mV at all temperatures studied (figure 4.8). On the other hand the holding potential seems to have little effect on τ_a. With a holding potential of -50 mV, a test pulse to -10 mV at 20°C elicited currents with a τ_a of 2.32 ± 0.25 ms (n = 9) which was not significantly different to that when the holding potential was -100 mV. This was slightly surprising since DHP sensitive current has been reported as activating faster than ω-CgTx sensitive current (Kasai & Neher, 1992). The Arrhenius plots of τ_a with holding potentials of -50 mV and -100 mV are similar (figure 4.9), and the Q_{10} value for τ_a with a holding potential of -50 mV (12.65, CI = 0.85 - 187.7, n = 12,8) was not significantly different to that when the holding potential was -100 mV, unlike the Q_{10} values for peak amplitude.

3. Effect of Temperature on Current Inactivation

In addition to the effects on current activation rate, figure 4.1 clearly shows that increases in temperature produce profound changes in inactivation kinetics. At 15 and 20°C there is very little inactivation of the current with time. By the end of the 150 ms test pulse the current only fell by 2.1 and 4.8% of the peak value in this example. However these values increased to 12.3 and 20.8% at 25 and 30°C respectively.

Exponential curves were fitted to data from at least the length of τ_a beyond the peak, to the end of the test pulse. When this was done, the situation was found to be rather complex. At 15°C, current inactivation was often too slow to be fitted accurately to data from a 150 ms test pulse. However, when this could be done (6 out of 16 cells), inactivation data was well fitted in every case by a single exponential function, as previously seen by some (Thompson & Wong, 1991), with a time constant (τ_i) of 174.0 ± 35.4 ms (n = 6). This inactivating component made up 26.38 ± 3.32% of the total peak current. At 20°C, it was more often possible to fit exponential functions (33 out of 41 cells), but again all were best fitted by single functions. In this case τ_i averaged 140.1 ± 21.7 ms (n = 33), and the inactivating portion comprised 19.95 ± 1.62% of the total peak current. Current inactivation in all cells at 25 and 30°C was fast enough to fit exponentials. A proportion of cells (9/18) at 25 and all those at 30°C (5) were fitted significantly better ($p < 0.001$) by double rather than single exponential functions, as seen in DRG (Tatebayashi & Ogata, 1992), SCG (Ikeda, 1991), cerebellar (Slesinger & Lansman, 1991a), and hippocampal cells (Kay, 1991). At 25°C, the data that was fitted by single exponentials had an average τ_i of 93.68 ± 7.77 ms (n = 9), with the inactivating component making up 21.01 ± 3.27% of the total current. For cells where inactivation was best described by double exponentials, these had $\tau_{i,s}$'s of 107.9 ± 17.49 (n = 9) and 82.13 ± 14.67 (n = 5) at 25 and 30°C, comprising 24.38 ± 2.51 and 22.65 ± 1.39% of total current. Average $\tau_{i,f}$'s were 11.63 ± 2.59 and 9.92 ± 2.71 ms making up 7.03 ± 2.35 and 15.75 ± 4.23%. The difference between inactivation at 20 and 30°C is illustrated in figure 4.10. From the raw data (figure 4.10A) it is clear that there

is a qualitative difference in the inactivation. This is much more evident when the data is normalised to the peak current amplitude at each temperature (figure 4.10B). The proportion of current made up of the single inactivating component is not significantly different at any temperature, and not significantly different from the slow inactivating component at higher temperatures. However, the percentage of total current that represents the fast inactivating component increases significantly ($p = 0.006$) between 25 and 30°C. This would be consistent with a hypothesis that the fast inactivating component is only seen as the temperature is increased. This conclusion is similar to that of Nobile et al. (1990), who demonstrated both a fast and a slow component of inactivation at 37°C in chick DRG. In these cells there was also around an order of magnitude difference between the two time constants. The authors suggested that heating led to the uncovering of a novel fast component.

Clearly a comparison of inactivation time constants at different temperatures is difficult. In those cells where inactivation was fitted by single exponential functions at all temperatures, the time constant was found to have a Q_{10} of 3.53 (CI = 0.92 - 13.50, n = 13,13). Taking the average values for τ_i from all cells gives a lower Q_{10} ranging from 1.54 to 2.24. The Q_{10} for $\tau_{i,s}$ from averaged data is 1.73, and for $\tau_{i,f}$ 1.37. However, to try to circumvent the problems of the different exponential fits between cells, it was decided to compare the percentage reduction in current amplitude between the peak and the end of the 150 ms test pulse. An Arrhenius plot of this measurement for collated data (figure 4.11) was linear between 15 and 30°C giving a Q_{10} similar to the value for τ_i from single exponentials, of 3.27 (CI = 0.71 - 15.08, n = 38,30). This is only

slightly higher than the value for inactivation observed by others (2.5, 20-30°C, Narahashi et al., 1987, and 2.7, 20-37°C, Nobile et al., 1990).

The voltage sensitivity of the inactivation time constants, like the inactivation kinetics, is also complex (figure 4.12 & 4.13). At 20°C it appears that the inactivation time constant is voltage insensitive. By contrast, at 30°C, $\tau_{i,f}$ shows marked voltage sensitivity, increasing by nearly two orders of magnitude when test voltages increase from -40 to -20 mV. This is somewhat at odds with the findings of some groups (Kay, 1991, Thompson & Wong, 1991), but in broad agreement with others (Nobile et al. 1990, Bossu et al. 1991b). In the cell shown in figure 4.13, at -40 mV $\tau_{i,f}$ was 0.11 ms (comprising 30.8 % of the peak amplitude), while at -10 mV $\tau_{i,f}$ was 11.36 ms (24.6% of total current). This is in broad agreement with the observations of Nobile et al. (1990). However, while this group of workers saw little or no voltage sensitivity of $\tau_{i,s}$ in DRG neurones at any temperature, this is not the case in DR. $\tau_{i,s}$, at 30°C increased with depolarisation, but to a much smaller extent (4-5 fold) than $\tau_{i,f}$, and the voltage range over which this occurred was more positive than that for $\tau_{i,f}$, being -30 to -10 mV. This would be commensurate with the two components representing two separate populations of calcium channels. The proportion of total current made up by the two inactivating components showed no clear voltage dependency, though as can be seen in figure 4.13, both inactivating components, and particularly the fast one, appear to be more prominent with smaller depolarisation pulses. This appears to occur in chromaffin cells, where the relative proportions of the fast inactivating component has been observed to decrease more rapidly with

depolarisation than the slow component (Bossu et al. 1991b).

4. Effect of Temperature on Current Tails

Deactivation of calcium currents was studied by analysing the tail currents occurring when the membrane potential was returned to its holding value. Possibly because of the very rapid nature of calcium tail currents in DR cells and the relatively slow settling time of the voltage clamp, measurements involving tail currents showed great variability. Data from the time the membrane potential settled at the holding level, until the tail current had clearly decayed fully was fitted by exponential functions. The situation was similar to that for current activation in that the data was normally well fitted by a single exponential component, as previously observed in sensory (Swandulla & Armstrong, 1988), and cerebellar neurones (Slesinger & Lansman, 1991a). However many groups have also reported an additional fast component (Fenwick et al. 1982, Byerly et al. 1984, Dubinsky & Oxford, 1984, Taylor, 1988, Bargas et al. 1991, Sala, 1991), and this was seen in some cells, particularly at low temperatures (11/19 at 15, 8/38 at 20, and 1/14 at 25°C). It is most likely that the fast tail component was not always seen due to difficulties in separating it from the capacitance artifact. However, another possibility is that double exponentials were found in several other studies as a result of poor space clamp (i.e. the membrane not being universally isopotential). This has certainly been reported to occur if cells are cultured long enough to develop significant dendritic arborisation (Slesinger & Lansman, 1991a). In these experiments, as a result of the isolation procedure, cells normally had few dendritic processes

(see figure 2.2). Unfortunately, no assessment of the extent of dendrites was made, so it is not possible to comment on whether double exponential tails were seen more frequently in cells with large dendrites, that may have possibly been poorly space clamped. In a few cells at 25°C (5/42), and all cells studied at 30°C, the tails were too rapid to fit accurately.

The temperature sensitivity of deactivation was assessed by comparing the time constants (τ_t) for single exponential functions fitted to tail currents at 15 to 25°C, when the membrane was returned to -100 from -10 mV. Between 15 and 25°C τ_t was much less sensitive than τ_a, the Q_{10} being 2.88 (CI = 0.36 - 23.28, n = 36,30), with the Arrhenius plot being linear in this range (figure 4.14). This Q_{10} value is similar to that seen in other cells where deactivation is one of the least temperature sensitive components of calcium currents (Taylor, 1988, Swandulla & Armstrong, 1988, Nobile et al. 1990).

Unlike inactivation and activation, tail current time constants demonstrated no obvious voltage sensitivity at any temperature over the range of voltages studied (figure 4.15). In addition, when the cells membrane potential was repolarised to -50 mV rather than -100 mV, the average τ_t at 20°C was also not significantly different at 2.66 ± 0.39 ms (n = 10) as opposed to 3.03 ± 0.33 ms (n = 38). This matches findings in sympathetic neurones (Sala, 1991). Figure 4.16 shows example tail currents generated when the return potential was -50 mV, along with an Arrhenius plot for τ_t. The Q_{10} for τ_t in this situation was 3.28 (CI = 0.15 - 72.35, n = 12,8), and was not significantly different to that when the return potential was -100 mV.

The Q_{10} values quoted in this chapter are summarised in table 4.2.

Table 4.1 - Best Fit Functions for Activation Data

This table details the number of cells for whom single exponentials fitted the data better than double exponentials, or vice versa, and which Hodgkin & Huxley equation fitted best. If there was no significant difference between fits, then the simplest function was assigned. The table also shows for how many cells the best exponential was better than the best Hodgkin & Huxley function. Details of the functions are given in chapter 2.

	15°C	20°C	25°C	30°C
Number of Cells	19	41	18	5
Exponentials:				
Single best	9	33	11	4
Double best	10	8	7	1
Hodgkin & Huxley:				
m^1 best	17	32	15	3
m^2 best	2	4	3	0
m^3 best	0	1	0	0
m^4 best	0	4	0	2
Exponential better than				
Hodgkin & Huxley:	18	39	18	3

Table 4.2 - Temperature Dependence of Calcium Currents

	Q_{10} Mean (95% CI, n = measurements, cells)
Peak Amplitude, H.P. -100 mV	2.47 (CI = 1.06 - 5.80, n = 42,32)
'Steady State' Amplitude, H.P. -100 mV	2.08 (CI = 1.00 - 4.30, n = 38,30)
Peak Amplitude, H.P. -50 mV	1.69 (CI = 1.07 - 2.66, n = 10,8)
Activation Time Constant, H.P. -100 mV	10.20 (CI = 1.19 - 87.56, n = 42,32)
Activation Time Constant, H.P. -50 mV	12.65 (CI = 0.85 - 187.7, n = 12,8)
Inactivation Time Constant, H.P. -100 mV	3.53 (CI = 0.92 - 13.50, n = 13,13)
Inactivation, % Reduction, H.P. -100 mV	3.27 (CI = 0.71 - 15.08, n = 38,30)
Tail Current Time Constant, H.P. -100 mV	2.88 (CI = 0.36 - 23.28, n = 36,30)
Tail Current Time Constant, H.P. -50 mV	3.28 (CI = 0.15 - 72.35, n = 12,8)

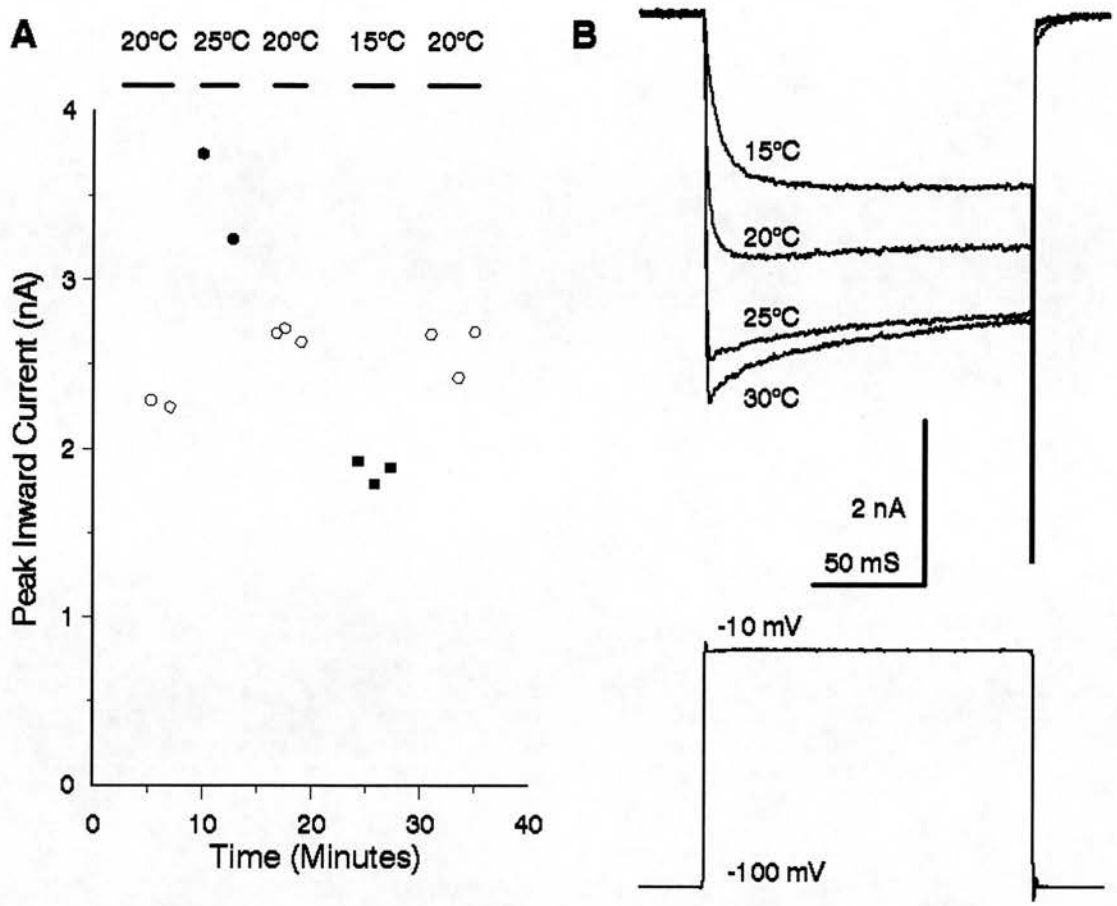

Figure 4.1: Effect of temperature on calcium current current amplitude. A. Graph of peak current amplitude plotted against time. Currents were elicited by voltage jumps from -100 to -10 mV. Control currents were recorded at 20°C (open circles), and temperature jumps were made to 25°C (filled circles), and 15°C (filled squares). The time spent at each of these temperatures is indicated by the horizontal bars. B. Examples of HVA currents recorded at 15, 20, 25 and 30°C, with the voltage protocol used to elicit them. Standard internal and external solutions. All data leak and capacity subtracted. Cell 26099003.

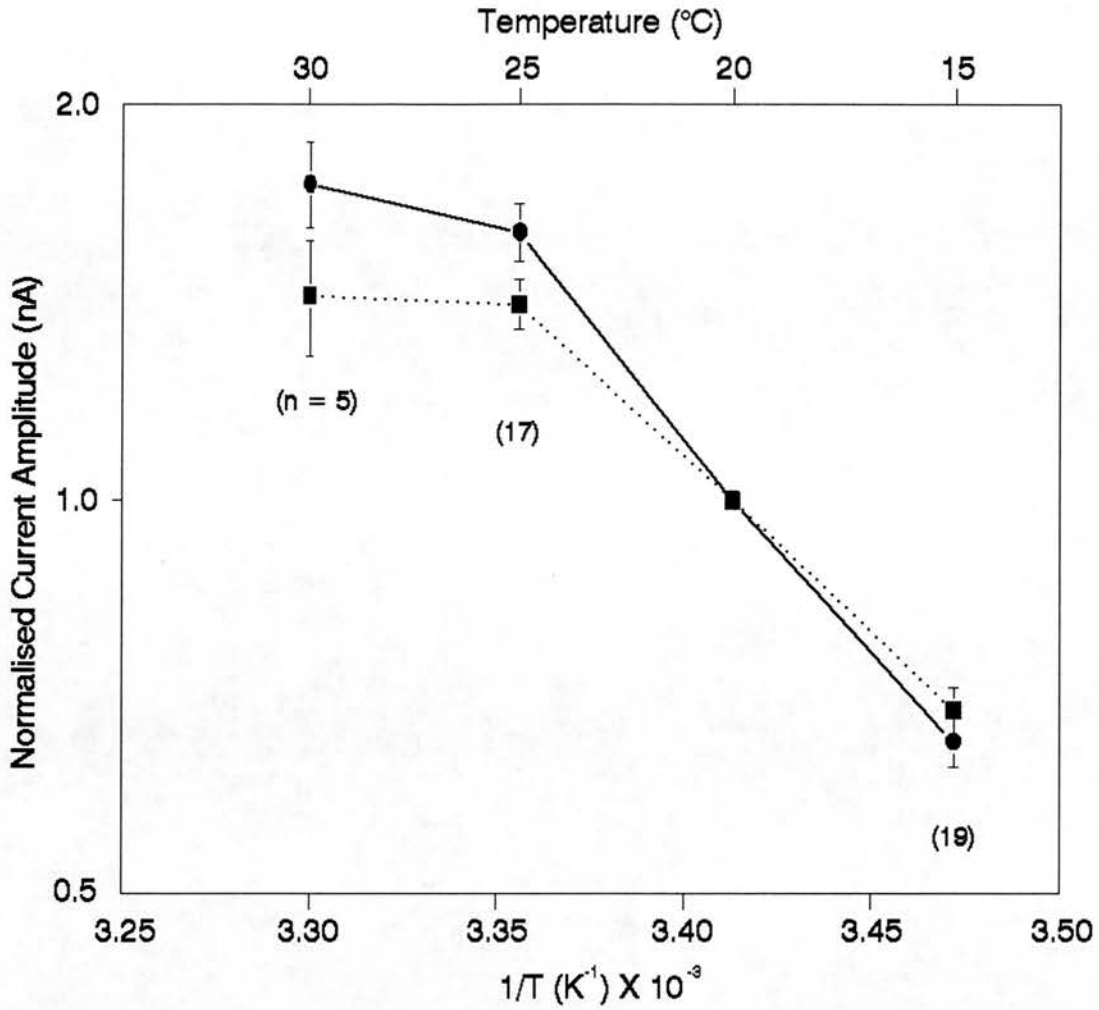

Figure 4.2: **Arrhenius plots of the peak and steady state current amplitude.** Currents were elicited by voltage steps from -100 to -10 mV, for 150 ms, and leak subtracted. Circles and the solid line represent the peak current amplitude, and the squares and the dotted line represents the 'steady state' amplitude, at the end of the voltage step. The ordinate is current amplitude normalised to that seen at 20°C (in 32 cells), plotted on a logarithmic scale. The lower abscissa is the reciprocal of the absolute temperature, and the upper, temperature in degrees Celsius. Data is plotted as means +/- SEM with the number of observations averaged indicated in parentheses.

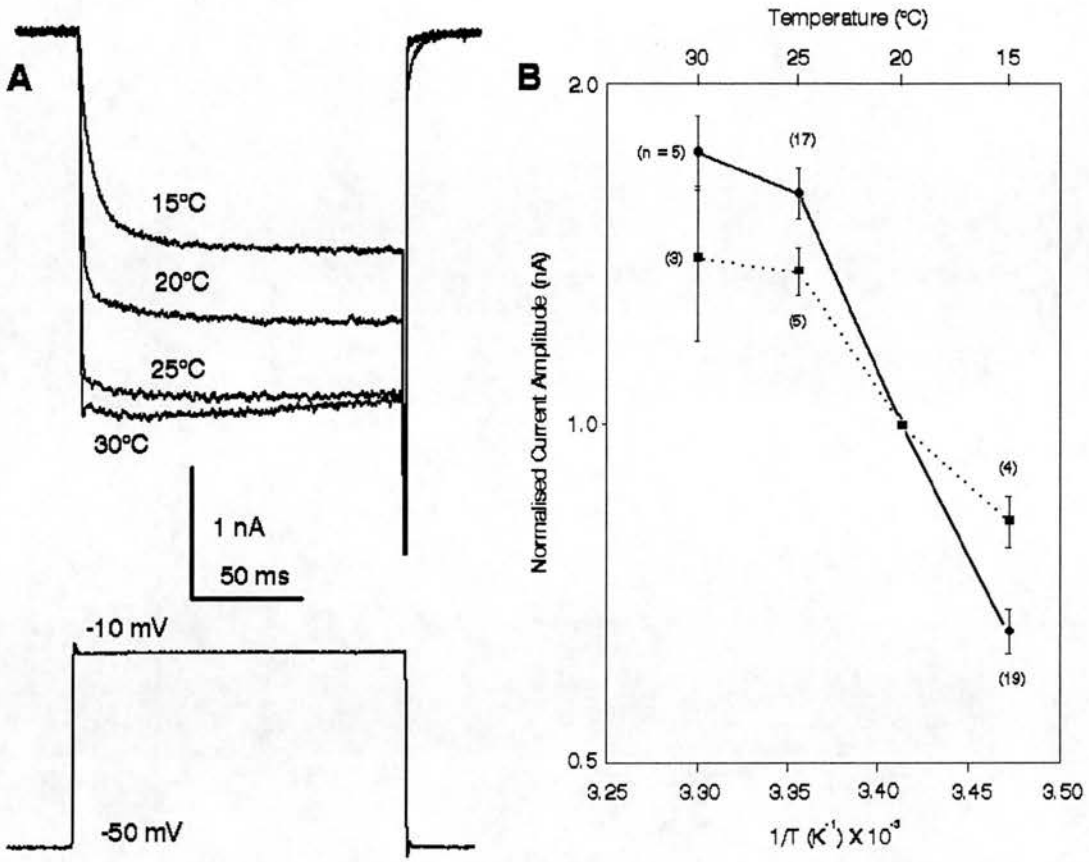

Figure 4.3: **Effect of temperature on HVA current amplitude with a holding potential -50 mV.** A. Examples of currents elicited by voltage steps from -50 to -10 mV at 15, 20, 25, 30°C. Same cell and conditions as in figure 4.1. B. Arrhenius plot of current amplitude elicited by voltage steps to -10 mV. The filled circles and solid line represents peak current data obtained when the cells holding potential was -100 mV (31 cells), while the filled squares and dotted line that obtained when the holding potential was -50 mV (8 cells). Details of the graph as for figure 4.2.

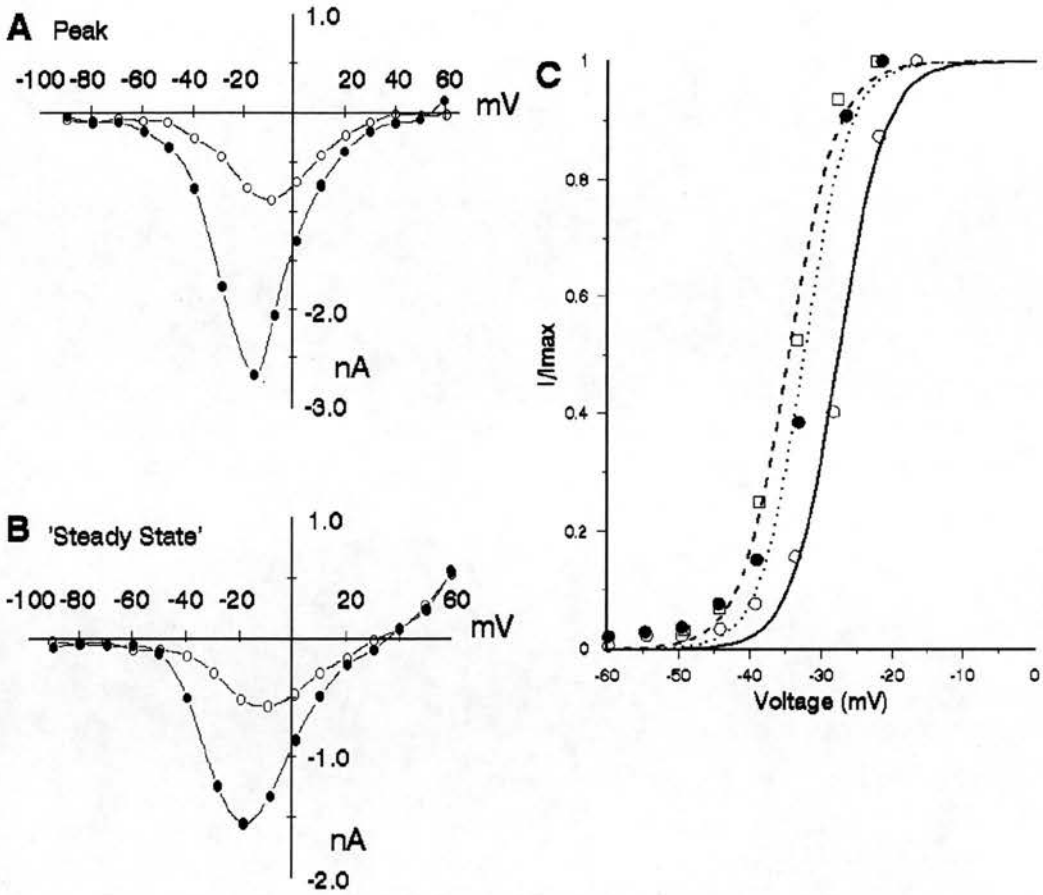

Figure 4.4: **Current/voltage relationship changes with temperature.** A. Plot of peak current amplitude against test potential from a holding potential of -100 mV. Open circles are currents at 20°C, and filled circles 25°C. Data leak subtracted and fitted with a cubic spline. Standard solutions. Cell 20119001. B. As for A. but 'steady state' current amplitude. C. I/Imax plotted against test potential at 20 (open circles), 25 (filled circles), and on return to 20°C (open squares). Data is fitted by modified boltzman functions whose V_h and k are -27.52 and 3.23 (solid line), -32.35 and 3.07 (dotted line), and -34.52 mV and 3.36 mV (dashed line) respectively. Cell 17019102.

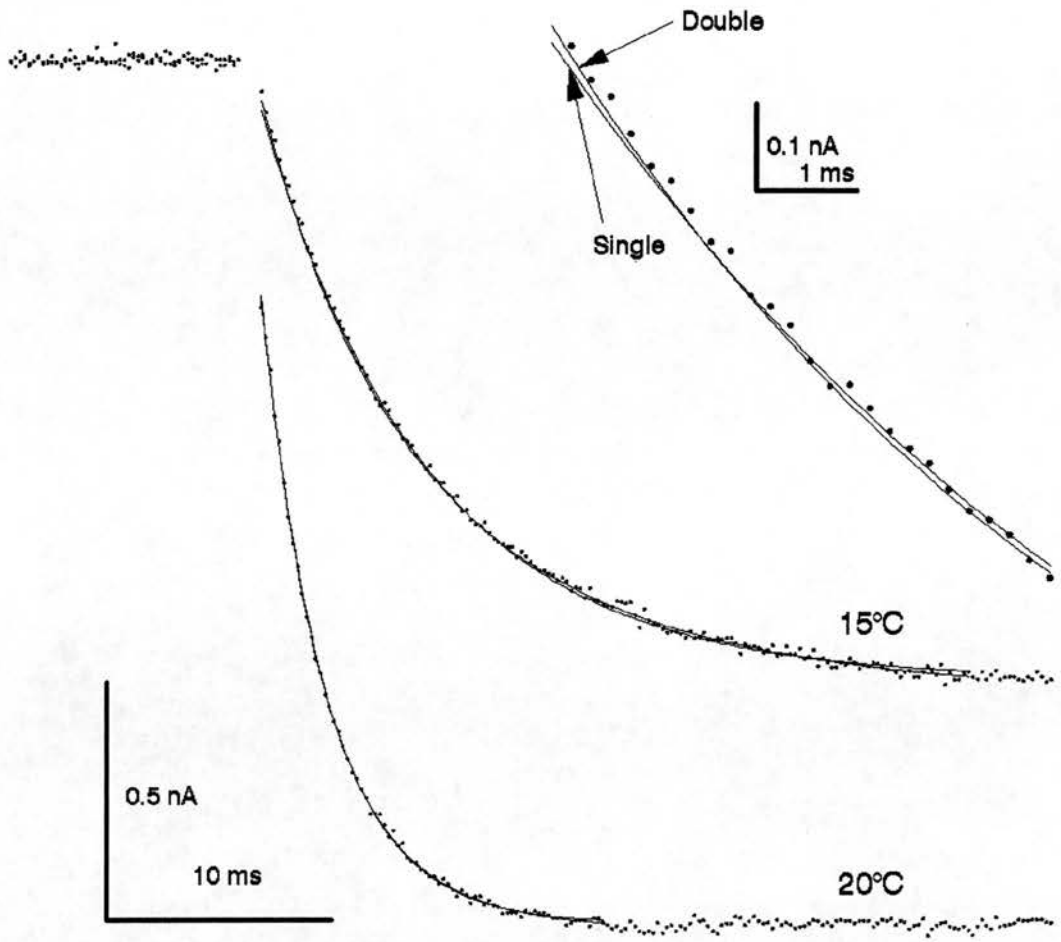

Figure 4.5: **Exponential curves fitted to current activation data.** Currents were elicited at 20 and 15°C, by voltage jumps from -100 to -10 mV. Leak and capacity subtracted data points (digitized at 5 kHz, no averaging) are overlayed with single and double exponential functions. The insert illustrates the first 5 ms of activation at 15°C on an expanded time base. At 15°C the data was best fitted by a double exponential function, while at 20°C the single exponential was best. Details of the curves used in this example are given in the text. Standard solutions. Cell 14029102.

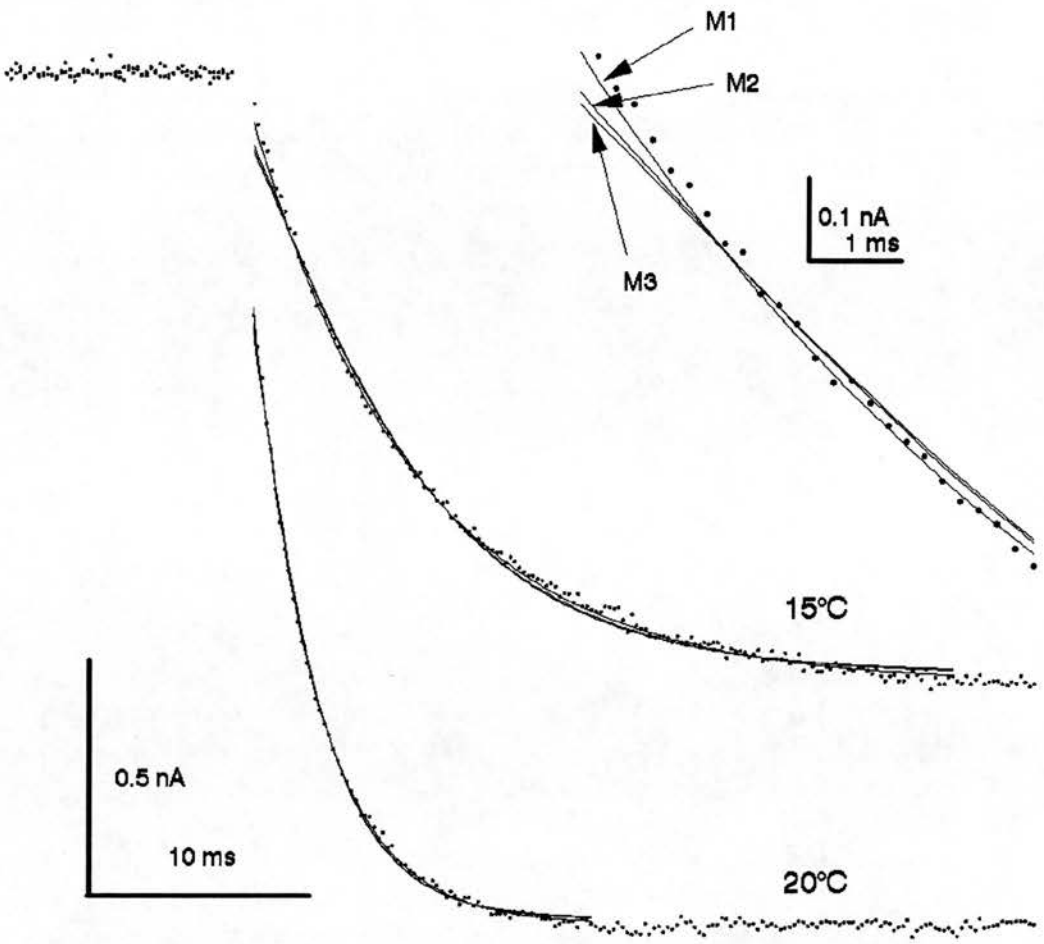

Figure 4.6: **Hodgkin and Huxley activation functions fitted to current activation data.** Same data and conditions as figure 4.5. Data at 15 and 20°C fitted with m^1, m^2, and m^3 functions. In each case the data was best fitted by the m^1 function. Insert illustrates the first 5 ms of activation at 15°C with the three curves. Details of all the curves is given in the text.

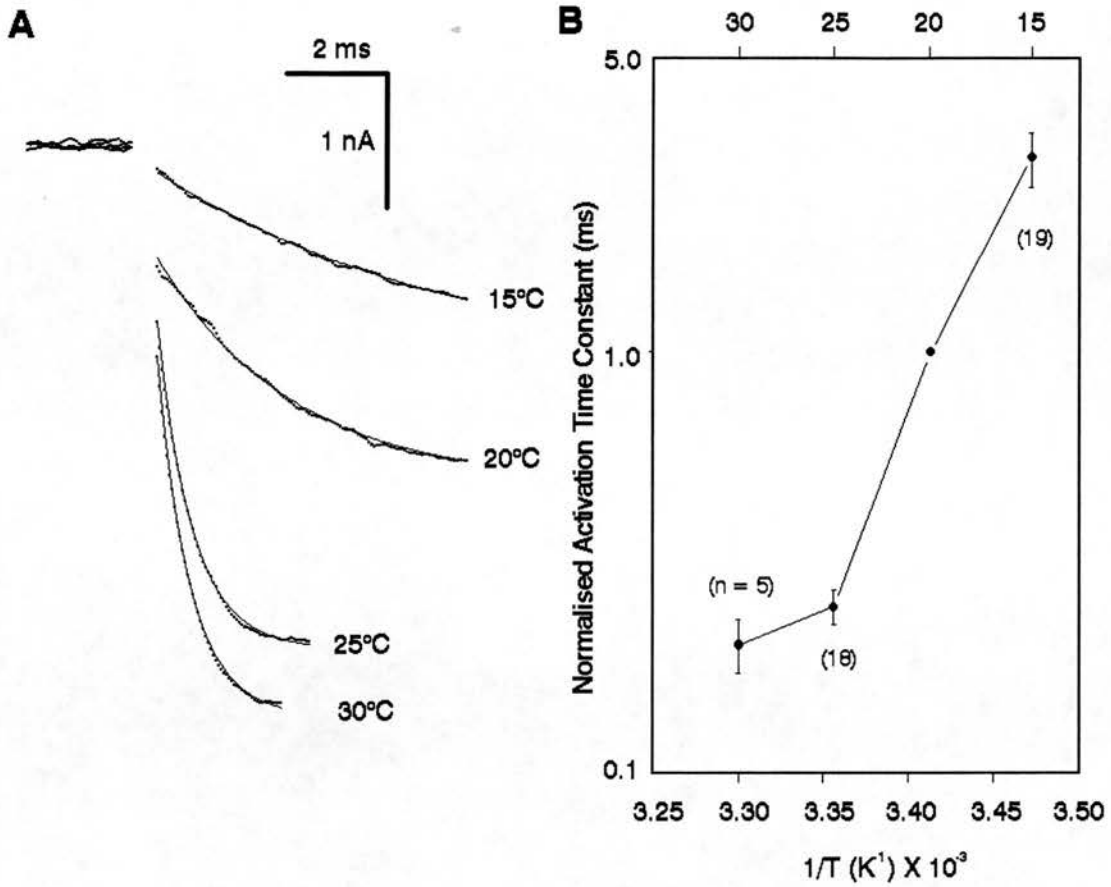

Figure 4.7: **Effect of temperature** on current **activation rate**. A. Examples of current activation elicited by voltage steps from -100 to -10 mV. Leak and capacity subtracted data (digitized at 20 kHz, no averaging) is plotted at 15, 20, 25, and 30°C, together with best fit single exponential functions, with time constants of 6.03, 2.60, 0.68, and 0.64 ms respectively. Standard solutions. Cell 26099003. B. Arrhenius plot of activation time constants derived from single exponential functions, and normalised to that seen at 20°C (in 32 cells). Details of the plot as for figure 4.2.

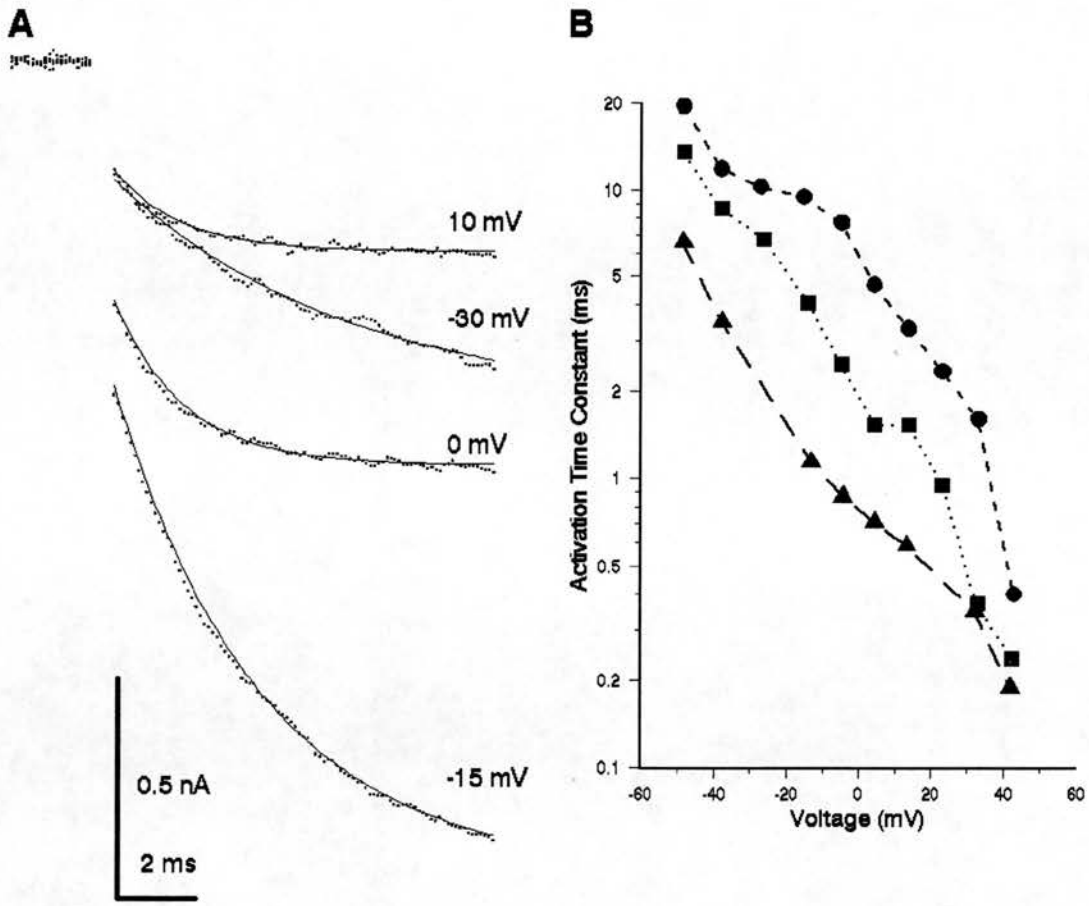

Figure 4.8: **Voltage dependency of HVA current activation rate.** A. Activation portion of current data recorded at 20°C by voltage jumps from -100 mV to the potentials indicated. Best fit single exponential functions are plotted through the data points (digitized at 20 kHz, forward averaged every 2 points), with time constants of 5.58 (-30 mV), 3.60 (-15 mV), 1.67 (0 mV) and 1.56 ms (10 mV). All data has been leak and capacity subtracted. Standard solutions. B. Plot of activation time constants against test potential at 15 (circles), 20 (squares), and 25°C (triangles). Note that the ordinate is on a logarithmic scale. Cell 21119002.

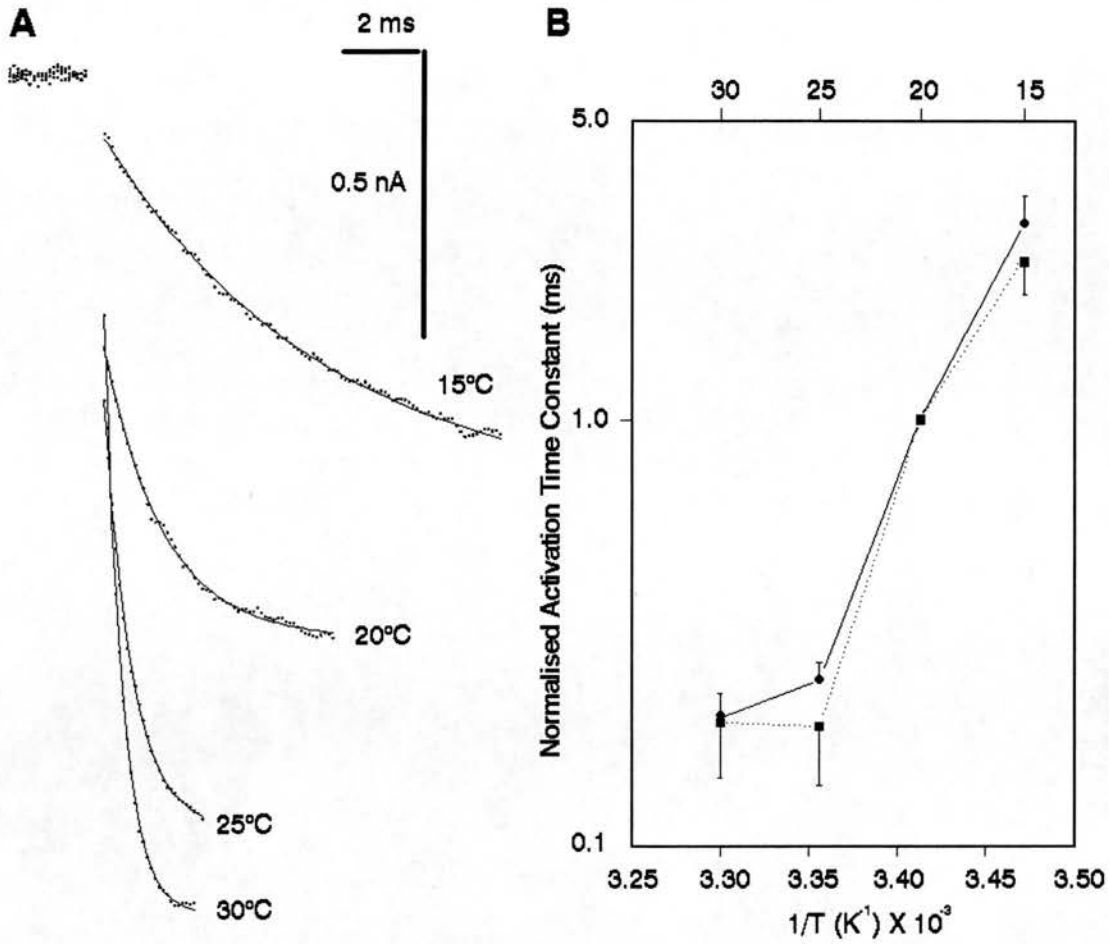

Figure 4.9: **Effect of temperature on current activation rate from a holding potential of** -50 mV. A. Examples of current activation elicited by voltage steps from -50 to -10 mV. Leak and capacity subtracted data (digitized at 10 kHz, no averaging) is plotted at 15, 20, 25, and 30°C, together with best fit single exponential functions, with time constants of 5.65, 1.51, 0.72, and 0.48 ms respectively. Standard solutions. Cell 26099003 (same as figure 4.7). B. Arrhenius plot of activation time constants derived from single exponential functions, and normalised to that seen at 20°C. Circles and solid line, H.P. -100 mV (32 cells). Squares and dotted line, H.P. -50 mV (8 cells). Details of the plot as for figure 4.2.

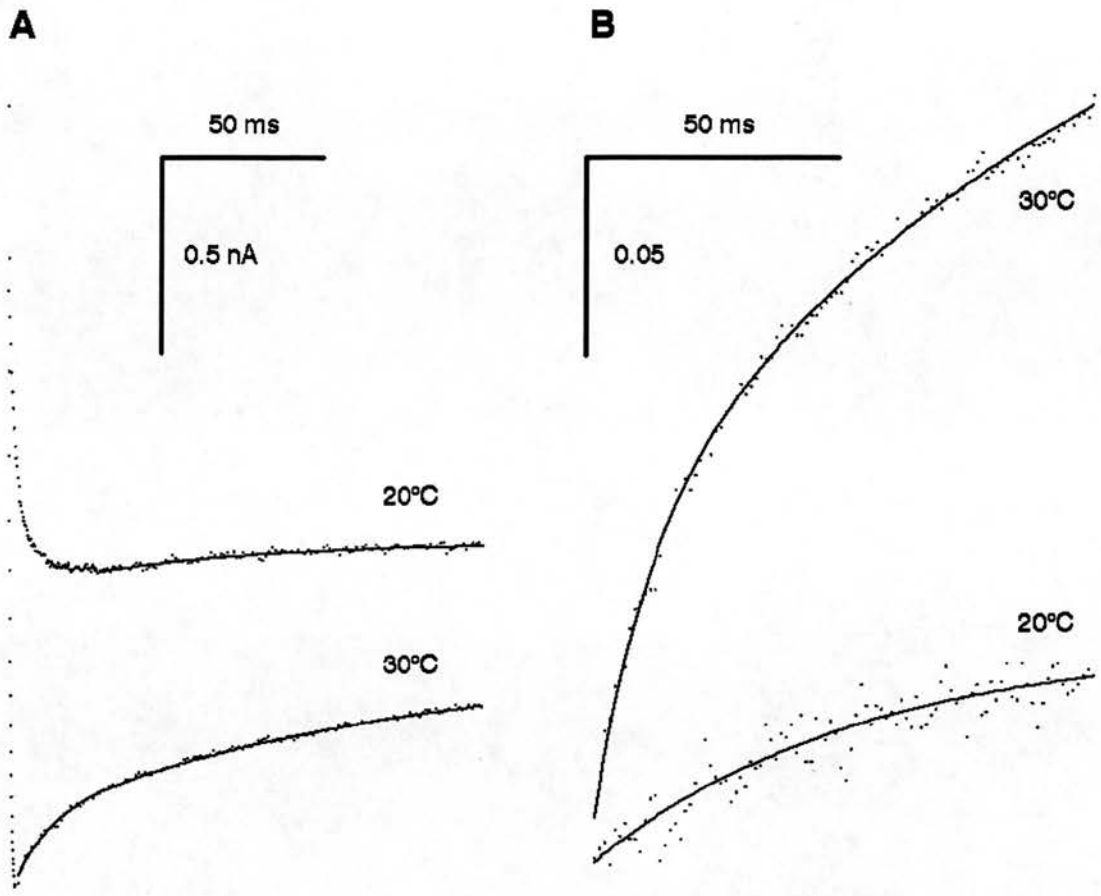

Figure 4.10: Effect of temperature on current inactivation. Currents were elicited by voltage jumps from -100 to -10 mV for 150 ms. A. Leak and capacity subtracted current data (digitized at 10 kHz, forward averaged every 5 points) recorded at 20 and 30°C, together with best fit exponential functions. B. Same data as in A, but normalised to the peak current amplitude. The data at 20°C is best fitted with a single exponential function with a time constant of 53.49 ms. The data at 30°C however, is best fitted by a double exponential function, with time constants of 10.75 and 121.3 ms. Standard solutions. Cell 26099003.

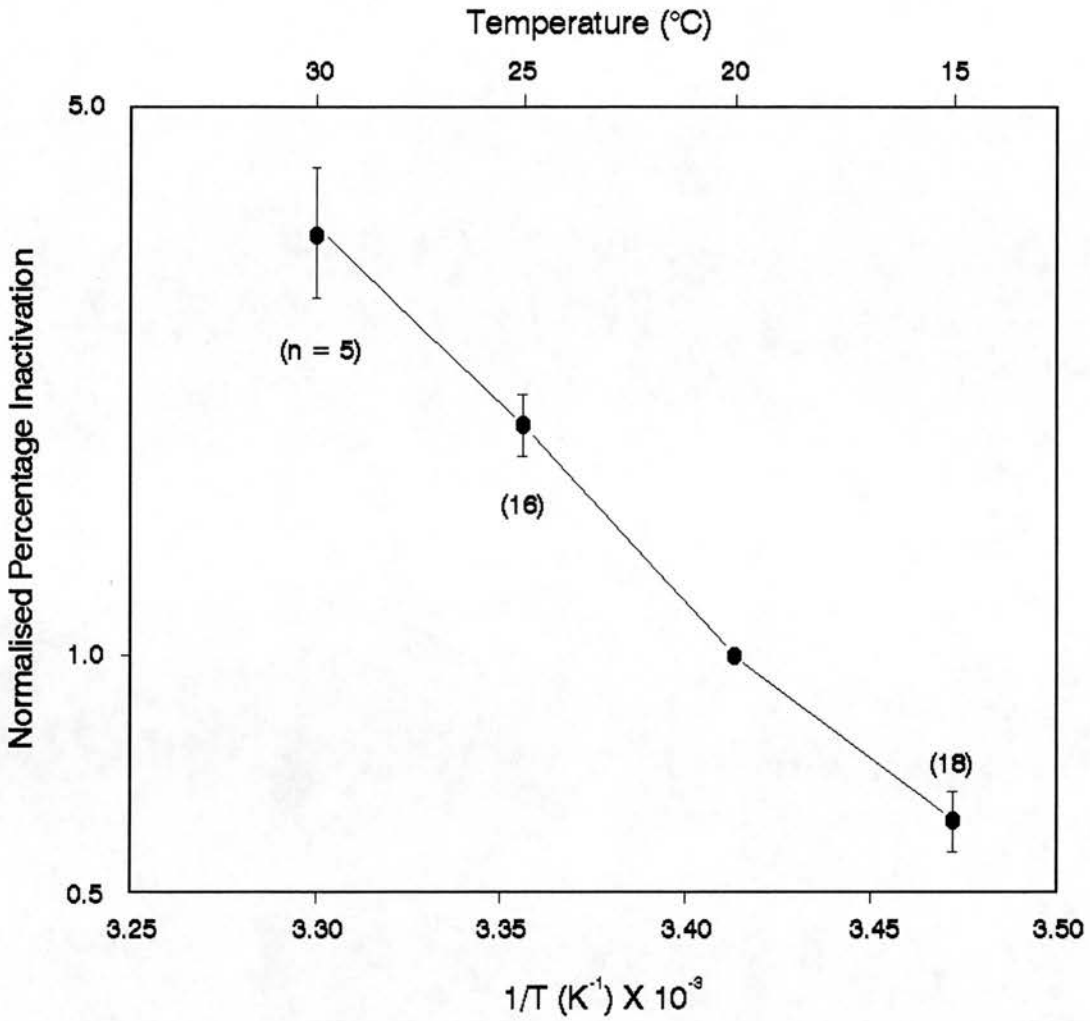

Figure 4.11: Arrhenius plot of percentage current inactivation between peak and 'steady state'. Currents were elicited by voltage steps from -100 to -10 mV for 150 ms, and inactivation assessed by calculating the percentage drop in current between the peak value, and that seen at the end of the voltage step. Percentages have been normalised to that seen at 20°C (in 30 cells). Details of the plot are otherwise as for figure 4.2. Standard solutions.

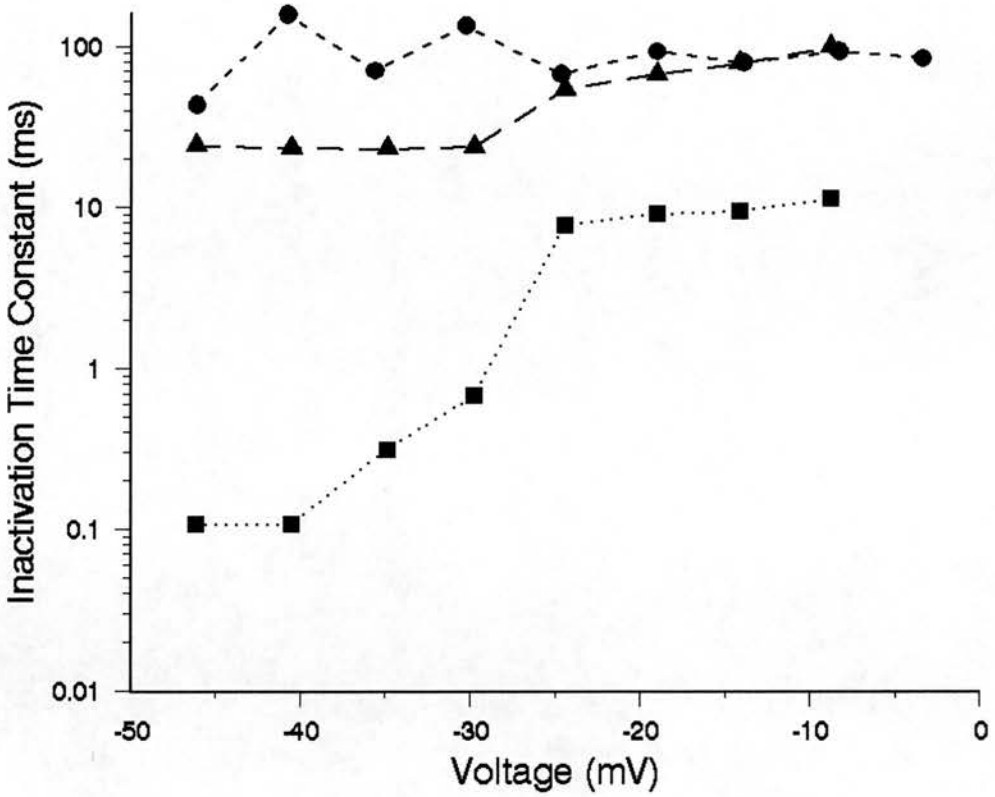

Figure 4.12: **Voltage dependence of peak current inactivation rate at 20 and 30°C.** Plot of inactivation time constants, derived from best fit exponential functions, against test potential, for currents elicited by voltage steps from -100 mV. Note that the ordinate is on a logarithmic scale. The circles and short dashed line represent the single component of inactivation at 20°C, the squares and dotted line the fast component at 30°C, and the triangles and long dashed line the slow component at 30°C. Standard solutions. Cell 10019101.

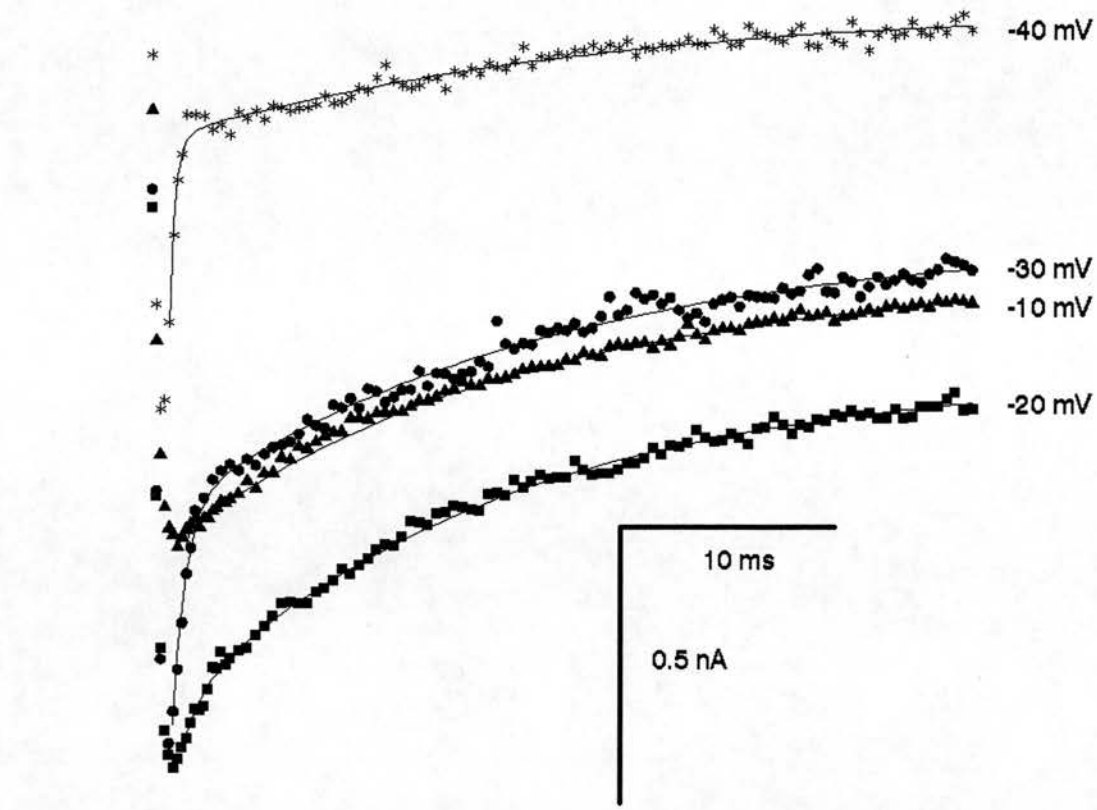

Figure 4.13: Voltage dependency of current inactivation. Currents were elicited at 30°C by voltage steps from -100 mV to -40 (asterisks), -30 (circles), -20 (squares), and -10 (triangles). Leak and capacity subtracted data points (digitized at 5 kHz, forward averaged every 2 points) are plotted together with best fit double exponential functions, with time constants of 0.11 and 23.84, 0.68 and 24.06, 9.21 and 67.15, and 11.36 and 99.48 ms respectively. Standard solutions. Cell 10019101.

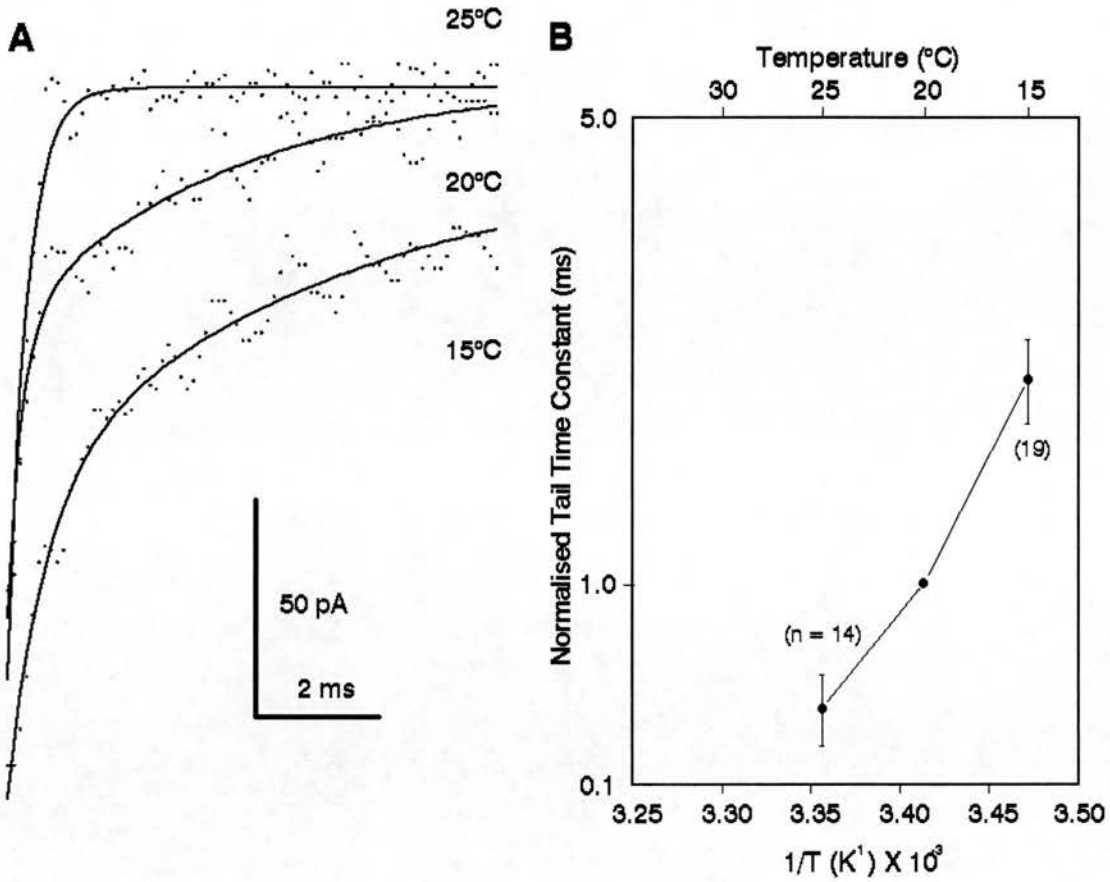

Figure 4.14: **Effect of temperature on tail currents.** A. Tail currents seen when the membrane potential was returned to -100 mV from a test potential of -10 mV for 150 ms. Leak and capacity subtracted data points (digitized at 20 kHz, forward averaged every 2 points) are plotted together with best fit exponential curves. At 15 and 20°C these were doubles with time constants of 5.03 and 0.60, and 3.59 and 0.24 ms. At 25°C the curve was a single with time constant 0.87 ms. Standard solutions. Cell 25099002. B. Arrhenius plot of time constants derived from single exponential functions fitted to tail currents, and normalised to that seen at 20°C (in 30 cells). Details of plot as for figure 4.2.

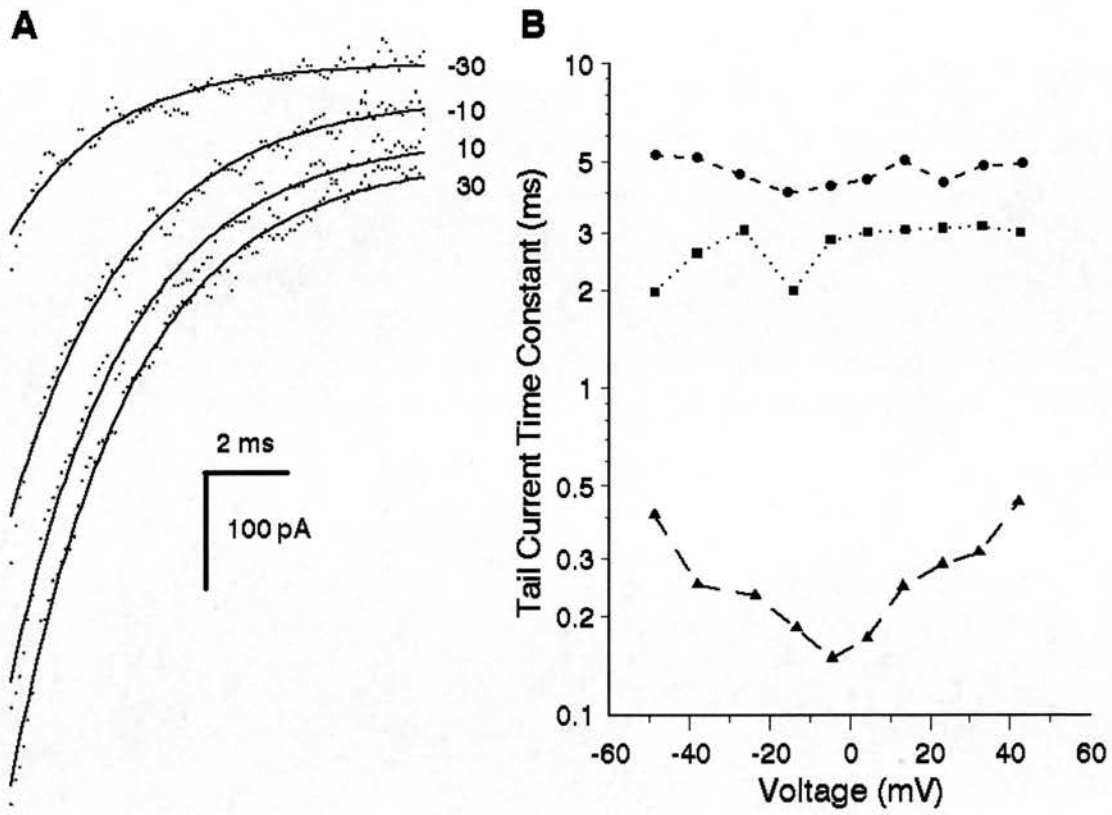

Figure 4.15: **Voltage dependency of tail currents.** A. Examples of tail currents elicited at 15°C when the membrane potential was repolarised to -100 mV from the test potentials indicated after 150 ms. Leak and capacity subtracted data points (digitized at 20 kHz, no averaging) are shown together with best fit single exponential functions with time constants of 2.39 (-30 mV), 2.89 (-10 mV), 2.84 (10 mV), and 2.89 ms (30 mV). B. Plot of tail current time constants derived from single exponential functions against test potential. Data is plotted for 15 (circles), 20 (squares), and 25°C (triangles). Standard solutions. Cell 21119002.

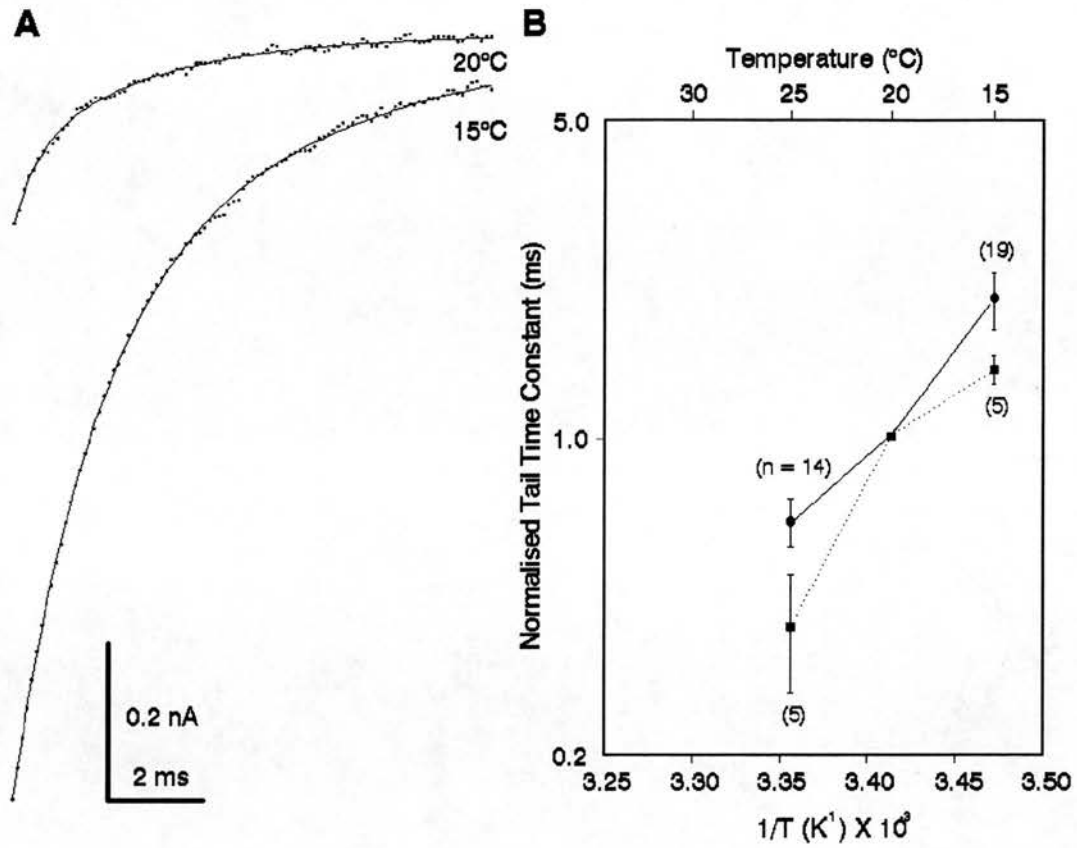

Figure 4.16: **Effect of temperature on tail currents with a holding potential of -50 mV.** A. Tail currents seen when the membrane potential was repolarised from -10 mV for 150 ms. Data points (digitized at 10 kHz, no averaging) are plotted with exponential curves with time constants of 1.68 and 5.39 ms at 15, and 0.52 and 2.81 ms at 20°C. Standard solutions. Cell 27099002. B. Arrhenius plot of time constants derived from single exponentials fitted to tail currents, and normalised to that seen at 20°C. Circles and solid line represent data obtained when the membrane potential was returned to -100 mV (30 cells), and the squares and dotted line when returned to -50 mV (8 cells).

Chapter 5 Effect of Receptor and G-Protein Activation on Temperature Dependence

1. Effect of 5-HT_{1A} Receptor Activation

To study both the effects of temperature on 5-HT_{1A} receptor mediated effects, and the effect of receptor activation on the temperature dependence of calcium currents, 50 μM 8-OH-DPAT was applied to DR cells. This dose has previously been shown to be supra-maximal (Penington & Kelly, 1990). 8-OH-DPAT was chosen as the agonist since this is less liable to oxidation than 5-HT itself, and so the applied concentration is less likely to be affected by changes in temperature. In addition, the concentration of 8-OH-DPAT, unlike that of 5-HT, is unlikely to be influenced by the process of neuronal uptake. The action of 8-OH-DPAT on HVA current, elicited by voltage steps from -100 to -10 mV for 150 ms, has been investigated in the temperature range 15 to 25°C.

Figure 5.1 illustrates currents with and without 8-OH-DPAT at 15 and 20°C. It can be seen that at both temperatures, activation of 5-HT_{1A} receptors by 8-OH-DPAT leads to a reduction in current amplitude, and a slowing of the activation rate. The 'steady state' HVA current was reduced by 29.0 ± 2.4 (n = 7), 27.6 ± 4.3 (n = 13), and 21.9 ± 1.7 % (n = 5) at 15, 20 and 25°C respectively. There was no significant difference or trend in this measurement with temperature. On the other hand, the percentage reduction of current, isochronal to the control peak, did show a trend to increase with temperature with values of 31.6 ± 3.4, 39.4 ± 4.3 and 37.8 ± 3.9 % for 15, 20, and 25°C. If pairs of values from the same cells were compared then an increase with increased temperature was just short of significance, with $p = 0.08$. The slowing of the activation rate was more clearly temperature dependent. The increase in τ_a at 15, 20 and 25°C was 1.62

± 0.35, 3.42 ± 0.87, and 14.54 ± 3.92. Pairs of values showed a highly significant increase with temperature ($p = 0.001$). This suggests with some certainty that the effect of 5-HT_{1A} receptor activation on activation kinetics is temperature dependent. This effect on activation may explain why the percentage reduction in peak amplitude shows more of a trend with temperature than the reduction in 'steady state' amplitude.

The effect of 8-OH-DPAT on the temperature dependence of current amplitude has been studied by comparing the control peak amplitude with the isochronal amplitude with 8-OH-DPAT, and the 'steady state' amplitudes (figure 5.2). The isochronal amplitude showed a Q_{10} of 2.01 (CI = 1.12 - 3.59, n = 13,11), which was lower than the value for the control peak (compare two Arrhenius plots in figure 5.2A), but was short of significance ($p = 0.08$). However the value is much nearer that for the control 'steady state' amplitude, and this may reflect that the decrease in amplitude is due to a predominant action on one type of calcium channel, such as the N-type, as has been suggested previously (Penington & Kelly, 1990). The 'steady state' Q_{10} value with 8-OH-DPAT was 2.20 (CI = 0.97 - 4.99, n = 13,11), very close to the control value.

The effect of 8-OH-DPAT on the temperature dependence of the activation rate was complicated by the finding that a higher proportion of currents in the presence of 8-OH-DPAT were best fitted by double rather than the single exponentials in controls (table 5.1), as seen for the action of D_2 DA agonists in pituitary cells (Keja et al. 1992). This was particularly marked at higher temperatures, where in controls very few sets of data were biexponential. The difference in the ability of double exponentials to fit data compared to singles

was often quite marked (figure 5.3). Activation in the presence of 8-OH-DPAT was almost exclusively best fitted by m^1 Hodgkin and Huxley functions at all temperatures (22/25), though these fits were less good than the best fit exponential function. The slowing of τ_a is reflected in the average value derived from single exponentials at 20°C being 2.30 ± 0.18 ms (n = 41) for controls, but 7.13 ± 2.03 ms (n = 13) in the presence of 8-OH-DPAT.

The difficulties associated with using different functions to fit the data from different cells was avoided by comparing all the data using τ_a derived from single exponentials. The Q_{10} for this value, in the presence of 8-OH-DPAT was 3.17 (CI = 0.79 - 12.41, n = 13,11). It can be seen from figure 5.4 that as in the control situation, the Arrhenius plot of τ_a was linear between 15 and 25°C, but that the Q_{10} value was highly significantly lower in the presence of 8-OH-DPAT ($p << 0.001$). This is commensurate with a hypothesis that the slowing of activation seen with 8-OH-DPAT involves an alteration in the activation process.

The effect of 8-OH-DPAT on tail currents has also been studied. In controls at 20°C, the average τ_t was 3.03 ± 0.33 (n = 38). With 8-OH-DPAT, this increased to 3.74 ± 0.41 (n = 13), an increase that was just short of significance ($p = 0.03$). The Q_{10} value for τ_t with 8-OH-DPAT, unlike τ_a, however showed no evidence of significant change, being 1.64 (CI = 0.15 - 17.60, n = 13,11), compared to 2.88 (CI = 0.36 - 23.28, n = 36,30, figure 5.5).

2. Effect of G-Protein Activation on Current Amplitude

It has been shown that the effects of 5-HT_{1A} receptor activation

are mediated via a pertussis toxin sensitive G-protein, and can be mimicked by direct G-protein activation (Penington et al. 1991). To examine if the effect of 8-OH-DPAT on temperature dependence could be mimicked in this way, 200 μM of the non-hydrolysable GTP analogue, GTPγS, was added to the pipette solution. This is a higher dose than has previously been studied in DR cells (30 μM, Penington et al. 1991), where effects could only be seen after over 10 minutes of recording. With 200 μM, the effects were qualitatively similar, but were present when recording began following the 5 minute equilibrium period, after obtaining whole cell mode.

Figure 5.6 illustrates currents elicited by 150 ms voltage steps from -100 mV to various depolarised levels, at 20 and 25°C. At fairly low levels of depolarisation, to between -60 and -40 mV, there was usually a clear peak amplitude seen in the current trace, and some evidence of current inactivation. This is shown in more detail in figure 5.7. The voltages required to elicit this current would suggest that this was LVA type current, and its form not dissimilar to the LVA current seen in the control situation, but it was perhaps more prominent.

With depolarisations to levels more positive than -40 mV, the current appears to be of a somewhat different qualitative nature to control HVA currents. They appear to increase in amplitude throughout the test pulse, with no clear peak being present (figures 5.6A & B, and 5.9A). In addition, the tail currents appear longer (compare figures 4.1B and 5.9A). Quantitatively HVA current in the presence of GTPγS is also different to controls. Since there is no peak present, it is only possible to compare 'steady state' current amplitudes directly (though clearly in the presence of GTPγS, this is far from a

steady state condition). At 20°C, control HVA currents had an average amplitude of 1.38 ± 0.09 nA (n = 41), while GTPγS currents were significantly lower at 1.05 ± 0.09 nA (n = 23, p = 0.01), as would be expected if GTPγS mimicked the actions of 5-HT.

Figure 5.6 shows the current voltage relationship with GTPγS at 20 and 25°C. In common with controls, there was a shift of the voltage required to elicit the maximum current to more negative values with increases in temperature. The voltage dependence was assessed by plotting Boltzman activation curves for the 'steady state' current amplitude (figure 5.8). These gave average V_h values of -27.46 ± 0.37 and -30.75 ± 1.75 mV (n = 6) at 20 and 25°C, that were not different to controls.

In common with 8-OH-DPAT, exposure to GTPγS does not lead to a significant change in the temperature dependence of current amplitude. Figure 5.9 shows current elicited by standard voltage steps from -100 to -10 mV, at 15, 20 and 25°C. The Q_{10} value for the 'steady state' amplitude was found to be 1.89 (CI = 0.73 - 4.89, n = 25,17, see figure 5.9B).

3. Effect of G-Protein Activation on Current Activation Rate

While there was considerable variability as to whether single or double exponentials best fitted current activation data in the presence of 8-OH-DPAT, this was not the case with GTPγS. It was found that in 42 out of 44 sets of data (23 cells), double exponentials were significantly better than single functions (see table 5.1, and figure 5.10), as has been found by others (Marchetti & Robello, 1989, Dolphin, 1991b). Table 5.2 details the $\tau_{a,f}$ and $\tau_{a,s}$ values, along

with the proportion of total current that each comprises. It should be noted that these percentages do not total 100% because the currents were not extrapolated back to time zero, but were taken from the time the voltage clamp settled. It can be seen that while the slow component stays at a steady proportion of around 15-16%, the fast component decreases with increases in temperature. This is probably due to a large proportion of $\tau_{a,f}$ activating during the settling time of the clamp at higher temperatures. Slowing of activation is not simply due to the addition of, or conversion of a proportion of τ_a to $\tau_{a,s}$, since the magnitude of $\tau_{a,f}$ at 20°C (3.06 ± 0.19, n = 23) is significantly ($p < 0.001$) greater than τ_a at the same temperature in the control situation (2.30 ± 0.18, n = 41). This is at odds with the view of Dolphin (1991b). Both $\tau_{a,f}$ and $\tau_{a,s}$ with GTPγS show a similar voltage dependency to τ_a seen in controls, in that they both decrease in amplitude dramatically with depolarisation (figure 5.11). m^1 Hodgkin and Huxley functions were best in 41 out of 44 cells, though these were invariably not as good as the best fit double exponential.

It was of particular interest to examine if the dramatic reduction in the Q_{10} for activation produced by 8-OH-DPAT was also caused by direct G-protein activation. This was found to be the case. Both $\tau_{a,f}$ and $\tau_{a,s}$ had similar Q_{10} values of 2.70 (CI = 0.18 - 40.30) and 2.69 (CI = 0.42 - 17.29, n = 23,15) that were highly significantly ($p \ll 0.001$) lower than the control value for τ_a (figure 5.12B). To check that this finding was not simply an artifact of the activation becoming biexponential, single τ_a values were also calculated for currents in the presence of GTPγS. These had a Q_{10} of 2.41 (CI = 0.25 - 23.12, n = 23,17), that was not significantly different to the values for $\tau_{a,f}$ or $\tau_{a,s}$ with GTPγS, or τ_a with 8-OH-DPAT, but again

was significantly lower than the Q_{10} for control τ_a.

4. Effect of G-Protein Activation on Current Tails

Like 8-OH-DPAT, GTPγS led to a prolongation of the tail current, such that τ_t increased to 3.85 ± 0.27 ms (n = 23), that was significantly longer than the control value (p = 0.002). This effect has not previously been reported in DR cells. To investigate this action of GTPγS further, cells containing internal solution with 200 μM GTPγS were also superfused with external solution containing cadmium. In common with control currents (see chapter 3), 200 μM cadmium led to a large but incomplete reduction of the 'steady state' current (91.3 ± 6.2%, n = 4), while 2 mM caused a more complete inhibition (96.1 ± 2.3%, n = 3). Interestingly, while 200 μM cadmium had little effect on τ_t in the presence of GTPγS (increasing it by 9.9 ± 5.8%, n = 4), 2 mM caused a large reduction in all cells tested (57.0 ± 9.6%, n = 3, figure 5.13). This suggests that GTPγS is prolonging the tail current of the relatively cadmium insensitive component. This component has the characteristics of LVA current (see chapter 3), and so is in keeping with the suggestion that in the presence of GTPγS there is proportionately more current seen with small depolarisations than in controls (see section 2 above, and figures 5.6B and 5.7). It may be noted that in figure 5.13, there is an apparent positive shift in the baseline current with the application of Cd^{2+} in both cells illustrated. This reflects a small decrease in the current required to hold the cells at -100 mV. The shift was extremely small being less than 0.03 nA, and at a normal

gain was lost in the current noise. There was an impression throughout this study that the holding current tended to decrease slightly with time, perhaps as a result of the cell membrane becoming more stable after the trauma of going 'whole cell'. However, any change that did occur was so small and variable, that it prevented careful assessment. It was therefore not possible to ascertain if Cd^{2+} had any significant effect on the holding current, as might be suggested by figure 5.13.

While the kinetics of the tail currents were changed by the addition of GTPγS to the internal solution, the voltage dependency of τ_t was unaltered, in that there was no clear relationship with the level of depolarisation (figure 5.14). Likewise as far as the temperature dependence of the tail currents was concerned, GTPγS had no effect, the Q_{10} for τ_t was 2.05 (CI = 0.19 - 22.61, n = 22,16), and not significantly different to the control value (figure 5.15).

5. Effect of Prepulses on GTPγS Action

Several groups have shown that the application of a depolarising prepulse shortly before the test pulse can partially reverse the action of agonists or direct G-protein activation (Grassi & Lux, 1989, Elmslie et al. 1990, Scott & Dolphin, 1990, Lopez & Brown, 1991, Tatebayashi & Ogata, 1992), including the action of 5-HT in DR (Penington et al. 1991). It was of particular interest to examine whether prepulses were able to reverse the slowing of the activation rate and the reduction in Q_{10} for τ_a, by both 8-OH-DPAT and GTPγS. While it has been reported that long prepulses (200 - 4000 ms) can cause a reduction in current amplitude (Slesinger & Lansman, 1991a),

in common with most investigations where similar prepulses (< 200 ms) have been applied (Elmslie et al. 1990, Penington et al. 1991, Lopez & Brown, 1991), no effect was seen on control currents at any temperature in any cell. Thus currents in DR do not seem capable of facilitation that is observed in chromaffin cells (Artalego et al. 1990, 1991), SCG neurones (Ikeda, 1991), or to a small degree in DRG cells (Scott & Dolphin, 1990, Tatebayashi & Ogata, 1992). One previous study has reported a reduction in peak current amplitude when using Ca^{2+} as the charge carrier, and recording at 35°C (Williams et al. 1991). Since in this case the reduction was greatly attenuated by 5 mM BAPTA, the effect was thought to be calcium mediated. As such, it would not be expected with the solutions used in this study. Figure 5.16A illustrates the effect of a prepulse to 60 mV for 100 ms applied 10 ms prior to a standard test pulse with and without 50 μM 8-OH-DPAT. It can be seen that the 44.4% reduction in peak current amplitude by 8-OH-DPAT was partially reversed by around 50%, but τ_a, which was increased 2.25 fold from 2.90 to 6.53 ms was returned to 2.98 ms by the prepulse. When a prepulse (to 40 mV, 20 ms prior to the test pulse) was applied to a cell containing GTPγS, while the amplitude of the peak current was increased by only 32.5%, the slow, biexponential, activation ($\tau_{a,f}$ = 3.87 ms, $\tau_{a,s}$ = 52.27 ms) was converted to one with a faster mono-exponential character (τ_a = 2.63 ms, figure 5.16B). If single exponentials for both currents are compared in this example, there was a 12.46 fold increase in τ_a induced by the prepulse.

Figure 5.17 illustrates the effect of the magnitude of the prepulse on currents elicited in the presence of GTPγS. As the level of depolarisation increased the percentage increase in current

amplitude goes up, as does the decrease in τ_a. The increase in amplitude seems to plateau with depolarisations to around 50 - 60 mV, while τ_a tends to stabilise at levels around 10 mV less. As it has been noted depolarisations beyond the apparent reversal potential (50 - 60 mV) often lead to cell deterioration (see chapter 3), and the fact that it was the affect on τ_a that was of most interest, a standard prepulse to 40 mV was chosen. Since the tail currents are prolonged with GTPγS, a standard interval of 20 ms between the prepulse and test pulse was used to allow the prepulse tail to decay as fully as possible. With this standard prepulse, in the presence of GTPγS at 20°C, the 'steady state' amplitude was increased by 11.3% and τ_a decreased 5.70 ± 2.04 fold (n = 7).

Examples of currents in the presence of GTPγS, with and without prepulses, at 15, 20, and 25°C are overlaid in figure 5.18A for comparison. It can be seen that the tail currents generated by the prepulses had nearly completely decayed at all temperatures, other than to a small degree at 15°C. The effect of the prepulse was to lead to a current that qualitatively appears much more akin to control HVA currents in DR cells. As such it was possible to calculate Q_{10} values for both peak and 'steady state' amplitudes. These had values of 1.95 (CI = 0.94 - 4.03) and 1.77 (CI = 0.54 - 5.77, n = 10,6, see figure 5.18B). The same trend of the peak having a Q_{10} value larger than 'steady state' as in controls occurred, but both values were less. However for the peak Q_{10}'s this was just short of significant ($p = 0.04$), and for the 'steady state' values was not significant ($p = 0.25$). Having a current peak with prepulses allowed the amplitude of currents in the presence of GTPγS to be measured isochronally to this, when no prepulse was applied in individual cells. The Q_{10} for this

amplitude, isochronal to the prepulse peak, was 2.75 (CI = 0.87 - 8.63, n = 10,6), and was significantly higher than the GTPγS 'steady state' Q_{10} (p = 0.007), again in line with controls. This would suggest the possibility that some proportions of the various components of HVA currents are not affected by G-protein activation.

Prepulses had a clear effect on the current activation rate. Rather than the activation of all cells at 20°C being biexponential, only 3 out of 7 cells had activation better fitted by a double rather than a single exponential function (see table 5.1). In addition, τ_a was increased 5.7 ± 2.0 fold (n = 7) compared to the activation with GTPγS without a prepulse, to 2.12 ± 0.26 ms. This value for τ_a was not significantly different to the control τ_a value (2.30 ± 0.18 ms, n = 41). Figure 5.19 illustrates current activation with GTPγS plus prepulses, and shows the Arrhenius plot for this τ_a, along with control and straight GTPγS τ_a's. The Q_{10} for τ_a with GTPγS plus a prepulse was 11.16 (CI = 1.32 - 94.75, n = 10,6), and so it can be clearly seen that prepulses led to a complete reversal of the decreased temperature sensitivity induced by GTPγS. Thus both the slowing of activation and the possible change in mechanism of activation (reflected by the lowering of the Q_{10} value) by GTPγS, are reversed by large depolarisations.

The prolonged τ_t seen with GTPγS is unaffected by prepulses, with the average value being 3.65 ± 0.77 (n = 7), nor is the Q_{10} for τ_t significantly affected (3.37, CI = 0.12 - 93.62, n = 10,6, see figure 5.20).

6. Effect of GDPβS

As a control for the action of GTPγS, 2 mM of the non-hydrolysable GDP analogue, GDPβS, was added to the internal solution used for some cells. Figure 5.21A illustrates currents recorded under such conditions. The Q_{10} values for peak (2.25, CI = 0.83 - 6.08, n = 13,9, figure 5.21B) and 'steady state' current amplitude (2.16, CI = 0.58 - 8.07, n = 13,9), τ_a (12.83, CI = 2.10 - 78.49, n = 13,9, figure 5.22A), and τ_t (1.50,CI = 0.27 - 8.42, n = 12,8, figure 5.22B), were all not significantly different from the control values. In addition, τ_t (3.10 ± 0.33 ms, n = 9) was likewise close to the control value, being near to significantly less then τ_t with GTPγS ($p = 0.04$). The value for the Q_{10} for τ_a was significantly higher than that seen with either 8-OH-DPAT or GTPγS ($p \ll 0.001$).

All the Q_{10} values for this section are detailed in table 5.3.

Table 5.1 - Best Fit Functions for Activation Data

This table details the number of cells activation data fitted significantly better by double rather than single exponential functions at different temperatures.

	15°C	20°C	25°C	30°C
Controls	10/19	8/41	7/18	1/5
8-OH-DPAT	4/7	6/13	3/5	
GTPγS	8/8	23/23	11/13	
GTPγS Plus Prepulse	2/5	3/7	0/3	
GDPβS	2/5	1/9	0/6	

Table 5.2 - Double Exponential Activation Functions with GTPγS

The table details the average fast ($\tau_{a,f}$), and the slow activation time constants ($\tau_{a,s}$), together with the percentage of the total current that these two components represent, and the total number of cells examined at each temperature.

	Number	$\tau_{a,f}$ (ms)	Percent	$\tau_{a,s}$ (ms)	Percent
15°C	8	5.69 ± 0.14	30.9 ± 2.0	48.13 ± 3.84	15.3 ± 2.1
20°C	23	3.06 ± 0.19	21.3 ± 2.2	34.23 ± 3.67	16.9 ± 1.3
25°C	11	2.92 ± 0.69	11.0 ± 3.9	22.15 ± 3.09	15.4 ± 2.1

Table 5.3 - Effect of Receptor or G-protein Activation on Temperature Dependence

	Q_{10} Mean (95% CI, n = measurements, cells)
Application of 50 μM 8-OH-DPAT	
Isochronal Amplitude	2.01 (CI = 1.12 - 3.59, n = 13,11)
'Steady State' Amplitude	2.20 (CI = 0.97 - 4.99, n = 13,11)
Activation Time Constant	3.17 (CI = 0.79 - 12.41, n = 13,11)
Tail Current Time Constant	1.64 (CI = 0.15 - 17.60, n = 13,11)
Application of 200 μM GTPγS	
'Steady State' Amplitude	1.89 (CI = 0.73 - 4.89, n = 25,17)
Amplitude Isochronal to Prepulse	2.75 (CI = 0.87 - 8.63, n = 10,6)
Peak Amplitude with Prepulse	1.95 (CI = 0.94 - 4.03, n = 10,6)
'Steady State' Amplitude with Prepulse	1.77 (CI = 0.54 - 5.77, n = 10,6)
Single Activation Time Constant	2.41 (CI = 0.25 - 23.12, n = 23,17)
Fast Double Activation Time Constant	2.70 (CI = 0.18 - 40.30, n = 23,15)
Slow Double Activation Time Constant	2.69 (CI = 0.42 - 17.29, n = 23,15)
Activation Time Constant with Prepulse	11.16 (CI = 1.32 - 94.75, n = 10,6)
Tail Current Time Constant	2.05 (CI = 0.19 - 22.61, n = 22,16)
Tail Current Time Constant with Prepulse	3.37 (CI = 0.12 - 93.62, n = 10,6)
Application of 1 mM GDPβS	
Peak Amplitude	2.25 (CI = 0.83 - 6.08, n = 13,9)
'Steady State' Amplitude	2.16 (CI = 0.58 - 8.07, n = 13,9)
Activation Time Constant	12.83 (CI = 2.10 - 78.49, n = 13,9)
Tail Current Time Constant	1.50 (CI = 0.27 - 8.42, n = 12,8)

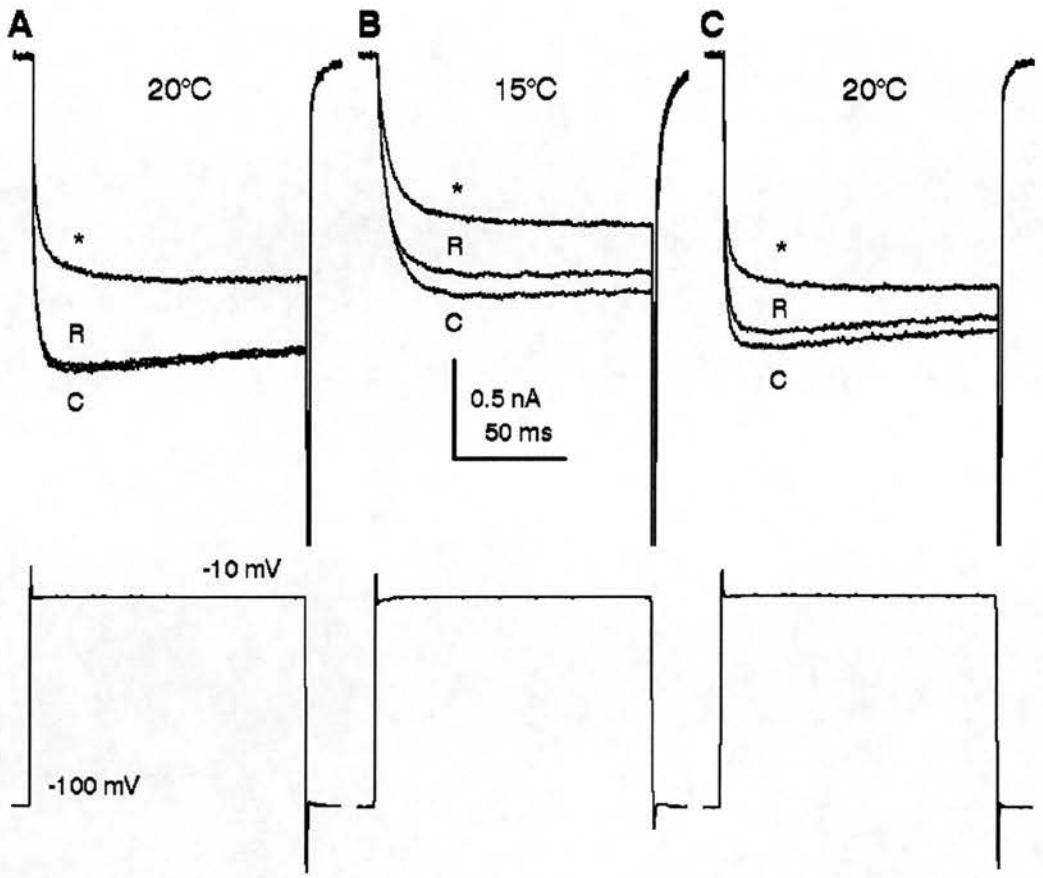

Figure 5.1: Effect of temperature on HVA current response to 8-OH-DPAT. Calcium currents were elicited by voltage steps from -100 to -10 mV for 150 ms at 20 (A), 15 (B), and 20°C (C). 50 μM 8-OH-DPAT was applied from a broken patch pipette brought to within 50 μm of the cell. The figure illustrates control currents (C), those recorded in the presence of 8-OH-DPAT (*), and recovery (R) at each temperature. Standard internal and external solutions. All data is leak and capacity subtracted. Cell 25099001.

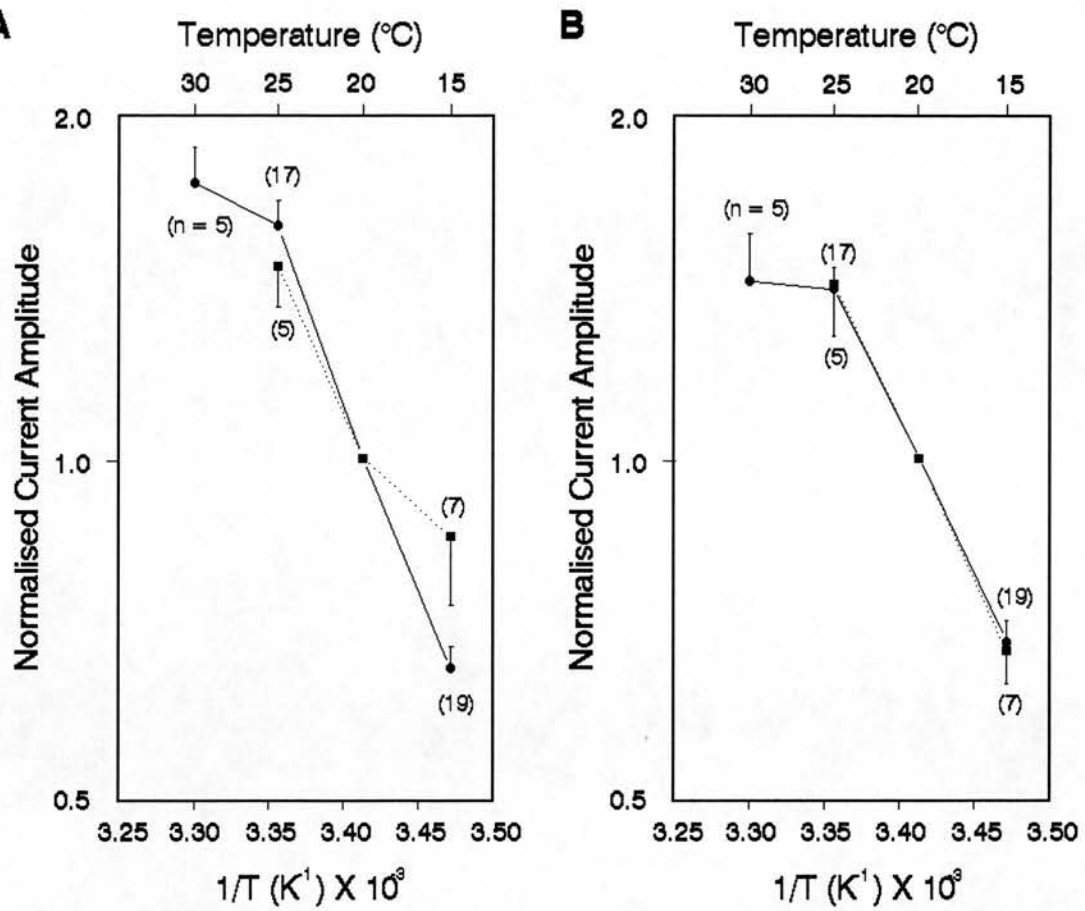

Figure 5.2: **Arrhenius plots of current amplitude in the presence and absence of 8-OH-DPAT.** All currents were elicited by voltage jumps from -100 to -10 mV for 150 ms. In both plots, control data is represented as circles, solid lines, and upward error bars, and measurements in the presence of 50 μM 8-OH-DPAT represented by squares, dotted lines, and downward error bars. A. Control peak current amplitudes (32 cells, as in figure 4.2), and amplitudes measured in the presence of 8-OH-DPAT isochronally with the control peak amplitude (11 cells). B. 'Steady-state' current amplitude measured at the end of the voltage step for controls, and with 8-OH-DPAT. Details of plot as for 4.2.

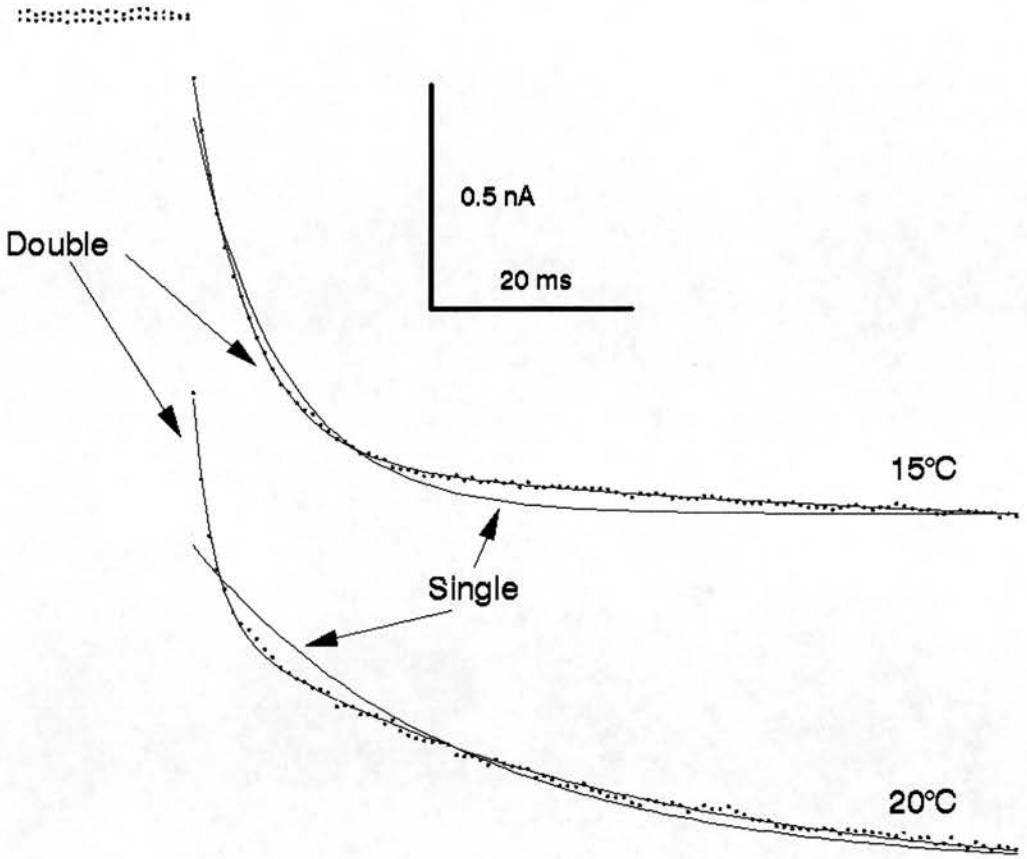

Figure 5.3: Current activation in the presence of 8-OH-DPAT. Currents were elicited by voltage steps from -100 to -10 mV while 50 μM 8-OH-DPAT was applied via a broken patch pipette positioned within 50 μm of the cell. Leak and capacity subtracted data points (digitised at 5 kHz, forward averaged every 2 points) are plotted together with best fit single and double exponential functions, at 15 and 20°C. The single exponentials had time constants of 79.36 and 26.73 ms, and the doubles 5.84 and 80.53, and 2.08 and 39.20 ms respectively. In both cases double exponentials fitted significantly better than singles ($p< 0.001$). Standard solutions. Cell 24099101.

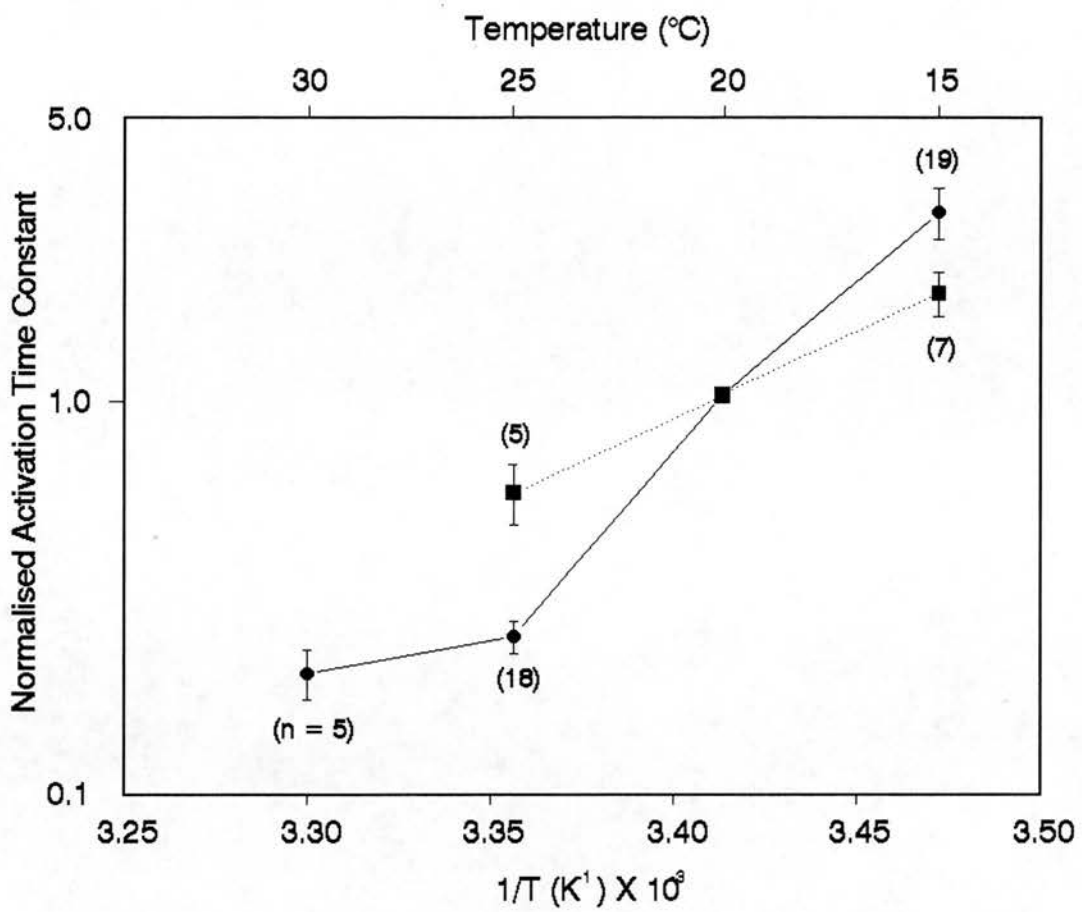

Figure 5.4: **Arrhenius plot of activation time constants.** Currents were elicited by voltage steps from -100 to -10 mV for 150 ms. All data has been leak and capacity subtracted. The graph illustrates Arrhenius plots of activation time constants derived from single exponential functions, normalised to that seen at 20°C. Circles and solid line represent control data (32 cells as in figure 4.7B), and the squares and dotted line data obtained in the presence of 50 μM 8-OH-DPAT (11 cells). Details of the plot as for figure 4.2.

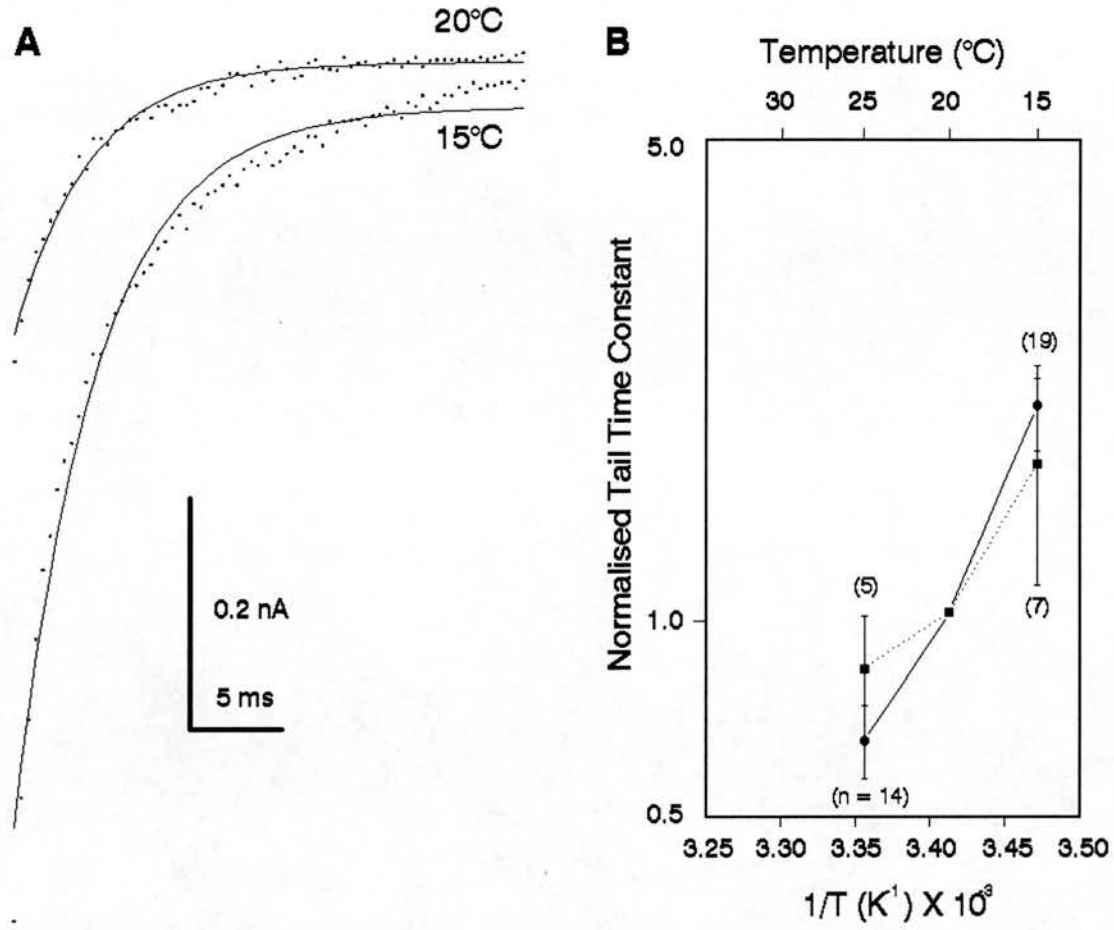

Figure 5.5: Effect of temperature on tail currents in the presence of 8-OH-DPAT. A. Tail currents seen when membrane potential was repolarised to -100 from a test potential of -10 mV for 150 ms, with 50 μM 8-OH-DPAT. Leak and capacity subtracted data points (digitised at 5 kHz, no averaging) plotted together with best fit single exponential functions with time constants of 3.20 and 4.59 ms at 20 and 15°C respectively. Standard solutions. Cell 25099101. B. Arrhenius plot of time constants derived from single exponential functions, normalised to that seen at 20°C. Circles and solid line, controls (30 cells), squares and dotted line with 8-OH-DPAT (11 cells). Details as in figure 4.2.

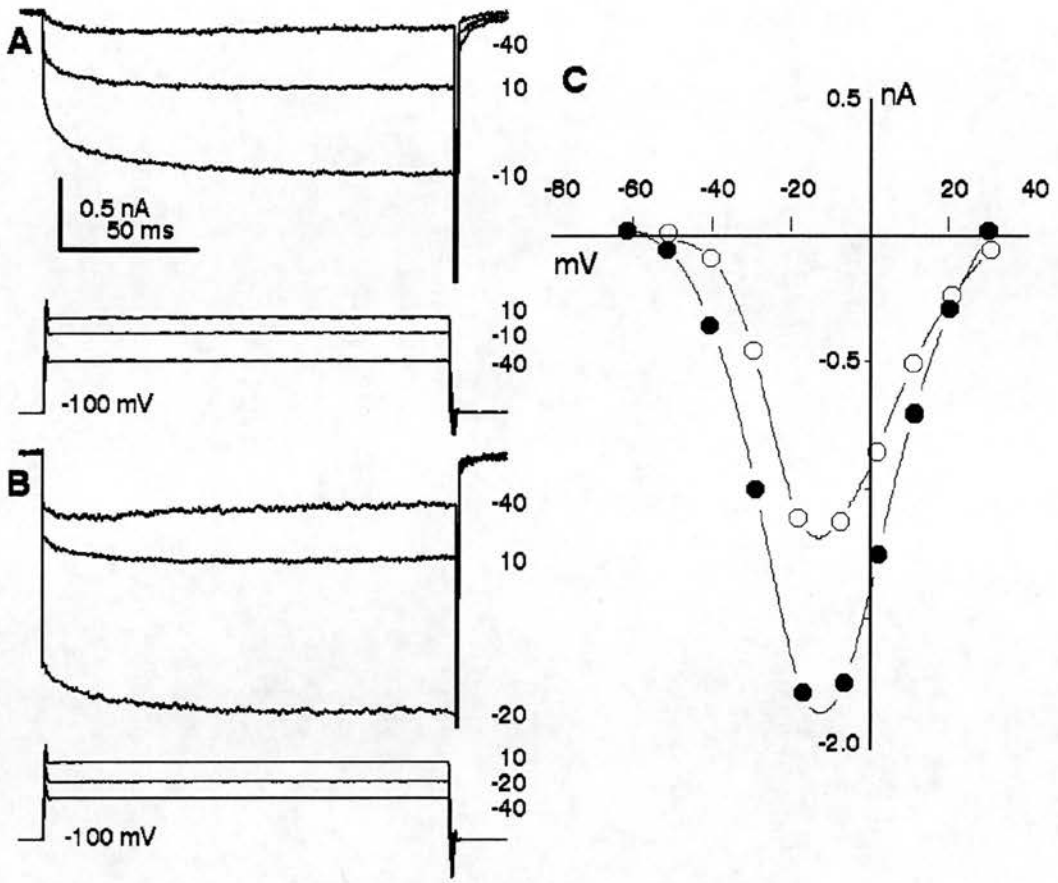

Figure 5.6: **Voltage dependency of calcium currents recorded in the presence of GTPγS.** A. Examples of currents recorded at 20°C with 200 μM GTPγS in the internal solution. Standard external solution. Currents were elicited by voltage jumps from a holding potential of -100 mV to test potentials shown on the right of the voltage traces and corresponding current traces. Data leak and capacity subtracted. B. As A but recorded at 25°C. C. 'Steady-state' current amplitude is plotted against the test potential achieved. Open circles, data recorded at 20°C, and solid circles data at 25°C. Points are fitted with a cubic spline curve. Cell 28119101.

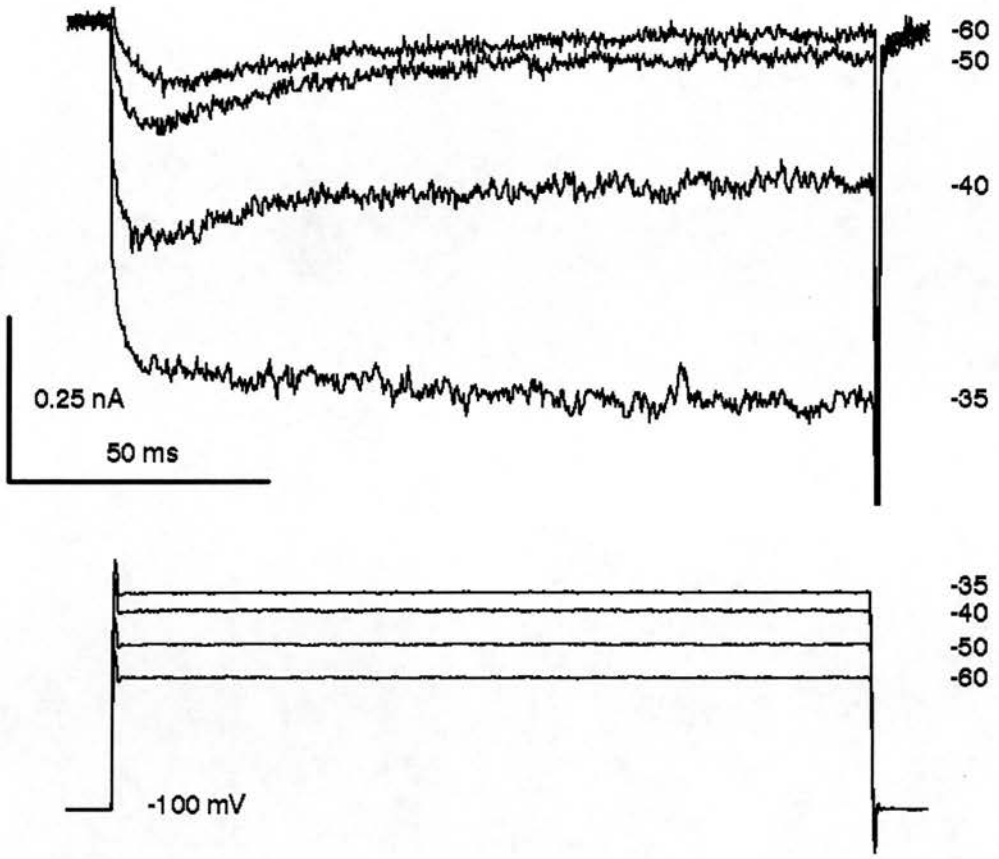

Figure 5.7: **Effect of small depolarisations on calcium currents in the presence of** GTPγS. Currents were elicited at 25°C by voltage steps from -100 mV to the test potentials indicated. Standard external solution, internal contained 200 μM GTPγS. Data leak and capacity subtracted. Cell 18109102.

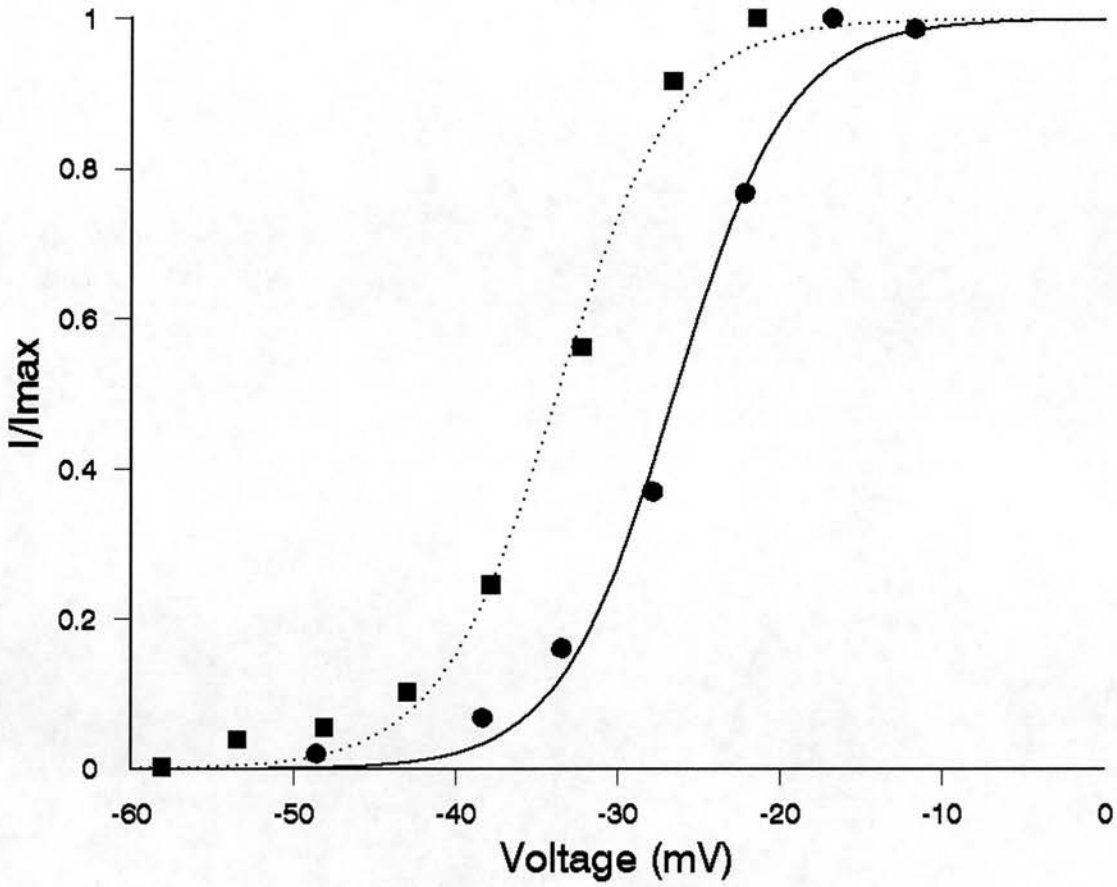

Figure 5.8: Voltage dependency of activation in the presence of GTPγS. 'Steady-state' current amplitude is normalised to the maximum value obtained by a voltage jump from an holding potential of -100 mV, and plotted against the test potential achieved. Circles represent data recorded at 20°C, while the squares represent data at 25°C. Data in each case is fitted with a modified Boltzman function. These have $V_{0.5}$'s of -26.49 and -33.70 ms, and k's of 3.52 and 3.66 mV respectively. Standard external solutions, internal contained 200 μM GTPγS. Cell 18109102.

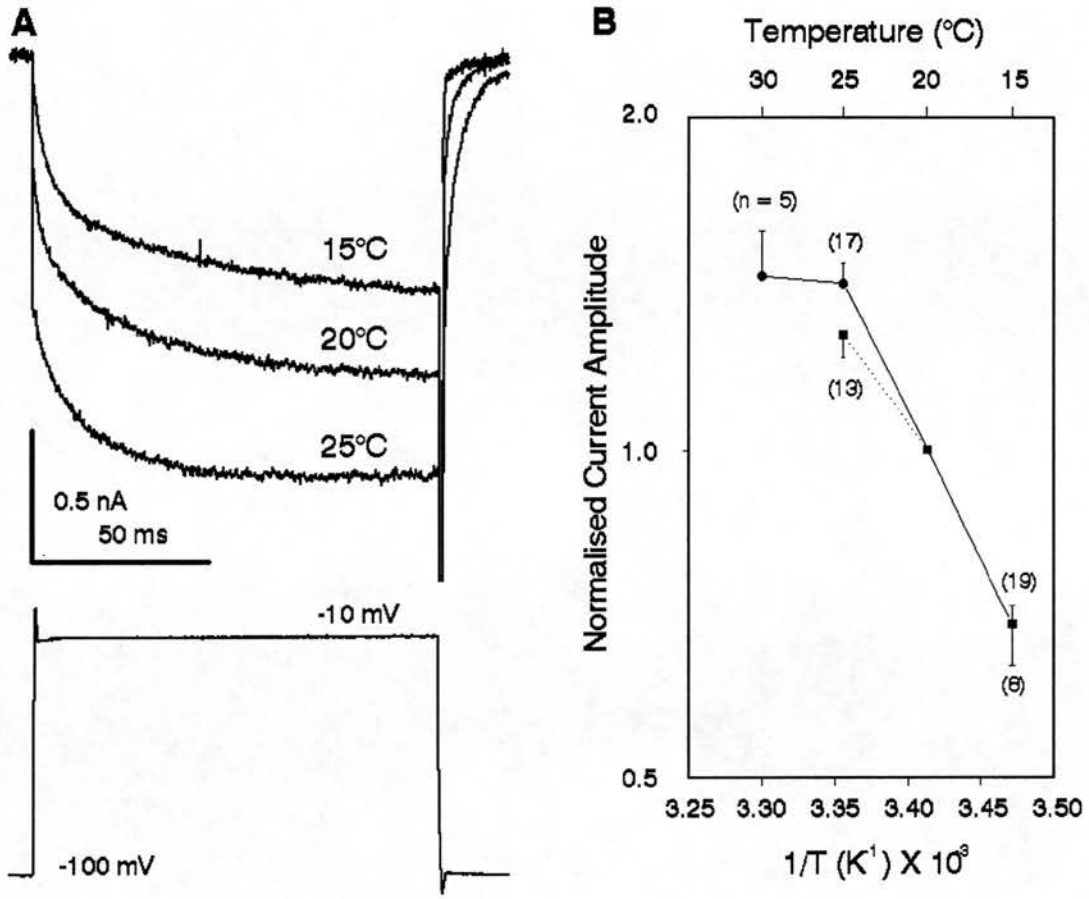

Figure 5.9: Effect of temperature on HVA calcium currents in the presence of GTPγS. A. Currents elicited by voltage jumps from -100 to -10 mV at 15, 20 and 25°C. Standard external solution, internal solution contained 200 μM GTPγS. Data leak and capacity subtracted. Cell 31059101. B. Arrhenius plot of 'steady-state' current amplitude at the end of the 150 ms voltage step. Circles, solid line, and upward error bars represent control data (30 cells, as in figure 4.2). Squares, dotted line, and downward error bars represent data recorded with GTPγS in the internal solution (17 cells). Note that the points for the two sets of data are overlaid at 15°C. Details of the plot as for 4.2.

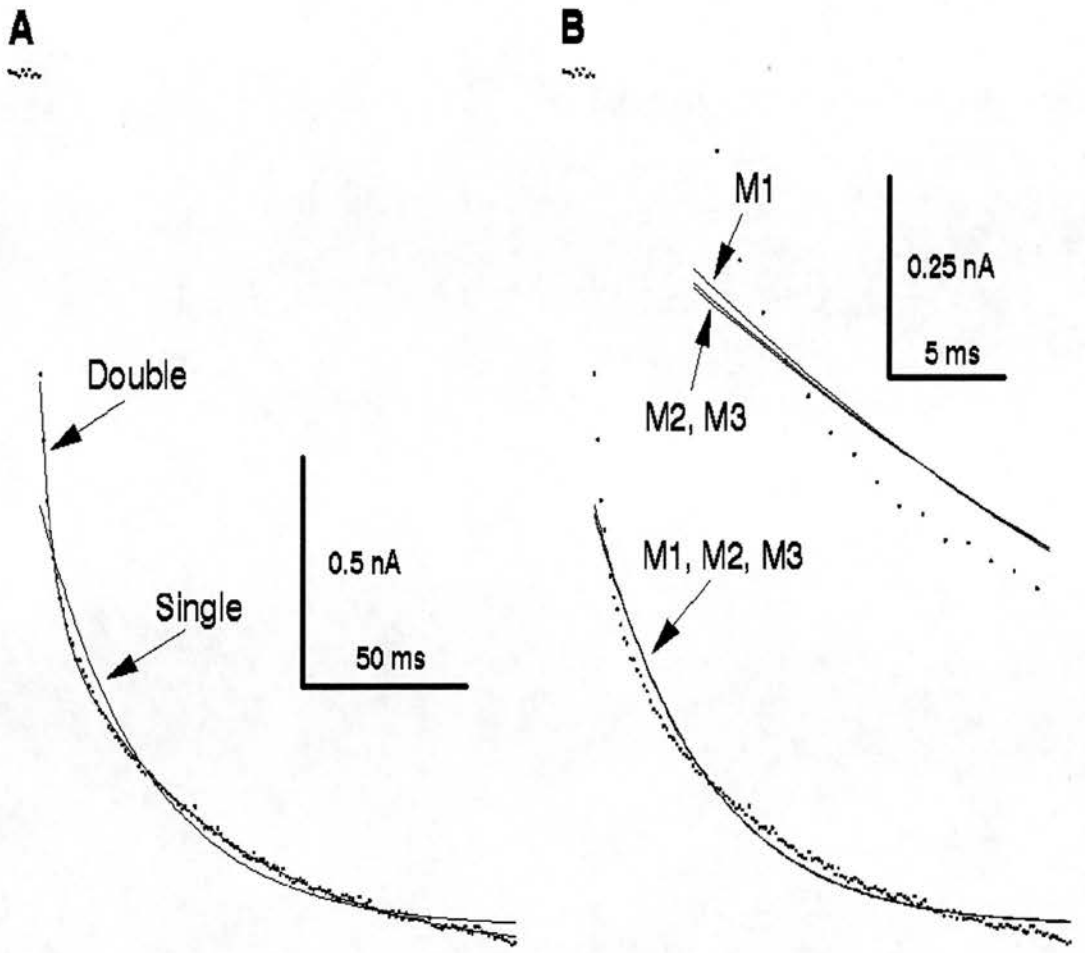

Figure 5.10: **Examples of exponential and Hodgkin and Huxley fits to the activation portion of current traces in the presence of GTPγS.** A current was elicited by a voltage step from -100 to -10 mV for 150 ms, at 20°C. Standard external solution, internal contained 200 μM GTPγS. Leak and capacity subtracted data points (digitised at 5 kHz, forward averaged every 5 points) are plotted together with best fit single and double exponential functions (A), and m^1, m^2, and m^3 Hodgkin and Huxley functions (B). In B, the first few points of the activation on an expanded time scale are also plotted as an insert. Details of the functions are given in the text. Cell 25069101.

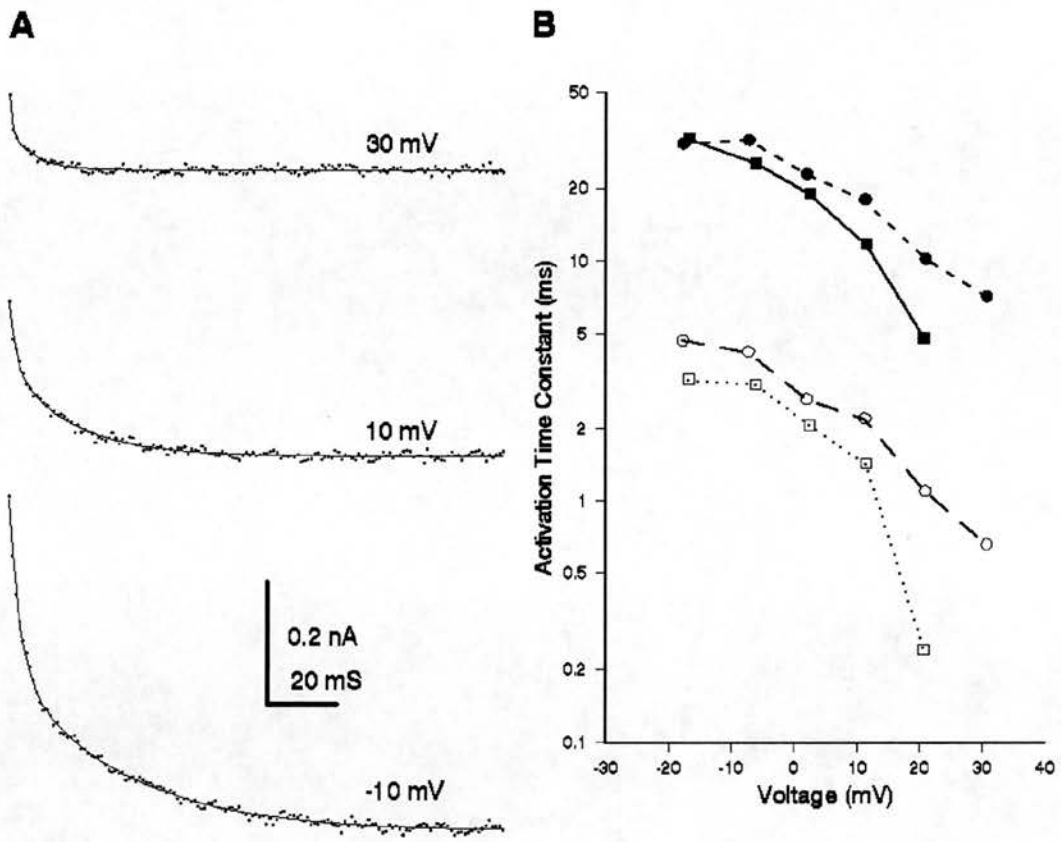

Figure 5.11: Voltage dependency of activation rate in the presence of GTPγS. A. Examples of current activation elicited by voltage jumps from -100 mV to the potentials marked, at 20°C . Data points (digitised at 5 kHz and forward averaged every 5 points) plotted together with double exponential functions with time constants of 18.10 & 3.04, 12.67 & 2.21, and 4.27 & 0.66 ms, at -10, 10 and 30 mV. Standard external solution, internal contained 200 μM GTPγS. B. Activation time constants plotted against test potential. Circles represent data at 20 and squares at 25°C. Open symbols are the fast time constant, and solid the slow time constant. Cell 28119101.

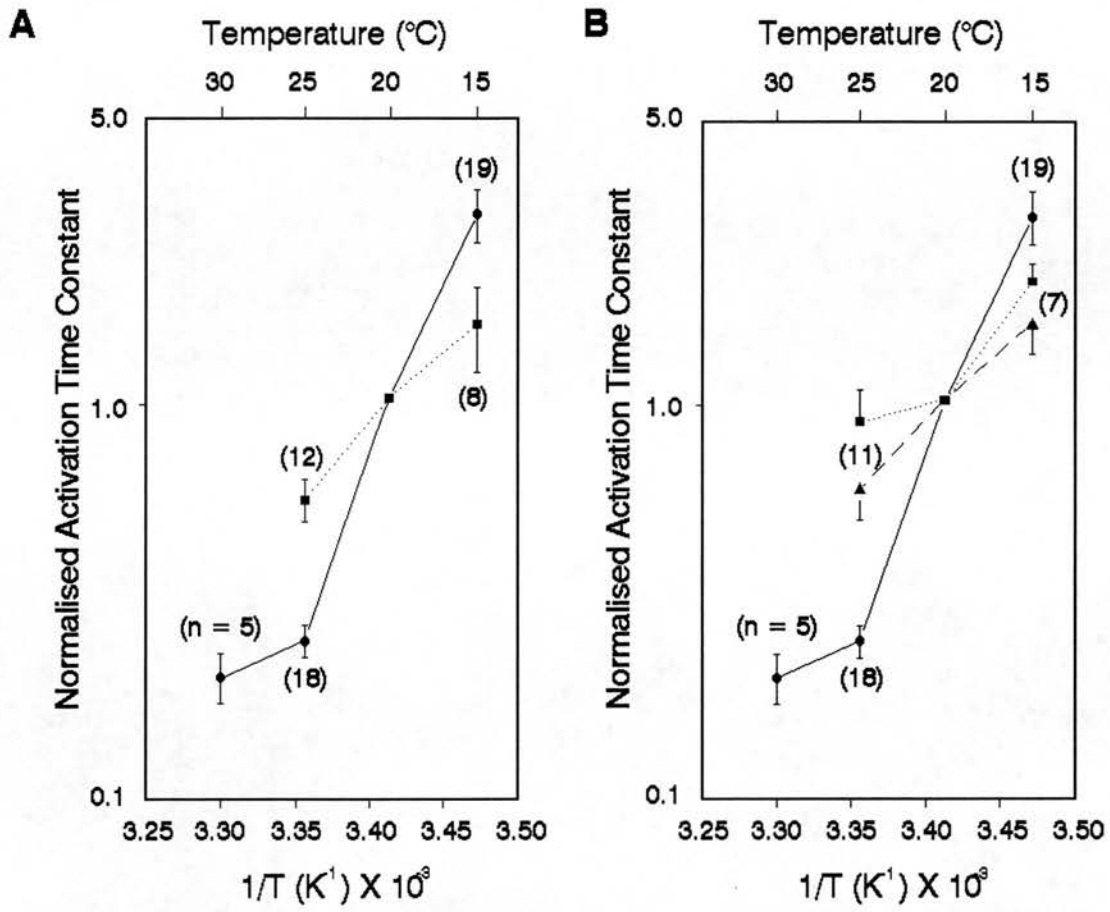

Figure 5.12: Arrhenius plots for activation time constants in the presence of GTPγS. All currents were elicited by voltage jumps from -100 to -10 mV for 150 ms. In both plots control data is represented by circles and solid lines (32 cells). In A, squares and dotted lines represent activation time constants derived from single exponential functions fitted to data when the internal solution contained 200 μM GTPγS (17 cells). In B, squares, dotted lines, and upward error bars represent the fast time constant derived from double exponential functions, while triangles, dashed lines, and downward error bars represent the slow component, both in the presence of 200 μM GTPγS (15 cells).

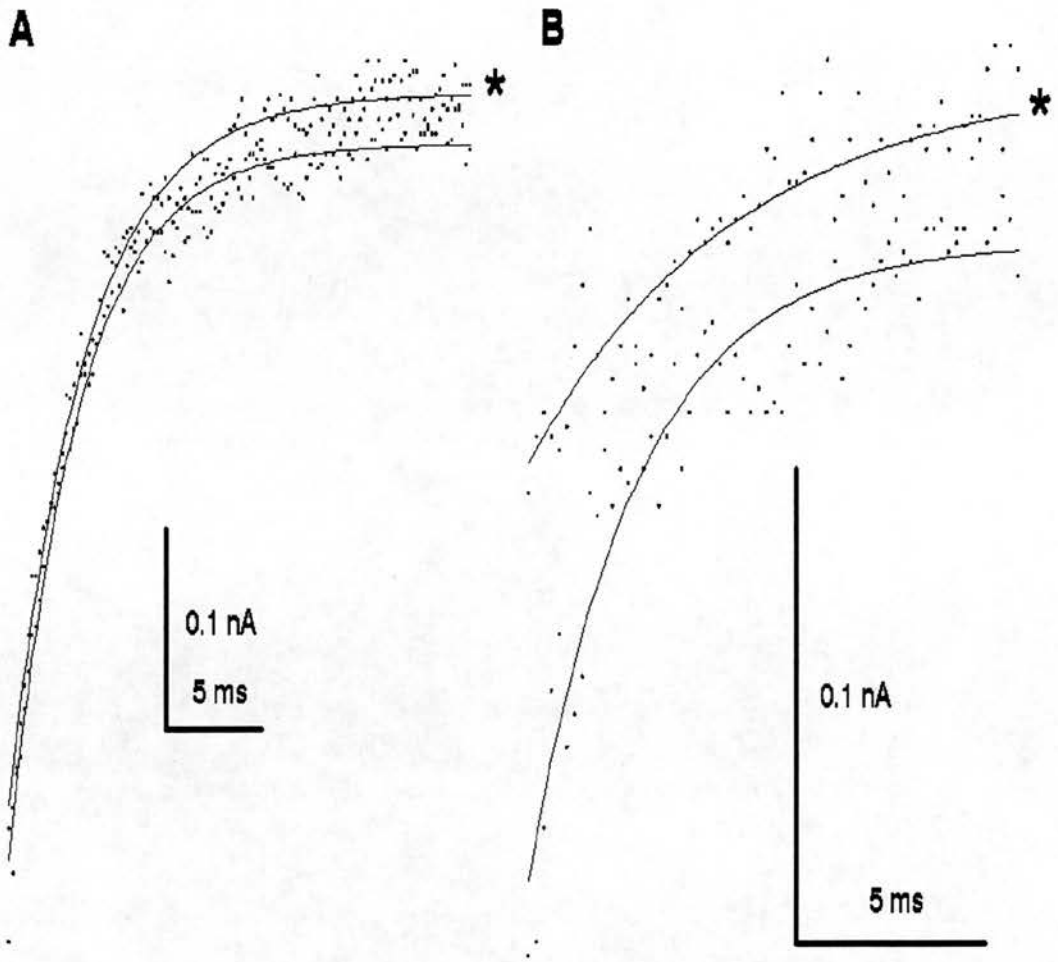

Figure 5.13: **Effect of cadmium on tail currents in the presence of GTPγS.** Tail currents recorded when the membrane potential was returned to -100 mV from a test potential of -10 mV. Internal solution contained 200 μM GTPγS. Data points (digitised at 5 kHz, no averaging) are plotted with best fit single exponential functions. A. Control current, and current recorded when the external solution contained 200 μM cadmium chloride (*). The exponentials had time constants of 3.71 and 3.98 ms respectively. Cell 27119102. B. Control current and current recorded with 2 mM cadmium in the external solution. Time constants 5.49 and 2.89 ms. Cell 20029202.

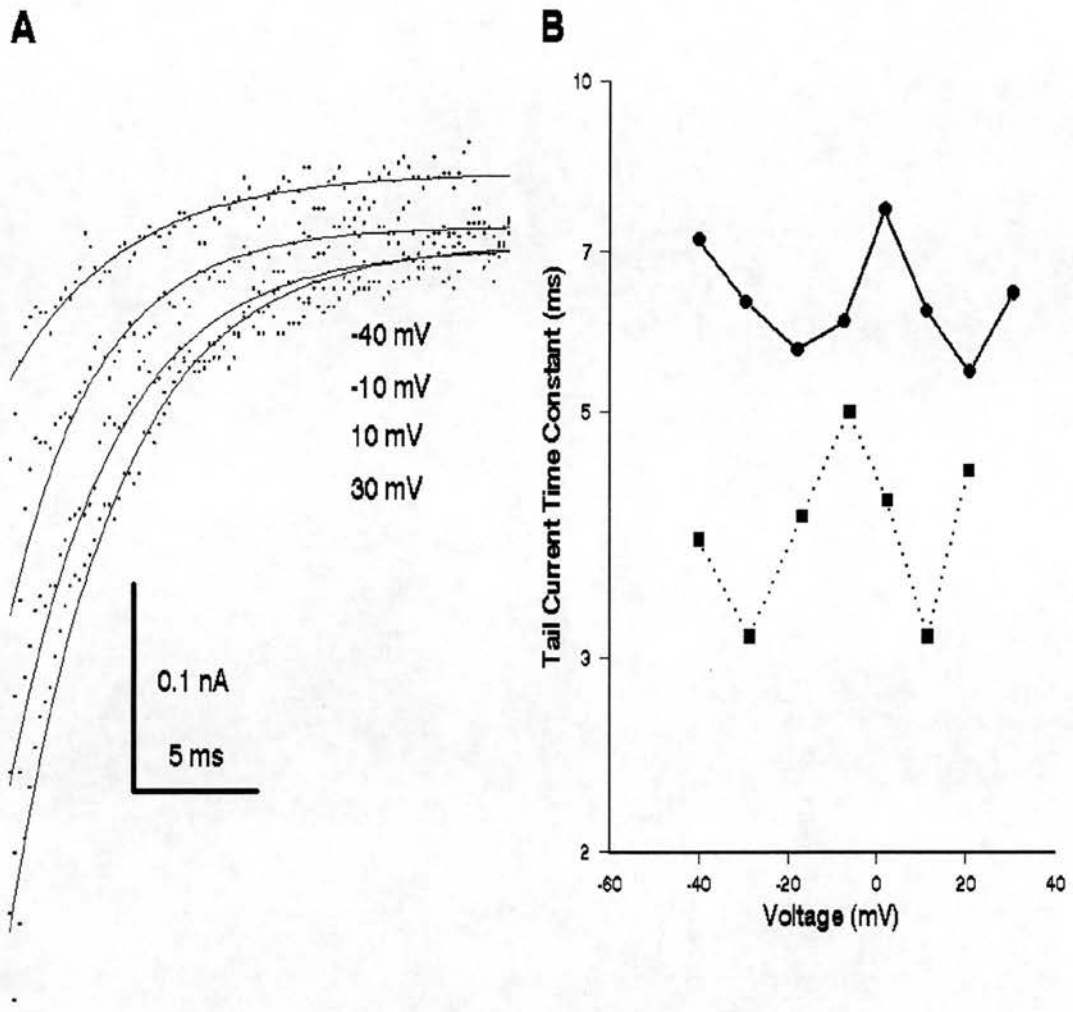

Figure 5.14: **Voltage dependency of tail currents in the presence of** GTPγS. A. Examples of tail currents elicited when the membrane potential was repolarised to -100 mV from the potentials marked, at 20°C. Data points (digitised at 5 kHz and forward averaged every 5 points) plotted together with single exponential functions. These had time constants of 7.18, 6.05, 6.19, and 6.42 ms, at -40, -10, 10 and 30 mV. Standard external solution, internal contained 200 μM GTPγS. B. Tail current time constants plotted against test potential. Circles represent data at 20 and squares at 25°C. Cell 28119101.

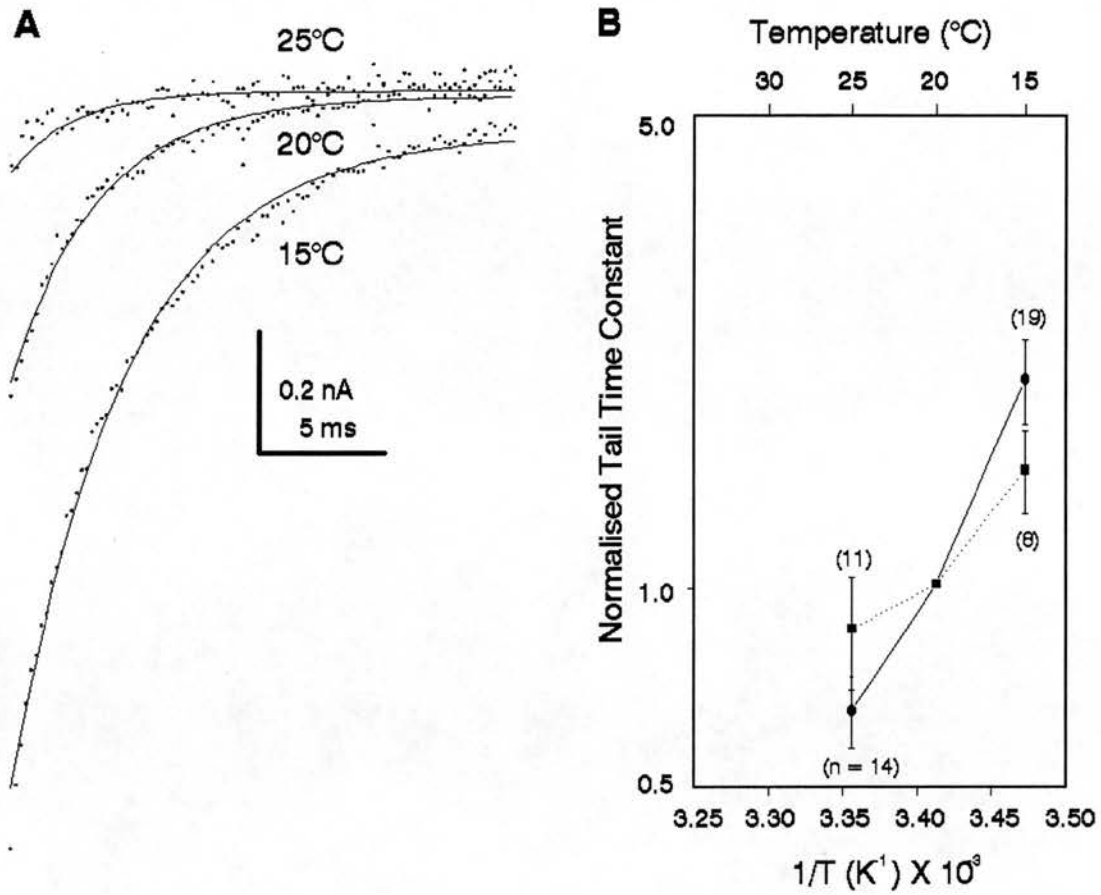

Figure 5.15: **Effect of temperature on tail currents in the presence of GTPγS.** A. Tail currents seen when the membrane potential was returned to -100 from a test potential of -10 mV for 150 ms. Standard external solution, internal contains 200 μM GTPγS. Leak and capacity subtracted data points (digitised at 5 kHz, no averaging) are plotted together with best fit single exponential functions with time constants of 2.39, 3.42 and 4.59 ms at 25, 20 and 15°C respectively. Cell 25099101. B. Arrhenius plot of time constants derived from single exponential functions. Circles and solid line, controls (30 cells), squares and dotted line with GTPγS (16 cells). Details as figure 4.2.

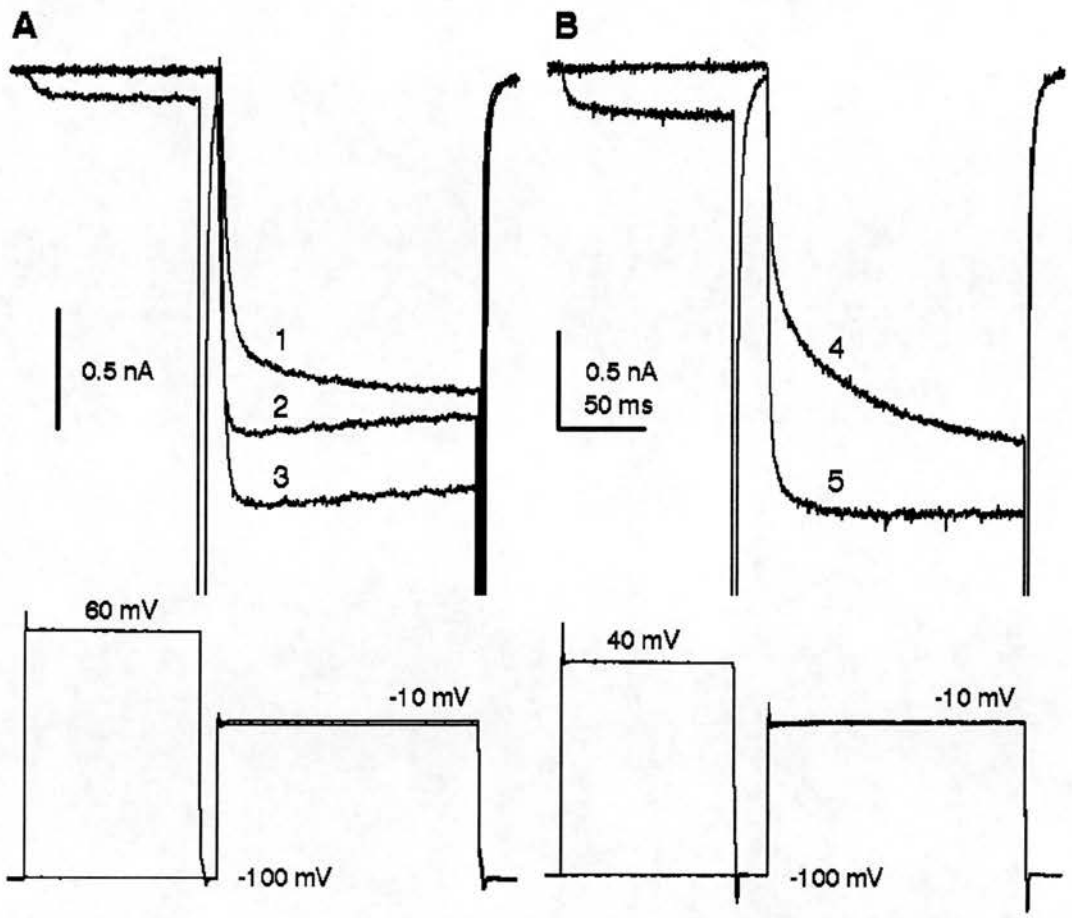

Figure 5.16: **Effect of depolarising prepulses on HVA currents.** A. Standard solutions. 3. Control current elicited by voltage step from -100 to -10 mV. 1. Application of 50 μM 8-OH-DPAT via a broken patch pipette. 2. Prepulse to 60 mV applied 10 ms prior to the test pulse, with 8-OH-DPAT still present. Cell 06029203. B. Standard external solution, internal contained 200 μM GTPγS. 4. Control current elicited by voltage step from -100 to -10 mV. 5. Prepulse to 40 mV applied 20 ms prior to the test pulse. Cell 25069101. All data leak and capacity subtracted.

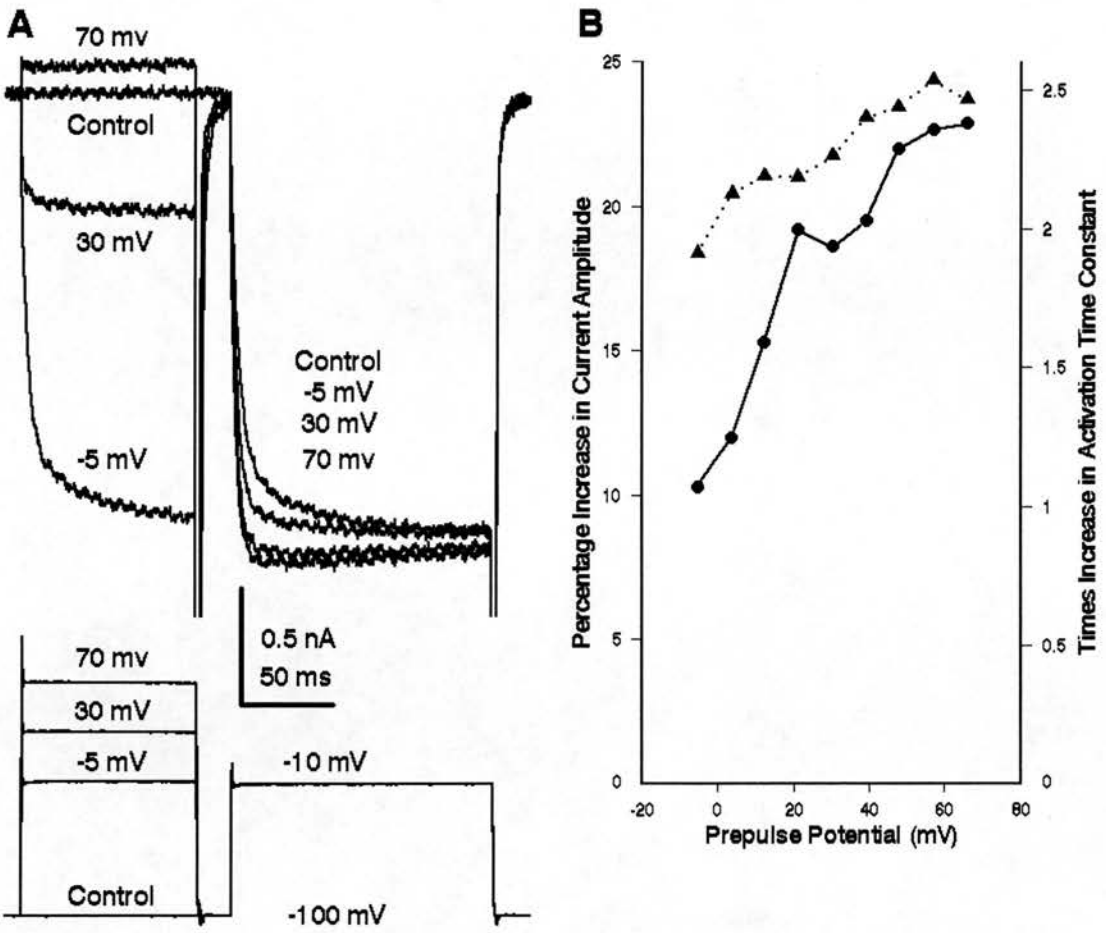

Figure 5.17: **Effect of size of depolarising prepulse on HVA current.** A. Currents elicited by voltage jumps from -100 to -10 mV with no prepulse (control), and with a prepulse for 100 ms, to -5, 30 and 70 mV 20 ms prior to the test pulse. Standard external solution, internal contained 200 μM GTPγS. Data leak and capacity subtracted. B. The percentage increase in current amplitude measured isochondrally with the peak seen with a prepulse to 70 mV (circles and solid line), and the increase in activation time constant derived from a single exponential function (triangles and dotted line), plotted against the prepulse potential. Cell 21019202.

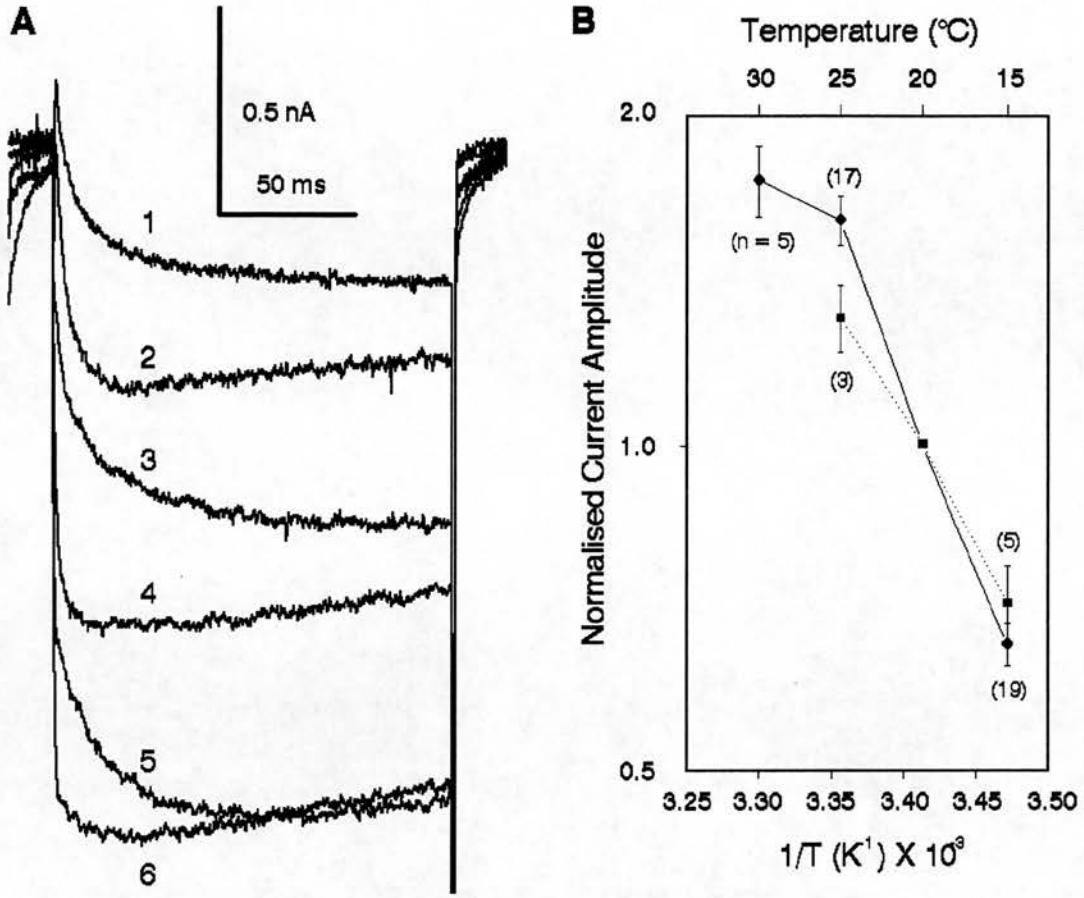

Figure 5.18: **Effect of prepulse on the temperature dependence of current amplitude in the presence of GTPγS.** A. Currents elicited by voltage steps from -100 to -10 mV with (even numbers) and without (odd numbers) a 100 ms prepulse to 40 mV, 20 ms prior to the test pulse. Currents recorded at 15 (1 & 2), 20 (3 & 4), and 25°C (5 & 6). Standard external solution, internal contained 200 μM GTPγS. Data leak and capacity subtracted. Cell 13069101. B. Arrhenius plot of control peak current amplitude (circles and solid line, 32 cells as in figure 4.2), and peak current amplitude with GTPγS plus a prepulse (squares and dotted line, 6 cells). Details of plot as for figure 4.2.

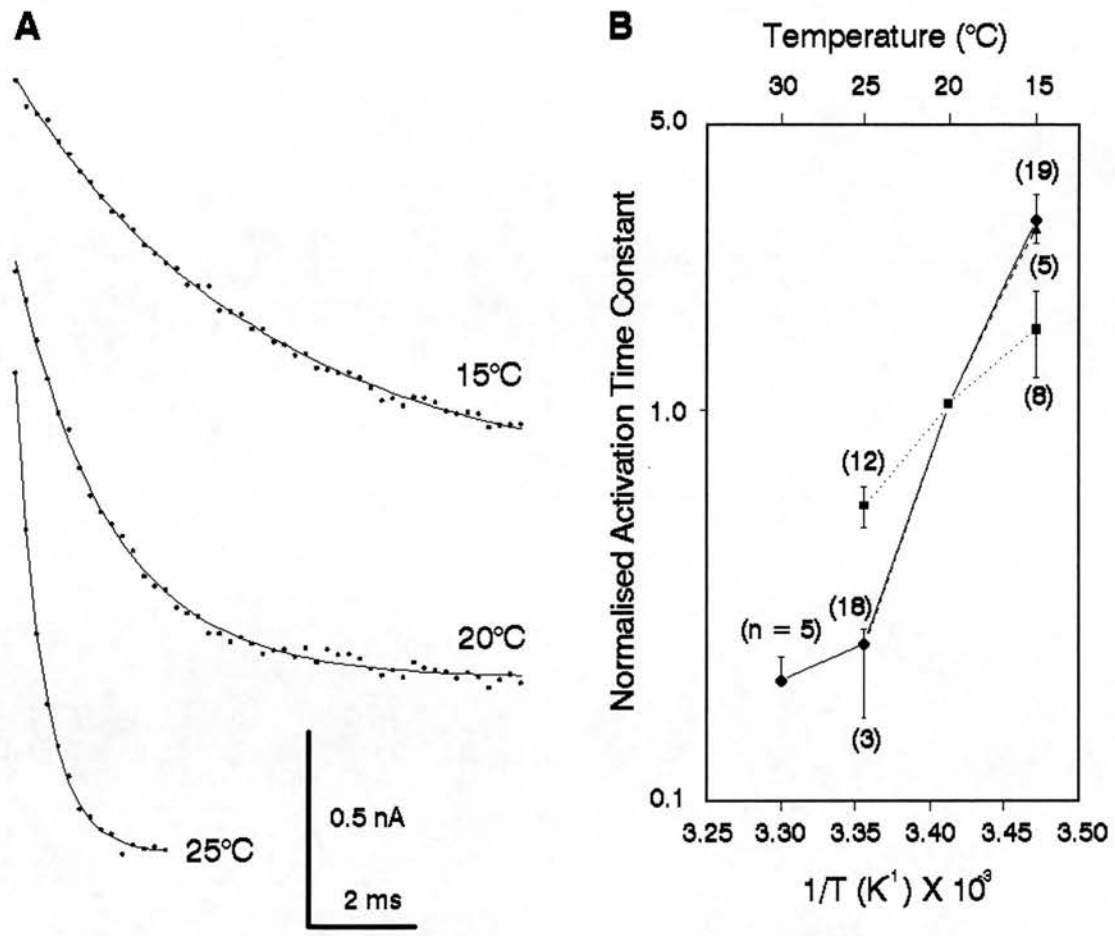

Figure 5.19: **Effect of temperature on current activation rate in the presence of GTPγS with prepulses.** A. Current data elicited by voltage steps from -100 to -10 mV, with prepulses to 40 mV for 100 ms applied 20 ms prior to the test pulse. Data points (digitised at 5 kHz, no averaging) plotted with best fit single exponentials with time constants of 4.61, 1.79, and 0.52 ms at 15, 20, and 25°C respectively. Internal solution contained 200 μM GTPγS. Cell 21069101. B. Arrhenius plot of activation time constants from single exponentials. Controls; circles, up error bars and solid line (32 cells). GTPγS; squares and dots (17 cells). GTPγS and prepulses; triangles, down error bars, and dashes (6 cells).

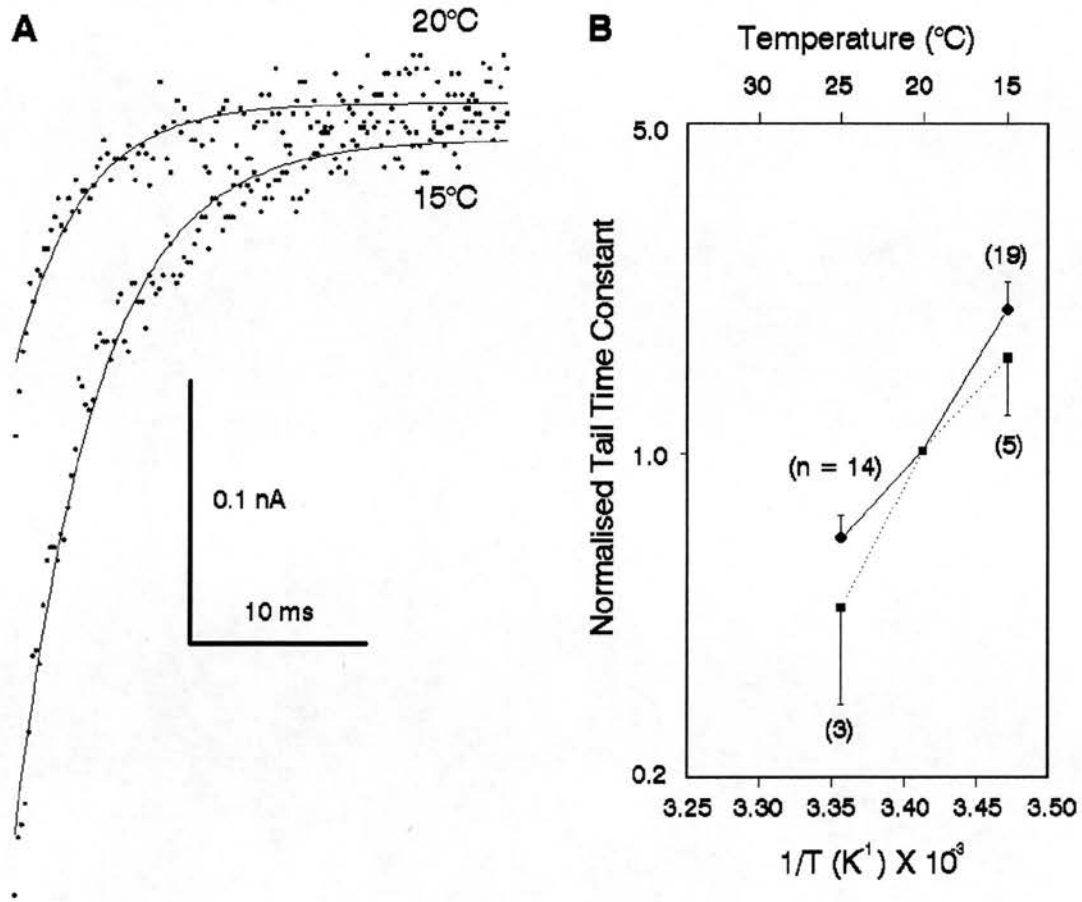

Figure 5.20: **Effect of temperature on tail currents in the presence of GTPγS with prepulses.** A. Current data elicited when the membrane potential was returned to -100 from a test potential of -10 mV, with prepulses to 40 mV for 100 ms applied 20 ms prior to the test pulse. Data points (digitised at 5 kHz, no averaging) plotted with best fit single exponentials with time constants of 4.65, 3.81 ms at 15 and 20°C respectively. Internal solution contained 200 μM GTPγS. Cell 19069103. B. Arrhenius plot of tail time constants from single exponentials. Controls; circles, up error bars and solid line (30 cells). GTPγS and prepulses; squares, down error bars, and dots (6 cells).

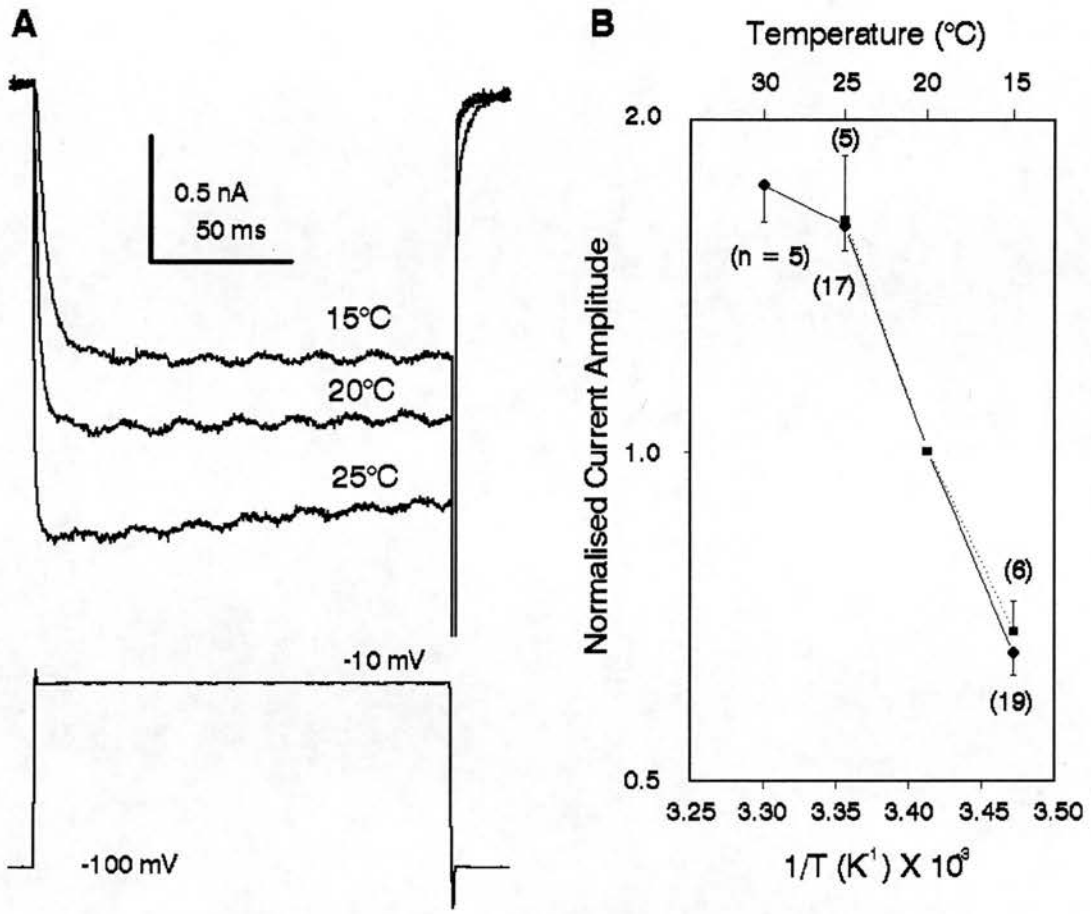

Figure 5.21: **Effect of temperature on currents in the presence of GDPβS.** A. Currents elicited by voltage steps from -100 to -10 mV at 15, 20 and 25°C. Standard external solution, internal contained 1 mM GDPβS. Data leak and capacity subtracted. Cell 12099001. B. Arrhenius plot of peak current amplitude. Control data (circles, down error bars and solid line, 32 cells, as in figure 4.2) is plotted along with that obtained with GDPβS (squares, up error bars and dotted line, 9 cells). Details of the plot as for figure 4.2.

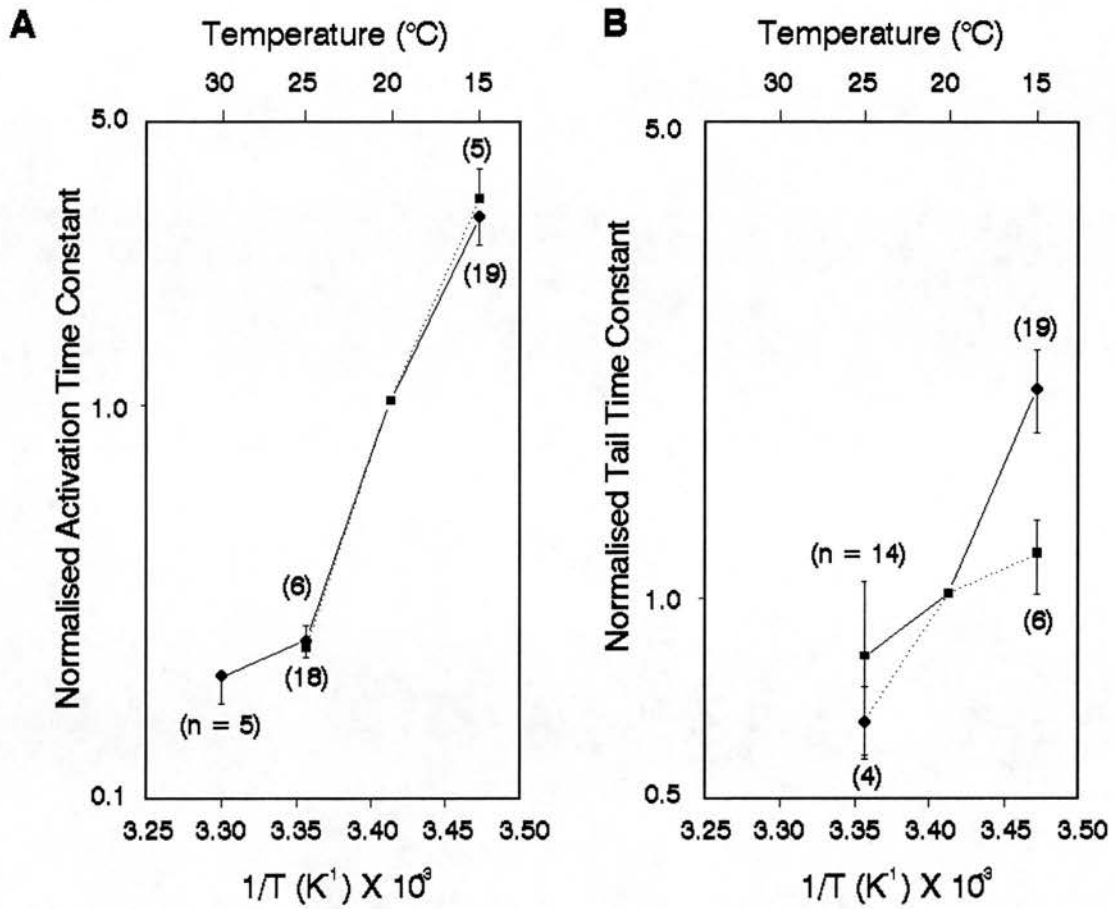

Figure 5.22: Effect of temperature on activation rate and current tails in the presence of GDPβS. A. Arrhenius plot of activation time constants derived from single exponential functions. Control data (circles, down error bars, and solid line, 32 cells) is plotted along with data recorded with 2 mM GDPβS in the internal solution (squares, up error bars, and dotted line, 9 cells). B. Arrhenius plot of tail current time constants derived from single exponential functions. Control data (circles and solid line, 30 cells) is plotted along with data recorded with GDPβS (squares and dotted line, 8 cells). Details of the plot as for figure 4.2.

Chapter 6 Effect of Inhibition of Phosphatases

The degree of phosphorylation of proteins is governed by the relative activity of the appropriate kinases and phosphatase (PP). Application of a relatively non-specific phosphatase inhibitor, OA at the crayfish neuromuscular junction, leads to increased transmitter release (Swain et al. 1991). This may be due to effects on calcium channels. A recent report has suggested that in the presence of GTPγS, increased levels of phosphorylation of an unknown protein, following the application of a phosphatase inhibitor, does in deed lead to increased calcium current amplitude in DRG neurones (Dolphin, 1992a & b). It was of great interest therefore, to examine the effect of phosphatase inhibition in DR cells, and in particular to see if this affected the activation kinetics or temperature dependence under different conditions.

1. Effect of Phosphatase Inhibition on Control Currents

1 μM of OA, was added to the internal solution used for some cells. The most obvious initial observation was that current amplitude rundown was altered by this (figure 6.1), with no obvious change in the inactivation rate, as has been observed in *Helix* neurones (Yakel, 1992). At 20°C, the average rate of run down was 0.28 ± 0.33 %/min (n = 5), which was just short of being significantly less ($p = 0.02$) than the control average of 1.08 ± 0.55 %/min (n = 6). However, as can be seen by comparing figures 3.5 and 6.1, the main difference seemed to be the amount of runup that occurred with OA. This amounted to 86.1 ± 30.2 % of the initial current amplitude (n = 5), and this was significantly more than in controls ($p = 0.002$). If the rundown was simply assessed from after the time at which the

maximum current was recorded, then the rate in the presence of OA was 1.42 ± 0.25 %/min, which was not significantly different from controls (1.16 ± 0.54). Thus it appears that inhibition of phosphatase action leads to an initial enhancement of current, with no effect on the subsequent rate of rundown of current amplitude.

The action of OA was also assessed on the voltage dependency of calcium currents. Figure 6.2 illustrates currents elicited by different depolarisations, in the presence of OA, together with an IV plot. Qualitatively the currents were similar to control currents, though with possibly less inactivation. The IV plot was also similar to controls, with a maximum current seen at around -10 mV, though the section of the curve to the left of the maximum was usually extremely steep. This was reflected by the finding that inclusion of OA in the pipette solution caused a significant shift of V_h of Boltzman activation functions in the positive direction to -19.06 ± 1.87 mV (n = 7), compared to -25.65 ± 1.11 mV (n = 16) seen in controls. However, while the V_h values were more positive, the rate of leftward shift with time was no different to controls at 0.27 ± 0.04 mV/min (n = 5) compared to 0.26 ± 0.07 mV/min (n = 6, see figure 6.3).

The other main quantitative effect seen with OA was that the maximum peak amplitude elicited by a voltage step from -100 to -10 mV at 20°C was significantly higher than controls ($p = 0.0002$), being 2.28 ± 0.15 nA (n = 14) compared to 1.56 ± 0.09 nA (n = 42). The average values for τ_a (2.85 ± 0.29 ms, n = 14) and τ_t (3.08 ± 0.42 ms, n = 14), were no different to the equivalent controls (2.30 ± 0.18, n = 41, and 3.03 ± 0.33 ms, n = 38).

The temperature dependence of current amplitude (figure 6.4) followed a familiar course, with the Q_{10} for the peak amplitude being

slightly higher than that for the 'steady state' amplitude (1.87, CI = 0.65 - 5.37, and 1.82, CI = 0.68 - 4.92 respectively, n = 12,6). Neither value was significantly different to control values, as was the case for the Q_{10}'s for τ_a and τ_t (figure 6.5) in the presence of OA (10.00, CI = 1.49 - 67.23, and 1.18, CI = 0.83 - 1.70, n = 12,6).

2. Effect of Phosphatase Inhibition on 8-OH-DPAT Action

Figure 6.6 illustrates currents recorded with 1 μM OA in the internal solution, with and without 50 μM 8-OH-DPAT being applied by diffusion from a broken patch pipette. The reduction in peak current amplitude by 8-OH-DPAT at 20°C was identical to controls (41.0 ± 5.4%, n = 9, versus 39.4 ± 4.3, n = 13), as were the Q_{10} values for the peak and 'steady state' amplitude (1.76, CI = 0.70 - 4.44, and 1.75, CI = 0.49 - 6.24, n = 12,6, figure 6.7). These were lower than the control values, but were not significantly different from values obtained with 8-OH-DPAT but no OA. It may therefore be that phosphorylation at sites sensitive to de-phosphorylation by PPs blocked by this dose of OA are not involved in the reduction in current amplitude mediated by 8-OH-DPAT.

As far as activation kinetics were concerned, while 8-OH-DPAT still led to an increase in τ_a, this was less than in the control situation when there was no OA in the internal solution, at 1.43 ± 0.15, compared to 3.42 ± 0.87 fold, though this did not reach the significance level (p = 0.05). However the activation data was less often biexponential (2/9 rather than 6/13). The rate of phosphorylation generally is likely to be considerably slower than the rate of activation of calcium currents, so it would seem unlikely that

phosphorylation has to occur for channels to open when the membrane potential is depolarised. However, the prevailing degree of phosphorylation may play a role in the mechanisms underlying current activation. If this is the case than it might be expected that OA might alter the Q_{10} value for τ_a. This is indeed the case and the reduction in the Q_{10} value seen with 8-OH-DPAT was reversed by OA to control levels (14.05, CI = 1.81 - 109.1, n = 12,6, figure 6.8A).

Tail current τ_t showed no evidence of being prolonged by 8-OH-DPAT in the presence of OA, the average time at 20°C being 2.40 ± 0.27 ms (n = 9), and the Q_{10} was also not dissimilar to the control value (1.93, CI = 0.56 - 6.66, n = 12,6, figure 6.8B).

3. Effect of Phosphatase Inhibition on GTPγS Action

The addition of OA along with GTPγS to the internal solution, led to currents with a different qualitative nature to those seen with GTPγS alone (figure 6.9A). The 'steady state' amplitude at 20°C was found to be slightly increased (1.20 ± 0.20, n = 7, versus 1.05 ± 0.09 nA, n = 23), but more obviously, the currents normally peaked during the test pulse. This peak amplitude was on average 1.32 ± 0.17 nA (n = 7), and significantly larger than the 'steady state' current amplitude with GTPγS alone (p = 0.001).

The Q_{10} values for the peak and 'steady state' amplitudes were 2.20, CI = 0.81 - 5.98, and 1.72, CI = 0.63 - 4.72, n = 14,7, figure 6.9B), being similar to control values, with the peak value being statistically higher than the 'steady state' when pairs were compared ($p < 0.001$).

Similar to the situation with 8-OH-DPAT, the addition of OA to the

internal solution along with GTPγS had a considerable effect on current activation. GTPγS had the effect of increasing τ_a from 2.30 ± 0.18 (n = 41) to 18.27 ± 2.59 ms (n = 22) at 20°C. However when OA was also present, the increase in τ_a was mostly reversed, the average being 3.98 ± 0.82 ms (n = 9). In addition, while the current activation of 23 out of 23 cells, with GTPγS at 20°C, was biexponential, this was the situation for only 2 out of 9 cells when OA was present.

Along with the return of the activation kinetics towards normal, OA also reversed the decrease in the Q_{10} value for τ_a induced by GTPγS, with it being 15.95 (CI = 0.99 - 257.4, n = 14,7) and not significantly different from the control (figure 6.10A).

OA also seemed to block the prolonged τ_t produced by GTPγS, with the average at 20°C being 3.06 ± 0.61 ms (n = 7), however this was not a significant effect. This may be due to excessive variability of the tail currents, which was also reflected in their Q_{10} value of 4.93 (CI = 0.31 - 77.96, n = 14,7, see figure 6.10B). While this is significantly higher than control, its relevance seems unclear.

The action of the more specific I1PP was also investigated. This inhibitor is able to increase calcium current amplitude in the presence of GTPγS in DRG cells (Dolphin, 1992a & b). Unfortunately the results with I1PP were very inconsistent (figure 6.11). The addition of 1 μM of the active fragment (residues 9 - 41) of this peptide, along with 200 μM GTPγS, to the internal solution led to a reduction in the quality of the seals between the pipettes and the cell membranes. Perhaps as a result of this, currents recorded with I1PP plus GTPγS were often of small amplitude, with the 'steady state' amplitude at 20°C averaging 0.53 ± 0.12 nA (n = 7). The nature of

the currents was also extremely variable, with some exhibiting slow biexponential activation, as seen with GTPγS alone, and some with fast mono-exponential activation, as in controls (figure 6.11). Of seven cells tested at 20°C, five showed clear current peaks during the 150 ms test pulse, while two increased in amplitude throughout. This inconsistency could be as a result of a long period being needed for the equilibrium of the intracellular concentration of a molecule as large as I1PP to be reached. The time constant (τ, in seconds) for this has been reported to be

$$\tau = \left(\frac{r}{r_o}\right)^3 \alpha R_A M^{1/3} \qquad (6.1)$$

where r is the cell radius in μm, r_o is 7.7, α is 0.6 ± 0.17, R_A is the access resistance in MΩ, and M is the molecular weight in daltons of the molecule in question (Pusch & Neher, 1988). The active fragment of I1PP contains 32 amino acids and so M would be approximately 32 X 150 = 4800 daltons. R_A is at least R_e and so 10 MΩ, and the minimum r was 10 μm. This gives τ = 227 minutes, clearly longer than the life span of the cells, so the concentration of I1PP between individual cells may well have varied enormously.

4. Effect of Phosphatase Inhibition on the Action of Prepulses

Figure 6.12 illustrates the effect of a depolarising prepulse prior to a standard test pulse with both GTPγS and 8-OH-DPAT, when the internal solution contained OA. It can be seen that while 8-OH-DPAT causes a 32.4% reduction in peak current, a prepulse had little effect

on reversing this. Not enough cells were examined to know if there was significantly less effect in this respect compared to controls. It can also be clearly seen that τ_a is very similar in all three current records in figure 6.12A, and these were 3.01, 2.61, and 2.87 ms for the control with OA, with 8-OH-DPAT and OA, and with 8-OH-DPAT, OA, and prepulse. Figure 6.12B shows the effect of a prepulse on currents elicited in the presence of both GTPγS and OA. In this case, the prepulse did lead to an increase in current amplitude, but again there was little effect on τ_a. The average increase in 'steady state' current amplitude was 9.5 ± 3.1% (n = 7), which was no different to the effect seen with no OA (11.3 ± 2.2%, n = 7). However, the increase in τ_a was only 1.33 ± 0.07 fold, which was significantly less than the controls (5.70 ± 2.04, p = 0.001). This is clearly to be expected since the addition of OA to GTPγS does lead to a reversal of the increased τ_a.

Figures 6.13 and 6.14 show that, as would be expected, prepulses in addition to GTPγS and OA had no effect on the Q_{10} values for the peak (1.82, CI = 0.64 - 5.20) and 'steady state' amplitudes (1.53, CI = 0.58 - 4.09), and τ_t (4.07, CI = 0.21 - 79.03, n = 14,7). The increase in the Q_{10} for τ_a induced by the inclusion of OA in the internal solution, was not further enhanced by prepulses (14.29, CI = 1.84 - 111.2, n = 14,7).

The Q_{10} values quoted in this chapter are summarised in table 6.1.

Table 6.1 - Effect of Phosphatase Inhibitor on Temperature Dependence

	Q_{10} Mean (95% CI, n = measurements, cells)
Application of 1 μM OA	
Peak Amplitude	1.87 (CI = 0.65 - 5.37, n = 12,6)
'Steady State' Amplitude	1.82 (CI = 0.68 - 4.92, n = 12,6)
Activation Time Constant	10.00 (CI = 1.49 - 67.23, n = 12,6)
Tail Current Time Constant	1.18 (CI = 0.83 - 1.70, n = 12,6)
Application of 1 μM OA + 50 μM 8-OH-DPAT	
Peak Amplitude	1.76 (CI = 0.70 - 4.44, n = 12,6)
'Steady State' Amplitude	1.75 (CI = 0.49 - 6.24, n = 12,6)
Activation Time Constant	14.05 (CI = 1.81 - 109.1, n = 12,6)
Tail Current Time Constant	1.93 (CI = 0.56 - 6.66, n = 12,6)
Application of 1 μM OA + 200 μM GTPγS	
Peak Amplitude	2.20 (CI = 0.81 - 5.98, n = 14,7)
'Steady State' Amplitude	1.72 (CI = 0.63 - 4.72, n = 14,7)
Peak Amplitude with Prepulse	1.82 (CI = 0.64 - 5.20, n = 14,7)
'Steady State' Amplitude with Prepulse	1.53 (CI = 0.58 - 4.09, n = 14,7)
Activation Time Constant	15.95 (CI = 0.99 - 257.4, n = 14,7)
Activation Time Constant with Prepulse	14.29 (CI = 1.84 - 111.2, n = 14,7)
Tail Current Time Constant	4.93 (CI = 0.31 - 77.96, n = 14,7)
Tail Current Time Constant with Prepulse	4.07 (CI = 0.21 - 79.03, n = 14,7)

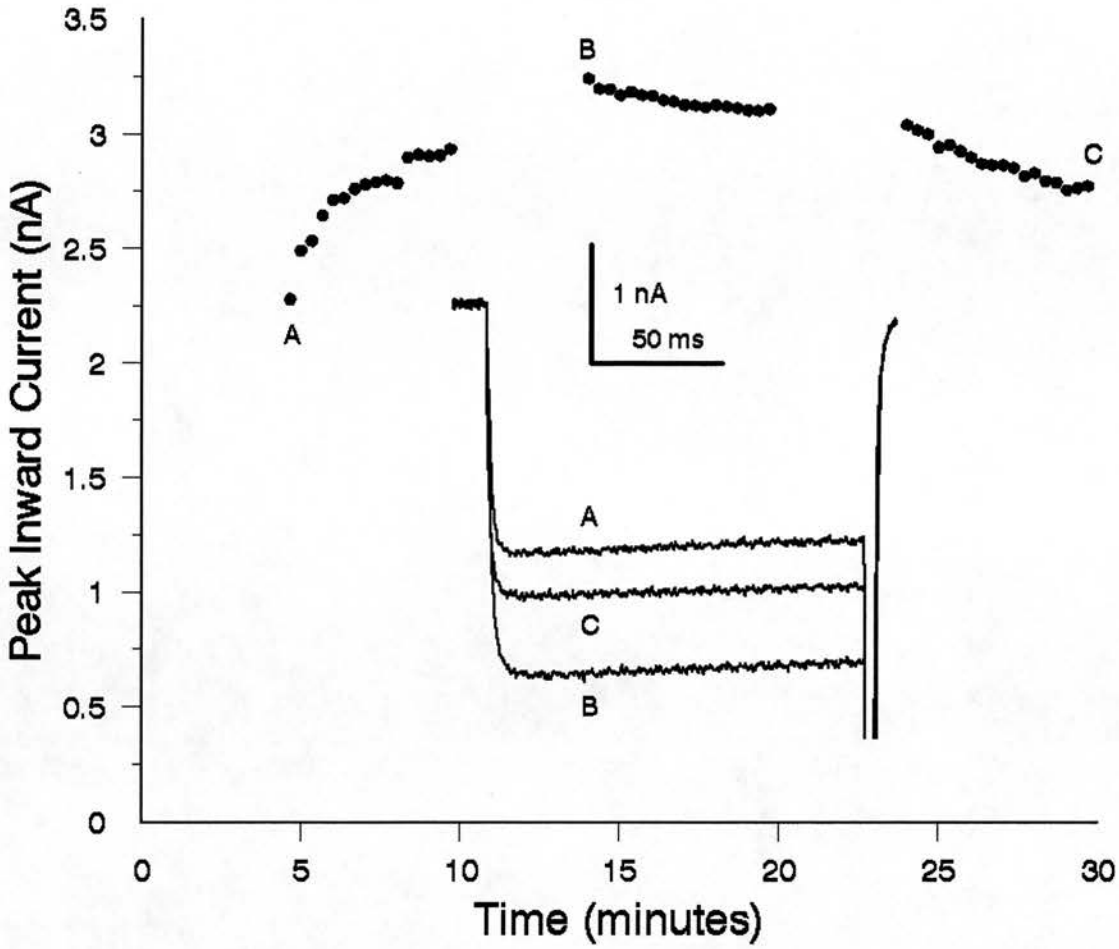

Figure 6.1: **Rundown of high threshold current in the presence of OA.** Currents were elicited by voltage steps from -100 to -10 mV every 20 seconds, at 20°C. Peak current is plotted against time. Time 0 is 5 minutes after whole-cell mode was achieved, and the bath solution was switched over to the standard external solution. Internal solution contained 1 μM OA. The breaks in the data beginning at times 0, 10, and 20 minutes are when the current voltage relationship was determined. The insert illustrates currents recorded at the beginning (A), the peak (B) and end (C) of the experiment. All data leak and capacity subtracted. Cell 22019202.

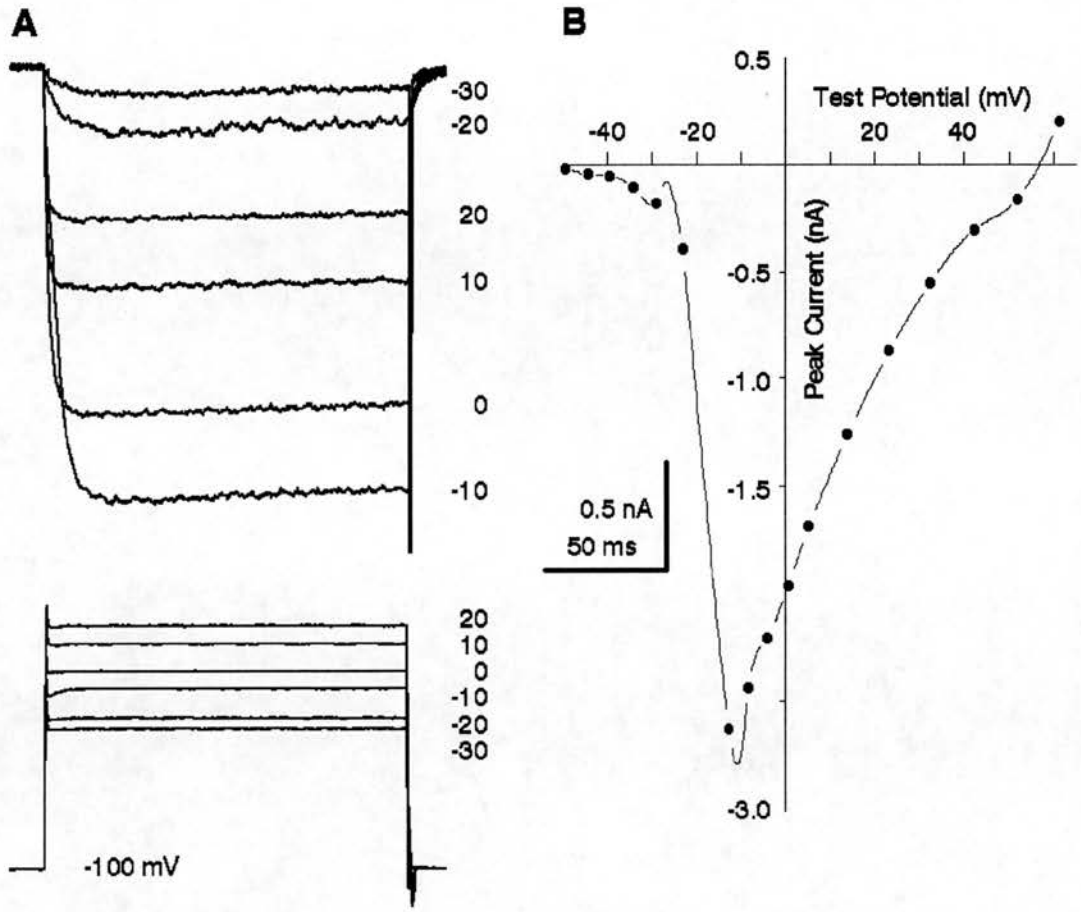

Figure 6.2: **Current/voltage relationship in the presence of OA.** A. Currents were elicited by voltage jumps from -100 mV to a series of depolarised levels for 150 ms, at 20°C. The nominal test potentials are illustrated alongside both the voltage and appropriate current traces. B. Plot of test potentials against peak current amplitude, with data fitted with a cubic spline. Examples of currents are leak and capacity subtracted, but the raw data is plotted in section B. Standard external solution, internal contained 1 μM OA. Cell 05029201.

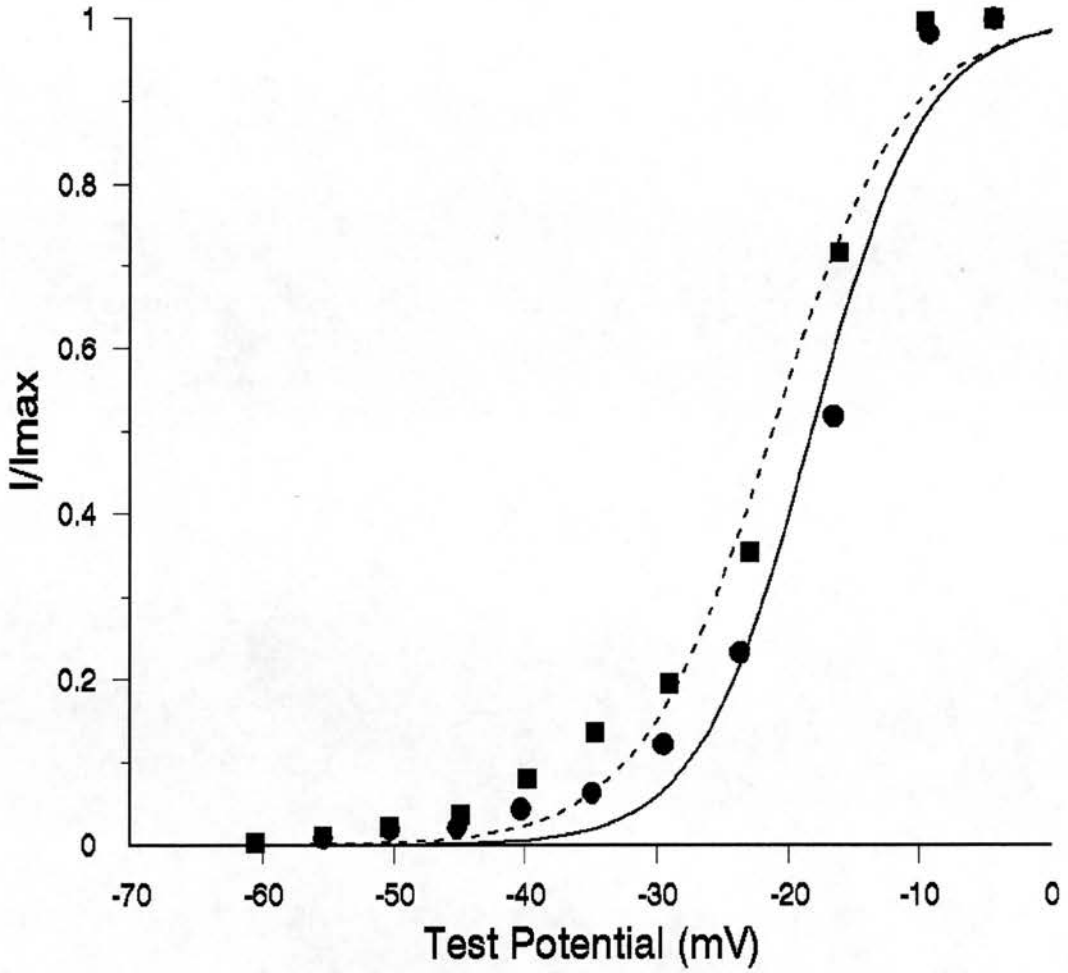

Figure 6.3: Voltage dependency of activation with time in the presence of OA. Current/voltage data was obtained, and the peak I/I_{max} plotted against the test potential, at times 0 (circles), and 30 minutes (squares) after the commencement of recording. Data is fitted by modified Boltzman activation functions whose V_h and k are -18.17 and 4.27 (solid line), and -21.19 and 5.06 mV (dashed line) at 0 and 30 minutes respectively. Standard external solution, internal contained 1 μM OA. Cell 22019201.

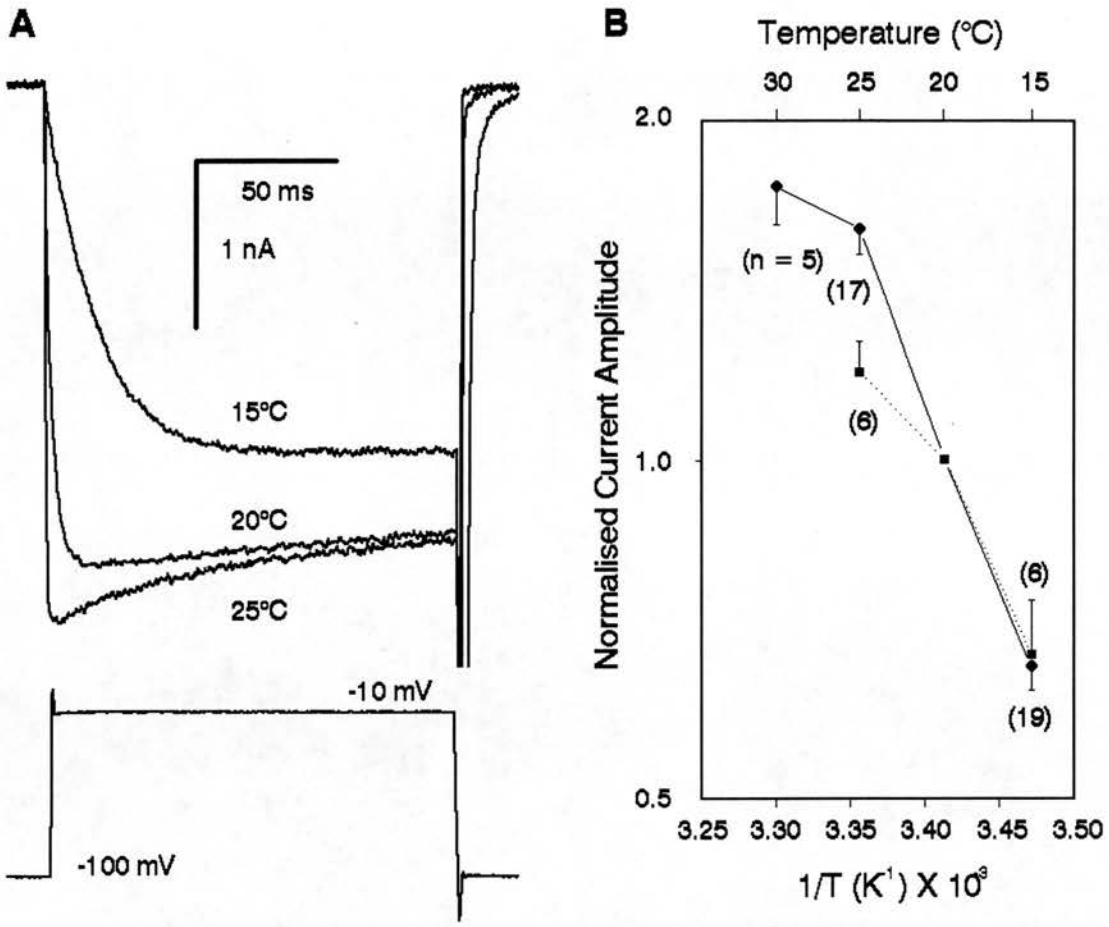

Figure 6.4: **Effect of temperature on currents in the presence of** OA. A. Currents elicited by voltage steps from -100 to -10 mV at 15, 20 and 25°C. Standard external solution, internal contained 1 μM OA. Data leak and capacity subtracted. Cell 31019201. B. Arrhenius plot of peak current amplitude. Control data (circles, down error bars and solid line, 32 cells, as in figure 4.2) is plotted along with that obtained with OA (squares, up error bars and dotted line, 6 cells). Details of the plot as for figure 4.2.

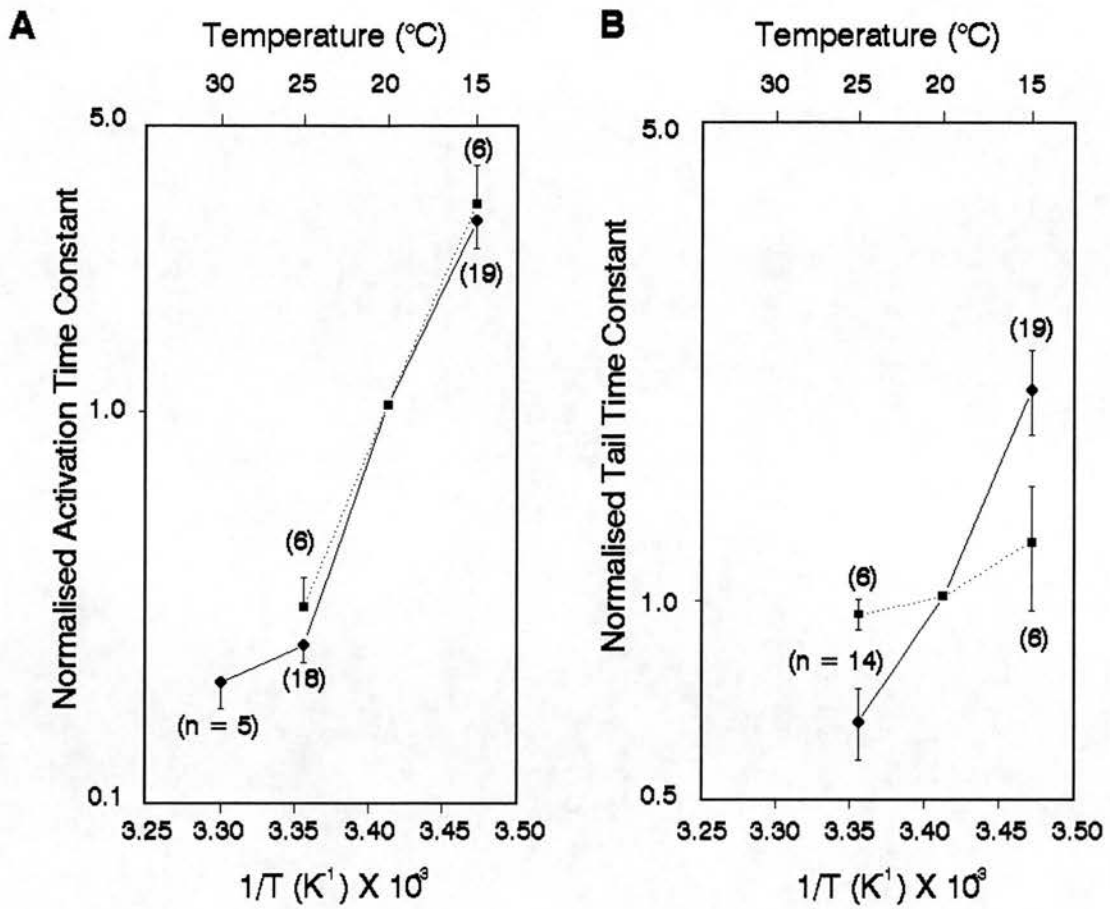

Figure 6.5: **Effect of temperature on activation rate and current tails in the presence of** OA. A. Arrhenius plot of activation time constants derived from single exponential functions. Control data (circles, down error bars, and solid line, 32 cells) is plotted along with data recorded with 1 μM OA in the internal solution (squares, up error bars, and dotted line, 6 cells). B. Arrhenius plot of tail current time constants derived from single exponential functions. Control data (circles and solid line, 30 cells) is plotted along with data recorded with 1 μM OA (squares and dotted line, 6 cells). Details of the plot as for figure 4.2.

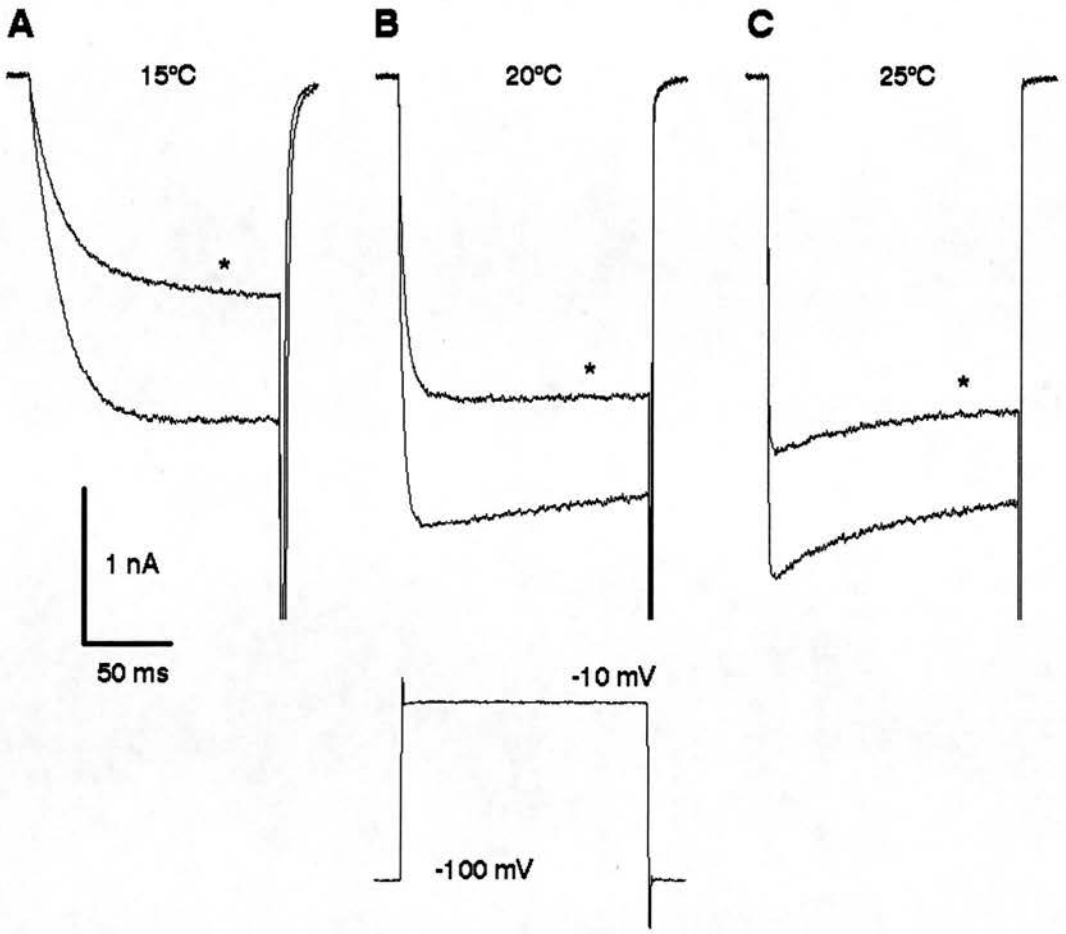

Figure 6.6: **Effect of temperature on currents in the presence of OA and 8-OH-DPAT.** Currents were elicited by voltage steps from -100 to -10 mV at 15 (A), 20 (B) and 25°C (C). 50 μM 8-OH-DPAT was applied via a broken patch pipette placed within 50 μm of the cell, for the traces marked with an asterisk (*). Standard external solution, internal contained 1 μM OA. Control data as in figure 6.4.

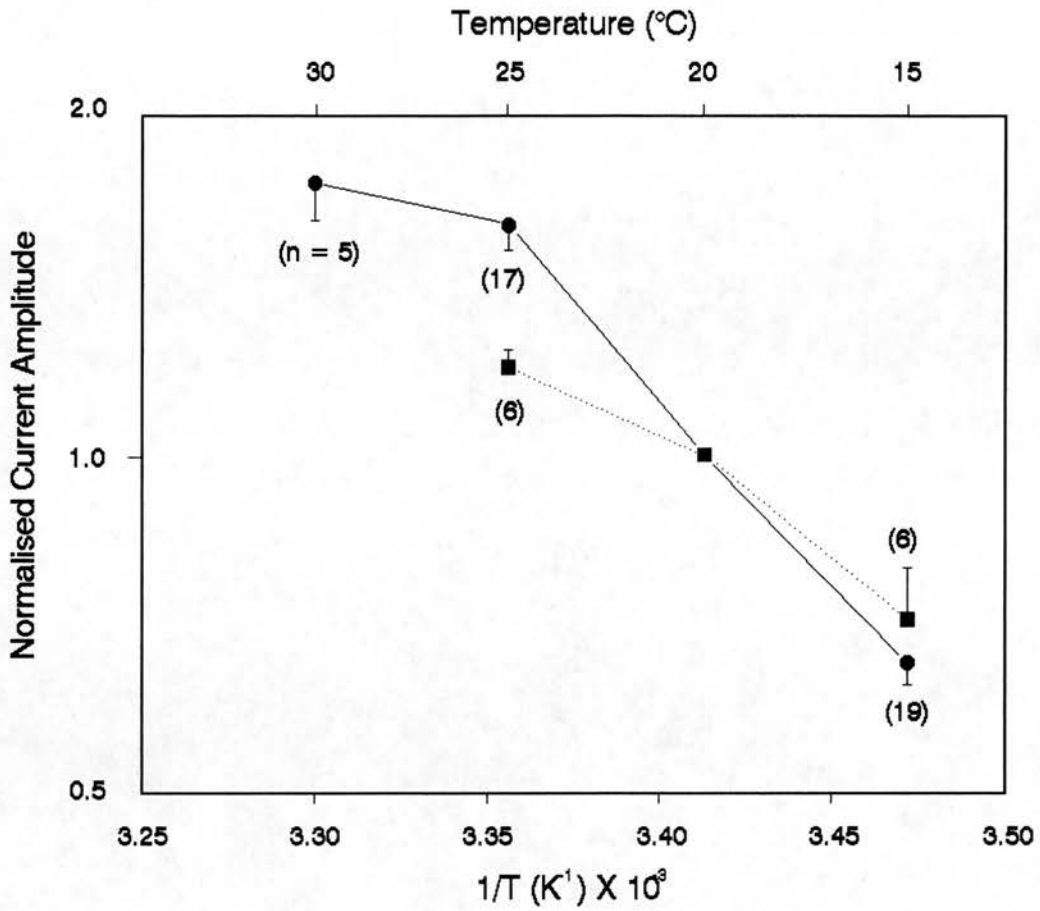

Figure 6.7: **Arrhenius plot of peak current amplitude in the presence of OA and 8-OH-DPAT.** Control data (circles, down error bars and solid line, 32 cells, as in figure 4.2) is plotted along with that obtained when the internal solution contained 1 μm OA and 50 μm 8-OH-DPAT was applied via a broken patch pipette (squares, up error bars and dotted line, 6 cells). Details of the plot as for figure 4.2.

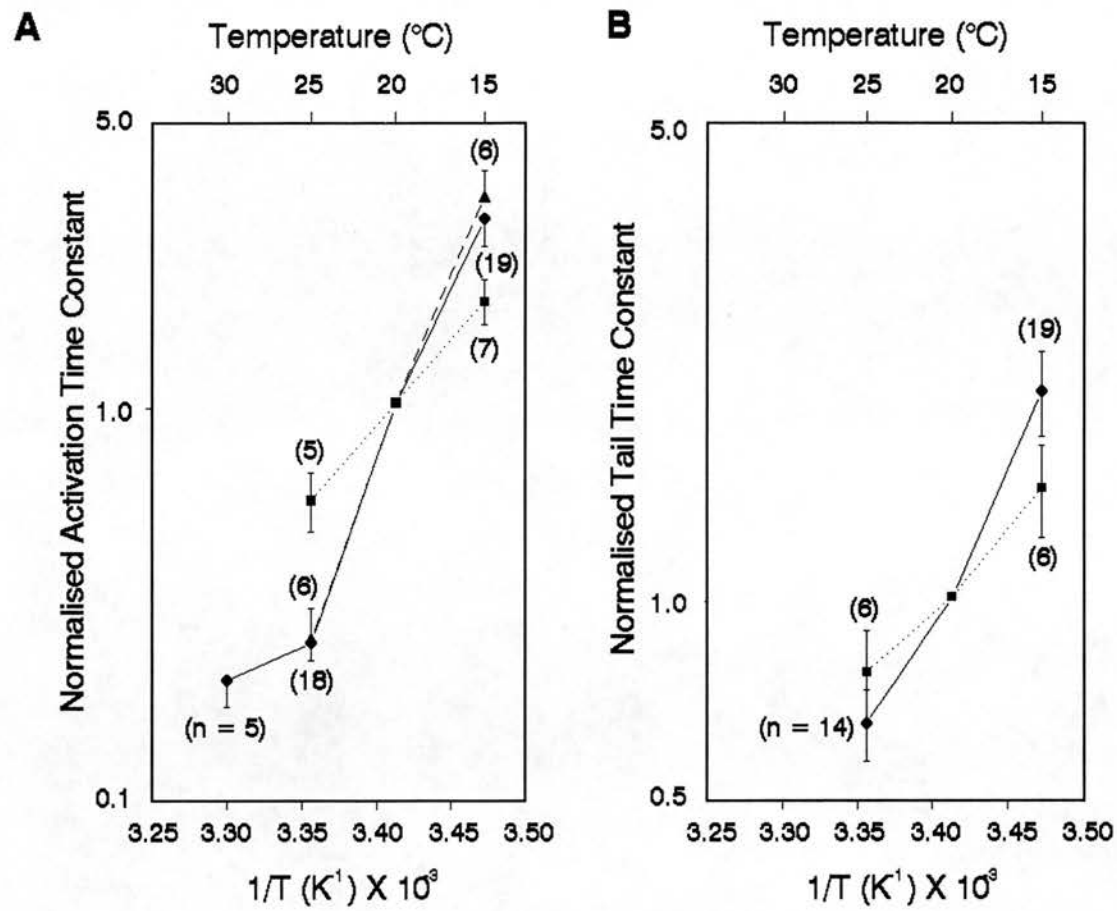

Figure 6.8: **Effect of temperature on activation rate and current tails in the presence of OA and 8-OH-DPAT.** A. Arrhenius plot of activation time constants derived from single exponential functions. Control data (circles, down error bars, solid line, 32 cells) is plotted along with data recorded with 50 μM 8-OH-DPAT (squares, dotted line, 6 cells), and data with 8-OH-DPAT when 1 μM OA was present in the internal solution (triangles, up error bars, dashed line). B. Arrhenius plot of tail current time constants derived from single exponential functions. Control data (circles and solid line, 30 cells) is plotted with data recorded with 8-OH-DPAT and 1 μm OA (squares and dotted line, 6 cells).

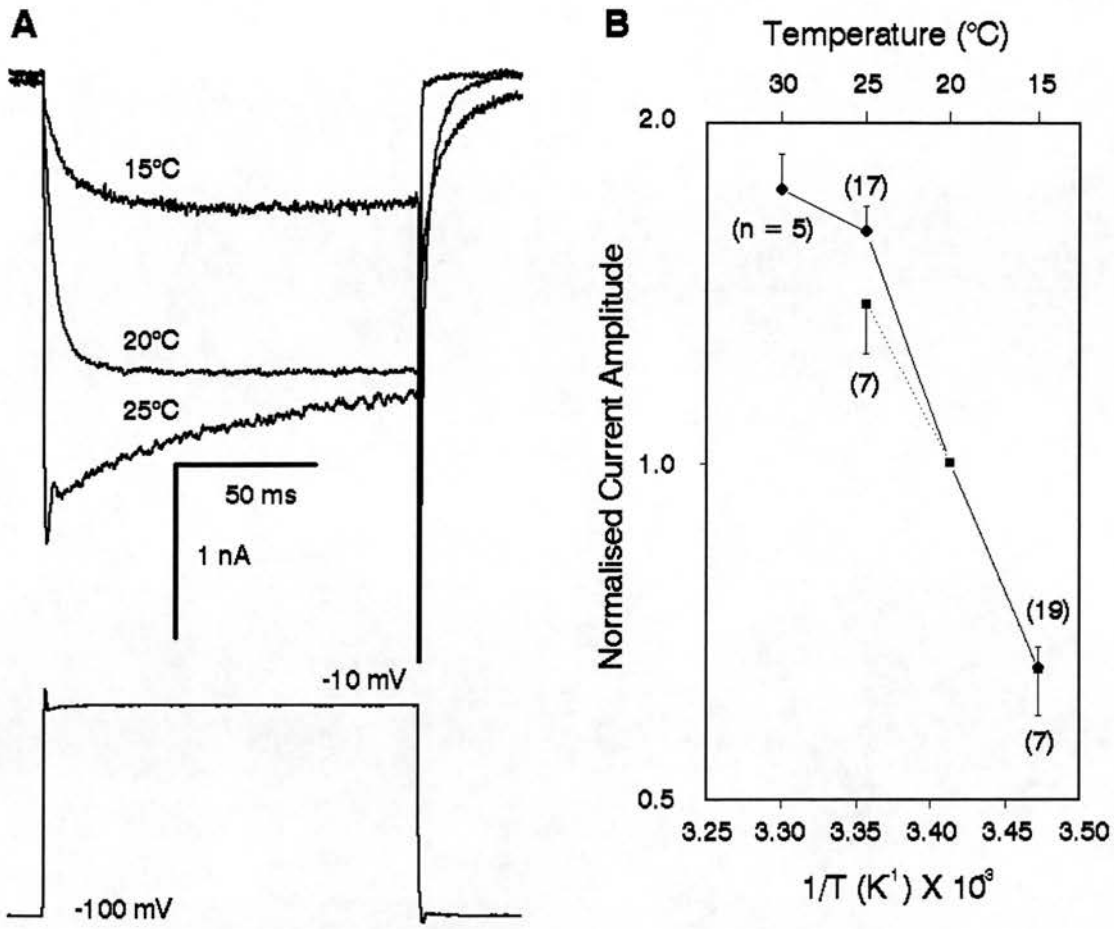

Figure 6.9: **Effect of temperature on currents in the presence of OA and GTPγS.** A. Currents elicited by voltage steps from -100 to -10 mV at 15, 20 and 25°C. Standard external solution, internal contained 1 μM OA, and 200 μM GTPγS. Cell 19029203. B. Arrhenius plot of peak current amplitude. Control data (circles, down error bars and solid line, 32 cells, as in figure 4.2) is plotted along with that obtained with OA and GTPγS in the internal solution (squares, up error bars and dotted line, 7 cells). Details of the plot as for figure 4.2.

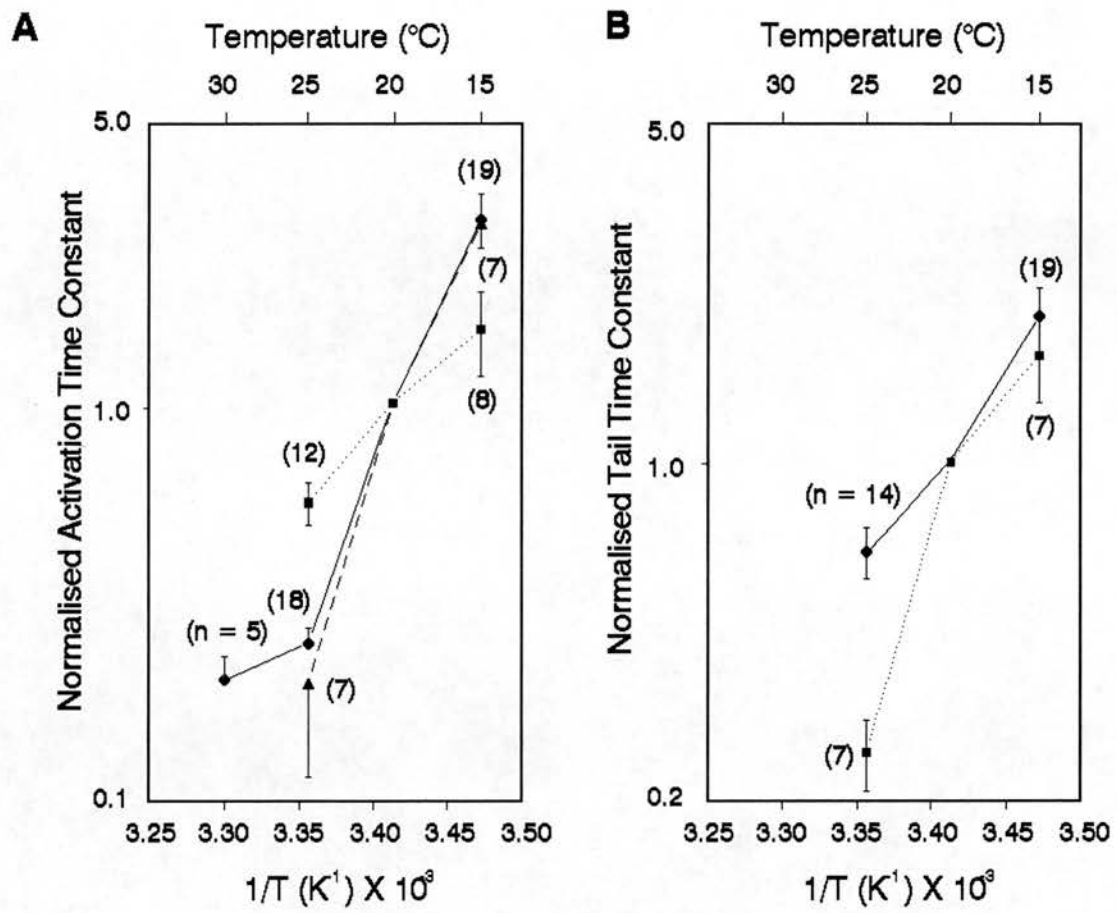

Figure 6.10: Effect of temperature on activation rate and current tails in the presence of OA and GTPγS. A. Arrhenius plot of activation time constants derived from single exponential functions. Control data (circles, up error bars, solid line, 32 cells) is plotted along with data recorded with 200 μM GTPγS (squares, dotted line, 17 cells), and data with GTPγS and 1 μM OA in the internal solution (triangles, down error bars, dashed line, 7 cells). B. Arrhenius plot of tail current time constants derived from single exponential functions. Control data (circles and solid line, 30 cells) is plotted along with data recorded with 200 μM GTPγS and 1 μM OA in the internal solution (squares and dotted line, 7 cells).

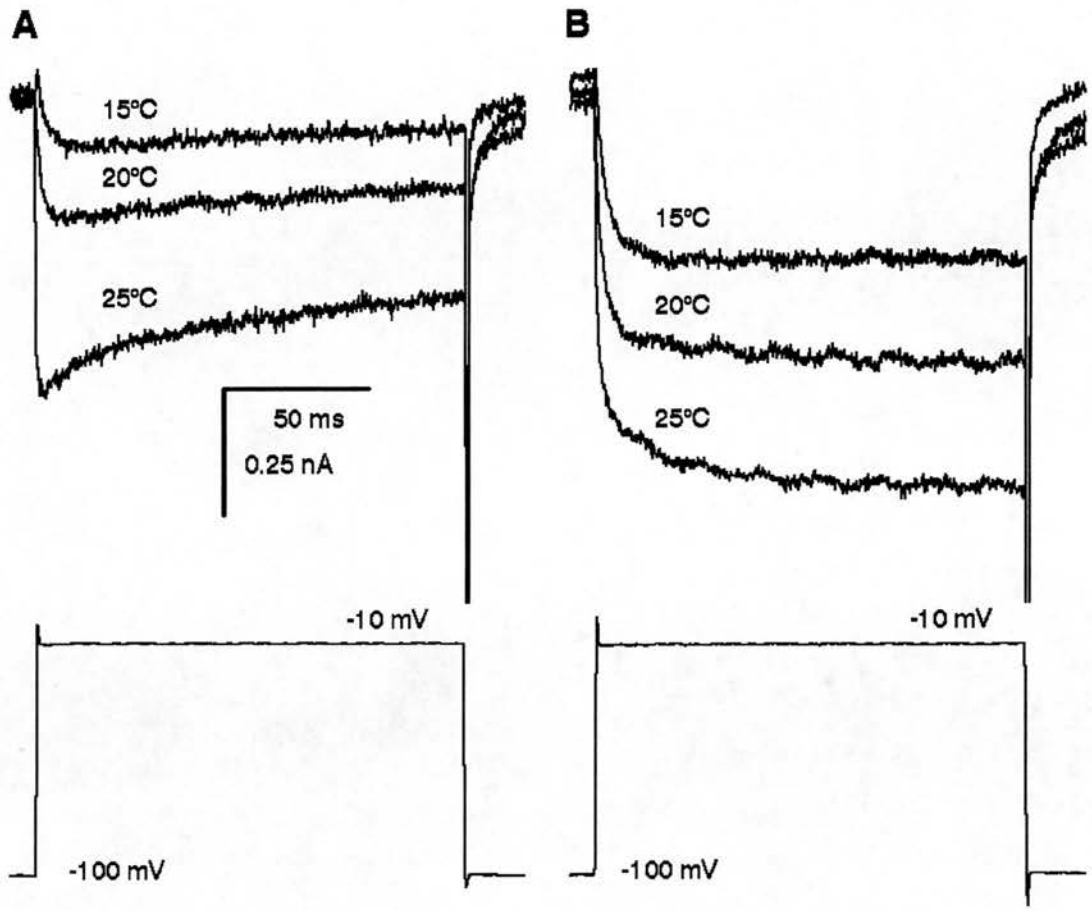

Figure 6.11: Effect of GTPγS and I1PP on HVA currents. In both examples the internal solution contained 200 μM GTPγS and 1 μM I1PP, and the data is leak and capacity subtracted. A. Example of currents elicited by voltage steps from -100 to -10 mV for 150 ms, at 15, 20, 25°C. In this case, τ_a had a Q_{10} of 8.6. Cell 03109102. B. An example of a cell were the activation kinetics steadily accelerated during the recording period. The currents illustrated were recorded at 25, 20 and 15°C, and in that order temporally. The τ_a values were 11.23, 4.23, and 3.75 ms respectively. Cell 04109102.

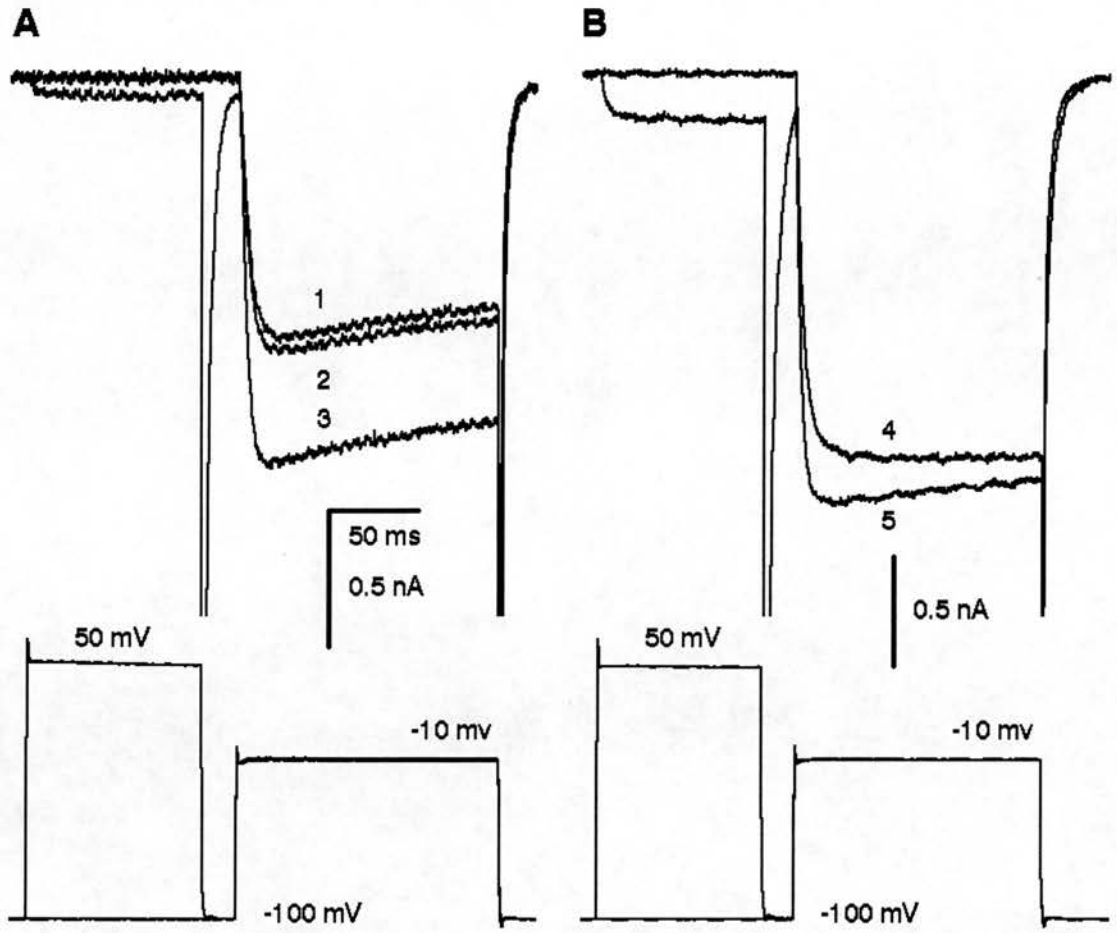

Figure 6.12: **Effect of depolarising prepulses on 8-OH-DPAT and GTPγS actions in the presence of OA.** A. Internal solution contained 1 μM OA. 3. Control current elicited by voltage step from -100 to -10 mV. 1. Application of 50 μM 8-OH-DPAT via a broken patch pipette. 2. Prepulse to 60 mV applied 10 ms prior to the test pulse, with 8-OH-DPAT still present. Cell 04029201. B. Internal solution contained OA and 200 μM GTPγS. 4. Control current elicited by voltage step from -100 to -10 mV. 5. Prepulse to 60 mV applied 10 ms prior to the test pulse. Cell 19029203. All data leak and capacity subtracted.

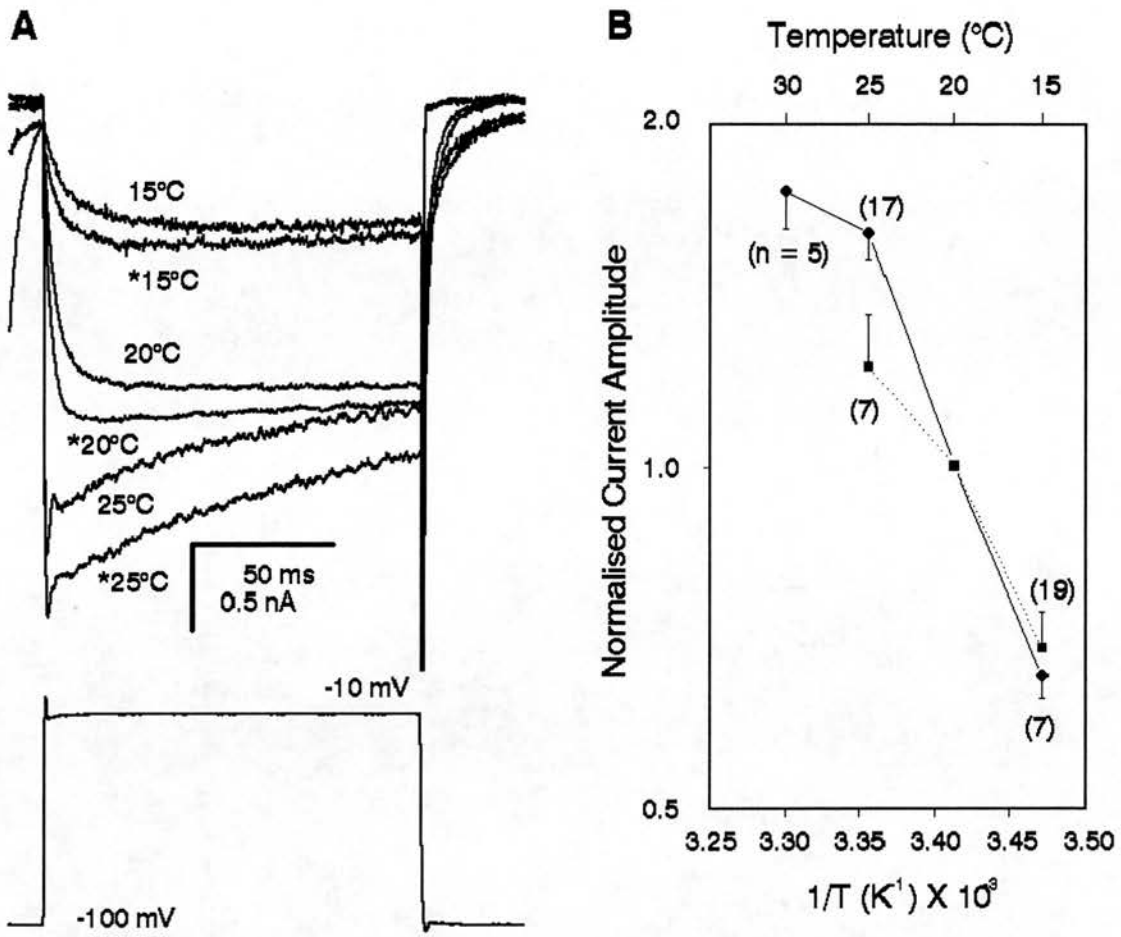

Figure 6.13: Effect of prepulses on current amplitude in the presence of GTPγS and OA. A. Currents elicited by voltage steps from -100 to -10 mV at 15, 20 and 25°C. Those marked with an asterisk were recorded with a 100 ms prepulse to 60 mV 10 ms prior to the test pulse. Standard external solution, internal contained 200 μM GTPγS and 1 μM OA. Data leak and capacity subtracted. Cell 19029203. B. Arrhenius plot of control peak current amplitude (circles and solid line, 32 cells, as in figure 4.2), and peak current amplitude with GTPγS and OA plus a prepulse (squares and dotted line, 7 cells). Details of plot as for figure 4.2.

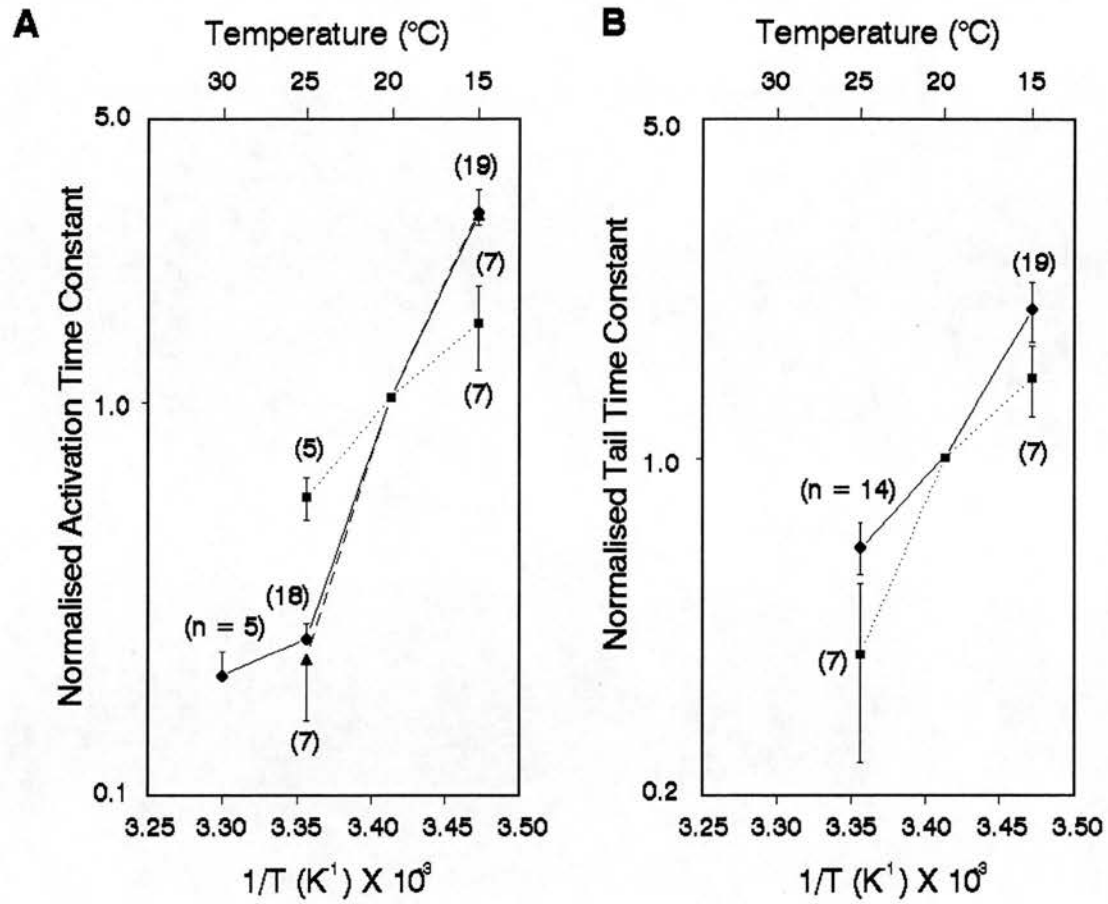

Figure 6.14: **Effect of temperature on activation rate and current tails in the presence of OA and GTPγS, with prepulses.** A. Arrhenius plot of activation time constants. Control data (circles, up error bars, solid line, 32 cells) is plotted with data recorded with 200 μM GTPγS (squares, dotted line, 17 cells), and data with GTPγS and 1 μM OA in the internal solution with test pulses preceded (10 ms) by a prepulse to 60 mV for 100 ms (triangles, down error bars, dashed line, 7 cells). B. Arrhenius plot of tail current time constants. Control data (circles and solid line, 30 cells) is plotted with data recorded with GTPγS and OA with prepulses (squares and dotted line, 7 cells).

Chapter 7 Discussion

1. Calcium Currents in Dorsal Raphé Neurones

The macroscopic appearance of the calcium currents reported here matches well with that previously published for DR neurones (Penington et al. 1991). This is also the case with regard to the voltage sensitivity, in particular the voltage threshold, the voltage required to elicit a maximum current, the experimentally derived reversal potential, and the effect of changes in holding potential were not significantly different to the previous reports.

One point of concern when using a slightly atypical internal solution (i.e. not a caesium based one) for these experiments, is that the ionic substitutions, and channel blockers used, do not lead to a complete isolation of calcium currents from other ionic conductances. The fact that around 95% of the current is blocked by cadmium is reassuring in this regard. Since a 2 mM concentration was required for this, it appears that, assuming that this was the actual concentration "seen" by the cells, calcium currents in DR are less sensitive to cadmium than in many other tissues, though there are reports of fairly high IC_{50} values in other preparations (40 μM, Boland & Dingledine, 1990). The component (around 17% of the total current) that showed least sensitivity to cadmium, in that it was only blocked by 2 mM, but not with 200 μM, would appear to be LVA or T-type current. Certainly the V_h for current activation for this component was significantly more negative than the control, and this hypothesis would be consistent with observations made in DRG neurones (Fox et al. 1987a, Gross & MacDonald, 1987).

The use of the patch-clamp technique has several advantages among which is a control of the intracellular medium. However, one of the

main disadvantages of this technique, or any employing intracellular perfusion, is that currents, including calcium, are often noticed to decrease with time, or 'rundown'. This has been noted by many groups (Kostyuk et al. 1981b, Byerly & Hagiwara, 1982, Fenwick et al. 1982, Lee & Tsien, 1984, Forscher & Oxford, 1985, Cota 1986, Belles et al. 1988, Ozawa et al. 1989). This is usually assumed to be as a result of diffusion into the pipette of soluble cytoplasmic constituents. Several groups have suggested that rundown can be reduced by the inclusion of various combinations of cAMP, ATP, Magnesium, catalytic subunit of AK, and calcium chelators like EGTA (Kostyuk et al. 1981b, Doroshenko et al. 1984, Lee & Tsien, 1984, Forscher & Oxford, 1985, Belles et al. 1988), though this action of cAMP or ATP is not always seen in heart cells (Irisawa & Kokubun, 1983, Lee & Tsien, 1984). However with both EGTA and MgATP in the pipette solution in this study, rundown was still observed. Over a period of 30 minutes or so from the start of whole-cell recording, this occurred at a rate of just over 1%/min. This was slow enough to allow reasonable assessment of the changes in amplitude with temperature or receptor agonists. In addition there was no significant change in any of the kinetic parameters with time at 20°C. However there was an impression that the fast inactivating component seen at 25 and more particularly at 30°C, did decrease significantly with time, though this was not measured, in line with the observations of some (Carbone & Lux, 1987a, Gross et al. 1990b, Bargas et al. 1991), but not others (Kay, 1991). Occasionally a small amount of 'runup' was seen in control situations, over the first few minutes of recording. This never amounted to much, and may have been due to an improvement in the cell-pipette seal over the initial stages of the experiment. Other than this there was no

clear separation of rundown into discrete periods with different rates, as seen in guinea pig myocardial cells (Belles et al. 1988).

The change in the voltage sensitivity of current activation with time is of a similar nature to that seen by Belles et al. (1988) in cardiac cells, were a parallel shift of current inactivation was also seen. The leftward shift in the voltage dependence could be explained by two possible mechanisms that involve the redistribution of ionic charges. Firstly while small ions tend to equilibrate rapidly between the cell and the pipette, large macromolecules (with a net negative charge) tend to remain inside the cell, with the small ions following a Donnan equilibrium, leading to the inside of the cell initially being more negative than the pipette (Marty & Neher, 1983). However, as the macromolecules slowly diffuse out of the cell, there is a decline in this Donnan potential. Since the direction and time course of the shift in the voltage dependence would correspond to that that would be expected for the change in Donnan potential, this has been proposed as a possible mechanism (Marty & Neher, 1983, Fernandez et al. 1984). The second possibility is that the shift could result from a change in the electric double layer at the inner surface of the membrane, with a consequent change in the effective field experienced by the gating charge. To account for the leftward shift observed in these experiments, the charge at the inner surface would have to become more positive, and this could result from the build up of barium ions that entered the cell each time it was depolarised. This is the explanation favoured by Belles et al. (1988). The same arguments can be used to explain the irreversible leftward shift in voltage sensitivity seen with increases in temperature. If the shift is due to a decrease in the Donnan potential, then it would be

expected that the reversal potential would also shift, while if it is due to a build up of cations on the intracellular surface of the membrane, this would not be the case. In both cases, one could predict that the shift would be greater at higher temperatures, either due to increased cation entry, or due to increased mobility in the aqueous solution of the macromolecules, though this latter factor would be expected to produce a smaller change (e.g. a Q_{10} in the range 1 - 1.5). The change in the buffering capacity of EGTA with temperature is negligible between 20 and 25°C (React version 2.01, G.L. Smith, Chelcom Software, 1986), and seems unlikely to be involved, since one would predict that this should be reversible. Although the reversal potential was not routinely measured during the experiments conducted to assess rundown, there was no clear evidence from those where full IV plots were performed at different temperatures, that the reversal potential changed (see figure 4.4), which certainly raises doubt over the shift being due to a Donnan potential change. The change in the rate of shift in V_h from 0.26 to 0.55 mV/min between 20 and 25°C would give a Q_{10} for this of 4.5. This would seem to be rather high for both hypotheses presented above, and in particular if increases in temperature simply speed up the movement of macromolecules in an aqueous solution.

It has been suggested, that calcium channel agonists, such as BayK 8644 stabilise the phosphorylated form of L-type channels (Armstrong & Eckert, 1987), act by promoting calcium channel phosphorylation (Dolphin, 1991a), or at least exposing a phosphorylation site to the action of kinases and PPs (Huang & McArdle, 1992). The fact that BayK 8644 also causes a shift of the current-voltage relationship in the hyperpolarising direction (Fox et al. 1987a, Taylor, 1988, Brown et

al. 1989, Meyers & Barker, 1989, Marchetti et al. 1991, Mogul & Fox, 1991, Scroggs & Fox, 1991, Huang & McArdle, 1992), suggests that phosphorylation may be involved in the change in voltage sensitivity with temperature. The high Q_{10} value for the shift in V_h would be more in favour of this. It may in fact be that the leftward shift in calcium current IV plots in DR neurones is a combination of an alteration in the phosphorylation state of calcium channels, along with a change in the electric field due to a build up of cations.

2. The Temperature Dependence of Calcium Currents in Dorsal Raphé

This study has confirmed that the temperature sensitivity of calcium current amplitudes are greater than that seen for sodium or potassium currents studied in a variety of tissues (see table 7.1). The cause of this difference is not immediately apparent. The amplitude Q_{10}'s for sodium and potassium are slightly influenced by a Q_{10} for their equilibrium potentials of 1.035 (Chiu, 1979, Beam & Donaldson, 1983). This might be higher for calcium since Ca^{2+} ions diffuse slower in the cytoplasm than in free water due to binding to molecules or sequestration (Augustine et al. 1987). However the high amplitude Q_{10} values may also reflect the greater complexity of calcium channels compared to those of sodium and particularly potassium. The findings described here are in broad agreement with previous work in vertebrate neuronal tissues on calcium currents, with at least one component of the current amplitude having a Q_{10} in the 2 - 2.5 range. Although it appears that the other component(s) have a lower Q_{10}, all the measurements of the temperature sensitivity of current amplitude are likely to be under estimated for several

possible reasons. Firstly, since the access resistance is likely to fall with increases in temperature, this will partly mask increases in current amplitude. For sodium currents in rat myelinated nerve fibres it is reported that the apparent Q_{10} for the current amplitude must be multiplied by the Q_{10} of the series resistance, about 1.4, to obtain the actual Q_{10} for amplitude (Schwarz, 1986). Secondly, there are the problems concerned with changes in voltage dependency. Currents were elicited by voltage steps to -10 mV, since initially at 20°C this was usually the potential that elicited a maximal current (see figure 4.4). However since the voltage sensitivity is changed by increases in temperature, and with time, it would be unusual for a step to -10 mV to elicit a maximal current at subsequent higher temperatures. In the cell illustrated in figure 4.4, at 20°C a step to -10 mV produced a leak subtracted peak current of -0.87 nA, while at 25°C this increased to -2.06 nA. However, to the nearest 10 mV, the maximum current at 25°C was actually elicited at -20 mV, and was -2.68 nA. The third possible reason for an underestimate of the Q_{10} for current amplitude is rundown, which itself is temperature dependent.

Accelerated rundown at 30°C, coupled with the shift in voltage dependency, probably accounts for the non-linearity of the Arrhenius plot of the peak current amplitude between 25 and 30°C (figure 4.2). It is possible that some non-linearity is due to a transition temperature occurring in these cells. This has previously been observed for calcium currents (Narahashi et al. 1987), though not by all workers (Taylor, 1988, Nobile et al. 1990), and occurred at 18-20°C. This is also the case for acetylcholine channel conductance (Fischbach & Lass, 1978), though it is a higher temperature than that seen for sodium currents (10°C, Hagiwara & Yoshii, 1980, Schwarz,

1979), and potassium currents (8°C, Kimura & Meves, 1979). All have been postulated to occur as a result in changes in the fluidity of the lipid membrane where the critical temperature for saturated fatty acid flexibility is 9-10°C (Chapman, 1975). Therefore a transition temperature for calcium current amplitude in DR neurones between 25 and 30°C seems rather unlikely. In addition, Narahashi's group observed a Q_{10} for peak current amplitude above 20°C in the same order (3) as observed here, while below this temperature the value was 15-17, far higher than anything observed in DR cells.

The most striking effect of temperature, as in other cells, is the acceleration of the rate of activation (see table 7.2). However in DR cells, the Q_{10} of over 10 for the activation time constant is particularly high. Changes in temperature are likely to affect the arrangement of the lipid molecules in the cell membrane. As a result, this would lead to changes in capacitance. Since the capacity compensation was not adjusted during recordings, it is possible that very rapid activation seen at high temperatures may have been contaminated with the capacitance artifact leading to an underestimate of τ_a and an over estimate of the Q_{10}. However, this seems unlikely since certainly in skeletal muscle fibres membrane capacitance actually decreases with temperature with a Q_{10} of about 1.03 (Del Castillo & Machne, 1953, Hodgkin & Nakajima, 1972). Thus if anything, the capacitance neutralisation of the voltage clamp would have been over rather than under compensated. It is interesting to note that although there is a change in the voltage sensitivity of current amplitude with temperature, no such change was seen for current activation (figure 4.8B), nor was the temperature sensitivity affected by changes in the holding potential. Following Arrhenius assumptions,

the Q_{10} gives an indication of the energy requirement of a process, and one of 2-3 would suggest an active process such as enzymatic involvement. However a Q_{10} in double figures is indicative of more complex processes, such as a multiple-step biochemical pathway, or the translocation of molecules through a non-aqueous medium (Morris & Clarke, 1981). Therefore it is tempting to hypothesize that upon depolarisation, for calcium channels to open several enzymatic reactions, and/or the movement of the various subunits of the channel in the lipid bilayer has to occur.

The opening of calcium channels appears to be far more complex than their closure, whether this occurs with time or repolarisation. While inactivation is difficult to assess accurately due to the changes in its nature with temperature, the simplistic measurement of the percentage reduction of current from the peak to the end of the 150 ms test pulse, does give a Q_{10} far lower than that for the activation rate time constant. In addition the Q_{10} for the tail currents is also much lower being in the 2-3 range (see table 7.3). This value for the tail currents is slightly higher than that found in other preparations where tail current kinetics are the least temperature sensitive parameter. It may be that the Q_{10} calculated here is an over estimate due to the difficulties in fitting the fast tail currents observed, or that channel deactivation is more temperature sensitive in DR cells than other neuronal preparations.

3. Calcium Channel Heterogeneity

It has been accepted for some time that high-threshold calcium currents in neuronal cells are composed of at least two current

components (Nowycky et al. 1985, Fox et al. 1987a), but there is now growing evidence that this may be an over simplification, with a component of HVA current that is insensitive to both DHPs and ω-CgTx in many cells (Regan et al. 1991). This is also the case in DR neurones (Penington et al. 1991). The data obtained in this study showing the effect of temperature adds a new dimension to the interpretation of the heterogeneous nature of HVA current.

The finding that the Q_{10} for peak amplitude is lowered when the holding potential is changed from -100 to -50 mV, coupled with the observation that the 'steady-state' current is also less temperature sensitive than the peak amplitude (see table 7.1), would be consistent with the view that the classical L-type, slowly or non-inactivating current (Fox, et al. 1987a), may be less temperature sensitive than the populations of channels that inactivate during the test pulse, or are inactivated by a holding potential of -50 mV. How the complex nature of the effect of temperature on inactivation may be explained in terms of the classical classification is not clear. The different voltage sensitivities of the two inactivating components seen at 25 and 30°C would possibly suggest that they are more likely to represent two populations of channels, or different states of channels, rather than one channel which undergoes a two stage process of closure. It therefore appears that there are at least three components of high-threshold current in DR cells at temperatures of 25°C or above. The first has a fast time constant for inactivation, is recruited only at higher temperatures, and accounts for around 15% of the total current at 30°C. The second has a slower time constant, is present at all temperatures tested, and accounts for 20 - 25%, while the third has a time constant too slow to measure using 150 ms voltage test pulses,

and makes up the balance. These proportions do not fit with those that are DHP or ω-CgTx sensitive, or insensitive to both (Penington et al. 1991). Coupled with observations that suggest that single N- and L-type calcium channels can carry two kinetically distinct components of current, one rapidly inactivating and the other sustained (Plummer & Hess, 1991, Slesinger & Lansman, 1991b), it is clear that differentiating the various components of HVA current from whole-cell records is fraught with difficulties. Since N-type channels may be able to switch to various inactivation states, it is possible that the results obtained in this study may be due to the channels favouring a fast inactivation state at higher temperatures. Alternatively, calcium channels may have two inactivating states that can be reached from either the closed state preceding the open state, or directly from the open state, as in the model for axonal sodium channels proposed by Armstrong and Gilly (1979).

Nobile and workers (1990) have suggested that the fast inactivating component in DRG cells, is linked to a calcium-dependent process, since the proportion of the total current made up of this component mirrors the changes in current amplitude with voltage. Figure 4.13 clearly demonstrates that this is not the case in DR cells. In addition, while calcium was used as the charge carrier by Nobile et al., barium was used in this study, which would not be expected to activate calcium dependent processes.

4. Action of 8-OH-DPAT and GTPγS on Tail Currents

An additional effect of 5-HT_{1A} receptor or G-protein stimulation has been observed in this study that has not previously been noted in

these cells, and that is that there is a significant increase in the tail current time constant. Since these elongated tails are relatively insensitive to cadmium, the most obvious explanation for this observation is an effect on LVA current. This would be supported by the previous observations that T-type current has a more slowly decaying tail than HVA current (Carbone & Lux, 1987a, Swandulla & Armstrong, 1988, Regan, 1991). 5-HT has previously been shown to enhance LVA current in both rat spinal motoneurones (Berger & Takahashi, 1990) and hippocampal lacunosum-moleculare interneurones (Fraser & MacVicar, 1991), while GTPγS at low doses is observed to increase T-type current in DRG neurones (Scott et al. 1990). It would therefore seem that a hypothesis of 5-HT increasing the tail current time constant in DR neurones by an action on LVA current mediated by 5-HT_{1A} receptors and a G-protein, is reasonable, though further pharmacological work is clearly necessary. The main argument against the hypothesis is that it would be expected that T-type current would be nearly completely inactivated by the end of a 150 ms test pulse, and therefore should be unable to contribute to the tail current. Recent single channel work on L-type current in cerebellar granule cells might help explain this anomaly. A component of this current flows through L-type channels that are closed at negative potentials following a large depolarisation, but then open after a delay (Slesinger & Lansman, 1991c). This delay can be explained by inactivated channels returning to rest via an open state after repolarisation. If T-type channels are held in the inactivated state until the end of a 150 ms voltage step, and then they also return to rest via an open state, then enhancement of T-type current might be expected to lead to an enlarged tail current, even after a 150 ms test

pulse. Further support for this idea comes from the work of Sala (1991) on frog sympathetic neurones, who has shown that the deactivation time course is not altered as channels inactivate, during progressively longer pulses. Prolonged tails have also been shown to occur in hippocampal interneurones in the presence of carbachol when LVA current is enhanced (Fraser & MacVicar, 1991, figure 8A, voltage step to -20 from -100 mV), though these authors do not discuss this. Clearly the definitive answer to the question of which channels underlie the prolonged tails is difficult to resolve from whole-cell recordings, especially with the LVA current in DR neurones being small and inconsistent. However clearly further investigation is required in this area.

5. Action of Agonists on HVA Calcium Currents and the Effect of Depolarising Prepulses

The partial reduction (50 - 60%) of the peak HVA current amplitude by 5-HT and 8-OH-DPAT previously shown (Penington & Kelly, 1990, Penington et al. 1991) has been confirmed here, as has the fact that not all cells isolated in the manner described respond to 5-HT agonists (89%). The possible reasons for this second observation are discussed in chapter 3.

This was the first detailed quantification of slowing of activation by a 5-HT agonist in DR. In the presence of 5-HT_{1A} agonists, activation is more commonly best fitted by double rather than single exponential functions. This could possibly be due to one of two reasons, either the general slowing of activation causes a normally unresolvable fast component to become resolvable, or the

whole nature of the mechanism of activation is altered. It has previously been suggested that GTPγS causes a slow activating component to be seen in addition to a fast component that has a similar time constant to activation in control DRG cells (Dolphin, 1991b). This has been postulated to be due to an activated G-protein interacting with just a proportion of channels. The results obtained here are not identical, since the fast component seen in the presence of GTPγS is significantly slower than the single control component. Whether this implies an effect of GTPγS on all HVA channels is not clear, but this would seem to be a possible implication. However the settling time of the voltage clamp used in this study was too poor to allow this matter to be resolved.

Further evidence has been acquired that the 5-HT response is mediated by a 5-HT_{1A} receptor, in that in addition to 8-OH-DPAT, ipsapirone also produces a similar response to 5-HT itself. Interestingly both 8-OH-DPAT and ipsapirone slow the activation time constant less than 5-HT, though this is only significant for ipsapirone, while the reduction in current amplitude was not significantly less for either. There is much speculation that many 5-HT_{1A} agonists, including 8-OH-DPAT and ipsapirone, are in fact only partial agonists, especially when acting at 5-HT_{1A} receptors in hippocampus (e.g. Andrade & Nicoll, 1987a & b). This may also be the case in DR, but may only be revealed by the perhaps more sensitive measurement of the slowing of activation.

While 9 out of 10 cells failed to respond to the application of DA, one cell did show an increase in current amplitude, and an acceleration in the activation rate. Assuming that this was not simply an artifact (the cell parameters suggested a healthy cell, and

plain external solution had no effect on the calcium current, while 5-HT caused a small inhibition), the most obvious explanation is that this was not a serotoninergic DR neurone. This would be supported by the observation that the control currents elicited from this cell, were not identical to those of most cells, in that they had a relatively slow activation rate (figure 3.8), that was more akin to that seen when cells were loaded with GTPγS. The effect was of interest in that DA has been shown to increase current amplitude and accelerate the activation rate of calcium currents recorded in bovine chromaffin cells (Artalejo et al. 1990, 1991). These cells contain channels defined on the basis of their voltage sensitivity, kinetics, pharmacological sensitivity, and single channel conductance, that match N- and L-type ones seen in vertebrate neurones (Bossu et al. 1991a & b). Depolarising prepulses of a similar nature to those used in this study are able to markedly "facilitate" these calcium currents (Fenwick et al. 1982, Artalego et al. 1990 & 1991). This is hypothesised to be due to the conversion of channels that are "reluctant" to open on depolarisation to being "willing". Macroscopically the control currents in chromaffin cells appear very similar to those recorded with GTPγS in this study, while prepulses have a similar affect in chromaffin cells to that seen in DR in the presence of GTPγS. Facilitation with prepulses has also been seen in SCG neurones, where it is hypothesised to occur as a result of conversion of "reluctant" to "willing" N-type channels, since it does not occur in the presence of ω-CgTx (Ikeda, 1991). It therefore would appear that the same type of channels are facilitated, as can be inhibited by transmitters in other neurones. Depolarising prepulses have also been shown to increase the open probability and lead to longer openings of

an HVA channel in cerebellar granule cells (Slesinger & Lansman, 1991b). These channels are reported to be DHP sensitive and so of the L-type. It is interesting that these same L-type channels have been reported capable of inactivating in two different modes (Slesinger & Lansman, 1991a & b), as have N-type channels in SCG (Plummer & Hess, 1991). Whether the finding of facilitation of L-type channels in cerebellum can be extrapolated to other cells, or reflects regional variations, is not known. The amount of facilitation possible in SCG is reduced by GDPβS, and greatly increased by GTPγS (Ikeda, 1991). Thus it may well be due to a voltage dependent removal of tonic G-protein mediated inhibition. Similar proposals have been suggested in neuronal cells for the action of transmitters and depolarising prepulses (Bean, 1989b, Elmslie et al. 1990). These state that "willing" channels are converted to "reluctant" by transmitters, and this is reversed by prepulses. The main difference between cells such as SCG, where facilitation with prepulses occurs, and DR neurones, may be that in the former there is basal activity of G-proteins, which does not occur in the latter.

There is thus a possible further explanation for the result seen here with DA, and that is that the cell was a serotoninergic DR neurone, with a local high level of 5-HT (e.g. due to release from a nearby cell in the dish, which is feasible if DR cells release 5-HT from the somatodendritic compartment (Héry et al. 1986, Becquet et al. 1990)), and this would explain why when further 5-HT was applied, only slight inhibition was seen. If this was the case then a hypothesis could be derived that normally DR calcium channels are "willing", but are made "reluctant" by 5-HT_{1A} receptor or G-protein activation (as originally proposed for 5-HT in DR cells by Penington et al. 1991).

It has been shown that "reluctant" channels can be converted back to "willing" ones by large depolarisations. However, it is also possible that DA can do the same. To test the second possibility, it would be of interest to investigate if DA has any action on DR neurones loaded with GTPγS.

6. Effect of Receptor and G-protein Activation on Temperature Dependence

In addition to having profound effects on activation kinetics, 5-HT_{1A} receptor and direct G-protein activation also have a major effect on the temperature dependence of the activation rate. While application of 8-OH-DPAT or GTPγS has no effect on the temperature dependence of calcium current amplitude or tail current kinetics, they both caused a reduction in the Q_{10} for the activation time constant from over 10 to around 3, an effect that is highly significant. This action does not appear to be an artifact of 8-OH-DPAT and GTPγS causing the activation to become biexponential, since the Q_{10} for both the time constants of double exponentials, and the time constant of the best fit single exponentials, are all of the same order (see table 7.2). This finding is, to my knowledge, completely novel.

If one follows Arrhenius assumptions and proposes a multi-step process and/or translocation of molecules in the lipid membrane to be the cause of the high Q_{10} normally seen for the activation rate, then it follows that this has been affected by G-protein activation. The Q_{10} in the presence of GTPγS of around 2.5 is of the same order as that for the kinetics of sodium and potassium currents in vertebrate nerve fibres (Frankenhoeuser & Moore, 1963, Moore, 1971, Chiu, 1979,

Kniffki et al. 1981, Collins & Rojas, 1982, Benoit et al. 1985, Schwarz, 1986, Schwarz & Eikof, 1987). The structure of voltage-dependent sodium and calcium channels, as far as is known, is rather similar. Certainly both contain very similar subunits which are thought to conduct the ions (α for the sodium, and α_1 for the calcium channel - see Catterall, 1988). However the quaternary structure of the calcium channel is more complex than the sodium one in that it is pentomeric rather than trimeric (certainly for the DHP binding channel, see chapter 1, section 4). It is possible that it is the complex interaction of the five subunits that endows calcium channels with such a high Q_{10} for activation. If this is so, an activated G-protein, or second messenger, may in some way, interact with the calcium channel complex to cause its mechanism of activation to appear more like that seen for sodium channels, and thus have a lower Q_{10}.

In the same way that depolarising prepulses, prior to the test pulse, are able to reverse much of the amplitude reduction and slowing of activation seen with 8-OH-DPAT and GTPγS, they are also able to reverse the decrease in Q_{10} for the activation time constant. It therefore appears that whatever the mechanism by which G-protein activation alters current activation, this is voltage dependent in that it is returned to normal by large depolarisations.

Interestingly, when 8-OH-DPAT is applied to DR cells, while the Q_{10} for activation kinetics decreases, that for the actual slowing of the activation rate by 8-OH-DPAT is rather high at around 9 (derived from averaged values for the increase in τ_a). The implications of this Q_{10} are unclear, but it may reflect the complex interaction of the G-protein with other molecules, possibly involving translocation in the membrane.

7. The Action of Phosphatases

Both the α_1 and β subunits of DHP binding calcium channels have multiple phosphorylation sites, and are substrates for cAMP- and calcium/calmodulin-dependent protein kinases plus protein kinase C (Campbell et al. 1988). The effect of phosphorylation on calcium channel activity is poorly understood. In cardiac cells, cAMP dependent phosphorylation of calcium channels appears to be the final step in the β-adrenergic enhancement of HVA current (see Hartzell et al. 1991 and reviews of Reuter, 1983, Bean, 1989a, Hess, 1990, Dolphin, 1991b). Also in cardiac cells, the chemical phosphatase 2,3-butanedione monoxime (BDM) reduces action potential duration through an effect on calcium currents (Bergey et al. 1981). BDM also suppresses calcium transients in rat skeletal muscle (Fryer et al. 1988). These observations may be due to BDM removing labile regulatory phosphate group(s) necessary for activation of calcium channels. Continual phosphorylation has previously been suggested as being a requirement to keep calcium channels in snail neurones primed for activation (Eckert & Chad, 1984).

Phosphorylation of smooth muscle calcium channels by calmodulin-dependent protein kinase II has been shown recently to lead to enhanced currents (McCarron et al. 1992). In mammalian neurones, increases in the level of phosphorylated sites by the use of phosphatase inhibitors has been shown to increase calcium conductance in DRG neurones (Dolphin, 1992a & b), though only in the presence of internal GTPγS. In this case, the phosphatase involved appears to be sensitive to the endogenous I1PP, and therefore of the phosphatase 1 (PP1) type (Cohen, 1989). The action of I1PP was identical and non-

additive to that of both forskolin and 8-Br-cAMP, suggesting the involvement of AK. Chronic application of dibutyl cAMP to cultured cells also leads to the enhancement of calcium currents thought to be of the T- and L- type (Eckert et al. 1990, Yamaguchi, 1990). In murine DRGs BDM reversibly reduces HVA calcium currents that can be reversed by the application of 8-Br-cAMP, while PKC activators have no effect (Huang & McArdle, 1992), again suggesting a role for AK. At a single channel level, the effect of BDM was observed to be due to a reduction in the percentage of time the channels spent in the open state.

AK may be involved in the rundown of calcium currents. The catalytic subunit of this kinase has been shown to increase calcium channel activity in a pituitary cell line (Armstrong & Eckert, 1987). In addition, adenosine thiotriphosphate (ATPγS), a non-hydrolysable analogue of ATP, prevents rundown of calcium currents in invertebrate neurones and vertebrate cardiac myocytes, an effect similar to that of cAMP or AK (Eckert et al. 1986, Kameyama et al. 1988). While ATPγS actually reduces calcium currents via a G-protein, perhaps by conversion to GTPγS, in rat nodose ganglia, the catalytic subunit of AK has been reported to decrease HVA current rundown by Gross et al. (1990a). The preferential action of the catalytic subunit on HVA current is in keeping with the feeling that this is much more prone to rundown that LVA (Carbone & Lux, 1987a, Fox et al. 1987a, Hagiwara et al. 1988, Bargas et al. 1991). Thus this kinase appears to have a regulatory role that may or may not also occur in DR cells in the light of the rather inconsistent results obtained with forskolin.

The few experiments performed with forskolin, suggest that adenylate cyclase is not involved in signal transduction following

receptor stimulation. This would be in keeping with previous work on calcium current modulation by transmitters (see chapter 1, section 5). While it was not seen in every cell, it does appear that either runup may be precipitated or enhanced by forskolin, or rundown decreased. This may be analogous to the effects of forskolin seen in DRG neurones (Dolphin 1991a & 1992b), and be due to an action of AK in enhancing, or maintaining, calcium currents in some way.

In DR neurones, application of OA led to a dramatic increase in runup with little or no effect on the rate and extent of rundown, and therefore had a similar action to forskolin in some cells. The concept and definition of 'runup' is somewhat vague. The idea that current amplitude may decline with time during whole-cell clamp, due to the loss of some aspect of channel maintenance, is well accepted. However runup is not such a universally recognised phenomena. In this work the term has been used in a fairly loose fashion to refer to an increase in current amplitude that occurs steadily over a number of minutes. The use of the term is not intended to implicitly imply any mechanism. However, the hypothesis is certainly formulated that, like rundown, runup may reflect the functional state of the channels, such as the basal degree of phosphorylation, and possibly unrelated to any change in phosphorylation that might be mediated by 5-HT_{1A} agonists. Effects of OA have previously been seen on calcium current amplitude with time, in smooth muscle cells (Lang et al. 1991), however the action was not quantified clearly enough to ascertain if the effect was due to increased runup, or decreased rundown. In *Helix* neurones, OA certainly appears to have a primary effect on rundown, with no clear evidence of an effect on runup as seen in DR (Yakel, 1992). The question therefore arises as to whether OA induced runup in DR is a

novel finding for calcium currents generally, or if there is simply a difference in nomenclature used. This is possible combined with variations in the perceived effect with different doses. This may well be the case for the action of AK. Gross et al. (1990b) report that in rat nodose ganglia cells, the catalytic subunit causes a dose dependent increase in HVA (but not LVA) current amplitude that takes some time to occur. At high doses (1 or 50 μg/ml) little rundown is seen, but particularly at the highest dose, it is not clear that recordings were made beyond the time a maximum current amplitude was recorded (see figures 3C & D, Gross et al. 1990b). With the lowest dose tested (0.1 μg/ml) the record of current amplitude (figure 3B, Gross et al. 1990b), appears extremely similar to figure 6.1 presented in this thesis. In this case a period of 'runup' (term not used by Gross et al.) was seen during the first 5-6 minutes of recording, when the amplitude increased by around 35-40% (measured from figure 3B, Gross et al. 1990b). From this point on, the rate of rundown was in the order of 3 %/min. In the control (figure 3A, Gross et al. 1990b), current 'runup' was less (10 - 15%), and rundown occurred at the rate of approximately 2.5 %/min. Thus at low concentrations, the catalytic subunit of AK seems to have a strikingly similar effect in nodose neurones to OA in DR cells.

Assuming that the action of OA in DR is mediated by an inhibition of a PP, a hypothesis can be formulated. It appears that some or all HVA calcium channels in DR are "maintained" or "enhanced" in their ability to pass current by a mechanism involving phosphorylation that is governed by an OA sensitive phosphatase, and a kinase that may be cAMP dependent. OA inhibits PP1, PP2A, and also PP2B, with no effect on PP2C (Cohen, 1989). An action on PP2B is unlikely in that it is

calcium dependent (Cohen, 1989), and the internal solution contained high levels of EGTA. So it would appear that the action of OA is likely to be mediated via an inhibition of PP1 or PP2A. Exactly by what mechanism this leads to an increase in current amplitude is not clear. Dolphin found that OA decreased DRG cell viability (1992a), and in addition, I1PP only led to an increase in current amplitude in the presence of GTPγS (1992b). It may well be, therefore, that the regulation of calcium channels is slightly different between DRG and DR. In addition, the action of I1PP in this example may have been somewhat different (see below).

It was suggested in section 1 above that the leftward shift in the voltage dependency of calcium currents with time and increases in temperature may involve the phosphorylation state of the channels. While OA had no effect on the rate of leftward shift, the V_h for the activation Boltzman function was significantly more positive. Therefore it seems unlikely that an action of PP1 or PP2A could be directly responsible for the leftward shift, but clearly the degree of phosphorylation of the channels does seem to affect the voltage-dependency. This is supported by the observation that the maximal current amplitude in the presence of ATPγS is elicited at more positive potentials than controls in nodose neurones (Gross et al. 1990a).

An effect of OA was noted on the action of 8-OH-DPAT and GTPγS in prolonging tail currents. There was no apparent increase in τ_t with 8-OH-DPAT in the presence of OA, and it was also less with GTPγS and OA than with GTPγS alone, though this latter effect was short of significance. It would therefore appear that the possible effect of 5-HT on LVA current discussed in section 4 above, may involve a

decrease in the phosphorylation state of the LVA channels or the G-protein that transduces the signal. Thus when phosphorylation is increased by OA, the response is blocked.

The most notable effect of OA was on the HVA response to 8-OH-DPAT and GTPγS. While the reduction in amplitude was little affected, the slowing of the activation rate was attenuated. Furthermore the decrease in Q_{10} was completely reversed (see table 7.2). Since a reduction in amplitude with some slowing still occured, an effect of OA could easily have been missed. It is a good illustration of the advantages of examining the temperature dependence of the activation rate, in that this was very clearly altered by OA. While OA had significant effects on the action of 8-OH-DPAT on both activation kinetics and Q_{10}, there was no significant reduction in amplitude inhibition by 8-OH-DPAT. This has important implications. Either it is simply that the reduction in current amplitude was variable enough to prevent it reaching significance, or, amplitude inhibition is mediated via a separate mechanism to retardation of activation, and is not simply a result of this, as has been suggested as a possibility by Swandulla et al. (1991b) and Dolphin (1991b). The dose of OA used was fairly low (Cohen, 1989), and application of a higher dose may clarify this in that all parameters may be affected significantly, though if they clearly had different sensitivities to OA, then the implication would still be that 5-HT_{1A} receptor activation has multiple actions on HVA current in DR neurones. If 5-HT has two actions on calcium currents, one a slowing of the activation rate that involves changes in an OA sensitive phosphorylation state, and the other a direct reduction in current amplitude, the physiological significance of these needs to be assessed. Since calcium entry through HVA channels

normally occurs during the relatively short period of time an action potential occurs, it may well be that slowing of activation has a greater influence on the increase in intracellular calcium, than the direct reduction in current amplitude. Clearly this needs to be assessed further by the use of action potential waveforms in voltage clamp, perhaps combined with internal calcium measuring fluorescence techniques.

There have been relatively few studies that have conclusively shown an involvement of phosphorylation in the action of transmitters on calcium currents in neurones. Certainly Dolphin has shown that in DRGs, in the presence of GTPγS, forskolin and phosphatase inhibitors are able to increase current amplitude and activation rate (Dolphin, 1991a, 1992a & b), though forskolin apparently has no effect on the action of baclofen (Dolphin et al. 1989). In this situation, the phosphatase and kinase that determine the phosphorylation state would seem to be PP1 and AK respectively. Clearly though in this situation it is difficult to tease apart possible separate effects on rundown, and G-protein action. Further work with specific inhibitors and active fragments of peptides is required to clarify which kinase and phosphatase are involved in DR neurones.

8. Implications for the Mechanism of Rundown, Calcium Channel Activation, and Modulation by 5-HT

Several models have been proposed for the action of transmitters on calcium currents, derived from detailed analysis of voltage dependence and kinetics (e.g. Grassi & Lux, 1989, Bean, 1989b, Marchetti & Robello, 1989, Elmslie et al. 1990, Lopez & Brown, 1991,

Swandulla et al. 1991b, Dolphin, 1991b, Kasai, 1992). These range from simple equilibria such as

$$M \rightleftharpoons C \rightleftharpoons O \qquad (7.1)$$

where M is the modulated, C the closed, and O the open states of the channel, to more complex arrangements such as

$$C \rightleftharpoons O \rightleftharpoons M \rightleftharpoons C' \rightleftharpoons O' \qquad (7.2)$$

where C′ and O′ are additional open and closed states (Kasai, 1992). Much of the argument between these models hinges on fine kinetic details and the concentration dependence of various transitions (for discussion of this see Kasai, 1992). Since different doses of 8-OH-DPAT or GTPγS have not been tested in this study, it is impossible to side one way or another. In addition, detailed analysis of the kinetics of the 8-OH-DPAT action have not been made. However information has been gained with regard to the possible mechanisms involved in receptor modulation of calcium currents, and a model to describe the hypotheses formed is presented here.

The phosphorylation state of any protein depends on the balance of the activity of the relevant kinases and phosphatases. The results obtained in this study suggest that when the level of phosphorylation of some protein is increased by the inhibition of phosphatases, the HVA calcium current activation rate is increased in the presence of a 5-HT_{1A} agonist or GTPγS. In the absence of a phosphatase inhibitor, but with 5-HT_{1A} receptor stimulation, or direct G-protein activation with GTPγS, the current activates upon depolarisation more slowly. It

can be presumed that under these conditions the level of phosphorylation will be lower than in the presence of a phosphatase inhibitor. It has been suggested that the protein whose phosphorylation state that is important in these circumstances could be the G-protein or the calcium channel (Dolphin, 1992b). This question can not be answered easily since it is not clear if high levels of phosphorylation are required for rapid activation in the absence of receptor stimulation. The fact that OA has no effect on activation rates in the control situation suggests that either the channels are already highly phosphorylated, or phosphorylation of channels does not determine the activation rate. In chromaffin cells, where depolarisation or dopamine are able to facilitate a large fast activating current, it has been shown that facilitation is suppressed by inhibitors of protein phosphorylation, or by injection of PP2A into cells (Artelejo et al. 1992b). If facilitation in chromaffin cells is due to the conversion of "reluctant" to "willing" channels, while in DR, 5-HT causes the opposite conversion, this would suggest that the rapid activation does indeed require phosphorylation of calcium channels (or possibly G-proteins, if these are intimately linked in the absence of receptor stimulation).

In recent years there has been considerable progress made in understanding the structure of calcium channels (see chapter 1, section 4). However to date these have been primarily concerned with those that bind DHPs (i.e. L-type). If an assumption is made that all voltage-dependent calcium channels are likely to have a fair degree of similarity in their structure, then it is possible to formulate some hypotheses as to the site and nature of the phosphorylation that affects current activation. As mentioned above, the two subunits that

are capable of being phosphorylated are α_1 and β (Campbell et al. 1988). Antibodies specific to the β subunit are able to precipitate radio labelled DHP receptors from digitonin solublised membranes (Leung et al. 1988). Since the α_1 subunit contains the DHP binding site (Sharp et al. 1987), precipitation of DHP receptors by β antibodies suggests a close association between α_1 and β subunits. α_1 subunits are the ion-conducting and voltage sensing component of calcium channels (Campbell et al. 1988). A study of chimaeric calcium channels derived from cDNA from slowly activating skeletal muscle or rapidly activating cardiac muscle channels suggests that it is repeat I of the α_1 subunit that determines the channel activation kinetics (Tanabe et al. 1991). β subunits are thought to be intrinsically involved in the regulation of calcium channel activity. Monoclonal β subunit antibodies are able to activate calcium channels reconstituted into planar lipid bilayers (Vilven et al. 1988). It has recently been shown by cotransfecting cell lines with various combinations of expression plasmids for the various subunits of skeletal muscle calcium channels, that while α_1 subunits alone are able to pass current, the activation kinetics are around 100 times slower than expected for channels studied in their native membranes (Lacerda et al. 1991). However when α_1 and β subunits are expressed together, the activation rate is near normal levels (Lacerda et al. 1991, Varadi et al. 1991).

A hypothesis may thus be formulated to account for rundown and the effect of 5-HT on activation, assuming a similarity between skeletal muscle and the various neuronal HVA calcium channels, and this is diagrammatically represented in figure 7.1. Much of this model is somewhat schematic, and rather speculative, though it generally fits

most of the data obtained in DR and other cells concerning rundown and modulation of calcium channels (particularly with regard to changes in the activation rate). The model illustrates opening of the channels on depolarisation in a simple fashion as the conversion from state 1 (closed) to state 2 (open). No account has been taken of inactivation, the routes of deactivation, or the possible multiple stages that may occur between state 1 and 2. However conversion from 1 to 2 occurs rapidly on depolarisation, and an interaction between α_1 and β subunits of the channel is necessary for this.

The closed channel may occur in three states (1,3 and 4). State 3 represents channels that are no longer able to open as a result of rundown. The conversion from state 1 to 3 has arbitrarily been illustrated as due to a loss of phosphorylation of the α_1 subunit of the channel. Under normal conditions this subunit would be maximally phosphorylated, but during the course of whole-cell clamp recordings, the kinase involved in this phosphorylation appears to be lost (may be due to diffusion into the pipette), or its activity is decreased by some mechanism (perhaps as a result of the decreased availability of cAMP). In this model, the α_1 subunit can not pass current when dephosphorylated. Rundown may thus be reversed or slowed down, or runup induced by catalytic subunits of AK, 8-Br-cAMP, or forskolin, and BDM may have the opposite effect (see section 7 above). This also occurs with OA in DR, due to a block of the action of a PP that mediates the dephosphorylation converting state 1 to state 3. Combined with data from other cell types in addition to DR, the kinase mediating the conversion from state 3 to 1 is likely to be AK while the PP converting 1 to 3 seems to be OA sensitive. The results in DR suggest a difference between runup and rundown, which may be

artifactual (see section 7), otherwise it is not clear how this relates to the model presented here.

The other closed state of the channel is state 4. This differs from state 1 in that the β subunit is no longer phosphorylated, and as a result is unable to interact with the α_1 subunit to enable rapid activation. Thus when a depolarisation occurs the channels activate slowly to enter open state 5. In the model presented by Marchetti & Robello (1989) a common open state is shared by both modulated (corresponding to state 4) and control (state 1) channels. It is not clear from results obtained here whether open states 2 and 5 in the present model differ in any way, so the two models may be compatible. Single channel data is likely to be required to answer this question. In the model of Bean (1989b) and Elmslie et al. (1990), state 1 would equate with "willing" and state 4 with "reluctant" channels. Under normal control conditions in DR, the β subunit would be hypothesised to normally be maximally phosphorylated and therefore able to interact with the α_1 subunit, in line with the view of Dolphin (1991a). This is somewhat different to chromaffin cells, where increased levels of phosphorylation of channels induced by depolarisation or dopamine, is required for rapid opening (Artalejo et al. 1992b). Conversion from state 4 to 1 should occur rapidly compared to the reverse transition, so that at rest most channels are in state 1. The β subunit is phosphorylated by a kinase that must differ from the kinase that phosphorylates the α_1 subunit in some way, in that no change in activation rate is seen with time. If there was a loss of the kinase phosphorylating the β subunit, then this model would predict that the activation rate would be seen to decrease with time. The phosphorylation of the β subunit is influenced by activation of G-

proteins, either directly, or via a non-freely diffusible second messenger, in such a way that the dephosphorylated form is favoured (note for simplicity, the model refers to direct action of the G-protein). This could involve the activated α subunit of the G-protein (i.e. α-GTP), or the G-protein dependent molecule, having a high affinity for, and so binding to, the dephosphorylated form of the β subunit of the calcium channel, preventing phosphorylation. As a result the interaction between α_1 and β is prevented. Alternatively, α-GTP or an intermediate may either enhance the PP activity or inhibit the kinase activity involved with the phosphorylation of the β subunit. Since EGTA was present at high concentrations, the possible kinases would be AK and PKC. However neither have been clearly shown to be involved in signal transduction in DR, or any preparation. Therefore, an enhancement of the PP or prevention of β subunit phosphorylation would seem the most likely possibilities. If the kinase involved is AK, to explain the observations that forskolin has no effect on signal transduction, it has to be assumed that the kinase is normally maximally active. The interaction of the G-protein in such a way that the channels activate from a different resting state, would be in keeping with the kinetic studies of Kasai & Aosaki (1989) and Kasai (1992).

The data obtained in this study would tend not to favour the model illustrated in equation 7.1, where the channel opens from state 4 via state 1. One of the pieces of evidence that has been put forward in support of model equation 7.1 is that in the presence of GTPγS, biexponential activation is seen, with the fast component having a similar time constant to control activation (Dolphin 1991b). This is not the case in DR. In addition the finding that the Q_{10} for both

$\tau_{a,f}$ and $\tau_{a,s}$ with GTPγS is significantly lower than the control time constant is not in keeping with model 7.1, but is more in favour of the model presented in this thesis.

It has been suggested that the apparent effect of prepulses in reversing the action of transmitters is in fact due to facilitation of channels not affected by receptor activation (Tatebayashi & Ogata, 1992). However the finding in DR that prepulses clearly reverse the action of GTPγS on the activation rate Q_{10} (see table 7.2) strongly suggests that this is not the case. Rather, the mechanism of activation appears to be altered by 8-OH-DPAT and GTPγS, and reversed back to the control mechanism by depolarisations. Therefore any hypothesis for the action of the G-protein has to take into account that this is reversed or inhibited in a voltage dependent way. Lopez and Brown (1991) have proposed a hypothesis where a G-protein dependent blocking molecule is coupled to calcium channels to produce inhibition of the current. In the model presented here, this may represent the interaction between α-GTP and the phosphatase, or dephosphorylated β subunit. Inhibition is reported to occur at a GTPγS concentration dependent rate, and unblocking is voltage dependent, being mediated by large depolarisations (Lopez & Brown, 1991). Since the unblocking is also GTPγS concentration dependent, it seems unlikely that depolarisation simply drives channels from state 4 to 5 rapidly without the reassociation of the β subunit. Therefore it would seem that the α-GTP action on the phosphatase or dephosphorylated β subunit is inhibited by large depolarisations. Then if the kinase is maximally active, the β subunits equilibrium would shift towards the phosphorylated form, and channel state 4 revert to 1 to allow rapid opening. This may be different to chromaffin cells where

voltage dependent phosphorylation is proposed to underlie current facilitation by depolarisations (Artalejo et al. 1992b). OA presumably works by either blocking the enhancement of the phosphatase activity by α-GTP, or decreasing the availability of dephosphorylated β subunits for α-GTP to bind to.

The model presented would account for many of the observations made not only in DR, but in other cell types as well. The action of OA in these cells, and I1PP in rat DRG (Dolphin, 1992a & b), may be similar in shifting the equilibrium between states 1 and 4 in the presence of GTPγS towards state 1, while the action of BDM in mouse DRG (Huang & McArdle, 1992) would be opposite to the action of OA in DR on the equilibrium between states 1 and 3. Clearly if the kinases and PPs involved in these two equilibria are similar, then teasing out the different effects may be difficult. Certainly both PPs in DR seem to be OA sensitive.

A potentially serious draw back of this model is that different classes of channels may be involved in the two equilibria between closed channels described. While several groups have suggested that HVA current is preferentially subject to rundown (Carbone & Lux, 1987a, Fox et al. 1987a, Hagiwara et al. 1988, Bargas et al. 1991), the action of BDM in mouse DRGs may be particularly L-type current related (Huang & McArdle, 1992) in that Bay K 8644 promotes the suppression of calcium current. However, since in this case 100% suppression results, while 47% occurs in the absence of Bay K 8644, it seems likely that N-type channels are also involved, since these are present in DRG neurones (Kostyuk et al. 1988). It may in fact be the case that Bay K 8644 simply promotes the action of BDM on L-type channels in the same way it has been suggested to promote

phosphorylation (Dolphin, 1991a), while N-type channels are susceptible in the control situation.

If the current activation rate is determined by an interaction between the α_1 and β subunits, and this interaction involves their repositioning in the membrane, and the dynamic equilibrium between the phosphatase and kinase determining the phosphorylation state of the β subunit, then this would be compatible with the high Q_{10} normally seen for the activation rate in DR. In most cell types, including DR neurones, closed channels are presumably primarily in state 1, to explain the rapid activation, and the lack of effect of prepulses in controls. However, in chromaffin and SCG cells, it would seem that there is either a significant basal activity of G-proteins, or lack of activity of the kinase converting state 4 to 1, that causes some channels to be in state 4, and thus open slowly. Depolarising prepulses are then able to relieve the action of the G-protein, or enhanced phosphorylation, leading to facilitation. This may explain why GDPβS decreases and GTPγS increases facilitation in SCG (Ikeda, 1991). If either an interaction with the subunits, or the phosphatase involved the movement of the G-protein and/or another molecule or subunit of the channel, in the membrane, then this would account for the high Q_{10} seen for the action of 8-OH-DPAT on the activation rate.

9. Conclusions

This study has confirmed many of the previous observations of calcium currents and their modulation by 5-HT in DR neurones. In addition, several new findings have been made.

It appears that phosphorylation, at a site that is dephosphory-

lated by an OA sensitive phosphatase, is involved in the maintenance or enhancement of HVA current in DR cells, as revealed by the runup that was observed with OA. The results with forskolin were somewhat inconclusive, so it is not clear if this phosphorylation is mediated by AK.

The temperature sensitivity of the HVA current amplitudes recorded is similar to previous work on calcium currents, but is generally higher than that seen for sodium and potassium currents, in other preparations. Analysis of the Q_{10} for current amplitude at different times during depolarising test pulses, together with using different holding potentials, suggests that the various components of HVA currents have different temperature sensitivities. In particular, it would seem that the fast inactivating component(s) that are inactivated when the H.P. is -50 mV have higher amplitude Q_{10}'s than the more sustained component(s) that remain at this H.P.

The analysis of inactivation at different temperatures, also provided information as to the heterogeneous nature of HVA calcium current in DR neurones. While at room temperature, there appeared to be both an inactivating and a more sustained component, when the temperature was increased above 25°C, a third component appeared to be recruited that inactivated fastest of all.

While inactivation and deactivation (as assessed from tail currents) have Q_{10}'s that are around 3, current activation is much more temperature sensitive, with a Q_{10} for the activation time constant of over 10. Several groups have previously suggested that calcium current activation is highly temperature sensitive, though none have shown such a high value for the Q_{10}. These figures, while rather circumstantial, are commensurate with a hypothesis that while

inactivation and deactivation may be active processes, activation has a higher energy requirement, such as would occur with a multistep series of reactions, and/or the translocation of molecules in the lipid membrane.

The action of the 5-HT_{1A} receptor agonist 8-OH-DPAT, and the non-hydrolysable GTP analogue, GTPγS, on current amplitude was studied, in addition to a careful analysis of the actions of these two drugs on the kinetic parameters of the currents. As has previously been shown, both lead to a partial reduction in current amplitude, together with a slowing of the activation rate. In addition, a novel action in DR has been identified. Both 8-OH-DPAT and GTPγS caused an increase in the duration of the tail current time constant. These broadened tails were relatively cadmium insensitive. Since the current which showed least sensitivity to cadmium, had many of the characteristics of LVA current, it has been proposed that activation of 5-HT_{1A} receptors enhances LVA current via a G-protein dependent mechanism, and that it is this enhancement that underlies the prolonged tail currents.

Analysis of the rate of activation with and without both 8-OH-DPAT and GTPγS, showed that these drugs caused a change from a fast monoexponential process, to a slower biexponential one. This was not simply due to the introduction of a second slow component, since even the faster of the two components with GTPγS was slower than the single control component.

In addition to the change in the kinetics of current activation, 8-OH-DPAT and GTPγS, but not GDPβS, caused the temperature sensitivity of activation to drop from over 10 to around 3.5. This is argued to be highly suggestive that G-protein activation leads to a change in the mechanism or process underlying current activation. Fast

activation, with a high Q_{10}, could be restored by the application of a large depolarising prepulse, prior to the test pulse. This is likely to be due to the depolarisation reversing the action of the G-protein, rather than simply facilitating some quiescent fast activating current.

Application of OA also lead to a reversal of the decrease in activation rate Q_{10} by both 8-OH-DPAT and GTPγS, together with a partial decrease in the slowing of current activation, though current amplitude was still reduced by 8-OH-DPAT. It has therefore been hypothesised that G-protein activation in some way causes HVA channels to tend to be dephosphorylated by an OA sensitive PP, from which state they open on depolarisation more slowly than if they were phosphorylated. This deposphorylation is blocked by OA, and also seems to be voltage sensitive, in that it is reversed by large depolarisations. It is also suggested that the phosphorylation site involved in determining the activation kinetics is different to the one involved in the maintenance or enhancement of HVA mentioned above. Since OA did not prevent current amplitude reduction by 8-OH-DPAT, it may be that inhibition of HVA current by transmitters in neurones involves more than one mechanism.

Table 7.1 - Amplitude Q_{10} Values

	Q_{10} Mean (95% CI, n = measurements, cells)
Peak, H.P. -100 mV	2.47 (CI = 1.06 - 5.80, n = 42,33)
'Steady State', H.P. -100 mV	2.08 (CI = 1.00 - 4.30, n = 38,30)
Peak, H.P. -50 mV	1.69 (CI = 1.07 - 2.66, n = 10,8)
8-OH-DPAT Isochronal	2.01 (CI = 1.12 - 3.59, n = 13,11)
8-OH-DPAT 'Steady State'	2.20 (CI = 0.97 - 4.99, n = 13,11)
GTPγS 'Steady State'	1.89 (CI = 0.73 - 4.89, n = 25,17)
GTPγS Isochronal to Prepulse	2.75 (CI = 0.87 - 8.63, n = 10,6)
GTPγS Peak with Prepulse	1.95 (CI = 0.94 - 4.03, n = 10,6)
GTPγS 'Steady State' with Prepulse	1.77 (CI = 0.54 - 5.77, n = 10,6)
GDPβS Peak	2.25 (CI = 0.83 - 6.08, n = 13,9)
GDPβS 'Steady State'	2.16 (CI = 0.58 - 8.07, n = 13,9)
Okadaic Acid Peak	1.87 (CI = 0.65 - 5.37, n = 12,6)
Okadaic Acid 'Steady State'	1.82 (CI = 0.68 - 4.92, n = 12,6)
Okadaic Acid + 8-OH-DPAT Peak	1.76 (CI = 0.70 - 4.44, n = 12,6)
Okadaic Acid + 8-OH-DPAT 'S. S.'	1.75 (CI = 0.49 - 6.24, n = 12,6)
Okadaic Acid + GTPγS Peak	2.20 (CI = 0.81 - 5.98, n = 14,7)
Okadaic Acid + GTPγS 'S. S.'	1.72 (CI = 0.63 - 4.72, n = 14,7)
Okadaic Acid + GTPγS Peak with Prepulse	1.82 (CI = 0.64 - 5.20, n = 14,7)
Okadaic Acid + GTPγS 'S. S.' with Prepulse	1.53 (CI = 0.58 - 4.09, n = 14,7)

Table 7.2 - Activation Time Constant Q_{10} Values

	Q_{10} Mean (95% CI, n = measurements, cells)
Control, H.P. -100 mV	10.20 (CI = 1.19 - 87.56, n = 42,32)
Control, H.P. -50 mV	12.65 (CI = 0.85 - 187.7, n = 12,8)
8-OH-DPAT	3.17 (CI = 0.79 - 12.41, n = 13,11)
GTPγS Single	2.41 (CI = 0.25 - 23.12, n = 23,17)
GTPγS Fast Double	2.70 (CI = 0.18 - 40.30, n = 23,15)
GTPγS Slow Double	2.69 (CI = 0.42 - 17.29, n = 23,15)
GTPγS with Prepulse	11.16 (CI = 1.32 - 94.75, n = 10,6)
GDPβS	12.83 (CI = 2.10 - 78.49, n = 13,9)
Okadaic Acid	10.00 (CI = 1.49 - 67.23, n = 12,6)
Okadaic Acid + 8-OH-DPAT	14.05 (CI = 1.81 - 109.1, n = 12,6)
Okadaic Acid + GTPγS	15.95 (CI = 0.99 - 257.4, n = 14,7)
Okadaic Acid + GTPγS with Prepulse	14.29 (CI = 1.84 - 111.2, n = 14,7)

Table 7.3 - Tail Current Time Constant Q_{10} Values

	Q_{10} Mean (95% CI, n = measurements, cells)
Control, H.P. -100 mV	2.88 (CI = 0.36 - 23.28, n = 36,30)
Control, H.P. -50 mV	3.28 (CI = 0.15 - 72.35, n = 12,8)
8-OH-DPAT	1.64 (CI = 0.15 - 17.60, n = 13,11)
GTPγS	2.05 (CI = 0.19 - 22.61, n = 22,16)
GTPγS with Prepulse	3.37 (CI = 0.12 - 93.62, n = 10,6)
GDPβS	1.50 (CI = 0.27 - 8.42, n = 12,8)
Okadaic Acid	1.18 (CI = 0.83 - 1.70, n = 12,6)
Okadaic Acid + 8-OH-DPAT	1.93 (CI = 0.56 - 6.66, n = 12,6)
Okadaic Acid + GTPγS	4.93 (CI = 0.31 - 77.96, n = 14,7)
Okadaic Acid + GTPγS with Prepulse	4.07 (CI = 0.21 - 79.03, n = 14,7)

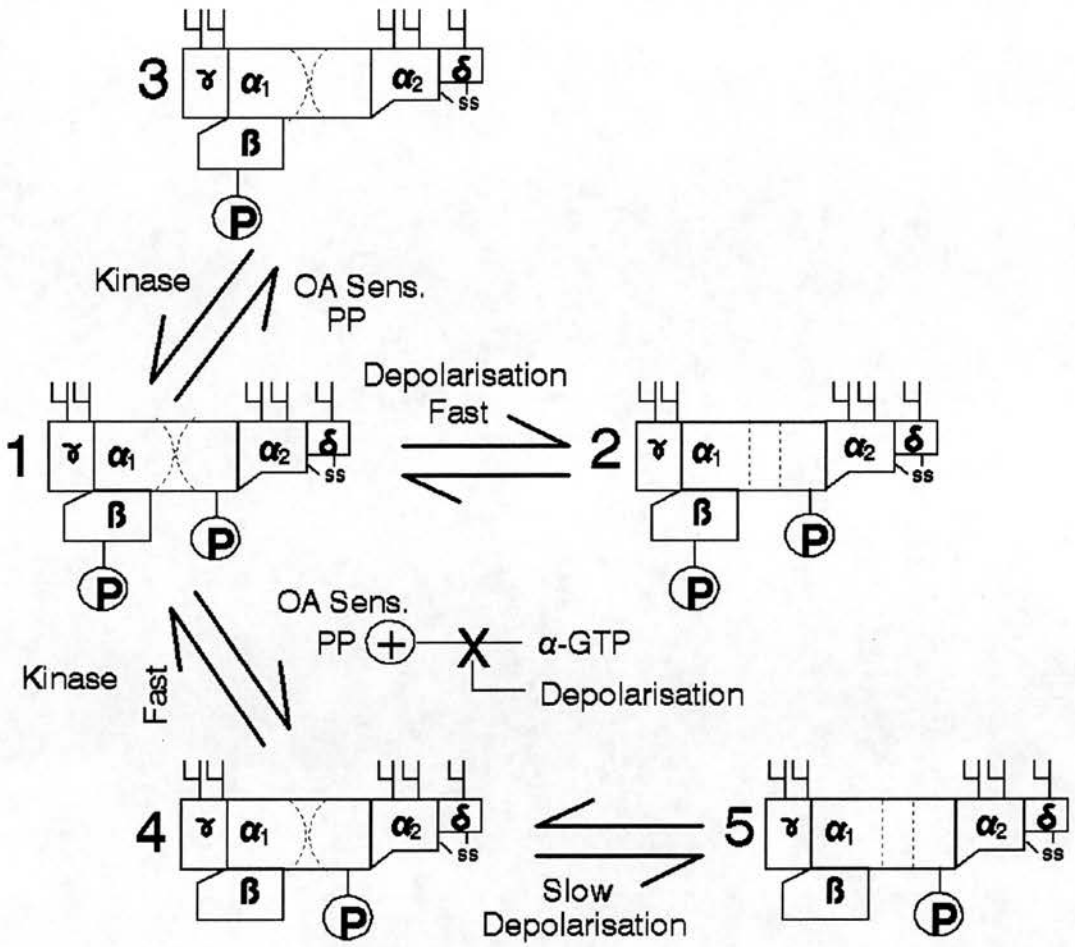

Figure 7.1: **Model for rundown and action of 5-HT on calcium channels in DR neurones.** Model described in detail in text. Basic structure of channel adapted from Catterall & Striessnig (1992). Appendages on γ, δ, and α_2 subunits represent glycosylation sites on the extracellular surface of the channel. P represents phosphorylation sites on the intracellular surface. ss = disulphide bond between α_2 and δ subunits. OA Sens. PP = OA sensitive phosphatases. α-GTP = activated α subunit of G-protein bound to GTP.

Appendix A Abbreviations

This appendix details all abbreviations that are used in more than one section in the text of this thesis. All are quoted in full the first time they are used in the text.

4-AP	-	4-aminopyridine
5-HT	-	5-hydroxytryptamine
8-OH-DPAT	-	8-hydroxy-2-(di-n-propylamino)tetraline
aCSF	-	artificial cerebrospinal fluid
AHP	-	after hyperpolarisation
AK	-	cAMP-dependent kinase
ATP	-	adenosine triphosphate
ATPγS	-	adenosine 5'-O-3-thiotriphosphate
BAPTA	-	1,2-bis(2-aminophenoxy)ethane N,N,N',N'-tetraacetic acid
BDM	-	2,3-butanedione monoxime
cAMP	-	cyclic adenosine monophosphate
cGMP	-	cyclic guanosine monophosphate
CI	-	confidence interval (95%)
DA	-	dopamine
DARPP	-	dopamine and cAMP regulated phosphoprotein
DHP	-	dihydropyridine
DR	-	dorsal raphé
DRG	-	dorsal root ganglia
EDTA	-	ethylene-diaminotetraacetic acid
EGTA	-	ethylene glycol-bis(β-aminoethyl ether)N,N,N',N'-tetraacetic acid

GABA - γ-aminobutyric acid

GDPβS - guanosine 5'-O-2-thiodiphosphate

GTPγS - guanosine 5'-O-3-thiotriphosphate

H.P. - holding potential

HVA - high voltage activated calcium current

I1PP - residues 9-14 of phosphatase inhibitor 1 peptide

IBMX - isobutylmethylxanthine

LHRH - leutinising hormone releasing hormone

LSD - D-lsergic acid diethylamide

LVA - low voltage activated calcium current

m^x - Hodgkin and Huxley fuction for current activation, where x is an integer. See equation 2.8

NA - noradrenaline

NAN 190 - 1-(2-meth-oxyphenyl)-4-[4-(2-phthalimmidobutyl] piperazine

OA - okadaic acid

OAG - 1-oleoyl-2-acetylglycerol

PKC - protein kinase C

PP - protein phosphatase

PTx - pertussis toxin

Q_{10} - temperature coefficient. See equations 1.2 and 1.3

SCG - superior cervical ganglion

SEM - standard error of the mean

TBA - tetrabutylammonium

TEA - tetraethylammonium

TTX - tetrodotoxin

V_h - voltage eliciting half maximal activation or inactivation

τ_a - activation rate time constant

$\tau_{a,f}$ - fast activation rate time constant derived from a double exponential function

$\tau_{a,s}$ - slow activation rate time constant derived from a double exponential function

τ_i - inactivation time constant

$\tau_{i,f}$ - fast inactivation time constant derived from a double exponential function

$\tau_{i,s}$ - slow inactivation time constant derived from a double exponential function

τ_t - tail current time constant

ω-Aga-IVA - IVA ω-toxin fraction from *Agelenopsis aperta*

ω-CgTx - GVIA ω-toxin fraction from *Conus geographicus*

Appendix B Analysis Programme

The following appendix lists the basis of the computor programme used for data analysis in this study, and the mathematical methods used in the programme are discussed in chapter 2. The programme is written in Borland Turbo Pascal, version 6.0, and is comprised of the main programme, named NewFit4, and several units, listed after the "use" command at the beginning of NewFit4. CRT and DOS are predefined units that allow manipulation of text on screen, and the use of procedures and functions that are equivolent to some common DOS commands, respectively. MyUtils is a unit that contains several personally defined procedures, such as pausing, and bullet proofed methods for entering characters. Direct2 receves a string variable from the programme on several occasions, and returns a drive, path and filename chosen from directory lists. Files containing columns of Ascii data are read by the Readfile unit. These files were generally produced from raw current and voltage data using the CED (UK) Patch and Voltage clamp programme, version 5.0. These files could be viewed together with calculated curves using the ViewFile unit. None of the above units are listed in this appendix. However, following the main NewFit4 programme, the Curves and NewMak2 units are listed. The first of these contains the procedures for fitting curves, and the second for making new Ascii files from others, such as by removing a specific section (e.g. the period of inactivation), and then forward averaging this section if required. Programme remark statements are contained in curly brackets e.g. {}.

```
Program NewFit4;   {Version 4.0     22/04/92}

     {$M 65520,0,300000}      {Sets heap to 300K to allow GoToDOS to run}
                              {and increases the size of the stack}

 uses CRT, DOS, MyUtils, Direct2, Curves, NewMak2, ViewFile, Readfile ;

 {Const CurveNo = 10;   number of curves able to fit:
                                                    1 = double inc exp
                                                    2 = single inc exp
                                                    3 = double dec exp
                                                    4 = single dec exp
                                                    5 = inc Boltz
                                                    6 = dec Boltz
                                                    7 = H & H M1
                                                    8 = H & H M2
                                                    9 = H & H M3
                                                   10 = H & H M4
                                                   Defined in curves unit}

 Type
    {CArray = Array[1..CurveNo] of Boolean;  defined in the curves unit}
    PointerR = ^PointerRecord;
    PointerRecord = RECORD
                    Name : string47;
                    Fits : Carray;
                    next : PointerR;
                    end;
Var
   MainMenuChoise : integer;
   Ch : char;
   FileName : string47;
   FitHead, FitTail : PointerR;
   HeapMark : Pointer;
   Conf : char;

 {********************  MAIN PROCEDURES AND FUNCTIONS **********************}

 PROCEDURE Init(Var FitHead, FitTail : PointerR;
                Var HeapMark : Pointer);

 Begin
    FitHead := Nil;
    FitTail := Nil;
    Mark(HeapMark);
 End;

 PROCEDURE TitlePage;     {gives some info about the programme in general}

 BEGIN
   clrscr;
   writeln;
   HighVideo;
   writeln('                              Newfit Version 4.0');
   writeln('                            R.H. McAllister-Williams');
```

```
  NormVideo;
  writeln;
  writeln(' This programme has three main functions:');
  writeln;
  writeln(' 1.  It can create ASCII files from standard CED output files,
or other ASCII');
  writeln('     files.  Sections can be removed from the source file and
averaged if');
  writeln('     wanted.  The final data can either be written to a new
destination file');
  writeln('     or added to an old one, to allow sections of data to be
joined together.');
  writeln;
  writeln(' 2.  CED output files, and files generated by this programme may
be plotted');
  writeln('     on sceen, together with curves.');
  writeln;
  writeln(' 3.  Curves can be fitted to ASCII files.  These can be of 3
main types:');
  writeln('     A.  Exponentials - single or double;');
  writeln('     B.  Boltzman''s;');
  writeln('     C.  Hodgekin & Huxley Kinetics.');
  writeln;
  HighVideo;
  Case Test8087 of
    0 : Write('    No co-processor; using software emulation');
    1 : Write('             8087 co-processor in use');
    2 : Write('             80287 co-processor in use');
    3 : Write('             80387 co-processor in use');
    End; {case}
  NormVideo;
  writeln;
  pause;
END;      {of TitlePage procedure}

PROCEDURE MainMenu;     {puts the main menu on the screen}

BEGIN
  clrscr;
  HighVideo;
  writeln;
  writeln;
  writeln('                                  èëëëëëëëëëëëëëëf');
  writeln('                                  ¤   Main Menu   ¤');
  writeln('                                  àëëëëëëëëëëëëëë¥');
  normVideo;
  writeln;
  writeln;
  writeln('                              1.  Create an ASCII file.');
  writeln;
  writeln('                              2.  View an ASCII file.');
  writeln;
  writeln('                              3.  Fit curves to files.');
  writeln;
  writeln('                              4.  Exit to DOS.');
  writeln;
```

```
  writeln('                          5.  Exit programme.');
END;    {of MainMenu procedure}

{****************************** MAKE PROCEDURES ************************}

PROCEDURE MakeTitlePage;       {title page for the make file section}

BEGIN
   clrscr;
   writeln;
   writeln;
   HighVideo;
   writeln('                          ASCII File Generation Section');
   NormVideo;
   writeln;
   writeln;
   writeln('        In this section, you need to choose a source file.
This must be');
   writeln('        of an ASCII type with two or three columns, separated
by spaces,');
   writeln('        the first of which will probably be time (e.g. a CED
DA0 text file,');
   writeln('        or a file generated by this programme).  If there are
three columns,');
   writeln('        you will be asked if you want 1 & 2, or 1 & 3.  The
file MUST start');
   writeln('        with either a letter, or the data.  You will be told
information');
   writeln('        about the file and asked what you want to do with it.
 If you do');
   writeln('        not know the start and finish times of the section you
want, either');
   writeln('        exit the programme, or use the view file section before
you go any');
   writeln('        further.  You must also specify a destination file
name.  Duplicates');
   writeln('        will only be checked for in D:\NewFit\Files, which is
also the directory');
   writeln('        the file will be written to.');
   writeln;
   writeln;
   pause;
END;      {of the MakeTitlePage procedure}

PROCEDURE MakeMenu;

BEGIN
  clrscr;
  HighVideo;
  writeln;
  writeln;
  writeln('                              èëëëëëëëëëëëëëëëëëëëf');
  writeln('                              ¤  Make File Menu  ¤');
  writeln('                              àëëëëëëëëëëëëëëëëëëë¥');
  normVideo;
  writeln;
```

```
  writeln;
  writeln('                              1.  Choose a source file.');
  writeln;
  writeln('                              2.  Exit to DOS.');
  writeln;
  writeln('                              3.  Exit to main menu.');
END;    {of MakeMenu procedure}

PROCEDURE MakeProcedure;{main MakeFile procedure, all others run from here}

Var
  MakeMenuChoise : integer;
  Ch : char;

BEGIN
   MakeTitlePage;
   Ch := 'Y';
   while Ch = 'Y' do    {setting up endless loop}
     begin
        MakeMenu;
        writeln;
        writeln;
        write('       Enter your selection:  ');
        GetGoodInt(1,3,MakeMenuChoise);
           Case MakeMenuChoise of
              1 : FileMake;   {goes to NewMak2 unit}
              2 : GoToDOS;
              3 : Exit;
           end;     {of case statement}
     end;   {of while loop}
END;    { of MakeProcedure}

{****************************** VIEW PROCEDURES ***********************}

PROCEDURE ViewTitlePage;  {title page for the view file section}

Begin
   clrscr;
   writeln;
   writeln;
   HighVideo;
   writeln('                               View File Section');
   NormVideo;
   writeln;
   writeln;
   writeln('     This section is able to plot on screen any ascii file that
consists');
   writeln('     of two columns of data.  The X variable must be in
accending order,');
   writeln('     though the data does not necessaily have to be "sampled"
at a uniform');
   writeln('     rate.  Curves can be plotted over the data.  To do this,
you need to');
   writeln('     know the value of the constants in the appropriate
equation.  This means');
   writeln('     you need to run the curve fitting routine on the data
```

```
first of all.');
   writeln('     A second set of data can also be plotted over the first
for comparison.');
   writeln;
   writeln;
   pause;
End;    {of the ViewTitlePage}

PROCEDURE ViewMenu;

BEGIN
  clrscr;
  HighVideo;
  writeln;
  writeln;
  writeln('                                    èëëëëëëëëëëëëëëëëëëf');
  writeln('                                    ¤  View File Menu  ¤');
  writeln('                                    àëëëëëëëëëëëëëëëëëë¥');
  normVideo;
  writeln;
  writeln;
  writeln('                                1.  Choose a file.');
  writeln;
  writeln('                                2.  Exit to DOS.');
  writeln;
  writeln('                                3.  Exit to main menu.');
END;    {of MakeMenu procedure}

PROCEDURE ViewProcedure;  {main view procedure, all others run from here}

Var
  ViewMenuChoise : integer;
  Ch : char;

Begin
   ViewTitlePage;
   Ch := 'Y';
   While Ch = 'Y' do
     begin
        ViewMenu;
        writeln;
        writeln;
        write('       Enter your selection:  ');
        GetGoodInt(1,3,ViewMenuChoise);
        Case ViewMenuChoise of
           1 : PlotGraph;      {goes to viewfile unit}
           2 : GoToDOS;
           3 : Exit;
        end;  { of case statement}
     end;  {of while loop}
 end;  {of procedure}

 {******************************** FIT PROCEDURES ************************}

  PROCEDURE FitTitlePage;       {title page for the curve fit section}
```

```
  BEGIN
     clrscr;
     writeln;
     writeln;
     HighVideo;
     writeln('                          Curve Fitting Section');
     NormVideo;
     writeln;
     writeln;
     writeln('        In this section, you choose files that you want
fitted, and');
     writeln('        specify with which curves.  Once you have selected
all the files');
     writeln('        that you want to do, you need to set the programme
running.');
     writeln;
     writeln;
     pause;
  END;      {of the FitTitlePage procedure}

 PROCEDURE FitMenu;

  BEGIN
    clrscr;
    HighVideo;
    writeln;
    writeln;
    writeln('                                    èëëëëëëëëëëëëëëf');
    writeln('                                    ¤   Fit Menu   ¤');
    writeln('                                    àëëëëëëëëëëëëëë¥');
    normVideo;
    writeln;
    writeln;
    writeln('                           1.  Choose a file.');
    writeln;
    writeln('                           2.  Run fitting procedure.');
    writeln;
    writeln('                           3.  Exit to DOS.');
    writeln;
    writeln('                           4.  Exit to main menu.');
  END;    {of FitMenu procedure}

  PROCEDURE GetCurves(Var FitPtr : PointerR);

    Var
      Ch : array[1..curveNo] of char;
      Count : integer;
      YN : Char;

    Begin
       YN := 'N';
       Window(1,1,80,25);
       Clrscr;
       writeln;
       Highvideo;
       writeln('                      Select Possible Curves');
```

```
        NormVideo;
        writeln;
        writeln('              1: Double Increasing Exponential...');
        writeln('              2: Single Increasing Exponential...');
        writeln('              3: Double Decreasing Exponential...');
        writeln('              4: Single Decreasing Exponential...');
        writeln('              5: Increasing Boltzman.............');
        writeln('              6: Decreasing Boltzman.............');
        writeln('              7: Hodgkin & Huxley M1.............');
        writeln('              8: Hodgkin & Huxley M2.............');
        writeln('              9: Hodgkin & Huxley M3.............');
        writeln('             10: Hodgkin & Huxley M4.............');
        While upcase(YN) = 'N' do
           Begin
              For Count := 1 to CurveNo do
                 begin
                   GotoXY(51,Count + 3);
                   GetGoodChar(YNChars,Ch[Count]);
                   if upcase(Ch[Count]) = 'Y' then
                      FitPtr^.Fits[Count] := True
                      Else FitPtr^.Fits[Count] := False;
                 end;  {of for loop}
              writeln;
              writeln;
              write(' Are you happy with these selections?  ');
              GetGoodChar(YNChars,YN);
           end;  {of while loop}
     End;   {of GetCurves procedure}

  PROCEDURE FitFileChoise(Var FitHead, FitTail : PointerR);

    Var
      Ans : string5;
      FileConf : char;
      message : MessArray;
      Line : integer;

    BEGIN
       FileConf := 'N';
       While upcase(FileConf) = 'N' do
         begin
            Repeat
              GetFile(FileName);
              window(1,1,80,25);
              clrscr;
              if FileName = 'NONE' then exit;
              CheckColumns(Ans,FileName);
              If Ans <> 'Two' then
                 begin
                    writeln;
                    Beep;
                    writeln('For the curve fitting section, the file must be
of two columns.');
                    writeln('Try again to select an appropriate file.');
                    writeln;
                    pause;
```

```
                end;
            until Ans = 'Two';
            ReadFileMessage(Message, Line, FileName);
            If Line > 0 then
               begin
                  writeln;
                  DisplayMessage(Message, FileName);
               end
               else begin
                  writeln;
                  writeln('File ',FileName,' does not contain a message.');
               end;
            writeln;
            write('Are you happy with the file that you have selected? (Y/N)
  ');
            GetGoodChar(YNChars, FileConf);
          end;  {of while loop}
        If FitHead = Nil then
          begin
            New(FitHead);
            FitHead^.name := FileName;
            GetCurves(FitHead);
            FitHead^.next := Nil;
            FitTail := FitHead;
          end
        Else begin
            New(FitTail^.next);
            if FitHead = FitTail then
               FitHead^.next := FitTail^.next;
            FitTail :=FitTail^.next;
            FitTail^.name := FileName;
            GetCurves(FitTail);
            FitTail^.next := Nil;
            end;
    END;  {of FileChoise}

  PROCEDURE RunFit(FitHead, FitTail : PointerR;
                   FileName : string47);

    Var
      Ch1, Ch2, Ch3 : char;
      Count1, Count2 : integer;
      Counter : integer;
      CurrPtr : PointerR;
      NoFiles : Boolean;

{----------------------- Sub-level RunFit procedures --------------------}

  PROCEDURE WriteList(FitHead : PointerR;
                      Var Count1 : integer);

    Var
      CurrPtr2 : PointerR;
      Count3  : integer;

    Begin
```

```
    CurrPtr2 := Nil;
    window(1,1,80,25);
    clrscr;
    writeln('       File                          DIE SIE DDE SDE IB  DB  M1
M2  M3  M4');
    writeln;
    CurrPtr2 := FitHead;
    If CurrPtr2 = Nil then
      begin
        Beep;
        HighVideo;
        writeln(' There are no files entered !!!!!!');
        NormVideo;
        writeln;
        NoFiles := True;
        pause;
        exit;
      end;
    Count1 := 0;
    While CurrPtr2 <> Nil do
      begin
         Count1 := Count1 + 1;
         with CurrPtr2^ do
           begin
              GotoXY(1, Count1 + 2);
              write(Count1, '.');
              GotoXY(5, Count1 + 2);
              write(name);
              for Count3 := 1 to CurveNo do
                 begin
                    GotoXY(30 + (Count3 * 4), Count1 + 2);
                    if Fits[Count3] then write('Y') else write('N');
                 end;
           end;  {of with clause}
         currptr2 := currptr2^.next;
      end;  {of while loop}
    currptr2 := Nil;
 end;  { of WriteList procedure}

PROCEDURE CorrectEntry(Var Count1 : integer;
                       Var FitHead : PointerR;
                       Var FileName : string47;
                       Count2 : integer);

 Var
   TempPtr, CurrPtr3 : PointerR;
   Ch1, Ch2, Ch3 : Char;
   Counter : integer;
   Ans : string5;
   FileConf : char;
   message : MessArray;
   Line : integer;

 Begin
    TempPtr := Nil;
    CurrPtr3 := Nil;
```

```
      CurrPtr := FitHead;
      Count1 := 0;
      While Count1 < Count2 do
        Begin
           Count1 := Count1 + 1;
           If Count1 = Count2 then
              begin
                 writeln;
                 write(' Delete file and curve selection ?  ');
                 GetGoodChar(YNChars, Ch3);
                 If upcase(Ch3) = 'Y' then
                    begin
                       Counter := 0;
                       TempPtr := FitHead;
                       If CurrPtr3 = FitHead then
                          begin
                             FitHead := FitHead^.next;
                             Dispose(CurrPtr3);
                          end
                          else begin
                             While Counter < (Count2 - 1) do
                                begin
                                   Counter := Counter + 1;
                                   If Counter = Count2 - 1 then
                                      begin
                                         TempPtr^.next := CurrPtr3^.next;
                                         Dispose(CurrPtr3);
                                      end;
                                   TempPtr := TempPtr^.next;
                                end;  {of while loop}
                          end;  {of else clause}
                       Exit;
                    end;  {of if ch3 = y}
                 writeln;
                 write(' Correct file name ?  ');
                 GetGoodChar(YNChars, Ch1);
                 If upcase(Ch1) = 'N' then
                   begin
                      FileConf := 'N';
                      While upcase(FileConf) = 'N' do
                        begin
                           Repeat
                             GetFile(FileName);
                             window(1,1,80,25);
                             clrscr;
                             if FileName = 'NONE' then exit;
                             CheckColumns(Ans,FileName);
                             If Ans <> 'Two' then
                                begin
                                   writeln;
                                   Beep;
                                   writeln('For the curve fitting section,
the file must be of two columns.');
                                   writeln('Try again to select an
appropriate file.');
                                   writeln;
```

```
                                    pause;
                                  end;
                            until Ans = 'Two';
                            ReadFileMessage(Message, Line, FileName);
                            If Line > 0 then
                               begin
                                  writeln;
                                  DisplayMessage(Message, FileName);
                               end
                               else begin
                                  writeln;
                                  writeln('File ',FileName,' does not contain
a message.');
                               end;
                            writeln;
                            write('Are you happy with the file that you have
selected? (Y/N)  ');
                            GetGoodChar(YNChars, FileConf);
                         end;  {of while loop}
                      CurrPtr3^.name := FileName;
                    end;   {of if upcase(ch1) = 'N'}
                writeln;
                write(' Correct curve selection ?  ');
                GetGoodChar(YNChars, Ch2);
                If upcase(Ch2) = 'N' then GetCurves(CurrPtr3);
             end; {of section if found record i.e. count1 = count2}
          CurrPtr3 := CurrPtr3^.next;
       end;  {of main while loop}
    CurrPtr3 := Nil;
    TempPtr := Nil;
  End;  {of CorrectEntry procedure}

{------------------------ Main level RunFit Procedure -----------------}

  BEGIN
    NoFiles := false;  {assume that there are files present}
    CurrPtr := Nil;
     Ch1 := 'N';
     While upcase(Ch1) = 'N' do
       begin
          WriteList(FitHead, Count1);
          If NoFiles = true then exit; {exit from RunFit procedure if there
                                        are no files}
          writeln;
          writeln;
          write(' Is it O.K. to run with these ?  ');
          GetGoodChar(YNchars, Ch1);
          If upcase(Ch1) = 'N' then
             begin
                writeln;
                write(' Return to fit menu?  ');
                GetGoodChar(YNChars,Ch2);
                If upcase(Ch2) = 'Y' then Exit;
                writeln;
                write('  Do you want to ammend an entry ?  ');
                GetGoodChar(YNChars, Ch3);
```

```
                If Upcase(Ch3) = 'Y' then
                  begin
                     WriteList(FitHead, Count1);
                     writeln;
                     write('  Enter the number of the file to be ammended:
 ');
                     GetGoodInt(1, Count1, Count2);
                     CorrectEntry(Count1, Fithead, FileName, Count2);
                  End
                  Else begin
                     beep;
                     writeln;
                     writeln('  Well what do you want ?');
                     writeln('  You are going to be returned to the fit
menu');
                     delay(1000);
                     Exit;
                  End;
             End;  {of if ch1 = N}
       End;  {of while loop}
     Counter := 0;
     CurrPtr := FitHead;
     while CurrPtr <> Nil do
       begin
          Counter := Counter + 1;
          with CurrPtr^ do
             FitCurves(name, Fits);
          CurrPtr := CurrPtr^.next;
       end;  { of while loop}
     CurrPtr := NIL
  END;   {of RunFit}

PROCEDURE FitProcedure;     {main fitting procedure, all others run from
here}

  Var
    FitMenuChoise : integer;

  BEGIN
     FitTitlePage;
     Ch := 'Y';
     while Ch = 'Y' do    {setting up endless loop}
       begin
          FitMenu;
          writeln;
          writeln;
          write('       Enter your selection:  ');
          GetGoodInt(1,4,FitMenuChoise);
             Case FitMenuChoise of
                1 : FitFileChoise(FitHead,FitTail);
                2 : Begin
                       RunFit(FitHead, FitTail, FileName);
                       Release(HeapMark);  {Clears heap}
                       Init(FitHead, FitTail, HeapMark);  {to prevent
dangling pointers}
                    end;
```

```
                3 : GoToDOS;
                4 : Exit;
              end;      {of case statement}
        end;    {of while loop}
   END;     { of FitProcedure}

{************************** MAIN PROGRAMME ******************************}

BEGIN
  Init(FitHead, FitTail, HeapMark);
  TitlePage;
  Ch:= 'Y';
  while ch = 'Y' do  {sets up endless loop which get out of if select 4 from
 menu}
     begin
        MainMenu;
        writeln;
        writeln;
        write('      Enter your selection:  ');
        GetGoodInt(1,6,MainMenuChoise);
            Case MainMenuChoise of
               1 : MakeProcedure;
               2 : ViewProcedure;
               3 : FitProcedure;
               4 : GoToDOS;
               5 : Begin
                     If FitHead = Nil then Halt
                       Else begin
                              RedAlert(350,200);
                              clrscr;
                              writeln;
                              HighVideo;
                              writeln('YOU HAVE NOT RUN THE FITFILE
 PROCEDURE ON SELECTED FILES !!!');
                              writeln;
                              write('Confirm you want to end:  ');
                              NormVideo;
                              GetGoodChar(YNChars, Conf);
                              If upcase(Conf) = 'Y' then
                                begin
                                   Release(HeapMark);
                                   Init(FitHead, FitTail, heapMark);
                                   Halt;
                                end;
                            end;  {of else clause}
                  end;  {of case of 4}
            end;    {of case statement}
     end;    {of while loop}
END.
```

```
UNIT CURVES;        {version 1.3  22/04/92}

{The unit containing the various functions that will be fitted to the data
and the Amoeba procedure.  Some procedures adapted and developed from
programmes written by Prof I.M.L.Donaldson}

{======================== Public section of unit ========================}

INTERFACE

Uses CRT, PRINTER, DOS, MyUtils;  {units used}

Const
   CurveNo = 10;

Type
   CArray = array[1..CurveNo] of Boolean;

PROCEDURE FitCurves(FileName : string47;
                    Fits : CArray);

 {======================== Private section of unit ========================}

IMPLEMENTATION

PROCEDURE FitCurves(FileName : string47;
                    Fits : CArray);

{********************* Main level Procedure Declarations ******************}
Const
    MaxNo = 1000;  {maximum no of points in a file}
    ftol = 1.0e-12; {tolerance, adjust as required}
    Maxmp = 6;   {sets the maximum values for mp and np that any curve uses}
    Maxnp = 5;
    MaxRuns = 8;   {sets maximum number of runs of fitting procedure}
    Tol = 0.00001;  {tolerance for improvement of reruns = 0.001%}

Type
   RealArr = Array[1..MaxNo,'x'..'y'] of real;
   glmpnp = ARRAY [1..Maxmp,1..Maxnp] OF extended;
   glmp = ARRAY [1..Maxmp] OF extended;
   glnp = ARRAY [1..Maxnp] OF extended;
   RunArray1 = ARRAY [1..MaxRuns,1..Maxnp] of real;
   RunArray2 = ARRAY [1..MaxRuns] of real;

Var
   year, month, day, hour, minute, sec, junk : word; {to get date and time}
   NumPoints : integer;
   mp, np : integer;
   Data : Realarr;
   InFile : Text;
   Counter : Integer;  {indicates which fit the unit is on}
   Counter2 : integer; {indicates which run the fit is on}
   IndexLimit : extended;
   pr : glnp;
   y : glmp;
```

```
   p : glmpnp;
   iter, ndim : integer;
   x : glnp;
   Total, Average : RunArray1;
   SumFunc, AvFunc : RunArray2;
   Ch : char;
   OK : boolean;

{********************* Sub-main level procedures ************************}

PROCEDURE Now; {gets date and time into the appropriately named variables}
begin
   GetDate(year,month,day,junk);
   GetTime(hour,minute,sec,junk);
end;

PROCEDURE GetLimit; {calculates indexlimit for the current data - see below}
  Begin
    IndexLimit := Data[numpoints,'x']/1350; { time constants must always >
 indexlimit}
  end;

PROCEDURE Initmpnp(Var mp, np : integer;   {sets mp and np to appropriate}
                   Var Total, Average : RunArray1; {values for the curve}
                   Var SumFunc, AvFunc : RunArray2);

  Var
    Count1, Count2 : integer;

  Begin
     if (counter = 1) OR (Counter = 3) then
       begin
          mp := 6;
          np := 5;
       end;
     if (Counter = 2) OR (Counter = 4) then
       begin
          mp := 4;
          np := 3;
       end;
     if (Counter = 5) OR (Counter = 6) then
       begin
          mp := 3;
          np := 2;
       end;
     if (Counter >= 7) AND (Counter <= 10) then
       begin
          mp := 5;
          np := 4;
       end;
     For Count1 := 1 to MaxRuns do
       begin
          SumFunc[Count1] := 0;
          AvFunc[Count1] := 0;
          For Count2 := 1 to np do
            begin
```

```
                Total[Count1, Count2] := 0;
                Average[Count1, Count2] := 0;
              end;
        end;  { of for loop}
  end; {of procedure}

PROCEDURE GetData;      {reads the input data from the file into array}

 Var
   Letters : GoodChars;
   chr1 : char;
   message : boolean;

 Begin
      Assign(Infile,FileName);        {open the input file for reading}
      Reset(Infile);
      GetLetterSet(Letters);
      message := true;
      while message = true do      {reads past any text}
        begin
           Chr1 := ' ';
           while (chr1 = ' ') OR (Chr1 = #10) OR (Chr1 = #13) do
             Read(InFile, Chr1);
           if chr1 in letters then readln(InFile)
             else message := false;
         end;  {of while loop}
      NumPoints := 0;
      While (Numpoints < MaxNo) And (NOT Eof(InFile)) do
         Begin
            NumPoints:=Numpoints+1;
            ReadLn(Infile, Data[NumPoints,'x'], Data[NumPoints,'y']);
         End;
      close(Infile);
   If Data[NumPoints,'x'] = 0 then
      numpoints := numpoints - 1;   {incase the end of file mark is after a
                                      blank row}
 End;     {of procedure}

PROCEDURE CheckOK(Counter, Numpoints : integer;
                  Var OK : Boolean);

Begin
   OK := True;
   If ((Counter = 1) OR (Counter = 3)) AND (NumPoints <= 6)
      then OK := False;
   If ((Counter = 2) OR (Counter = 4)) AND (NumPoints <= 4)
      then OK := False;
   If ((Counter = 5) OR (Counter = 6)) AND (NumPoints <= 3)
      then OK := False;
   If ((Counter >= 7) AND (Counter <= 10)) AND (NumPoints <= 5)
      then OK := False;
end;

FUNCTION func(pr : glnp) : extended;
{N.B. Counter coming in through the "Backdoor" but not being altered}
```

```
 Var
   j : integer;
   sum : extended;
   stem : extended;  {the part of the m^x function going to be raised to
                      the power of x}

{To avoid floating point overflow, whch can occur relatively easily, the
 programme calculates 'indexlimit' before func is called}

Begin

{insert constraints on parameters; if broken, func:=1.0e30, ie HUGE and
 EXIT}
{-------------------------------------------------------------------------}

        If (((Counter = 1) OR (Counter = 3)) AND
                  {constraints for double exps}
        ((pr[2]<=0) OR (pr[3]<=indexlimit) OR (pr[4]<=0) OR
        (pr[5]<=indexlimit))) then
          Begin
             func := 1.0e30;
             Exit; {abandon this try without further waste of time!}
          end;
        If (((Counter = 2) OR (Counter = 4)) AND
             {constraints for single exps}
        ((pr[2]<=0) OR (pr[3]<=indexlimit))) then
          begin
             func := 1.0e30;
             Exit;
          end;
        If (((Counter = 5) OR (Counter = 6)) AND  {constaints for Boltzmans}
        ((pr[1]>=0) OR (pr[2]<=0))) then
          begin
             func := 1.0e30;
             Exit;
           end;
        If (((Counter >= 7) AND (Counter <= 10)) AND {constaints for M^x}
        ((pr[2]<0) OR (pr[2]>1) OR (pr[3]>1) OR (pr[3]<0) OR
        (pr[4]<=Indexlimit))) then
          begin
             func :=1.0e30;
             Exit;
           end;
{-------------------------------------------------------------------------}
        sum:=0;
         for j:= 1 to numpoints do
           begin
               If Counter = 1 then
                  sum:=sum + sqr(data[j,'y']-(pr[1]-pr[2]*exp(-
data[j,'x']/pr[3])-pr[4]*exp(-data[j,'x']/pr[5])));
               If Counter = 2 then
                  sum:=sum + sqr(data[j,'y'] -(pr[1]-pr[2]*exp(-
data[j,'x']/pr[3])));
               If Counter = 3 then
                  sum:=sum + sqr(data[j,'y'] -(-pr[1]+pr[2]*exp(-
data[j,'x']/pr[3])+pr[4]*exp(-data[j,'x']/pr[5])));
```

```
                If Counter = 4 then
                   sum:=sum + sqr(data[j,'y'] -(-pr[1]+pr[2]*exp(-
data[j,'x']/pr[3])));
                If Counter = 5 then
                   sum:=sum + sqr(data[j,'y'] -(1/(1+exp(-(data[j,'x']-
pr[1])/pr[2]))));
                If Counter = 6 then
                   sum:=sum + sqr(data[j,'y'] -(1/(1+exp(+(data[j,'x']-
pr[1])/pr[2]))));
                If ((Counter >= 7) AND (Counter <= 10)) then
                   begin
                      Stem := pr[2] - (pr[2] - pr[3]) * exp(-
data[j,'x']/pr[4]);
                      if Counter = 8 then
                         stem := stem * stem;
                      if Counter = 9 then
                         stem := stem * stem * stem;
                      if Counter = 10 then
                         stem := stem * stem * stem * stem;
                      sum := sum + sqr(data[j,'y'] -(pr[1] * stem));
                   end;
             end; {of calculating the sum of the sqr of the difference}
          func := sum; {sum of sq of differences of data from 'fitted' curve}
     end; {function func}

PROCEDURE amoeba(VAR p: glmpnp; VAR y: glmp; ndim: integer;
          ftol: extended; VAR iter: integer);

{This procedure is taken from "Numerical Receipes" by Press et al. 1986}

{ Programs using routine AMOEBA must supply an external function
func(pr:glnp):extended whose minimum is to be found. They must
also define types
TYPE
   glmpnp = ARRAY [1..mp,1..np] OF real;
   glmp = ARRAY [1..mp] OF real;
   glnp = ARRAY [1..np] OF real;
where mp and np are physical dimensions
NB all REAL types altered to EXTENDED for maximum precision and speed of
80N87 co-processors}

LABEL 99;
CONST
   alpha=1.0;
   beta=0.5;
   gamma=2.0;
   itmax=3000; { maximum no. of iterations}
VAR
   mpts,j,inhi,ilo,ihi,i: integer;
   yprr,ypr,rtol: extended;
   pr,prr,pbar: glnp;
BEGIN
   mpts := ndim+1;
   iter := 0;
   WHILE true DO BEGIN
      ilo := 1;
```

```
IF (y[1] > y[2]) THEN BEGIN
   ihi := 1;
   inhi := 2
END ELSE BEGIN
   ihi := 2;
   inhi := 1
END;
FOR i := 1 to mpts DO BEGIN
   IF (y[i] < y[ilo]) THEN  ilo := i;
   IF (y[i] > y[ihi]) THEN BEGIN
      inhi := ihi;
      ihi := i
   END ELSE IF  (y[i] > y[inhi]) THEN
      IF (i <> ihi) THEN  inhi := i
END;
rtol := 2.0*abs(y[ihi]-y[ilo])/(abs(y[ihi])+abs(y[ilo]));
IF (rtol < ftol) THEN GOTO 99;
IF (iter = itmax) THEN BEGIN
   writeln('pause in AMOEBA - too many iterations'); readln
END;
iter := iter+1;
FOR j := 1 to ndim DO pbar[j] := 0.0;
FOR i := 1 to mpts DO
   IF (i <> ihi) THEN FOR j := 1 to ndim DO pbar[j] := pbar[j]+p[i,j];
FOR j := 1 to ndim DO BEGIN
   pbar[j] := pbar[j]/ndim;
   pr[j] := (1.0+alpha)*pbar[j]-alpha*p[ihi,j]
END;
ypr := func(pr);
IF (ypr <= y[ilo]) THEN BEGIN
   FOR j := 1 to ndim DO prr[j] := gamma*pr[j]+(1.0-gamma)*pbar[j];
   yprr := func(prr);
   IF (yprr < y[ilo]) THEN BEGIN
      FOR j := 1 to ndim DO p[ihi,j] := prr[j];
      y[ihi] := yprr
   END ELSE BEGIN
      FOR j := 1 to ndim DO p[ihi,j] := pr[j];
      y[ihi] := ypr
   END
END ELSE IF  (ypr >= y[inhi]) THEN BEGIN
   IF (ypr < y[ihi]) THEN BEGIN
      FOR j := 1 to ndim DO p[ihi,j] := pr[j];
      y[ihi] := ypr
   END;
   FOR j := 1 to ndim DO prr[j] := beta*p[ihi,j]+(1.0-beta)*pbar[j];
   yprr := func(prr);
   IF (yprr < y[ihi]) THEN BEGIN
      FOR j := 1 to ndim DO p[ihi,j] := prr[j];
      y[ihi] := yprr
   END ELSE BEGIN
      FOR i := 1 to mpts DO
         IF (i <> ilo) THEN BEGIN
            FOR j := 1 to ndim DO BEGIN
               pr[j] := 0.5*(p[i,j]+p[ilo,j]);
               p[i,j] := pr[j]
            END;
```

```
                y[i] := func(pr)
              END
          END
        END ELSE BEGIN
          FOR j := 1 to ndim DO p[ihi,j] := pr[j];
          y[ihi] := ypr
        END
    END;
99:   END;

PROCEDURE DoFit(Var p : glmpnp;     {calls Amoeba to find coefficients for
min S of sq}
              Var x : glnp;
              Var y : glmp;
              Var ndim : integer;
              Data : RealArr;
              mp, np, Counter : integer);

Var
  Count1, Count2 : integer;

Begin
{initialize the vertices of the simplex}
    If ((Counter = 1) OR (Counter = 3)) then
       begin
          p[1,1]:=data[numpoints,'y'];p[1,2]:=1.0;p[1,3]:=10.0;p[1,4]:=1.0;
p[1,5]:=5.5;
          p[2,1] := 1.0; p[2,2] := 1.0; p[2,3] := 1.0; p[2,4]:=1.0;
p[2,5]:=1.0;
          p[3,1] := 1.0; p[3,2] := 1.0; p[3,3] := 1.0; p[3,4]:=0.0;
p[3,5]:=0.5;
          p[4,1] := 1.0; p[4,2] := 1.0; p[4,3] := 0.5; p[4,4]:=0.5;
p[4,5]:=1.0;
          p[5,1] := 1.0; p[5,2] := 1.0; p[5,3] := 1.0; p[5,4]:=1.0;
p[5,5]:=1.0;
          p[6,1] := 1.0; p[6,2] := 1.0; p[6,3] := 1.0; p[6,4]:=0.5;
p[6,5]:=0.5;
       end;
    If ((Counter = 2) OR (Counter = 4)) then
       begin
          p[1,1] := data[numpoints,'y']; p[1,2] := 1.0; p[1,3] := 1.0;
          p[2,1] := 1.0; p[2,2] := 1.0; p[2,3] := 1.0;
          p[3,1] := 1.0; p[3,2] := 1.0; p[3,3] := 1.0;
          p[4,1] := 0.0; p[4,2] := 2.0; p[4,3] := 0.5;
       end;
    If ((Counter = 5) OR (Counter = 6)) then
       begin
          p[1,1] := -100; p[1,2] := 1.0;
          p[2,1] := -10.0; p[2,2] := 1.0;
          p[3,1] := -1.0; p[3,2] := 5.0;
       end;
    If ((Counter >= 7) AND (Counter <= 10)) then
       begin
          p[1,1] := data[1,'y']; p[1,2] := 1; p[1,3] := 0; p[1,4] := 10;
          p[2,1] := 0; p[2,2] := 1; p[2,3] := 0; p[2,4] := 10;
          p[3,1] := 0.5; p[3,2] := 0.5; p[3,3] := 0; p[3,4] := 0;
```

```
          p[4,1] := 0; p[4,2] := 0.5; p[4,3] := 0.4; p[4,4] := 10;
          p[5,1] := 1; p[5,2] := 1; p[5,3] := 0; p[5,4] := 1;
       end;
  ndim := np;
  FOR Count1 := 1 to mp DO BEGIN
     FOR Count2 := 1 to np DO BEGIN
        x[Count2] := p[Count1,Count2]
     END;
     y[Count1] := func(x)
  END;
   amoeba(p,y,ndim,ftol,iter);
  end;

PROCEDURE ReRun(Var p : glmpnp;
                Var x : glnp;
                Var y : glmp;
                Var ndim  : integer;
                Data : RealArr;
                mp, np, Counter : integer);  {re-run using value of
exponent as one of the vertices}
            {leave one vertex unchanged for the re-run}

Var
  Count1, Count2 : integer;

begin
   If ((Counter = 1) OR (Counter = 3)) then
     begin
        p[2,1] := 10*p[1,1]; p[2,2] := 0.1*p[1,2]; p[2,3] := 1.0;
p[2,4]:=1.0; p[2,5]:=1.0;
        p[3,1] := 0.0; p[3,2] := 10*p[1,2]; p[3,3] := 0.1*p[1,3];
p[3,4]:=0.0; p[3,5]:=0.5;
        p[4,1] := 0.0; p[4,2] := 0.0; p[4,3] := 10*p[1,3];
p[4,4]:=0.1*p[1,4]; p[4,5]:=1.0;
        p[5,1] := 0.0; p[5,2] := 0.0; p[5,3] := 1.0; p[5,4]:=10*p[1,4];
p[5,5]:=0.1*p[1,5];
        p[6,1] := 0.1*p[1,1]; p[6,2] := 0.0; p[6,3] := 1.0; p[6,4]:=0.5;
p[6,5]:=10*p[1,5];
     end;
   If ((Counter = 2) OR (Counter = 4)) then
     begin
        p[2,1] := 0.1*p[1,1]; p[2,2] := 10*p[1,2]; p[2,3] := 10.0;
        p[3,1] := 1.0; p[3,2] := 0.1*p[1,2]; p[3,3] := 10*p[1,3];
        p[4,1] := 10*p[1,1]; p[4,2] := 1.0; p[4,3] := 0.1*p[1,3];
     end;
   If ((Counter = 5) OR (Counter = 6)) then
     begin
        p[2,1] := -100.0; p[2,2] := 0.5;
        p[3,1] := -0.5; p[3,2] := 100.0;
     end;
   If ((Counter >= 7) AND (Counter <= 10)) then
     begin
        p[2,1] :=0.1*p[1,1]; p[2,2] :=10*p[1,2]; p[2,3] := 1; p[2,4] := 10;
        p[3,1] :=1.0; p[3,2] :=0.1*p[1,2]; p[3,3] :=10*p[1,3]; p[3,4] := 1;
        p[4,1] :=10*p[1,1]; p[4,2] :=1.0; p[4,3] :=0.1*p[1,3]; p[4,4] :=
0.1*p[1,4];
```

```
        p[5,1] := 0; p[5,2] := 1; p[5,3] := 0; p[5,4] := 10*p[1,4];
      end;
      ndim := np;
        FOR Count1 := 1 to mp DO BEGIN
         FOR Count2 := 1 to np DO BEGIN
         x[Count2] := p[Count1,Count2]
      END;
      y[Count1] := func(x)
   END;
    amoeba(p,y,ndim,ftol,iter);
end;

PROCEDURE CalcAvs(Var Total, Average : RunArray1;
                  Var SumFunc, AvFunc : RunArray2;
                  mp, np : integer;
                  p : glmpnp;
                  y : glmp;
                  Counter2 : integer);

Var
  Count1, Count2 : integer;

Begin
   For Count1 := 1 to np do {calcs av. value of simplex at the vertices}
     begin
        Total[Counter2, Count1] := 0;
        for Count2 := 1 to mp do
           Total[Counter2, Count1] := Total[Counter2, Count1] + p[Count2,
Count1];
        Average[Counter2, Count1] := Total[Counter2, Count1]/mp;
     end;
   SumFunc[Counter2] := 0; {Calcs av. value of function at the vertices}
   for Count2 := 1 to mp do
      SumFunc[Counter2] := SumFunc[Counter2] + y[Count2];
   AvFunc[Counter2] := SumFunc[Counter2]/mp;
End;  {of procedure}

PROCEDURE PrintHeading(Counter : integer;
                       Day, Month, year, Hour, Minute, Sec : word;
                       FileName : string47);

Begin
   clrscr;
   writeln;
   writeln(' Date: ',Day,'-',Month,'-',Year,'    Time:
',Hour,':',Minute,':',Sec);
   writeln(' File: ',FileName,'      Number of data pairs: ',numpoints);
   writeln;
   writeln(lst);
   writeln(lst,' Date: ',Day,'-',Month,'-',Year,'    Time:
',Hour,':',Minute,':',Sec);
   writeln(lst,' File: ',FileName,'      Number of data pairs: ',numpoints);
   writeln(lst);
   writeln(' Results of fit, averages of vertices:');
   writeln(lst,' Results of fit, averages of vertices:');
   writeln;
```

```
   writeln(lst);
   If Counter = 1 then
     begin
        Writeln(' Double Increasing Exponential Function');
        writeln(lst,' Double Increasing Exponential Function');
     end;
   If Counter = 2 then
     begin
        writeln(' Single Inreasing Exponential Function');
        writeln(lst,' Single Inreasing Exponential Function');
     end;
   If Counter = 3 then
     begin
        writeln(' Double Decreasing Exponential Function');
        writeln(lst,' Double Decreasing Exponential Function');
     end;
   If Counter = 4 then
     begin
        writeln(' Single Decreasing Exponential Function');
        writeln(lst,' Single Decreasing Exponential Function');
     end;
   If Counter = 5 then
     begin
        writeln(' Increasing Boltzman Function');
        writeln(lst,' Increasing Boltzman Function');
     end;
   If Counter = 6 then
     begin
        writeln(' Decreasing Boltzman Function');
        writeln(lst,' Decreasing Boltzman Function');
     end;
   If ((Counter >= 7) AND (Counter <= 10)) then
     begin
        writeln(' Hogkin & Huxley M',Counter - 6,' Kinetic Function');
        writeln(lst,' Hogkin & Huxley M',Counter - 6,' Kinetic Function');
     end;
   writeln;
   writeln(lst);
   If ((Counter = 1) OR (Counter = 3)) then
     begin
       writeln('Iters.':4,'A':10,'B':10,'τ1':10,'C':10,'τ2':10,'Function':12
);
       writeln(lst,'Iters.':8,'A':10,'B':10,'τ1':10,'C':10,'τ2':10,'Function
':12);
     end;
   If ((Counter = 2) OR (Counter = 4)) then
     begin
        writeln('Iters.':4,'A':10,'B':10,'τ':10,'Function':12);
        writeln(lst,'Iters.':8,'A':10,'B':10,'τ':10,'Function':12);
     end;
   If ((Counter = 5) OR (Counter =6)) then
     begin
        writeln('Iters.':4,'V↑':10,'k':10,'Function':12);
        writeln(lst,'Iters.':4,'V↑':10,'k':10,'Function':12);
     end;
   If ((Counter >= 7) AND (Counter <= 10)) then
```

```
     begin
       writeln('Iters.':4,'Imax':10,'m∞':10,'m0':10,'τ':10,'Function':12);
       writeln(lst,'Iters.':8,'Imax':10,'m∞':10,'m0':10,'τ':10,'Function':12
);
     end;
   writeln;
   writeln(lst);
End;  {of procedure}

PROCEDURE PrintResults(Average : RunArray1;
                       AvFunc : RunArray2;
                       iter : integer;
                       Counter2 : integer);

Var
  Count1 : integer;

Begin
   write(iter:4,'    ');
   write(lst,iter:4,'    ');
   For Count1 := 1 to np do
      begin
         write(Average[Counter2,Count1]:10:4);
         write(lst,Average[Counter2,Count1]:10:4);
      end;
   writeln(AvFunc[Counter2]:12:6);
   writeln(lst,AvFunc[Counter2]:12:6);
End;  {of procedure}

PROCEDURE Variance (Data : RealArr;
                    y : glmp;
                    numpoints: integer;
                    mp, np : integer);

 Var
   sum, sumsq, ssqtot, curve, errsq, curvsq, F : extended;
   Count1 : integer;

 Begin
     sum := 0;
     sumsq:=0;
     For Count1 := 1 to numpoints do
        begin
           sum := sum + data[Count1,'y'];
           sumsq:=sumsq + sqr(data[Count1,'y']);
        end;
     ssqtot := (sumsq - sqr(sum)/numpoints);
       {this is the total sum of squares of deviations from the mean
       of the data for the total of (numpoints-1) degrees of freedom}
     errsq := 0;
     For Count1 := 1 to mp do  { find the total then the average value}
       errsq := errsq + y[Count1]; { of 'func' at the mp vertices; this is}
       errsq := errsq/mp;  { average value of the sum of sq of deviations}
        {from the fitted curve ie the 'error' with (numpoints-np-1) d of f}
        {Thus the variation removed by fitting the curve is (ssqtot-sum) for
          np d of f}
```

```
      curvsq := ssqtot - errsq;
       { and the mean square (variance) for the regression is.. }
      curve := curvsq/np;
       {and the error mean square is ... }
      sum := errsq/(numpoints - np - 1);
       {thus the variance ratio, F with np and numpoints-np-1 d of f in the
        numerator and denominator respectively is.. }
      F := curve/sum;
    writeln('Analysis of variance');
    writeln('Source':10,'D of F':10,'    Sum of Sq.':10,'   Mean
square':10,'F':10);
    writeln;
    writeln('curve':10,np:10,'   ',curvsq:10:6,'   ',curve:10:6,'
    ',F:10:6);
    writeln('Error':10,(numpoints-np-1):10,'   ',errsq:10:6,'
  ',sum:10:6);
    writeln('Total':10,(numpoints-1):10,'   ',ssqtot:10:6);
         {Now print the results as well, if required }
    writeln(lst);writeln(lst);
    writeln(lst,'-----------------------------------------------------');
    writeln(lst,'Analysis of variance');
    writeln(lst);
    writeln(lst,'Source':10,'D of F':10,'    Sum of Sq.':10,'   Mean
square':10,'F':10);
    writeln(lst);
    writeln(lst,'curve':10,np:10,'   ',curvsq:10:6,'   ',curve:10:6,'
    ',F:10:6);
    writeln(lst,'Error':10,(numpoints-np-1):10,'   ',errsq:10:6,'
  ',sum:10:6);
    writeln(lst,'Total':10,(numpoints-1):10,'   ',ssqtot:10:6);
    writeln(lst,^L); { if printing, eject the page}
end; {of procedure}

{************************ Main level Procedure ***************************}

Begin
   GetData;
   GetLimit;
   Counter := 0;
   While Counter < CurveNo do
     begin
        Counter := Counter + 1;
        If Fits[Counter] then  {i.e. wanting to fit curve no. "counter"}
          begin
             Now;
             PrintHeading(Counter, Day, Month, Year, Hour, Minute, Sec,
FileName);
             Initmpnp(mp, np, Total, Average, SumFunc, AvFunc);
             CheckOK(Counter, NumPoints, OK);
             If OK then
               begin
                  Counter2 := 1;
                  DoFit(p, x, y, ndim, data, mp, np, Counter);
                  CalcAvs(Total, Average, SumFunc, AvFunc,
mp,np,p,y,Counter2);
                  Beep;
```

```
                    Delay(500);
                    Beep;
                    PrintResults(Average, AvFunc, iter, Counter2);
                    Repeat
                       Counter2 := Counter2 + 1;
                       ReRun(p, x, y, ndim, data, mp, np, Counter);
                       CalcAvs(Total, Average, SumFunc, AvFunc,
 mp,np,p,y,Counter2);
                       Beep;
                       Delay(500);
                       Beep;
                       PrintResults(Average, AvFunc, iter, Counter2);
                    until (Counter2 = MaxRuns) OR (((AvFunc[Counter2-1] -
 AvFunc[Counter2])/AvFunc[Counter2-1]) <= Tol);
                    Variance(Data, y, numpoints, mp, np);
                end  {of if OK}
                else begin
                  Beep;
                  delay(500);
                  Beep;
                  writeln;
                  writeln('There are too few points in this file to make a
 sensible fit !');
                  Delay(2000);
                  writeln(lst);
                  writeln(lst,'There are too few points in this file to make
 a sensible fit !');
                  writeln(lst,^L);  {to eject page}
                end;  {of if Not OK}
            end; { of if wanting curve}
        end; {of original while loop}
    Quack;
end;  {of main level procedure}
END.  {of unit}
```

```
UNIT NewMak2;    {version 2.31D    30/03/92}
{This unit replaces the old MakeFile programme, and it runs from the
NewFit4 programme}

{======================== Public Section of Unit ============================}

INTERFACE

Uses CRT, PRINTER, DOS, MyUtils, Direct2, ReadFile;

PROCEDURE FileMake;

{======================== Private Section of Unit ===========================}

IMPLEMENTATION

PROCEDURE FileMake;

{************************ Main level NewMak2 Procedure Declarations *****}

var
  FileName, OutFileName : string47;
  Xdata, Ydata : DataPoint;
  Message : MessArray;
  Xmin, Xmax, Ymax, Ymin, TimeDiffS, TimeDiffF, Start, Finish : real;
  NumPoints, Line, Average : Integer;
  RunOnce, Update, Uniform, Convert : Boolean;
  Source, QPrint, Ch1 : char;
  ANS : string5;

{************************ Sub NewMak2 Procedures ************************}

PROCEDURE Questions(Var OutFileName : string47;
                    Var Update : Boolean;
                    Var Start, Finish : real;
                    Var Average : Integer;
                    Var Convert : boolean;
                    Xmax, Xmin : real;
                    Xdata, Ydata : Datapoint);

Var
  Qold, QAv, Chr, Qexist, Conf, QConv : char;
  QUpdate, QOverwrite, Count : integer;
  Name : string[12];
  FileConf : char;
  line : integer;
  message : MessArray;
  Ans : string5;

Begin
  If RunOnce = true then
    begin
       writeln;
       writeln;
       write('Do you want to use the same destination file?  ');
       GetGoodChar(YNChars, Qold);
```

```
    end;
  If ((RunOnce = false) OR (upcase(Qold) = 'N')) then
    begin
       writeln;
       write('Do you want to update/overwrite an existing file?  ');
       GetGoodChar(YNChars, Qexist);
    end;
  If (upcase(Qexist) = 'Y') OR (upcase(Qold) = 'Y') then
    begin
       writeln;
       writeln;
       writeln('Select   1. for overwite;');
       writeln('or       2. for update.');
       GetGoodInt(1,2,QUpdate);
       If QUpdate = 2 then
         Update := true
         else update := false;
       If Upcase(Qexist) = 'Y' then
         begin
            FileConf := 'N';
            While upcase(FileConf) = 'N' do
              begin
                Repeat
                 GetFile(OutFileName);
                 window(1,1,80,25);
                 clrscr;
                 if OutFileName = 'NONE' then exit;
                 CheckColumns(Ans,OutFileName);
                 If (Ans <> 'Two') AND (update = true) then
                  begin
                   writeln;
                   Beep;
                   writeln('To update a file, it must be of two columns.');
                   writeln('Try again to select an appropriate file.');
                   writeln;
                   pause;
                  end;
                until (Ans = 'Two') OR (update = false);
                ReadFileMessage(Message, Line, OutFileName);
                If Line > 0 then
                   begin
                       writeln;
                       DisplayMessage(Message, OutFileName);
                    end
                    else begin
                       writeln;
                       writeln('This file does not contain a message.');
                    end;
                writeln;
                write('Are you happy with the file that you have selected?
(Y/N)  ');
                GetGoodChar(YNChars, FileConf);
              end;  {of while loop}
            window(1,1,80,25);
            clrscr;
         end;
```

```
    end  {of If clause}
    else begin
       Chr := 'Y';
       While Chr = 'Y' do
         begin
            Repeat              {start of getting file name procedure}
              writeln;
              writeln;
              write('Enter the destination file name:  ');
              readln(Name);
              writeln;
              write(Name,'  Confirm this is correct (Y/N)  ');
              GetGoodChar(YNChars,conf);
            until upcase(conf) ='Y';  {O.K. got file name and happy with it}
            OutFileName := 'D:\NewFit\Files\' + Name;
            If Exist(OutFileName) then
               begin
                  writeln;
                  writeln('This file already exists');
                  writeln('Select   1.  to choose new file;');
                  writeln('         2.  to overwrite the file;');
                  writeln('or       3.  to update the file;');
                  GetGoodInt(1,3,QOverwrite);
                  Case QOverwrite of
                    1 : Begin
                          Chr := 'Y';
                          Update := false;
                        end;
                    2 : Begin
                          Chr := 'N';
                          update := false;
                        end;
                    3 : begin
                          Chr := 'N';
                          Update := true;
                        end;
                  end;  {of case clause}
              end   {of if statement}
              else Chr := 'N';
        end;   {of while loop}
  end;  {of else clause}
Repeat
   writeln;
   writeln;
   write('Enter the start time of the section you want to write to file:
');
   Readln(Start);
   If (Start < Xmin) or (Start > Xmax) then
      writeln('This is outside of the time range of the source file');
   If (Start >= Xmin) AND (Start < Xmax) then
      begin
         Count := 1;
         While Xdata^[Count] < start do
            Count := Count + 1;
         If NOT (Round(Xdata^[Count] * 100) = Round(start * 100)) then
            writeln('This exact time does not exist');
```

```
         end;
      until (Start>=Xmin) AND (Start<Xmax) AND
 (Round(Xdata^[Count]*100)=Round(start*100));
  Repeat
      writeln;
      write('Enter the finish time of the section you want to write to file:
  ');
      Readln(Finish);
      If (Finish < Start) or (Finish > XMax) then
         begin
            writeln('This is either less than the start time,');
            writeln('or outside of the time range of the source file');
         end;
      If (Finish > Start) AND (Finish <= Xmax) then
         begin
            Count := 1;
            While Xdata^[Count] < Finish do
               Count := Count + 1;
            If NOT (Round(Xdata^[Count] * 100) = Round(Finish * 100)) then
               writeln('This exact time does not exist');
          end;
      until (Finish>Start) AND (Finish<=Xmax) AND
 (Round(Xdata^[Count]*100)=Round(Finish*100));
  writeln;
  write('Do you want to forward average the data?  ');
  GetGoodChar(YNChars, QAv);
  If upcase(QAv) = 'Y' then
     begin
        writeln;
        write('Forward average how many points (1 - 10)?   ');
        GetGoodInt(1,10,Average);
     end
     else Average := 1;
  writeln;
  writeln;
  If update then
    begin
      writeln('CAUSION !!!!!');
      writeln('If you choose to convert, then you should be sure that the');
      writeln('file to be updated is also in milliseconds, otherwise
 problems');
      writeln('will result when the new data is written to the file');
      writeln;
      writeln;
    end;
  write('Do you want to convert from seconds to milliseconds?  ');
  GetGoodChar(YNChars, QConv);
  If upcase(QConv) = 'Y' then Convert := true else Convert := false;
end;  {of Questions procedure}


PROCEDURE WriteFileMessage (OutFileName, FileName : string47;
                            Message : MessArray;
                            Start, Finish : real;
                            Average : Integer;
                            convert : boolean);
```

```
Var
  OutFile : Text;
  Count : integer;
  st, fn : real;

Begin
   Assign(OutFile, OutFileName);
   Rewrite(OutFile);
   Writeln(OutFile,'Source File:  ',FileName);
   Writeln(OutFile,'Source file message:');
   count := 1;
   while message[count] <> '' do
     begin
        writeln(outFile, message[count]);
        count := count + 1;
     end;
   writeln(OutFile,'New Information:');
   If convert = False then
    write(OutFile,'Data taken from between ',start:0:2,' and ',Finish:0:2,'
 ms.')
     else begin
       st := start * 1000;
       Fn := finish * 1000;
       write(OutFile,'Data taken from between ', st:0:2,' and ', Fn:0:2,'
 ms.');
     end;
   writeln(OutFile,' Forward averaged ',Average);
   close(OutFile);
end;  {of WriteFileMessage procedure}

PROCEDURE WriteFileData(OutFileName : string47;
                        Xdata,Ydata : DataPoint;
                        Start, Finish : real;
                        Average : integer;
                        TimeDiffS : real);

Var
  Count1, Count2 : integer;
  Sindex, Findex : integer;
  Xsum, Ysum, Xav, Yav, Xfirst, Xfinal : single;
  OutFile : text;

Begin
   Assign(OutFile, OutFileName);
   Append(OutFile);
   Sindex := Round(Start/(TimeDiffS));
   Findex := Round(Finish/(TimeDiffS));
   Count1 := 0;
   Repeat
      Xsum := 0;
      Ysum := 0;
      For Count2 := 0 to (Average -1) do
        begin
           Xsum := Xsum + Xdata^[Sindex + Count2 + (Count1 * Average)];
           Ysum := Ysum + Ydata^[Sindex + Count2 + (Count1 * Average)];
        end;
```

```
      Xav := Xsum/Average;
      Yav := Ysum/Average;
      If count1 = 0 then Xfirst := Xav;
      If Convert then Xfinal := (Xav - Xfirst) * 1000  {converting to ms}
      else Xfinal := Xav - Xfirst;   {to zero times}
      writeln(OutFile, Xfinal:0:3,' ',Yav:0:3);
      count1 := count1 + 1;
   Until Findex - Sindex - (Count1 * Average) + 1 < Average;
   close(OutFile);
End;   { of WriteFileData}

PROCEDURE UpDateFile(Var Message : MessArray;
                     Var Line : integer;
                     OutFileName : string47;
                     Xdata,Ydata : Datapoint;
                     Start, Finish : single;
                     Average : integer;
                     TimeDiffS : real);

Var
  XOld, Yold : array1;
  Count, Count1, Count2, Count3, Count4, Count5, count6, count7 : integer;
  OldNumpoints, Sindex, Findex : integer;
  OutFile : text;
  Chr, Conf : char;
  Xsum, Ysum, Xav, Yav, Xfirst, Xfinal, TimeDiff : single;
  Ans : string5;
  SAverage, SStart, SFinish, SLast : string;

Begin
   CheckColumns(Ans,OutFileName);
   If Ans <> 'Two' then
     begin
        window(1,1,80,25);
        clrscr;
        writeln;
        beep;
        writeln('This file does not have two columns of data!!!!!!');
        writeln;
        writeln('It is incompatable with this procedure. ');
        writeln('You will therefore have to go through the question section
 again.');
        writeln;
        pause;
        exit;
     end;
   ReadFileMessage(Message, line, outfilename);
   Assign(OutFile, OutFileName);
   Reset(outFile);
   For Count5 := 1 to line do
      Readln(OutFile);
   Count6 := 0;
   While (Not eof(OutFile)) AND (count6 < maxno) do
     begin
        readln(OutFile, XOld[Count6], Yold[Count6]);
        Count6 := count6 +1;
```

```
    end;
  OldNumpoints := Count6-1;
  Conf := 'N';
  While upcase(Conf) = 'N' do
    begin
       writeln;
       writeln;
       write('Do you want the times to run continuously?  ');
       GetGoodChar(YNChars, Chr);
       If Upcase(Chr) = 'N' then
         begin
            beep;
            writeln;
            writeln('Are you sure you don''t want the time to run
continuously?  ');
            GetGoodChar(YNChars, Conf);
         end
         else conf := 'Y';
    end;  {of while loop}
  Message[line+1] := 'New Information:';
  If convert = False then
   begin
     str(Start:0:2,SStart);
     str(Finish:0:2,SFinish);
    end
    else begin
      str((Start*1000):0:2,SStart);
      str((Finish*1000):0:2,SFinish);
    end;
  Message[line+2] := 'Data taken from between ' + SStart + ' and ' +
SFinish + ' ms.';
  str(Average,SAverage);
  Message[line+3] := ' Forward averaged '+ SAverage;
  If upcase(Chr) = 'Y' then
     begin
       Message[line+4] := 'Times running continuously.';
       str(Xold[OldNumpoints]:0:2,Slast);
       Message[line+5] := 'Last time of old version of file:  ' + Slast;
       Line := line+5;
     end
     else begin
       Message[line+4] := 'Times not running continuously';
       Line := line+4;
     end;
  Rewrite(outFile);
  For Count7 := 1 to line do
     writeln(outfile,message[count7]);
           {putting the new message into the file}
  For Count2 := 0 to OldNumpoints do
    writeln(OutFile, XOld[Count2]:0:3,' ',YOld[Count2]:0:3);
           {putting the old data back into the file}
  Sindex := Round(Start/(TimeDiffS));
  Findex := Round(Finish/(TimeDiffS));
  Count3 := 0;
  Repeat
     Xsum := 0;
```

```
      Ysum := 0;
      For Count4 := 0 to (Average -1) do
        begin
           Xsum := Xsum + XData^[Sindex + Count4 + (Count3 * Average)];
           Ysum := Ysum + YData^[Sindex + Count4 + (Count3 * Average)];
        end;
      Xav := Xsum/Average;
      Yav := Ysum/Average;
      If count3 = 0 then Xfirst := Xav;
      If (upcase(Chr) = 'Y') then
         If not convert then
            Xfinal := Xav-Xfirst+XOld[OldNumpoints]+(Average*TimeDiffS)
            else Xfinal := (Xav-Xfirst) * 1000 + XOld[OldNumpoints] +
 (Average*TimeDiffS*1000)
         Else If not convert then Xfinal := Xav - Xfirst
            else Xfinal := (Xav - Xfirst) * 1000;
      writeln(OutFile, Xfinal:0:3,' ',Yav:0:3);
           { putting the new data into the file}
      count3 := count3 + 1;
   Until Findex - Sindex - (Count3 * Average) + 1 < Average;
   close(OutFile);
end;  {of update procedure}

{************************ Main NewMak2 Procedure ************************}

Begin
   RunOnce := false;
   update := false;
   clrscr;
   Ch1 := 'N';
   While upcase(Ch1) = 'N' do
     begin
       GetFile(FileName);
       If FileName = 'NONE' then Exit;
       window(1,1,80,25);
       clrscr;
       ReadFileMessage(Message, Line, FileName);
       If Message[1] <> '' then DisplayMessage(Message, FileName)
          else writeln('File ',Filename,' does not contain a message.');
       writeln;
       write('Is this file O.K?   ');
       GetGoodChar(YNChars,Ch1);
     end;
   CheckColumns(Ans,FileNAme);
   If (Ans = 'One') OR (Ans = 'More') then
    begin
      writeln;
      beep;
      writeln('This File is not of a compatabale type!!!!!');
      writeln('Check that there are two or three columns of data present.');
      writeln;
      pause;
      exit;
    end;
   New(Xdata);
   New(Ydata);
```

```
  ReadFileData(XData,YData,TimeDiffS,TimeDiffF,Numpoints,XMax,Xmin,Ymax,
Ymin,FileName,message,Line);
  If Numpoints = 0 then
     begin
        writeln;
        beep;
        writeln('This file does not appear to contain data!!!!!');
        writeln('You will need to try again.');
        writeln;
        pause;
        exit;   {no data in file, or incompatible file type}
     end;
  DisplayMessage(Message,FileName);
  DisplayDetails(NumPoints,TimeDiffS,TimeDiffF,uniform,Xmax,Xmin,Ymax,
Ymin,FileName);
  If Not(Uniform) then
    begin
      writeln;
      beep;
      writeln('This file has not been sampled at a uniform rate!!!!!');
      writeln('The source file must have been sampled at a uniform rate,');
      writeln('for this procedure to work properly.');
      writeln;
      pause;
      exit;
    end;
  Source := 'Y';
  while upcase(Source) = 'Y' do
    begin
      Questions(OutFileName,UpDate,Start,Finish,Average,Convert,Xmax,Xmin,
Xdata,Ydata);
       If Update = true then
         begin
            ReadFileMessage(Message, Line, OutFileName);
           UpdateFile(Message,line,OutFileNAme,Xdata,Ydata,Start,Finish,
Average,TimeDiffS);
         end
         else begin
            WriteFileMessage(OutFileName, FileName, Message, Start, Finish,
Average, convert);
            WriteFileData(OutFileName, XData, YData, Start, Finish,
Average,TimeDiffS);
         end;
       writeln;
       writeln;
       write('Do you want a printout of the destination file''s message ?
 ');
       GetGoodChar(YNChars, QPrint);
       If upcase(QPrint) = 'Y' then
         begin
            ReadFileMessage(Message, Line, OutFileName);
            PrintMessage(Message, Line, OutFileName);
         end;
       RunOnce := true;
       writeln;
       writeln;
```

```
        write('Do you want more from the same source file?  ');
        GetGoodChar(YNChars, Source);
      end;   {of while loop}
   Dispose(Xdata);
   Dispose(Ydata);
End;  {of FileMake Procedure}

END.  {of Unit}
```

References

References

Adrian, R.H. & Marshall, M.W. (1977). Sodium current in mammalian muscle. *Journal of Physiology* **268**, 223-250.

Aghajanian, G.K. (1985). Modulation of a transient outward current in serotonergic neurones by alpha-1-adrenoceptors. *Nature* **315**, 501-503.

Aghajanian, G.K., Foote, W.E. & Sheard, M.H. (1968). Lysergic acid diethylamide: Sensitive neuronal units in the midbrain raphe. *Science* **161**, 706-708.

Aghajanian, G.K., Haigler, H.J. & Bloom, F.E. (1972). Lysergic acid diethylamide and serotonin: Direct actions on serotonin-containing neurons in rat brain. *Life Sciences* **11**, 615-622.

Aghajanian, G.K. & Lakoski, J.M. (1984). Hyperpolarisation of serotonergic neurons by serotonin and LSD: Studies in brain slices showing increased k^+ conductance. *Brain Research* **305**, 181-185.

Aghajanian, G.K. & VanderMaelen, C.P. (1982). Intracellular recordings from serotonergic dorsal raphe neurons: Pacemaker potentials and the effect of LSD. *Brain Research* **238**, 463-469.

Aitken, A., Klee, C.B. & Cohen, P. (1984). The structure of the B subunit of calcineurin. *European Journal of Biochemistry* **139**, 663-671.

Akaike, N., Kostyuk, P.G. & Osipchuk, Y.V. (1989). Dihydropyridine-sensitive low-threshold calcium channels in isolated rat hypothalamic neurones. *Journal of Physiology* **412**, 181-195.

Akasu, T., Tsurusaki, M. & Tokimasa, T. (1990). Reduction of the N-type calcium current by noradrenaline in neurones of rabbit vesical parasympathetic ganglia. *Journal of Physiology* **426**, 439-452.

Anderson, C.S. & Dunlap, K. (1988). Single L-type calcium channels in dorsal root ganglion neurones can be modulated by norepinepherine. *Society of Neurosciences Abstracts* **14**, 262.5.

Andrade, R. & Aghajanian, G.K. (1985). Opiate and α_2-adrenoceptor-induced hyperpolarisations of locus ceruleus neurones in brain slices: Reversal by cyclic adenosine 3′:5′-monophosphate analogues. *Journal of Neuroscience* **5**, 2359-2364.

Andrade, R. & Nicoll, R.A. (1987a). Pharmacologically distinct actions of serotonin on single pyramidal neurons of the rat hippocampus recorded in vitro. *Journal of Physiology* **394**, 99-124.

Andrade, R. & Nicoll, R.A. (1987b). Novel anxiolytics discriminate between postsynaptic serotonin receptors mediating different physiological responses on single neurons of the hippocampus. *Naunyn-Schmiedeberg's Archives of Pharmacology* **336**, 5-10.

References

Aosaki, T. & Kasai, H. (1989). Characterization of two kinds of high-voltage-activated Ca-channel currents in chick sensory neurons. Differential sensitivity to dihydropyridines and omega-conotoxin GVIA. *Pflugers Archives.European Journal of Physiology* 414, 150-156.

Armstrong, C.M. & Gilly, W.F. (1979). Fast and slow steps in the activation of sodium channels. *Journal of General Physiology* 74, 691-711.

Armstrong, C.M. & Matteson, D.R. (1985). Two distinct populations of calcium channels in a clonal line of pituitary cells. *Science* 227, 65-66.

Armstrong, D.L. & Eckert, R. (1987). Voltage-activated calcium channels that must be phosphorylated to respond to membrane depolarisation. *Proceedings of the National Academy of Science USA* 84, 2518-2522.

Artalejo, C.R., Ariano, M.A., Perlman, R.L. & Fox, A.P. (1990). Activation of facilitation calcium channels in chromaffin cells by D_1 dopamine receptors through a cAMP/protein kinase A-dependent mechanism. *Nature* 348, 239-242.

Artalejo, C.R., Dahmer, M.K., Perlman, R.L. & Fox, A.P. (1991). Two types of Ca^{2+} currents are found in bovine chromaffin cells: Facilitation is due to the recruitment of one type. *Journal of Physiology* 432, 681-707.

Artalejo, C.R., Perlman, R.L. & Fox, A.P. (1992a). Omega-conotoxin GVIA blocks a Ca^{2+} current in bovine chromaffin cells that is not of the "classic" N type. *Neuron* 8, 85-95.

Artalejo, C.R., Rossie, S., Perlman, R.L. & Fox, A.P. (1992b). Voltage-dependent phosphorylation may recruit Ca^{2+} current facilitation in chromaffin cells. *Nature* 358, 63-66.

Augustine, G.J., Charlton, M.P. & Smith, S.J. (1987). Calcium action in synaptic transmitter release. *Annual Review of Neuroscience* 10, 633-693.

Baker, P.F. (1984). Intracellular perfusion and dialysis: application to large nerve and muscle cells. In: *Intracellular perfusion of excitable cells*. Vol. 5, Eds. Kostyuk, P.G. & Krishtal, O.A. John Wiley & Sons, Chichester. p. 1-18.

Baraban, J.M. & Aghajanian, G.K. (1981). Noradrenergic inervation of serotoninergic neurons in the dorsal raphe: Demonstration by electron microscopic autoradiography. *Brain Research* 204, 1-11.

Bargas, J., Surmeier, D.J. & Kitai, S.T. (1991). High- and low-voltage activated calcium currents are expressed by neurons cultured from rat embryonic rat neostriatum. *Brain Research* 541, 70-74.

Barhanin, J., Coppola, T., Schmid, A., Borsotto, M. & Lazdunski, M. (1987). The calcium channel antagonists receptor from rabbit skeletal muscle. *European Journal of Biochemistry* 164, 525-531.

References

Barnes, S. & Davies, J.A. (1988). The effects of calcium channel agonists and antagonists on the release of endogenous glutamate from cerebellar slices. *Neuroscience Letters* 92, 58-63.

Beam, K.G. & Donaldson, P.L. (1983). A quantitative study of potassium channel kinetics in rat skeletal muscle from 1 to 37°C. *Journal of General Physiology* 81, 485-512.

Bean, B.P. (1985). Two kinds of calcium channels in canine atrial cells. *Journal of General Physiology* 86, 1-30.

Bean, B.P. (1989a). Classes of calcium channels in vertebrate cells. *Annual Review of Physiology* 51, 367-384.

Bean, B.P. (1989b). Neurotransmitter inhibition of neuronal calcium currents by changes in channel voltage dependence. *Nature* 340, 153-156.

Bean, B.P. (1989c). Multiple types of calcium channels in heart muscle and neurons. Modulation by drugs and neurotransmitters. *Annals of the New York Academy of Sciences* 560, 334-345.

Becquet, D., Faudon, M. & Hery, F. (1990). The role of serotonin release and autoreceptors in the dorsalis raphe nucleus in the control of serotonin release in the cat caudate nucleus. *Neuroscience* 39, 639-647.

Beech, D.J., Bernheim, L. & Hille, B. (1992). Pertussis toxin and voltage dependence distinguish multiple pathways modulating calcium channels of rat sympathetic neurons. *Neuron* 8, 97-106.

Beech, D.J., Bernheim, L., Mathie, A. & Hille, B. (1991). Intracellular Ca^{2+} buffers disrupt muscarinic suppression of Ca^{2+} current and M current in rat sympathetic neurons. *Proceedings of the National Academy of Science USA* 88, 652-656.

Belehradek, J. (1935). Temperature and living matter. In: *Protoplasma-Monographier,* vol. 8, Verlag von Gebruder Borntraeger,

Belles, B., Malécot, C.O., Hescheler, J. & Trautwein, W. (1988). "Run-down" of the Ca current during long whole-cell recordings in guinea pig heart cells: Role of phosphorylation and intracellular calcium. *Pflugers Archives. European Journal of Physiology* **411**, 353-360.

Benoit, E., Corbier, A. & Dubois, J.M. (1985). Evidence for two transient sodium currents in the frog node of Ranvier. *Journal of Physiology* 361, 339-360.

Benson, G.C. & Gordon, A.R. (1945). The conductance of aqueous solutions of calcium chloride at temperatures from 15° to 45°C. *Journal of Chemistry and Physics* 13, 473-474.

Berger, A.J. & Takahashi, T. (1990). Serotonin enhances a low-voltage-activated calcium current in rat spinal motoneurons. *Journal of Neuroscience* 10, 1922-1928.

References

Bergey, J.L., Reiser, J., Wiggins, J.R. & Freeman, A.R. (1981). Oximes: 'Enzymatic' slow channel antagonists in canine cardiac Purkinje fibres? *European Journal of Pharmacology* 71, 307-319.

Bernheim, L., Beech, D.J. & Hille, B. (1991). A diffusable second messenger mediates one of the pathways coupling receptors to calcium channels in rat sympathetic neurons. *Neuron* 6, 859-867.

Bley, K.R., Madison, D.V. & Tsien, R.W. (1987). Multiple types of calcium channels in hippocampal neurons: Characterization and localization. *Society of Neurosciences Abstracts* 13, 1010.

Bley, K.R. & Tsien, R.W. (1988). LHRH and substance P inhibit N and L-type calcium channels in frog sympathetic neurons. *Biophysics Journal* 53, 235a.

Blumenthal, D.K., Takio, K., Hansen, R.S. & Krebs, E.G. (1986). Dephosphorylation of cAMP-dependent protein kinase regulatory subunit (Type II) by calmodulin-dependent protein phosphatase. *The Journal of Biological Chemistry* 261, 8140-8145.

Boland, L.M., Allen, A.C. & Dingledine, R. (1991a). Inhibition by bradykinin of voltage-activated barium current in a rat dorsal root ganglion cell line: Role of protein kinase C. *Journal of Neuroscience* 11, 1140-1149.

Boland, L.M., Brown, T.A. & Dingledine, R. (1991b). Gadolinium block of calcium channels: Influence of bicarbonate. *Brain Research* 563, 142-150.

Boland, L.M. & Dingledine, R. (1990). Multiple components of both transient and sustained barium currents in a rat dorsal root ganglion cell line. *Journal of Physiology* 420, 223-245.

Borsotto, M., Barhanin, J., Fosset, M. & Lazdunski, M. (1985). The 1,4-dihydropyridine receptor associated with the skeletal muscle voltage dependent calcium channel. Purification and subunit composition. *The Journal of Biological Chemistry* 260, 14255-14263.

Bossu, J.-L., De Waard, M. & Feltz, A. (1991a). Inactivation characteristics reveal two calcium currents in adult bovine chromaffin cells. *Journal of Physiology* 437, 603-620.

Bossu, J.-L., De Waard, M. & Feltz, A. (1991b). Two types of calcium chammels are expressed in adult bovine chromaffin cells. *Journal of Physiology* 437, 621-634.

Bossu, J.-L. & Feltz, A. (1986). Inactivation of the low-threshold transient calcium current in rat sensory neurons: Evidence for a dual process. *Journal of Physiology* 376, 341-357.

Bossu, J.-L., Feltz, A. & Thomann, J.M. (1985). Depolarization elicits two distinct calcium currents in vertebrate sensory neurons. *Pflugers Archives. European Journal of Physiology* 403, 360-368.

References

Bossu, J.-L., Rodeau, J.L. & Feltz, A. (1989). Decay kinetics of calcium currents in rat sensory neurones: Analysis at two internal free calcium concentrations. *Pflugers Archives. European Journal of Physiology* 414, 89-91.

Bramwell, G. (1974). Factors affecting the activity of 5-HT-containing neurons. *Brain Research* 79, 515-519.

Brehm, P. & Eckert, R. (1978). Calcium entry leads to inactivation of calcium channel in Paramecium. *Science* 202, 1203-1206.

Breitweiser, G.E. & Szabo, G. (1985). Uncoupling of cardiac muscarinic and β-adrenergic receptors from ion channels by a guanine nucleotide analogue. *Nature* 317, 538-540.

Brown, A.M., Morimoto, K., Tsuda, Y. & Wilson, D.L. (1981). Calcium current-dependent and voltage-dependent inactivation of calcium channels in Helix aspersa. *Journal of Physiology* 320, 193-218.

Brown, A.M., Tsuda, Y. & Wilson, D.L. (1983). A description of activation and conduction in calcium channels based on tail and turn-on current measurements in the snail. *Journal of Physiology* 344, 549-583.

Brown, D.A., Docherty, R.J. & McFadzean, I. (1989). Calcium channels in vertebrate neurons. Experiments on a neuroblastoma hybrid model. *Annals of the New York Academy of Sciences* 560, 358-372.

Brown, T.H., Perkel, D.H., Norris, J.C. & Peacock, J.H. (1981a). Electrotonic structure and specific membrane properties of mouse dorsal root ganglion neurons. *Journal of Neurophysiology* 45, 1-15.

Brown, T.H., Fricke, R.A. & Perkel, D.H. (1981b). Passive electrical constants in three classes of hippocampal neurons. *Journal of Neurophysiology* 46, 812-827.

Burlhis, T.M. & Aghajanian, G.K. (1987). Pacemaker potentials of serotonergic dorsal raphe neurons: Contribution of a low-threshold Ca^{2+} conductance. *Synapse* 1, 582-588.

Byerly, L., Chase, P.B. & Stimers, J.R. (1984). Calcium current activation kinetics in neurones of the snail Lymnaea Stagnalis. *Journal of Physiology* 348, 187-207.

Byerly, L. & Hagiwara, S. (1982). Calcium currents in internally perfused nerve cell bodies of lymnea stagnalis. *Journal of Physiology* 322, 503-528.

Cachelin, A.B., de Peyer, J.E., Kokubun, S. & Reuter, H. (1983). Ca^{2+} channel modulation by 8-bromocyclic AMP in cultured heart cells. *Nature* 304, 462-464.

Campbell, K.P., Leung, A.T. & Sharp, A.H. (1988). The biochemistry and molecular biology of the dihydropyridine-sensitive calcium channel. *Trends in Neurosciences* 11, 425-430.

References

Carafoli, E. (1987). Intracellular calcium homeostasis. *Annual Review of Biochemistry* 56, 395-433.

Carbone, E. & Lux, H.D. (1984a). A low voltage-activated, fully inactivating Ca channel in vertebrate sensory neurones. *Nature* 310, 501-502.

Carbone, E. & Lux, H.D. (1984b). A low voltage-activated calcium conductance in emdryonic chick sensory neurones. *Biophysics Journal* 46, 413-418.

Carbone, E. & Lux, H.D. (1987a). Kinetics and selectivity of a low-voltage-activated calcium current in chick and rat sensory neurones. *Journal of Physiology* 386, 547-570.

Carbone, E. & Lux, H.D. (1987b). Single low-voltage-activated calcium channels in chick and rat sensory neurones. *Journal of Physiology* 386, 571-601.

Carbone, E. & Lux, H.D. (1989). Modulation of Ca channels in peripheral neurons. *Annals of the New York Academy of Sciences* 560, 346-357.

Catterall, W.A. (1988). Structure and function of voltage-sensitive ion channels. *Science* 242, 50-61.

Catterall, W.A. & Striessnig, J. (1992). Receptor sites for Ca^{2+} channel antagonists. *Trends in Pharmacology* 12, 256-262.

Caulfield, M.P., Robbins, J. & Brown, D.A. (1992). Neurotransmitters inhibit the omega-conotoxin-sensitive component of Ca current in neuroblastoma X glioma hybrid (NG108-15) cells, not the nifedipine-sensitive component. *Pflugers Archives. European Journal of Physiology* 420, 486-492.

Cavalié, A., McDonald, T.F., Pelzer, D. & Trautwein, W. (1985). Temperature-induced transitory and steady-state changes in the calcium current of guinea pig ventricular myocytes. *Pflugers Archives. European Journal of Physiology* 405, 294-296.

Chalmers, D.T. & Watson, S.J. (1991). Comparitive anatomical distribution of 5-HT_{1A} receptor mRNA and 5-HT_{1A} binding in rat brain - a combined in situ hybridisation/in vitro receptor autoradiographic study. *Brain Research* 561, 51-60.

Chapman, D. (1975). Phase transitions and fluidity characteristics of lipids and cell membranes. *Quarterly Review of Biophysics* **8**, 185-235.

Charlton, M.P. & Augustine, G.J. (1990). Classification of presynaptic calcium channels at the squid giant synapse: Neither T-, L- nor N-type. *Brain Research* 525, 133-139.

Chen, C., Zhang, J., Vincent, J.-D. & Israel, J.-M. (1990). Two types of voltage-dependent calcium current in rat somatotrophs are reduced by somatostatin. *Journal of Physiology* 425, 29-42.

References

Chernevskaya, N.I., Obukhov, A.G. & Krishtal, O.A. (1991). NMDA receptor agonists selectively block N-type calcium channels in hippocampal neurons. *Nature* 349, 418-420.

Chiu, S.Y. (1979). A transition temperature for the maximal sodium conductance in mammalian node of Ranvier. *Biophysics Journal* 25, 193a.

Cohen, P. (1988). Protein phosphorylation and hormone action. *Proceedings of the Royal Society.Series B* 234, 115-144.

Cohen, P. (1989). The structure and regulation of protein phosphatases. *Annual Review of Biochemistry* 58, 453-508.

Cohen, P. & Cohen, P.T.W. (1989). Protein phosphatases come of age. *The Journal of Biological Chemistry* 264, 21435-21438.

Collins, C.A. & Rojas, E. (1982). Temperature dependence of the sodium channel gating kinetics in the node of Ranvier. *Quarterly Journal of Experimental Physiology* 67, 41-55.

Constanti, A. & Galvan, M. (1983). Fast inward-rectifying current accounts for anomalous rectification in olfactory cortex neurones. *Journal of Physiology* 385, 153-178.

Cota, G. (1986). Calcium channel currents in pars intermedia cells of the rat pituitary gland. *Journal of General Physiology* 88, 83-105.

Cota, G., Nicola Siri, L. & Stefani, E. (1983). Calcium-channel gating in frog skeletal muscle membrane: Effect of temperature. *Journal of Physiology* 338, 395-412.

Cox, D.H. & Dunlap, K. (1992). Pharmacological discrimination of N-type from L-type calcium current and its selective modulation by transmitters. *Journal of Neuroscience* 12, 906-914.

Crunelli, V., Forda, S., Brooks, P.A., Wilson, K.C.P., Wise, J.C.M. & Kelly, J.S. (1983). Passive membrane properties of neurones in the dorsal raphe and periaqueductal grey recorded in vitro. *Neuroscience Letters* 40, 263-268.

Cruz, L.J. & Olivera, B.M. (1986). Calcium channel antagonists. *The Journal of Biological Chemistry* 261, 6230-6233.

Curtis, B.M. & Catterall, W.A. (1984). Purification of the calcium antagonist receptor of the voltage-sensitive calcium channel from skeletal muscle transverse tubules. *Biochemistry* 23, 2113-2117.

Dahlstrom, A. & Fuxe, K. (1964). Evidence for the existance of monoamine-containing neurons in the central nervous system. I. Demonstation of monoamines in cell bodies of brain neurons. *Acta Physiology Scandinavia* 62, Suppl. 232, 1-55.

de Montigny, C., Blier, P. & Chaput, Y. (1984). Electrophysiologically-identified serotonin receptors in the rat CNS. *Neuropharmacology* 23, 1511-1520.

References

De Waard, M., Feltz, A. & Bossu, J.-L. (1991). Properties of a high-threshold voltage-activated calcium current in rat cerebellar granule cells. *European Journal of Neuroscience* 3, 771-777.

Deisz, R.A. & Lux, H.D. (1985). Gamma-aminobutyric acid-induced depression of calcium currents of chick sensory neurons. *Neuroscience Letters* 56, 205-210.

Deitmer, J.W. (1984). Evidence for two voltage-dependent calcium currents in the membrane of the ciliate stylonychia. *Journal of Physiology* 355, 137-159.

Del Castillo, J. & Machne, X. (1953). Effect of temperature on the passive electrical properties of the muscle fibre membrane. *Journal of Physiology* 120, 431-434.

Descarries, L., Watkins, K.C., Garcia, S. & Beaudet, A. (1982). The serotonin neurons of the nucleus raphe dorsalis of adult rats. *Journal of Comparitive Neurology* 207, 239-254.

Docherty, R.J. (1988). Gadolinium selectively blocks a component of calcium current in rodent neuroblastoma X glioma hybrid (NG108-15) cells. *Journal of Physiology* 398, 33-47.

Docherty, R.J. & McFadzean, I. (1989). Noradrenaline-induced inhibition of voltage-sensitive calcium currents in NG108-15 hybrid cells. *European Journal of Neuroscience* 1, 132-140.

Doerner, D., Pitler, T.A. & Alger, B.E. (1988). Protein kinase C activators block specific calcium and potassium current components in isolated hippocampal neurones. *Journal of Neuroscience* 8, 4069-4078.

Dolphin, A.C. (1988). Is p21-ras a real G protein? *Trends in Neurosciences* 11, 287-291.

Dolphin, A.C. (1991a). Ca^{2+} channel currents in rat sensory neurones: Interaction between guanine nucleotides, cyclic AMP and Ca^{2+} channel ligands. *Journal of Physiology* 432, 23-43.

Dolphin, A.C. (1991b). Regulation of calcium channel activity by GTP binding proteins and second messengers. *Biochimica et Biophysica Acta* 1091, 68-80.

Dolphin, A.C. (1992a). The effect of phosphatase inhibitors on calcium currents in cultured rat dorsal root ganglion neurones. *Journal of Physiology* 446, 39P.

Dolphin, A.C. (1992b). The effect of phosphatase inhibitors and agents increasing cyclic-AMP-dependent phosphorylation on calcium currents in cultured dorsal root ganglion neurones: Interaction with the effect of G protein activation. *Pflugers Archives. European Journal of Physiology* 421, 138-145.

Dolphin, A.C., Forda, S.R. & Scott, R.H. (1986). Calcium-dependent currents in cultured rat dorsal root ganglion neurones are inhibited by an adenosine analogue. *Journal of Physiology* 373, 47-61.

References

Dolphin, A.C., McGuirk, S.M. & Scott, R.H. (1989). An investigation into the mechanism of inhibition of calcium channel currents in cultured sensory neurones of the rat by guanine nucleotide analogues and (-)-baclofen. *British Journal of Pharmacology* 97, 263-273.

Dolphin, A.C. & Scott, R.H. (1986). Inhibition of calcium currents in cultured rat dorsal root ganglion neurones by (-)-baclofen. *British Journal of Pharmacology* 88, 213-220.

Dolphin, A.C. & Scott, R.H. (1987). Calcium channel currents and their inhibition by (-)-baclofen in rat sensory neurones: Modulation by guanine nucleotides. *Journal of Physiology* 386, 1-17.

Dolphin, A.C. & Scott, R.H. (1988). Ca^{2+} agonists/antagonists and GTP. *Trends in Pharmacology* 9, 394-395.

Dolphin, A.C. & Scott, R.H. (1989a). Modulation of Ca^{2+}-channel currents in sensory neurons by pertussis toxin-sensitive G-proteins. *Annals of the New York Academy of Sciences* 560, 387-390.

Dolphin, A.C. & Scott, R.H. (1989b). Interaction between calcium current ligands and guanine nucleotides in cultured rat sensory and sympathetic neurones. *Journal of Physiology* 413, 271-288.

Dolphin, A.C. & Scott, R.H. (1990). Activation of calcium channel currents in rat sensory neurons by large depolarizations: Effect of guanine neucleotides and (-)-baclofen. *European Journal of Neuroscience* 2, 104-108.

Dooley, D.J., Lupp, A., Hertting, G. & Osswald, H. (1988). Omega-conotoxin GVIA and pharmacological modulation of hippocampal noradrenaline release. *European Journal of Pharmacology* 148, 261-267.

Doroshenko, P. & Neher, E. (1991). Pertusis-toxin-sensitive inhibition by (-)baclofen of Ca signals in bovine chromaffin cells. *Pflugers Archives. European Journal of Physiology* 419, 444-449.

Doroshenko, P.A., Kostyuk, P.G., Martynyuk, A.E., Kursky, M.D. & Vorobetz, Z.D. (1984). Intracellular protein kinase and calcium inward currents in perfused neurones of the snail Helix pomatia. *Neuroscience* 11, 263-267.

Douglas, W.W. & Tarashevich, P.S. (1982). Slowing effects of dopamine and calcium-channel blockers on frequency of sodium spikes in rat pars intermedia cells. *Journal of Physiology* 326, 201-211.

Dryer, S.E., Dourado, M.M. & Wisgirda, M.E. (1991). Properties of Ca^{2+} currents in acutely dissociated neurons of the chick ciliary ganglion: Inhibition by somatostatin-14 and somatostatin-28. *Neuroscience* 44, 663-672.

Dubinsky, J.M. & Oxford, G.S. (1984). Ionic currents in two strains of rat anterior pituitary tumour cells. *Journal of General Physiology* 83, 309-339.

References

Dunlap, K. & Fischback, G.D. (1978). Neurotransmitters decrease the calcium component of sensory neurone action potentials. *Nature* 276, 837-839.

Dunlap, K. & Fischback, G.D. (1981). Neurotransmitters decrease the calcium conductance activated by depolarization of embryonic chick sensory neurones. *Journal of Physiology* 317, 519-535.

Eckert, R. & Chad, J.E. (1984). Inactivation of Ca channels. *Progress in Biophysics and Molecular Biology* 44, 215-267.

Eckert, R., Chad, J.E. & Kalman, D. (1986). Enzymatic regulation of calcium current in dialysed and intact molluscan neurons. *Journal of Physiology (Paris)* 81, 318-324.

Eckert, R., Hescheler, J., Krautwurst, D., Schultz, G. & Trautwein, W. (1990). Calcium currents of neuroblastoma X glioma hybrid cells after cultivation with dibutyl cyclic AMP and nickel. *Pflugers Archives. European Journal of Physiology* 417, 329-335.

Ellis, S.B., Williams, M.E., Ways, N.R., Brenner, R., Sharp, A.H., Leung, A.T., Campbell, K.P., McKenna, E., Koch, W.J., Hui, A., Schwartz, A. & Harpold, M.M. (1988). Sequence and expression of mRNAs encoding α_1 and α_2 subunits of a DHP-sensitive calcium channel. *Science* 241, 1661-1664.

Elmslie, K.S. (1992). Calcium current modulation in frog sympathetic neurones: Multiple neurotransmitters and G proteins. *Journal of Physiology* 451, 229-246.

Elmslie, K.S., Zhou, W. & Jones, S.W. (1990). LHRH and GTPγS modify calcium current activation in bullfrog sympathetic neurons. *Neuron* 5, 75-80.

Ewald, D.A., Sternweis, P.C. & Miller, R.J. (1988a). Guanine nucleotide-binding protein G_0-induced coupling of neuropeptide Y receptors to Ca^{2+} channels in sensory neurons. *Proceedings of the National Academy of Science USA* 85, 3633-3637.

Ewald, D.A., Miller, R.J. & Sternweis, P.C. (1988b). C-kinase and G-proteins mediate inhibition of Ca^{2+} currents by neuropeptide Y in rat dorsal root ganglion neurons. *Biophysics Journal* 53, 234a.

Fatt, P. & Ginsborg, B.L. (1958). The ionic requirements for the production of action potentials in crustacean muscle. *Journal of Physiology* 142, 516-543.

Fatt, P. & Katz, B. (1953). The electrical properties of crustacean muscle fibres. *Journal of Physiology* 120, 171-204.

Fedulova, S.A., Kostyuk, P.G. & Veselovsky, N.S. (1985). Two types of calcium channels in the somatic membrane of newborn rat dorsal root ganglion neurones. *Journal of Physiology* 359, 431-446.

References

Fenwick, E.M., Marty, A. & Neher, E. (1982). Sodium and calcium channels in bovine chromaffin cells. *Journal of Physiology* **331**, 599-635.

Fernandez, J.M., Fox, A.P. & Krasne, S.P. (1984). Membrane patches and whole-cell membranes: A comparison of electrical properties in the rat clonal pituitary (GH3) cells. *Journal of Physiology* **356**, 565-585.

Finkel, A.S. & Redman, S. (1984). Theory and operation of a single microelectrode voltage clamp. *Journal of Neuroscience Methods* **11**, 101-127.

Fischbach, G.D. & Lass, Y. (1978). A transition temperature for acetylcholine channel conductance in chick myoballs. *Journal of Physiology* **280**, 527-536.

Fisher, R.E., Gray, R. & Johnston, D. (1988). β-Adrenoceptor modulation of calcium channels in acutely exposed CA3 pyramidal neurons of adult guinea pig hippocampus. *Society of Neurosciences Abstracts* **14**, 262.9.

Fleckenstein, A. (1983). History of calcium antagonists. *Circulation Research* **52** (suppl.I), 3-16.

Forscher, P. & Oxford, G.S. (1985). Modulation of calcium channels by norepinepherine in internally dialyzed avian sensory neurons. *Journal of General Physiology* **85**, 743-763.

Forscher, P., Oxford, G.S. & Schulz, D. (1986). Noradrenaline modulates calcium channels in avian dorsal root ganglion cells through tight receptor coupling. *Journal of Physiology* **379**, 131-144.

Forsythe, I.D. & Coates, R.T. (1988). A chamber for electrophysiological recording from cultured neurones allowing perfusion and temperature control. *Journal of Neuroscience Methods* **25**, 19-27.

Foulkes, J.G., Ernst, V. & Levin, D.H. (1983). Separation and identification of Type 1 and Type 2 protein phosphatases from rabbit reticulocyte lysates. *The Journal of Biological Chemistry* **258**, 1439-1443.

Fox, A.P., Nowycky, M.C. & Tsien, R.W. (1987a). Kinetic and pharmacologial properties distinguishing three types of calcium currents in chick sensory neurones. *Journal of Physiology* **394**, 149-172.

Fox, A.P., Nowycky, M.C. & Tsien, R.W. (1987b). Single-channel recordings of three types of calcium channels in chick sensory neurons. *Journal of Physiology* **394**, 173-200.

Franckowiak, G., Bechem, M., Schramm, M. & Thomas, G. (1985). The optical isomers of the 1,4-dihydropyridine Bay K 8644 show opposite effects on Ca channels. *European Journal of Pharmacology* **114**, 223-226.

References

Frankenhaeuser, B. & Moore, L.E. (1963). The effect of temperature on the sodium and potassium permeability changes in myelinated nerve fibres of Xenopus Laevis. *Journal of Physiology* **169**, 431-437.

Franklin, J.L., Fickbohm, D.J. & Willard, A.L. (1992). Long-term regulation of neuronal calcium currents by prolonged changes of membrane potential. *Journal of Neuroscience* 12, 1726-1735.

Franks, F. (1981). Biophysics and biochemistry of low temperatures and freezing. In: *Effects of low temperatures on biological membranes*, Eds. Morris, G.J. & Clarke, A. Academic Press, London.

Fraser, D.D. & MacVicar, B.A. (1991). Low-threshold transient calcium current in rat hippocampal lacunosum-moleculare interneurons: Kinetics and modulation by neurotransmitters. *Journal of Neuroscience* 11, 2812-2820.

Fryer, M.W., Gage, P.W., Neering, I.R., Dulhunty, A.F. & Lamb, G.D. (1988). Paralysis of skeletal muscle by butanedione monoxime, a chemical phosphatase. *Pflugers Archives. European Journal of Physiology* 411, 76-79.

Fukuda, A., Minami, T., Nabekura, J. & Oomura, Y. (1987). The effects of noradrenaline on neurones in the rat dorsal motor nucleus of the vagus, in vitro. *Journal of Physiology* 393, 213-231.

Gahwiler, B.H. & Brown, D.A. (1987). Muscarine affects calcium currents in rat hippocampal pyramidal cells in vitro. *Neuroscience Letters* 76, 301-306.

Galizzi, J-P., Fosset, M., Romey, G., Laduron, P. & Lazdunski, M. (1986). Neuroleptics of the diphenylbutylpiperidine series are potent calcium channel inhibitors. *Proceedings of the National Academy of Science USA* 83, 7513-7517.

Galvan, M. & Adams, P.R. (1982). Control of calcium current in rat sympathetic neurons by norepinepherine. *Brain Research* 244, 135-144.

García, J. & Stefani, E. (1987). Appropriate conditions to record activation of fast Ca^{2+} channels in frog skeletal muscle. *Pflugers Archives. European Journal of Physiology* 408, 646-648.

Gilman, A.G. (1987). G proteins: Transducers of receptor-generated signals. *Annual Review of Biochemistry* 56, 615-649.

Glaser, T., Rath, M., Traber, J., Zilles, K. & Schleicher, A. (1985). Autoradiographic identification and topographical analyses of high affinity serotonin receptor subtypes as a target for the novel putative anxiolytic TVX Q 7821. *Brain Research* 358, 129-136.

Glennon, R.A., Naiman, N.A., Lyon, R.A. & Titeler, M. (1988a). Arylpiperazine derivatives as high-affinity 5-HT1A serotonin ligands. *Journal of Medicinal Chemistry* 31, 1968-1971.

References

Glennon, R.A., Naiman, N.A., Pierson, M.E., Titeler, M., Lyon, R.A. & Weisberg, E. (1988b). NAN-190: An arylpiperazine analog that antaganizes the stimulus effects of the 5-HT_{1A} agonist 8-hydroxy-2-(di-n-propylamino)tetralin (8-OH-DPAT). *European Journal of Pharmacology* **154**, 339-341.

Glossmann, H. & Ferry, D.R. (1983). Solubilization and partial purification of putative calcium channels labelled with [3H]-nimodipine. *Naunyn-Schmiedeberg's Archives of Pharmacology* **323**, 279-291.

Godfraind, T., Miller, R.J. & Wibo, M. (1986). Calcium antagonists and calcium entry blockade. *Pharmacological Reviews* **38**, 321-416.

Gottmann, K., Dietzel, I.D., Lux, H.D., Huck, S. & Rohrer, H. (1988). Development of inward currents in chick sensory and autonomic neuronal precursor cells in culture. *Journal of Neuroscience* **8**, 3722-3732.

Grassi, F. & Lux, H.D. (1989). Voltage-dependent GABA-induced modulation of calcium currents in chick sensory neurones. *Neuroscience Letters* **105**, 113-119.

Gray, R. & Johnston, D. (1987). Noradrenaline and β-adrenoceptor agonists increase activity of voltage dependent calcium channels in hippocampal neurons. *Nature* **327**, 620-622.

Green, K.A. & Cottrell, G.A. (1988). Actions of baclofen on components of the Ca-current in rat and mouse DRG neurons in culture. *British Journal of Pharmacology* **94**, 235-245.

Gross, R.A. & MacDonald, R.L. (1987). Dynorphine A selectively reduces a large transient (N-type) calcium current in mouse dorsal root ganglion neurons in cell culture. *Proceedings of the National Academy of Science USA* **84**, 5469-5473.

Gross, R.A. & MacDonald, R.L. (1988a). Activation of A-kinase reduces the N-type calcium current in mouse sensory neurons by enhancing inactivation. *Society of Neurosciences Abstracts* **14**, 262.8.

Gross, R.A. & MacDonald, R.L. (1988b). Barbiturates and nifedipine have different and selective effects on calcium currents of mouse DRG neurons in culture: A possible basis for differing clinical actions. *Neurology* **38**, 443-451.

Gross, R.A., MacDonald, R.L. & Ryan-Jastrow, T. (1989). 2-Chloroadenosine reduces the N calcium current of cultured mouse sensory neurones in a pertussis toxin-sensitive manner. *Journal of Physiology* **411**, 585-595.

Gross, R.A., Uhler, M.D. & MacDonald, R.L. (1990a). The reduction of neuronal calcium currents by ATP-γ-S is mediated by a G protein and occurs independently of cyclic AMP-dependent protein kinase. *Brain Research* **535**, 214-220.

References

Gross, R.A., Uhler, M.D. & MacDonald, R.L. (1990b). The cyclic AMP-dependent protein kinase catalytic subunit selectively enhances calcium currents in rat nodose neurones. *Journal of Physiology* 429, 483-496.

Gurney, A.M. & Nerbonne, J.M. (1984). Nifedipine blockade of neuronal calcium currents. *Society of Neurosciences Abstracts* 10, 868.

Hagiwara, N., Irisawa, H. & Kameyama, M. (1988). Contribution of two types of calcium currents to the pacemaker potentials of rabbit sino-atrial node cells. *Journal of Physiology* 395, 233-253.

Hagiwara, S. & Byerly, L. (1981). Calcium channels. *Annual Review of Neuroscience* 4, 69-125.

Hagiwara, S. & Nakajima, S. (1966a). Differences in Na and Ca spikes as examined by application of tetrodotoxin, procaine, and manganese ions. *Journal of General Physiology* 49, 793-806.

Hagiwara, S. & Nakajima, S. (1966b). Effects of the intracellular Ca ion concentration upon the excitability of the muscle fiber membrane of the barnacle. *Journal of General Physiology* 49, 807-818.

Hagiwara, S., Ozawa, S. & Sand, O. (1975). Voltage clamp analysis of two inward current mechanisms in the egg cell membrane of a star fish. *Journal of General Physiology* 65, 617-644.

Hagiwara, S. & Yoshii, M. (1980). Effect of temperature on the anomalous rectification of the membrane of the egg of the starfish, Mediaster Aequalis. *Journal of Physiology* 307, 517-527.

Hahnel, C., Gottmann, K., Wittinghofer, A. & Lux, H.D. (1992). p21ras oncogene protein selectively increases low-voltage-activated Ca^{2+} current density in embryonic chick dorsal root ganglion neurons. *European Journal of Neuroscience* 4, 361-368.

Hamill, O., Marty, A., Neher, E., Sakmann, B. & Sigworth, F.J. (1981). Improved patch-clamp techniques for high-resolution current recording from cells and cell-free membrane patches. *Pflugers Archives. European Journal of Physiology* 391, 85-100.

Hamilton, S.L., Yatani, A., Brush, K., Schwartz, A. & Brown, A.M. (1987). A comparison between the binding and electrophysiological effects of dihydropyridines on cardiac muscle. *Molecular Pharmacology* 31, 221-231.

Hartzell, H.C., Méry, P.-F., Fischmeister, R. & Szabo, G. (1991). Sympathetic regulation of cardiac calcium current is due exclusively to cAMP-dependent phosphorylation. *Nature* 351, 573-576.

Hemmings, C.F.B., Greengard, P., Tuang, H.Y.L. & Cohen, P. (1984). DARPP-32, a dopamine-regulated neuronal phosphoprotein, is a potent inhibitor of protein phosphatase-1. *Nature* 310, 503-505.

References

Héry, F., Faudon, M. & Fueri, C. (1986). Release of serotonin in structures containing serotonergic nerve cell bodies: Dorsalis raphé nucleus and nodose ganglia of the cat. *Annals of the New York Academy of Sciences* 473, 239-255.

Héry, F., Faudon, M. & Ternaux, J.P. (1982). *In vivo* release of serotonin in two raphe nuclei (raphe dorsalis and magnus) of the cat. *Brain Research Bulletin* 8, 123-129.

Hescheler, J., Rosenthal, W., Trautwein, W. & Schultz, G. (1987). The GTP-binding protein, G_0, regulates neuronal calcium channels. *Nature* 325, 445-447.

Hess, P. (1990). Calcium channels in vertebrate cells. *Annual Review of Neuroscience* 13, 337-356.

Hess, P., Lansman, J.B. & Tsien, R.W. (1984). Different modes of Ca channel gating behaviour favoured by dihydropyridine Ca agonists and antagonists. *Nature* 311, 538-544.

Hille, B. (1984). *Ionic Channels of Excitable Membranes*. Sinauer Associates *INC*, Sunderland, Massachusetts.

Hillyard, D.R., Monje, V.D., Mintz, I.M., Bean, B.P., Nadasdi, L., Ramachandran, J., Miljanich, G., Azimi-Zoonooz, A., McIntosh, J.M., Cruz, L.J., Imperial, J.S. & Olivera, B.M. (1992). A new conus peptide ligand for mammalian presynaptic Ca2+ channels. *Neuron* 9, 69-77.

Hiraga, A. & Cohen, P. (1986). Phosphorylation of the glycogen-binding subunit of protein phosphatase-1G by cyclic AMP-dependent protein kinase promotes translocation of the phosphatase from glycogen to cytosol in rabbit skeletal muscle. *European Journal of Biochemistry* 161, 763-769.

Hirning, L.D., Fox, A.P., McClesky, E.W., Olivera, B.M., Thayer, S.A., Miller, R.J. & Tsien, R.W. (1988a). Dominant role of N-type Ca^{2+} channels in evoked release of norepinepherine from sympathetic neurones. *Science* 239, 57-60.

Hirning, L.D., Fox, A.P. & Miller, R.J. (1990). Inhibition of calcium currents in cultured myenteric neurons by neuropeptide Y: Evidence for direct receptor/channel coupling. *Brain Research* 532, 120-130.

Hirning, L.D., Miller, R.J. & Fox, A.P. (1988b). Modulation of calcium transients and calcium currents in cultured rat myenteric neurons by neuropeptide Y. *Biophysics Journal* 53, 234a.

Hladky, S.B. & Haydon, D.A. (1972). Ion transfer across lipid membranes in the presence of gramicidin A. I Studies of the unit conductance channel. *Biochimica et Biophysica Acta* 274, 294-312.

Hockberger, P., Toselli, M., Swandulla, D. & Lux, H.D. (1989). A diacylglycerol analogue reduces neuronal calcium currents independently of protein kinase C activation. *Nature* 338, 340-342.

References

Hodgkin, A.L. & Huxley, A.F. (1952). A quantitative description of membrane current and its application to conduction and excitation in nerve. *Journal of Physiology* **117**, 500-544.

Hodgkin, A.L., Huxley, A.F. & Katz, B. (1952). Measurment of current-voltage relations in the mebrane of the giant axon of Loligo. *Journal of Physiology* **116**, 424-448.

Hodgkin, A.L. & Nakajima, S. (1972). Effects of diameter on electrical constants of frog skeletal muscle fibres. *Journal of Physiology* **221**, 105-120.

Hof, R.P., Rüegg, U.T, Hof, A. & Vogel, A. (1985). Stereoselectivity at the calcium channel: Opposite action of the enantiomers of a 1,4-dihydropyridine. *Journal of Cardiovascular Pharmacology* **7**, 689-693.

Holmes, C.F.B., Campbell, D.G., Caudwell, F.B., Aitken, A. & Cohen, P. (1986). The protein phosphatases involved in cellular regulation. *European Journal of Biochemistry* **155**, 173-182.

Holz, G.G., Rane, S.G. & Dunlap, K. (1986). GTP-binding proteins mediate transmitter inhibition of voltage-dependent calcium channels. *Nature* **672**, 670-672.

Horn, J.P. & McAfee, D.A. (1980). α-adrenergic inhibition of calcium-dependent potentials in rat sympathetic neurone. *Journal of Physiology* **301**, 191-204.

Hosey, M.M., Borsotto, M. & Lazdunski, M. (1986). Phosphorylation and dephosphorylation of the major component of the voltage dependent Ca channel in skeletal muscle membranes by cyclic AMP and Ca-dependent processes. *Proceedings of the National Academy of Science USA* **83**, 3733-3737.

Hosey, M.M. & Lazdunski, M. (1989). Calcium channels: Molecular pharmacology, structure and regulation. *Journal of Membrane Biology* **104**, 81-105.

Huang, F.L. & Glinsmann, W.H. (1976). Separation and characterisation of two phosphorylase phosphatase inhibitors from rabbit skeletal muscle. *European Journal of Biochemistry* **70**, 419-426.

Huang, G.-J. & McArdle, J.J. (1992). Novel suppression of an L-type calcium channel in neurones of murine dorsal root ganglia by 2,3-butanedione monoxime. *Journal of Physiology* **447**, 257-274.

Hui, A., Ellinor, P.T., Krizanova, O., Wang, J.-J., Diebold, R.J. & Schwartz, A. (1991). Molecular cloning of multiple subtypes of a novel rat brain isoform of the α_1 subunit of the voltage-dependent calcium channel. *Neuron* **7**, 35-44.

Huston, E. & Dolphin, A.C. (1990). The effect of the isomers of 202-791 and the $GABA_B$ agonist baclofen on glutamate release from depolarised cultured rat cerebellar neurones. *British Journal of Pharmacology* **99**, 129P.

Huston, E., Scott, R.H. & Dolphin, A.C. (1990). A comparison of the effect of calcium channel ligands and $GABA_B$ agonists and antagonists on transmitter release and somatic calcium channel currents in cultured neurons. *Neuroscience* 38, 721-729.

Ikeda, S.R. (1991). Double-pulse calcium channel current facilitation in adult rat sympathetic neurones. *Journal of Physiology* 439, 181-214.

Ikeda, S.R. & Schofield, G.G. (1989). Somatostatin blocks calcium current in rat sympathetic ganglion neurones. *Journal of Physiology* 409, 221-240.

Ingebritsen, T.S., Blair, J., Guy, P., Witters, L. & Hardie, D.G. (1983b). The protein phosphatases involved in cellular regulation: Fatty acid synthesis, cholestrol synthesis and glycolysis/ gluconeogenesis. *European Journal of Biochemistry* 132, 275-281.

Ingebritsen, T.S. & Cohen, P. (1983a). The protein phosphatases involved in cellular regulation: Classification and substrate specificities. *European Journal of Biochemistry* 132, 255-261.

Ingebritsen, T.S. & Cohen, P. (1983b). Protein phosphatases: Properties and role in cellular regulation. *Science* 221, 331-338.

Ingebritsen, T.S., Stewart, A.A. & Cohen, P. (1983a). The protein phosphatases involved in cellular regulation: Measurement of Type 1 and Type 2 protein phosphatases in extracts of mammalian tissues and assessment of their physiological roles. *European Journal of Biochemistry* 132, 297-307.

Innis, R.B. & Aghajanian, G.K. (1987). Pertussis toxin blocks 5-HT-1A and GABA-B receptor-mediated inhibition of serotonergic neurons. *European Journal of Pharmacology* 143, 195-204.

Innis, R.B., Nestler, E.J. & Aghajanian, G.K. (1988). Evidence for G-protein mediation of serotonin- and $GABA_B$- induced hyperpolarisation of rat dorsal raphe neurons. *Brain Research* 459, 27-36.

Inoue, I., Pant, H.C., Tasaki, I. & Gainer, H. (1976). Release of proteins from the inner surface of squid giant axon membrane labelled with tritiated N-ethyl maleimide. *Journal of General Physiology* 68, 385-395.

Irisawa, H. & Kokubun, S. (1983). Modulation by intracellular ATP and cyclic AMP of the slow inward current in isolated single ventricular cells of the guinea pig. *Journal of Physiology* **338**, 321-337.

Ito, H., Sakanaski, M., Kawamura, T. & Nishi, K. (1984). Effects of organic Ca^{2+}-antagonists on membrane characteristics of nodose ganglion cells in the rabbit. *Archives Internationales de Pharmacodynamie et de Therapie* 271, 53-63.

Janis, R.A. & Triggle, D.J. (1983). New developments in Ca^{2+} channel antagonists. *Journal of Medicinal Chemistry* 26, 775-785.

References

Jones, S.W. & Jacobs, L.S. (1990). Dihydropyridine actions on calcium currents of frog sympathetic neurons. *Journal of Neuroscience* **10**, 2261-2267.

Kalman, D., O'Lague, P.H., Erxleben, C. & Armstrong, D.L. (1988). Calcium-dependent inactivation of the dihydropyridine sensitive calcium channels in GH3 cells. *Journal of General Physiology* **92**, 531-548.

Kameyama, M., Kameyama, A., Nakayama, T. & Kaibara, M. (1988). Tissue extract recovers cardiac calcium channels from 'run-down'. *Pflugers Archives. European Journal of Physiology* **412**, 328.

Kaneda, M. & Akaike, N. (1989). The low-threshold Ca current in isolated amygdaloid neurons in the rat. *Brain Research* **497**, 187-190.

Kanze, D.L., Hamilton, S.L., Hawkes, M.J. & Brown, A.M. (1987). Dihydropyridine binding and calcium channel function in clonal rat adrenal medullary tumor cells. *Molecular Pharmacology* **31**, 401-409.

Kasai, H. (1992). Voltage- and time-dependent inhibition of neuronal calcium channels by a GTP-binding protein in a mammalian cell line. *Journal of Physiology* **448**, 189-209.

Kasai, H. & Aosaki, T. (1989). Modulation of Ca-channel current by an adenosine analog mediated by a GTP-binding protein in chick sensory neurons. *Pflugers Archives. European Journal of Physiology* **414**, 145-149.

Kasai, H., Aosaki, T. & Fukuda, A. (1987). Presynaptic Ca-antagonist ω-conotoxin irreversibly blocks N-type Ca-channels in chick sensory neurons. *Neuroscience Research* **4**, 228-235.

Kasai, H. & Neher, E. (1992). Dihydropyridine-sensitive and ω-conotoxin-sensitive calcium channels in a mammalian neuroblastoma-glioma cell line. *Journal of Physiology* **448**, 161-188.

Kass, R.S. & Sanguinetti, M.C. (1984). Inactivation of calcium current in the calf cardiac Purkinji fibre: evidence for voltage- and calcium-mediated mechanisms. *Journal of General Physiology* **84**, 705-726.

Katada, T. & Ui, M. (1980). Slow interaction of islet-activating protein with pancreatic islets during primary culture to cause reversal of α-adrenergic inhibition of insulin secretion. *The Journal of Biological Chemistry* **255**, 9580-9588.

Kay, A.R. (1991). Inactivation kinetics of calcium current of acutely dissociated CA1 pyramidal cells of the mature guinea-pig hippocampus. *Journal of Physiology* **437**, 27-48.

Kay, A.R. & Wong, R.K.S. (1986). Isolation of neurons suitable for patch-clamping from adult mammalian central nervous systems. *Journal of Neuroscience Methods* **16**, 227-238.

References

Keja, J.A., Stoof, J.C. & Kits, K.S. (1992). Dopamine D_2 receptor stimulation differentially affects voltage-activated calcium channels in rat pituitary melanotropic cells. *Journal of Physiology* **450**, 409-435.

Kimura, J.E. & Meves, H. (1979). The effect of temperature on the asymmetrical charge movement in squid giant axons. *Journal of Physiology* 289, 479-500.

Kniffki, K.D., Siemen, D. & Vogel, W. (1981). Development of sodium permeability inactivation in nodal membranes. *Journal of Physiology* 313, 37-48.

Knight, D.E., von Grafenstein, H. & Athayde, C.M. (1989). Calcium-dependent and calcium-independent exocytosis. *Trends in Neurosciences* 12, 451-458.

Kongsamut, S., Kamp, T.J., Miller, R.J. & Sanguinetti, M.C. (1985). Calcium channel agonist and antagonist effects of the sterioisomers of the dihydropyridine 202-791. *Biochemical and Biophysical Research Communications* 130, 141-148.

Kongsamut, S., Lipscombe, D. & Tsien, R.W. (1989). The N-type Ca channel in frog sympathetic neurons and its role in α-adrenergic modulation of transmitter release. *Annals of the New York Academy of Sciences* 560, 312-333.

Kostyuk, P.G., Akaike, N., Osipchuk, Y., Savchenko, A. & Shuba, Y. (1989). Gating and permeation of different types of Ca channels. *Annals of the New York Academy of Sciences* 560, 63-79.

Kostyuk, P.G., Krishtal, O.A. & Pidoplichko, V.I. (1981a). Calcium inward current and related charge movements in the membrane of snail neurones. *Journal of Physiology* 310, 403-421.

Kostyuk, P.G., Krishtal, O.A. & Shakhovalov, Y.A. (1977). Separation of sodium and calcium currents in the somatic membrane of mollusc neurones. *Journal of Physiology* 270, 545-568.

Kostyuk, P.G. & Shirokov, R.E. (1989). Deactivation kinetics of different components of calcium inward current in the membrane of mice sensory neurones. *Journal of Physiology* 409, 343-355.

Kostyuk, P.G., Shuba, Y.M. & Savchenko, A.N. (1988). Three types of calcium channels in the membranes of mouse sensory neurones. *Pflugers Archives. European Journal of Physiology* 411, 661-669.

Kostyuk, P.G., Veselovsky, N.S. & Fedulova, S.A. (1981b). Ionic currents in the somatic membrane of rat dorsal root ganglion neurons. II. Calcium currents. *Neuroscience* 7, 2431-3437.

Kramer, R.H., Kaczmarek, L.K. & Levitan, E.S. (1991). Neuropeptide inhibition of voltage-gated calcium channels mediated by mobilization of intracellular calcium. *Neuron* 6, 557-563.

References

Kuan, Y.F., Scholfield, C.N. & Steel, L. (1985). Effect of Ca antagonists on axonal Ca/Ba spikes in slices of guinea-pig brain. *Journal of Physiology* 362, 35P.

Kukita, F. (1982). Properties of sodium and potassium channels of the squid giant axon far below 0°C. *Journal of Membrane Biology* 68, 151-160.

Kunze, D.L. & Ritchie, A.K. (1990). The DHP sensitive calcium channel in GH3 cells exhibits multiple conductance levels. *Biophysics Journal* 57, 396a.

Lacerda, A.E., Kim, H.S., Ruth, P., Perez-Reyes, E., Flockerzi, V., Hofmann, F., Birnbaumer, L. & Brown, A.M. (1991). Normalization of current kinetics by interaction between the α_1 and β subunits of the skeletal muscle dihydropyridine-sensitive Ca^{2+} channel. *Nature* 352, 527-530.

Lang, R.J., Ozolins, I.Z. & Paul, R.J. (1991). Effects of okadaic acid and ATPγS on cell length and Ca^{2+}-channel currents recorded in single smooth muscle cells of the guinea-pig taenia caeci. *British Journal of Pharmacology* 104, 331-336.

Laurenza, A., Sutkowski, E.McH. & Seaman, K.B. (1989). Forskolin: A specific stimulator of adenylate cyclase or a diterpene with multiple sites of action ? *Trends in Pharmacology* 10, 442-446.

Lawrence, J., Penington, N.J. & Kelly, J.S. (1989). Identification of acutely dissociated neurones from the slices of adult rat brain stem as projecting neurones of the Nucleus Raphe Dorsalis. *Neuroscience Letters, Supplement* 36, 99.

Lee, K.S. & Tsien, R.W. (1984). High selectivity of calcium channels in single dialysed heart cells of the guinea pig. *Journal of Physiology* 354, 253-272.

Lester, R.A.J. & Jahr, C.E. (1990). Quisqualate receptor-mediated depression of calcium currents in hippocampal neurons. *Neuron* 4, 741-749.

Leung, A.T., Imagawa, T., Block, B., Franzini-Armstrong, C. & Campbell, K.P. (1988). Biochemical and ultrastructural characterization of the 1,4-dihydropyridine receptor from rabbit skeletal muscle. *The Journal of Biological Chemistry* 263, 994-1001.

Leung, A.T., Imagawa, T. & Campbell, K.P. (1987). Structural characterisation of the 1,4-dihydropyridine receptor of the voltage dependent calcium channel from rabbit skeletal muscle. Evidence for two distinct high molecular weight subunits. *The Journal of Biological Chemistry* 262, 7943-7946.

Lipscombe, D., Madison, D.V., Poenie, M., Reuter, H., Tsien, R.Y. & Tsien, R.W. (1988). Spatial distribution of calcium channels and cytosolic calcium transients in growth cones and cell-bodies of sympathetic neurons. *Proceedings of the National Academy of Science USA* 85, 2398-2402.

References

Lipscombe, D. & Tsien, R.W. (1987). Noradrenaline inhibits N-type Ca channels in isolated frog sympathetic neurones. *Journal of Physiology* 390, 84P.

Lledo, P.M., Homburger, V., Bockaert, J. & Vincent, J.-D. (1992). Differential G-protein-mediated coupling of D_2 dopamine receptors to K^+ and Ca^{2+} currents in rat anterior pituitary. *Neuron* 8, 455-463.

Llinás, R. & Sugimori, M. (1980). Electrophysiological properties of *in vitro* Purkinje cell dendrites in mammalian cerebellar slices. *Journal of Physiology* 305, 171-195.

Llinás, R., Sugimori, M., Lin, J.-W. & Cherksey, B. (1989). Blocking and isolation of a calcium channel from neurons in mammalian and cephalopods utilizing a toxin fraction (FTX) from funnel-web spider poison. *Proceedings of the National Academy of Science USA* **86**, 1689-1693.

Llinás, R. & Yarom, Y. (1981). Properties and distribution of ionic conductances generating electroresponsiveness of mammalian inferior olivary neurones in vitro. *Journal of Physiology* 315, 569-584.

Llinás, R. & Yarom, Y. (1986). Specific blockage of the low threshold calcium channel by high molecular weight alcohols. *Society of Neurosciences Abstracts* 12, 174.

Llinás, R., Yarom, Y. & Sugimori, M. (1981). Isolated mammalian brain in vitro: New technique for analysis of electrical activity of neuronal circuit function. *Federation Proceedings* 40, 2240-2245.

Lopez, H.S. & Brown, A.M. (1991). Correlation between G protein activation and reblocking kinetics of calcium channel currents in rat sensory neurons. *Neuron* 7, 1061-1068.

Lux, H.D. & Brown, A.M. (1984). Patch and whole cell calcium currents recorded simultaneously in snail neurons. *Journal of General Physiology* 83, 727-750.

MacDonald, R.L., Skerritt, J.H. & Werz, M.A. (1986). Adenosine agonists reduce voltage-dependent calcium conductance of mouse sensory neurones in cell culture. *Journal of Physiology* 370, 75-90.

MacDonald, R.L. & Werz, M.A. (1986). Dynorphin A decreases voltage dependent calcium conductance of mouse dorsal root ganglion neurones. *Journal of Physiology* 377, 237-249.

Madison, D.V., Fox, A.P. & Tsien, R.W. (1987). Adenosine reduces an inactivating component of calcium current in hippocampal CA3 neurons. *Biophysics Journal* 51, 30a.

Magura, I.S., Prevarskaya, N.B. & Zachar, J. (1985). Temperature-dependent properties of delayed outward current channels in somatic membrane of snail neurons. *General Physiology and Biophysics* 4, 97-99.

Malouf, N.N., McMahon, D.K., Hainsworth, C.N. & Kay, B.K. (1992). A two-motif isoform of the major calcium channel subunit in skeletal muscle. *Neuron* 8, 899-906.

Marchetti, C., Carbone, E. & Lux, H.D. (1986). Effects of dopamine and noradrenaline on Ca channels of cultured sensory and sympathetic neurons of chick. *Pflugers Archives. European Journal of Physiology* 406, 104-111.

Marchetti, C., Carignani, C. & Robello, M. (1991). Voltage-dependent calcium currents in dissociated granule cells from rat cerebellum. *Neuroscience* 43, 121-133.

Marchetti, C. & Robello, M. (1989). Guanosine-5'-O-(3-thiotriphosphate) modulates kinetics of voltage-dependent calcium current in chick sensry neurones. *Biophysics Journal* 56, 1267-1272.

Marcinkiewicz, M., Verge, D., Gozlan, H., Pichat, L. & Hamon, M. (1984). Autoradiographic evidence for the heterogeneity of 5-HT_1 sites in the rat brain. *Brain Research* 291, 159-163.

Marty, A. & Neher, E. (1983). Tight-seal whole-cell recording. In: *Single channel recording*, Eds. Sakmann, B. & Neher, E. Plenum Press, New York. p. 107-122.

Mathie, A., Bernheim, L. & Hille, B. (1992). Inhibition of N- and L-type calcium channels by muscarinic receptor activation in rat sympathetic neurons. *Neuron* 8, 907-914.

McCall, R.B. & Clement, M.E. (1989). Identification of serotonergic and sympathetic neurons in medullary raphe nuclei. *Brain Research* 477, 172-182.

McCarron, J.G., McGeown, J.G., Reardon, S., Ikebe, M., Fay, F.S. & Walsh Jr., J.V. (1992). Calcium-dependent enhancement of calcium current in smooth muscle by calmodulin-dependent protein kinase II. *Nature* 357, 74-77.

McCarthy, R.T. & TanPiengco, P.E. (1992). Multiple types of high-threshold calcium channels in rabbit sensory neurons: high-affinity block of neuronal L-type by nimodipine. *Journal of Neuroscience* 12, 2225-2234.

McClesky, E.W., Fox, A.P., Feldman, D.H., Cruz, L.J., Olivera, B.M., Tsien, R.W. & Yoshikami, D. (1987). ω-Conotoxin: Direct and persistent blockade of specific types of calcium channels in neurons but not in muscle. *Proceedings of the National Academy of Science USA* 84, 4327-4331.

McCobb, D.P. & Beam, K.G. (1991). Action potential waveform voltage-clamp commands reveal striking differences in calcium entry via low and high voltage-activated calcium channels. *Neuron* 7, 119-127.

McFadzean, I. & Docherty, R.J. (1989). Noradrenaline- and enkephalin-induced inhibition of voltage-sensitive calcium currents in NG108-15 hybrid cells. *European Journal of Neuroscience* 1, 141-147.

References

McFadzean, I., Mullaney, I., Brown, D.A. & Milligan, G. (1989). Antibodies to the GTP binding protein G_o, antagonise noradrenaline-induced calcium current inhibition in NG108-15 hybrid cells. *Neuron* 3, 177-182.

Menon-Johansson, A.S. & Dolphin, A.C. (1992). Inhibition of $GABA_B$ modulation of calcium channel currents in cultured rat dorsal root ganglion neurones by loading replated cells with anti-G-protein antibodies. *Journal of Physiology* 452, 35P.

Meyers, D.E.R. & Barker, J.L. (1989). Whole-cell patch-clamp analysis of voltage-dependent calcium conductances in cultured embryonic rat hippocampal neurons. *Journal of Neuroscience* **61**, 467-477.

Middlemiss, D.N. (1984). Stereoselective blockade at $[^3H]$5-HT binding sites and at the 5-HT autoreceptor by propranolol. *European Journal of Pharmacology* 101, 289-293.

Miller, R.J. (1985). How many types of calcium channels exist in neurones? *Trends in Neurosciences* 8, 45-47.

Miller, R.J. (1987). Multiple calcium channels and neuronal function. *Science* 235, 46-52.

Miller, R.J. & Freedman, S.B. (1984). Are dihydropyridine binding sites voltage sensitive calcium channels? *Life Sciences* 34, 1205-1221.

Mintz, I.M., Adams, M.E. & Bean, B.P. (1992b). P-type calcium channels in rat central and peripheral neurons. *Neuron* 9, 85-95.

Mintz, I.M., Venema, V.J., Swiderek, K.M., Lee, T.D., Bean, B.P. & Adams, M.E. (1992a). P-type calcium channels blocked by the spider toxin Ω-Aga-IVA. *Nature* 355, 827-829.

Mogul, D.J. & Fox, A.P. (1991). Evidence for multiple types of Ca^{2+} channels in acutely isolated hippocampal CA3 neurones of the guinea-pig. *Journal of Physiology* 433, 259-281.

Moore, L.E. (1971). Effect of temperature and calcium ions on rate constants of myelinated nerve. *American Journal of Physiology* 221, 131-137.

Morgan, J.L. & Curran, T. (1989). Stimulus-transcription coupling in neurons: Role of cellular immediate early genes. *Trends in Neurosciences* 12, 459-462.

Mori, Y., Friedrich, T., Kim, M.-S., Mikami, A., Nakai, J., Rúth, P., Bosse, E., Hofmann, F., Flockerzi, V., Furuichi, T., Mikoshiba, K., Imoto, K., Tanabe, T. & Numa, S. (1991). Primary structure and functional expression from complementary DNA of a brain calcium channel. *Nature* 350, 398-402.

Morris, G.J. & Clarke, A. (1981). *Effects of low temperatures on biological membranes*. Academic Press, London.

References

Morton, M.E., Caffrey, J.M., Brown, A.M. & Froehner, S.C. (1988). Monoclonal antibody to the α-subunit of the dihydropyridine-binding complex inhibits calcium currents in BC3HI myocytes. *Journal of Biological Chemistry* 263, 613-616.

Mosko, S.S. & Jacobs, B.L. (1974). Midbrain raphe neurons: spontaneous activity and response to light. *Physiology and Behaviour* 13, 589-593.

Mosko, S.S. & Jacobs, B.L. (1976). Recording of dorsal raphe unit activity in vitro. *Neuroscience Letters* 2, 195-200.

Murase, K. & Randic, M. (1983). Electrophysiological properties of rat spinal dorsal horn neurones in vitro: Calcium-dependent action potentials. *Journal of Physiology* 334, 141-153.

Murphy, T.H., Worley, P.F. & Baraban, J.M. (1991). L-type voltage sensitive calcium channels mediate synaptic activation of immediate early genes. *Neuron* 7, 625-635.

Myers, D.E.R. & Barker, J.L. (1989). Whole-cell patch clamp analysis of voltage-dependent calcium conductances in cultured embryonic rat hippocampal neurons. *Journal of Neurophysiology* 61, 467-477.

Nakazawa, K., Inoue, K., Ohara-Imaizumi, M., Fujimori, K. & Takanaka, A. (1991). Inhibition of Ca-channels by diazepam compared with that by nicardipine in phaeochromocytoma PC12 cells. *Brain Research* 553, 44-50.

Narahashi, T., Tsunoo, A. & Yoshii, M. (1987). Characterization of two types of calcium channels in mouse neuroblastoma cells. *Journal of Physiology* 383, 231-249.

Neher, E. (1986). Concentration profiles of intracellular Ca^{2+} in the presence of a diffusable chelator. In: *Calcium electrogenesis and neuronal functioning*, Eds. Heinemann, U., Klee, M., Neher, E. & Singer, W. Springer Verlag, Heidelberg. p. 80-95.

Nelder, J.A. & Mead, R. (1965). A simplex method for function minimization. *Computor Journal* 7, 308-312.

Nerbonne, J.M. & Gurney, A.M. (1987). Blockade of Ca^{2+} and K^{+} currents in bag cell neurons of aplysia californica by dihydropyridine Ca^{2+} antagonists. *Journal of Neuroscience* 7, 882-893.

Nestler, E.J., Walaas, S.I. & Greengard, P. (1984). Neuronal phosphoproteins: Physiological and clinical implications. *Science* 225, 1357-1364.

Nistri, A. & Cherubini, E. (1991). Depression of a sustained calcium current by kainate in rat hippocampal neurones in vitro. *Journal of Physiology* 435, 465-481.

Nobile, M., Carbone, E., Lux, H.D. & Zucker, H. (1990). Temperature sensitivity of Ca currents in chick sensory neurones. *Pflugers Archives. European Journal of Physiology* 415, 658-663.

References

Noda, M., Shimizu, S., Tanabe, T., Takai, T. & Kayano, T. (1984). Primary structure of Electrophorus electricus sodium channels deduced from cDNA sequence. *Nature* 312, 121-127.

North, R.A. & Yoshimura, M. (1984). The actions of noradrenaline on neurones of the rat substantia gelatinosa in vitro. *Journal of Physiology* 349, 43-55.

Nowycky, M.C., Fox, A.P. & Tsien, R.W. (1985). Three types of calcium channel with different calcium agonist sensitivity. *Nature* 316, 440-443.

Nussinovitch, I. (1989). Somatosatin inhibits two types of voltage-activated calcium currents in rat growth-hormone secreting cells. *Brain Research* 504, 136-138.

O'Dell, T.J. & Alger, B.E. (1991). Single calcium channels in rat and guinea-pig hippocampal neurones. *Journal of Physiology* **436**, 739-767.

Ogura, A. & Amano, T. (1984). Serotonin-receptor coupled with membrane electrogenesis in a rat glioma clone. *Brain Research* 297, 387-391.

Ogura, A. & Takahashi, M. (1984). Differential effect of a dihydropyridine derivative to block Ca^{2+} entry pathways in neuronal preparations. *Brain Research* 301, 323-330.

Oyama, Y., Tsuda, Y., Sahakibara, S. & Akaike, N. (1987). Synthetic ω-conotoxin: A potent calcium channel blocking neurotoxin. *Brain Research* 424, 58-64.

Ozawa, S., Tsuzuki, K., Iino, M., Ogura, A. & Kudo, Y. (1989). Three types of voltage-dependent calcium current in cultured rat hippocampal neuron. *Brain Research* 495, 329-336.

Paxinos, G. & Watson, C. (1982). *The rat brain in stereotaxic coordinates*. Academic Press, Australia.

Penington, N.J., Fox, A.P. & Kelly, J.S. (1992). Simultaneous modulation of Ca^{2+} and K^{+} currents by 5-hydroxytryptamine studied using action potential waveforms in rat dorsal raphe neurones. (In Press)

Penington, N.J. & Kelly, J.S. (1990). Serotonin receptor activation reduces calcium current in an acutely dissociated adult central neuron. *Neuron* 4, 751-758.

Penington, N.J., Kelly, J.S. & Fox, A.P. (1991). A study of the mechanism of Ca^{2+} current inhibition produced by serotonin in rat dorsal raphe neurons. *Journal of Neuroscience* 11, 3594-3609.

References

Pelech, S., Cohen, P., Fischer, M.J., Pogson, C.I., El-Maghrabi, M.R. & Pilkis, S.J. (1984). The protein phosphatases involved in cellular regulation: Antibody to protein phosphatase-2A as a probe of phosphatase structure and function. *European Journal of Biochemistry* 145, 39-49.

Perney, T.M., Hirning, L.D., Leeman, S.E. & Miller, R.J. (1986). Multiple calcium channels mediate neurotransmitter release from peripheral neurons. *Proceedings of the National Academy of Science USA* 83, 6656-6659.

Pfaffinger, P.J., Martin, J.M., Hunter, D.D., Nathanson, N.M. & Hille, B. (1985). GTP-binding proteins couple cardiac muscarinic receptors to a K channel. *Nature* 317, 536-538.

Plummer, M.R. & Hess, P. (1991). Reversible uncoupling of inactivation in N-type calcium channels. *Nature* 351, 657-659.

Plummer, M.R., Logothetis, D.E. & Hess, P. (1989). Elementary properties and pharmacological sensitivites of calcium channels in mammalian peripheral neurons. *Neuron* 2, 1453-1463.

Plummer, M.R., Rittenhouse, A., Kanevsky, M. & Hess, P. (1991). Neurotransmitter modulation of calcium channels in rat sympathetic neurons. *Journal of Neuroscience* 11, 2339-2348.

Pongs, O., Keeskemethy, N., Mueller, R., Krah-Jentzens, I., Baumann, A., Kiltz, H.H., Canal, I., Llamazares, S. & Ferrus, A. (1988). Shaker encodes a family of putative potassium channel proteins in the nervous system of Drosophila. *EMBO Journal* 7, 1087-1096.

Press, W.H., Flamney, B.P., Teukolskey, S.A. & Vetterling, W.T. (1986). *Numerical receipes*. Cambridge University Press, Cambridge.

Protti, D.A., Szczupak, L., Scornik, F.S. & Uchitel, O.D. (1991). Effect of ω-conotoxin GVIA on neurotransmitter release at the mouse neuromuscular junction. *Brain Research* 557, 336-339.

Pusch, M. & Neher, E. (1988). Rates of diffusional exchange between small cells and a measuring patch pipette. *Pflugers Archives. European Journal of Physiology* 411, 204-211.

Rainnie, D.G., Penington, N.J. & Kelly, J.S. (1987). On the hyperpolarising action of 5-HT on dorsal raphé neurones in vitro. *Neuroscience Letters, Supplement* 29, S72.

Rane, S.G. & Dunlap, K. (1986). Kinase C activator 1,2-oleoylacetylglycerol attenuates voltage-dependent calcium current in sensory neurons. *Proceedings of the National Academy of Science USA* 83, 184-188.

Rane, S.G., Holz, G.G. & Dunlap, K. (1987). Dihydropyridine inhibition of neuronal calcium current and substance P release. *Pflugers Archives. European Journal of Physiology* 409, 361-366.

References

Regan, L.J. (1987). Calcium channels in freshly-dissociated rat cerebellar Purkinje cells. *Society of Neurosciences Abstracts* 13, 100.

Regan, L.J. (1991). Voltage-dependent calcium currents in Purkinji cells from rat cerebellar vermis. *Journal of Neuroscience* 11, 2259-2269.

Regan, L.J., Sah, D.W.Y. & Bean, B.P. (1991). Ca^{2+} channels in rat central and peripheral neurons: High-threshold current resistant to dihydropyridine blockers and ω-conotoxin. *Neuron* 6, 269-280.

Reuter, H. (1983). Calcium channel modulation by neurotransmitters, enzymes and drugs. *Nature* 301, 569-574.

Reuveny, E. & Narahashi, T. (1991). Potent blocking action of lead on voltage-activated calcium channels in human neuroblastoma cells SH-SY5Y. *Brain Research* 545, 312-314.

Rosenberg, R.L., Hess, P., Reeves, J.P., Smilowitz, H. & Tsien, R.W. (1986). Calcium channels in planar lipid bilayers: Insights into mechanisms of ion permeation and gating. *Science* 231, 1564-1566.

Ryan-Jastrow, T., Gross, R.A. & MacDonald, R.L. (1988). 2-Chloroadenosine selectively reduces the N-calcium current of mouse dorsal root ganglion neurons in a pertussis toxin-sensitive manner. *Society of Neurosciences Abstracts* 14, 262.6.

Sah, D.W.Y. (1990). Neurotransmitter modulation of calcium current in rat spinal cord. *Journal of Neuroscience* 10, 136-141.

Sala, F. (1991). Activation kinetics of calcium currents in bull-frog sympathetic neurones. *Journal of Physiology* 437, 221-238.

Sanguinetti, M.C. & Kass, R.S. (1984). Voltage-dependent block of calcium channel current by dihydropyridine calcium channel antagonists. *Circulation Research* 55, 336-348.

Schauf, C.L. (1973). Temperature dependence of the ionic current kinetics of Myxicola giant axons. *Journal of Physiology* 235, 197-205.

Scholz, K.P. & Miller, R.J. (1991). $GABA_B$ receptor-mediated inhibition of Ca^{2+} currents and synaptic transmission in cultured rat hippocampal neurones. *Journal of Physiology* 444, 669-686.

Schroeder, J.E., Fischbach, P.S. & McClesky, E.W. (1990). T-type calcium channels: Heterogenous expression in rat sensory neurons and selective modulation by phorbol esters. *Journal of Neuroscience* 10, 947-951.

Schroeder, J.E., Fischbach, P.S., Zheng, D. & McClesky, E.W. (1991). Activation of μ opioid receptors inhibits transient high- and low-threshold Ca^{2+} currents, but spares a sustained current. *Neuron* 6, 13-20.

Schwarz, J.R. (1986). The effect of temperature on Na currents in rat myelinated nerve fibres. *Pflugers Archives. European Journal of Physiology* 406, 397-404.

Schwarz, J.R. & Eikof, G. (1987). Na currents and action potentials in rat myelinated nerve fibres at 20 and 37°C. *Pflugers Archives. European Journal of Physiology* 409, 569-577.

Schwarz, W. (1979). Temperature experiments on nerve and muscle membranes of frogs. Indications for a phase transition. *Pflugers Archives. European Journal of Physiology* 382, 27-34.

Scott, R.H. & Dolphin, A.C. (1987). Activation of a G protein promotes agonist responses to calcium channel ligands. *Nature* 330, 760-762.

Scott, R.H. & Dolphin, A.C. (1990). Voltage-dependent modulation of rat sensory neurone calcium channel currents by G protein activation: Effect of a dihydropyridine antagonist. *British Journal of Pharmacology* 99, 629-630.

Scott, R.H., Wootton, J.F. & Dolphin, A.C. (1990). Modulation of neuronal T-type calcium channel currents by photoactivation of intracellular guanosine 5'-o(3-thio)triphosphate. *Neuroscience* 38, 285-294.

Scroggs, R.S. & Fox, A.P. (1991). Distribution of dihydropyridine and ω-conotoxin-sensitive calcium currents in acutely isolated rat and frog sensory neuron somata: diameter-dependent L channel expression in frog. *Journal of Neuroscience* 11, 1334-1346.

Scroggs, R.S. & Fox, A.P. (1992a). Calcium current variation between acutely isolated adult rat dorsal root ganglion neurons of different size. *Journal of Physiology* 445, 639-658.

Scroggs, R.S. & Fox, A.P. (1992b). Multiple Ca^{2+} currents elicited by action potential waveforms in acutely isolated adult rat dorsal root ganglion neurons. *Journal of Neuroscience* 12, 1789-1801.

Sevcik, C. (1982). Temperature dependence of tetrodotoxin effect in squid giant axons. *Journal of Physiology* 325, 187-194.

Seward, E.P., Hammond, C. & Henderson, G. (1991). μ-Opioid-receptor-mediated inhibition of the N-type calcium-channel current. *Proceedings of the Royal Society. Series B* 224, 129-135.

Seward, E.P. & Henderson, G. (1990). Characterization of two components of the N-like high-threshold-activated calcium channel current in differentiated SH-SY5Y cells. *Pflugers Archives. European Journal of Physiology* 417, 223-230.

Sharp, A.H., Imagawa, T., Leung, A.T. & Campbell, K.P. (1987). Identification and characterisation of the dihydropyridine-binding subunit of the skeletal muscle dihydropyridine receptor. *The Journal of Biological Chemistry* 262, 12309-12315.

References

Sharp, T., Bramwell, S.R., Clark, D. & Grahame-Smith, D.G. (1989). *In vivo* measurement of extracellular 5-hydroxytryptamine in hippocampus of the anaesthetized rat using microdialysis: Changes in relation to 5-hydroxytryptaminergic neuronal activity. *Journal of Neurochemistry* 53, 234-240.

Sharp, T., Bramwell, S.R. & Grahame-Smith, D.G. (1990). Release of endogenous 5-hydroxytryptamine in rat ventral hippocampus evoked by electrical stimulation of the dorsal raphe nucleus as detected by microdialysis: sensitivity to tetrodotoxin, calcium and calcium antagonists. *Neuroscience* 39, 629-637.

Shen, K.-Z. & Surprenant, A. (1990). Mechanisms underlying presynaptic inhibition through α_2-adrenoceptors in guinea-pig submucosal neurones. *Journal of Physiology* 431, 609-628.

Sheng, M. & Greenberg, M.E. (1990). The regulation and function of *c-fos* and other immediate early genes in the nervous system. *Neuron* 4, 477-485.

Sinton, C.M. & Fallon, S.L. (1988). Electrophysiological evidence for a funtional differentiation between subtypes of the 5-HT_1 receptor. *European Journal of Pharmacology* 157, 173-181.

Slesinger, P.A. & Lansman, J.B. (1991a). Inactivation of calcium currents in granule cells cultured from mouse cerebellum. *Journal of Physiology* 435, 101-121.

Slesinger, P.A. & Lansman, J.B. (1991b). Inactivating and non-inactivating dihydropyridine-sensitive Ca^{2+} channels in mouse cerebellar granule cells. *Journal of Physiology* 439, 301-323.

Slesinger, P.A. & Lansman, J.B. (1991c). Reopening of calcium channels in mouse cerebellar neurons at resting membrane potentials during recovery from inactivation. *Neuron* 7, 755-762.

Smith, S.J. & Augustine, G.J. (1988). Calcium ions, active zones and synaptic transmitter release. *Trends in Neurosciences* 11, 458-464.

Snutch, T.P., Leonard, J.P., Gilbert, M.M., Lester, H.A. & Davidson, N. (1990). Rat brain expresses a heterogenous family of calcium channels. *Proceedings of the National Academy of Science USA* 87, 3391-3395.

Song, S.-Y., Saito, K., Noguchi, K. & Konishi, S. (1989). Different GTP-binding proteins mediate regulation of calcium channels by acetylcholine and noradrenaline in rat sympathetic neurons. *Brain Research* 494, 383-386.

Song, S.-Y., Saito, K., Noguchi, K. & Konishi, S. (1991). Adrenergic and cholinergic inhibition of Ca^{2+} channels mediated by different GTP-binding proteins in rat sympathetic neurons. *Pflugers Archives. European Journal of Physiology* 418, 592-600.

Sprouse, J.S. & Aghajanian, G.K. (1985). Serotonergic dorsal raphe neurons: electrophysiological responses in rats to 5-HT_{1A} and 5-HT_{1B} receptor subtype ligands. *Society of Neurosciences Abstracts* **11**, 47.

Sprouse, J.S. & Aghajanian, G.K. (1986). (-)-Propranolol blocks the inhibition of serotonergic dorsal raphe cell firing by 5-HT_{1A} selective agonists. *European Journal of Pharmacology* **128**, 295-298.

Sprouse, J.S. & Aghajanian, G.K. (1987). Electrophysiological responses of serotonergic dorsal raphe neurons to 5-HT_{1A} and 5-HT_{1B} agonists. *Synapse* **1**, 3-9.

Sprouse, J.S. & Aghajanian, G.K. (1988). Responses of hippocampal pyramidal cells to putative serotonin 5-HT_{1A} and 5-HT_{1B} agonists: A comparitive study with dorsal raphe neurons. *Neuropharmacology* **27**, 707-715.

Stanley, E.F. (1991). Single calcium channels on a cholinergic presynaptic nerve terminal. *Neuron* **7**, 585-591.

Stanley, E.F. & Goping, G. (1991). Characterization of a calcium current in a vertebrate cholinergic presynaptic nerve terminal. *Journal of Neuroscience* **11**, 985-993.

Steinbusch, H.W.M. (1981). Distribution of serotonin-immunoreactivity in the central nervous system of the rat - cell bodies and terminals. *Neuroscience* **6**, 557-618.

Steinbusch, H.W.M., Nieuwenhuys, R., Verhofstad, A.A.J. & Van Der Kooy, D. (1981). The nucleus raphe dorsalis of the rat and its projection upon the caudatoputamen. A combined cytoarchitectonic, immunohistochemical and retrograde transport study. *Journal of Physiology* (Paris) **77**, 157-174.

Sternweis, P.C. & Robishaw, J.D. (1984). Isolation of two proteins with high affinity for guanine nucleotides from membranes of bovine brain. *Journal of Biological Chemistry* **259**, 13806-13813.

Strålfors, P., Hiraga, A. & Cohen, P. (1985). The protein phosphatases involved in cellular regulation: Purification and characterisation of the glycogen-bound form of protein phosphatase-1 from rabbit skeletal muscle. *European Journal of Biochemistry* **149**, 295-303.

Strathmann, M., Wilkie, T.M. & Simon, M.I. (1989). Diversity of the G-protein family: Sequence from five additional α subunits in the mouse. *Proceedings of the National Academy of Science USA* **86**, 7407-7409.

Streit, J. & Lux, H.D. (1990). Calcium current inactivation during nerve-growth-factor-induced differentiation of PC12 cells. *Pflugers Archives. European Journal of Physiology* **416**, 368-374.

Strong, J.A., Fox, A.P., Tsien, R.W. & Kaczmarek, L.K. (1987). Stimulation of protein kinase C recruits covert calcium channels in aplysia bag neurons. *Nature* **325**, 714-717.

Surprenant, A., Shen, K.-Z., North, R.A. & Tatsumi, H. (1990). Inhibition of calcium currents by noradrenaline, somatostatin and opioids in guinea-pig submucosal neurones. *Journal of Physiology* 431, 585-608.

Sutor, B. & Zieglgansberger, W. (1987). A low-voltage activated transient calcium current is responsible for the time-dependent depolarizing inward rectification of rat neocortical neurons in vitro. *Pflugers Archives. European Journal of Physiology* 410, 102-111.

Swain, J.E., Robitaille, R., Dass, G.R. & Charlton, M.P. (1991). Phosphatases modulate transmission and serotonin facilitation at synapses: Studies with the inhibitor okadaic acid. *Journal of Neurobiology* 22, 855-864.

Swandulla, D. & Armstrong, C.M. (1988). Fast deactivating calcium channels in chick sensory neurons. *Journal of General Physiology* 92, 197-218.

Swandulla, D., Carbone, E. & Lux, H.D. (1991b). Do calcium channel classifications account for neuronal calcium channel diversity? *Trends in Neurosciences* 14, 46-51.

Swandulla, D., Hans, M., Zipser, K. & Augustine, G.J. (1991a). Role of residual calcium in synaptic depression and posttetanic potentiation: Fast and slow calcium signalling in nerve terminals. *Neuron* 7, 915-926.

Takahashi, M., Seagar, M.J., Jones, J.F., Reber, B.F.X. & Catterall, W.A. (1987). Subunit structure of dihydropyridine-sensitive calcium channels from skeletal muscle. *Proceedings of the National Academy of Science USA* 84, 5478-5482.

Takenoshita, M. & Steinbach, J.H. (1991). Halothane blocks low-voltage-activated calcium current in rat sensory neurons. *Journal of Neuroscience* 11, 1404-1412.

Tanabe, T., Adams, B.A., Numa, S. & Beam, K.G. (1991). Repeat 1 of the dihydropyridine receptor is critical in determining calcium channel activation kinetics. *Nature* 352, 800-803.

Tanabe, T., Takeshima, H., Mikami, A., Flockerzi, V., Takahashi, H., Kangawa, K., Kojima, M., Matsuo, H., Hirose, T. & Numa, S. (1987). Primary structure of the receptor for calcium channel blockers from skeletal muscle. *Nature* 328, 313-318.

Tang, C.M., Presser, F. & Morad, M. (1988). Amiloride selectively blocks the low-threshold (T) calcium channel. *Science* 240, 213-215.

Tasaki, I., Singer, I. & Takenaka, T. (1965). Effects of intracellular and external environments on the excitability of squid axon. A macromolecular approach. *Journal of General Physiology* 48, 1095-1123.

Tatebayashi, H. & Ogata, N. (1992). Kinetic analysis of the $GABA_B$-mediated inhibition of the high-threshold Ca^{2+} current in cultured rat sensory neurones. *Journal of Physiology* 447, 391-407.

Taube, J.S. & Schwartzkroin, P.A. (1984). Questionable effectiveness of nitrendipine and verapamil in selectively blocking postsynaptic calcium channels in hippocampus. *Society of Neurosciences Abstracts* 10, 75.

Taussig, R., Sanchez, S., Rifo, M., Gilman, A.G. & Belardetti, F. (1992). Inhibition of the ω-conotoxin-sensitive calcium current by distinct G proteins. *Neuron* 8, 799-809.

Taylor, W.R. (1988). Two-suction-electrode voltage-clamp analysis of the sustained calcium current in cat sensory neurones. *Journal of Physiology* 407, 405-432.

Thompson, S.M. & Wong, R.K.S. (1991). Development of calcium current subtypes in isolated rat hippocampal pyramidal cells. *Journal of Physiology* 439, 671-689.

Tillotson, D. (1979). Inactivation of Ca conductance dependent on entry of Ca ions in molluscan neurons. *Proceedings of the National Academy of Science USA* 76, 1497-1500.

Tonks, N.K. & Cohen, P. (1983). Calcineurin is a calcium ion-dependent, calmodulin-stimulated protein phosphatase. *Biochimica et Biophysica Acta* 747, 191-193.

Toselli, M. & Taglietti, V. (1990). Pharmacological characterisation of voltage-dependent calcium currents in rat hippocampal neurons. *Neuroscience Letters* 112, 70-75.

Tricklebank, M.D., Forler, C. & Fozard, J.R. (1985). The involvement of subtypes of the $5\text{-}HT_1$ receptor and of catecholaminergic systems in the behavioural response to 8-hydroxy-2-(di-n-propylamino)tetralin in the rat. *European Journal of Pharmacology* 106, 271-275.

Triggle, D.J. & Janis, R.A. (1987). Calcium channel ligands. *Annual Review of Pharmacology and Toxicology* 27, 347-369.

Trombley, P.Q. & Westbrook, G.L. (1992). L-AP4 inhibits calcium currents and synaptic transmission via a G-protein-coupled glutamate receptor. *Journal of Neuroscience* 12, 2043-2050.

Trulson, M.E. & Frederickson, C.J. (1987). A comparison of the electrophysiological and pharmacological properties of serotonin-containing neurons in the nucleus raphe dorsalis, raphe medianus and raphe pallidus recorded from mouse brain slices. *Brain Research Bulletin* 18, 179-190.

Trulson, M.E. & Jacobs, B.L. (1979). Raphe activity in freely moving cats: Correlation with level of behavioural arrousal. *Brain Research* 163, 135-150.

References

Tsien, R.W. (1983). Calcium channels in excitable cell membranes. *Annual Review of Physiology* 45, 341-358.

Tsien, R.W., Lipscombe, D., Madison, D.V., Bley, K.R. & Fox, A.P. (1988). Multiple types of neuronal calcium channels and their selective modulation. *Trends in Neurosciences* 11, 431-438.

Tsunoo, A., Yoshii, M. & Narahashi, T. (1986). Block of calcium channels by enkephalin and somatostatin in neuroblastoma-glioma hybrid NG108-15 cells. *Proceedings of the National Academy of Science USA* 83, 9832-9836.

Usowicz, M.M., Porzig, H., Becker, C. & Reuter, H. (1990). Differential expression by nerve growth factor of two types of Ca^{2+} channels in rat phaeocromocytoma cell lines. *Journal of Physiology* 426, 95-116.

VanderMaelen, C.P. & Aghajanian, G.K. (1983a). Electrophysiological and pharmacological characterisation of serotonergic dorsal raphe neurons recorded extracellularly and intracellularly in rat brain slices. *Brain Research* 289, 109-119.

VanderMaelen, C.P. & Aghajanian, G.K. (1983b). Evidence for a calcium-activated potassium conductance in serotonergic dorsal raphe neurons. *Society of Neurosciences Abstracts* 9, 500.

Varadi, G., Lory, P., Schultz, D., Varadi, M. & Schwartz, A. (1991). Acceleration of activation and inactivation by the β subunit of the skeletal muscle calcium channel. *Nature* 352, 159-162.

Verge, D., Daval, G., Patey, A., Gozlan, H., El Mestikawy, S. & Hamon, M. (1985). Presynaptic 5-HT autoreceptors on serotonergic cell bodies are of the 5-HT_{1A} subtype. *European Journal of Pharmacology* 113, 463-464.

Vilven, J., Leung, A.T., Imagawa, T., Sharp, A.H., Campbell, K.P. & Coronado, R.L. (1988). Interaction of calcium channels of skeletal muscle with monoclonal antibodies specific for its dihydropyridine receptor. *Biophysics Journal* 53, 556a.

von Spreckelsen, S., Lollike, K. & Treiman, M. (1990). Ca^{2+} and vasopressin release in isolated rat neurohypophysis: Differential effects of four classes of Ca^{2+} channel ligands. *Brain Research* 514, 68-76.

Wang, H.-L., Reisine, T. & Dichter, M. (1990). Somatostatin-14 and somatostatin-28 inhibit calcium currents in rat neocortical neurons. *Neuroscience* 38, 335-342.

Wang, X., Lemos, J.R., Dayanithi, G., Nordmann, J.J. & Treistman, S.N. (1991). Ethanol reduces vasopressin release by inhibiting calcium currents in nerve terminals. *Brain Research* 551, 338-341.

Wang, X., Treistman, S.N. & Lemos, J.R. (1992). Two types of high-threshold calcium currents inhibited by omega-conotoxin in nerve terminals of rat neurohypothesis. *Journal of Physiology* 445, 181-199.

Wanke, E., Ferroni, A., Malgaroli, A., Ambrosini, A., Pozzan, T. & Meldolesi, J. (1987). Activation of a muscarinic receptor selectively inhibits a rapidly inactivated Ca^{2+} current in rat sympathetic neurons. *Proceedings of the National Academy of Science USA* 84, 4313-4317.

Werz, M.A. & MacDonald, R.L. (1982). Opioid peptides decrease calcium-dependent action potential duration of mouse dorsal root ganglion neurons in cell culture. *Brain Research* 239, 315-321.

Wiley, J.W., Gross, R.A., Fox, N. & MacDonald, R.L. (1988). Neuropeptide Y and phorbol esters reduce the N-type calcium current of adult rat nodose neurons by different mechanisms. *Society of Neurosciences Abstracts* 14, 262.7.

Williams, J.S., Grupp, I.L., Grupp, G., Vaghy, P.L., Dumont, A., Schwartz, A., Yatani, A., Hamilton, S.L. & Brown, A.M. (1985). Profile of the oppositely acting enantiomers of the dihydropyridine 202-791 in cardiac preparations. *Biochemical and Biophysical Research Communications* 131, 13-21.

Williams, J.T., Colmers, W.F. & Pan, Z.Z. (1988). Voltage- and Ligand-Activated Inwardly Rectifying Currents in Dorsal Raphe Neurons in vitro. *Journal of Neuroscience* 8, 3499-3506.

Williams, J.T. & North, R.A. (1985). Catecholamine inhibition of calcium action potentials in rat locus coeruleus neurones. *Neuroscience* 14, 103-109.

Williams, K.R., Hemmings, H.C., LoPresti, M.B., Konigsberg, W.H. & Greengard, P. (1986). DARPP-32, a dopamine- and cyclic AMP-regulated neuronal phosphoprotein. *The Journal of Biological Chemistry* 261, 1890-1903.

Williams, M.E., Feldman, D.H., McCue, A.F., Brenner, R., Velicelebi, G., Ellis, S.B. & Harpold, M.M. (1992). Structure and functional expression of α_1, α_2 and β subunits of a novel human neuronal calcium channel subtype. *Neuron* 8, 71-84.

Williams, P.J., MacVicar, B.A. & Pittman, Q.J. (1990a). Electrophysiological properties of neuroendocrine cells of the intact rat pars intermedia: Multiple calcium currents. *Journal of Neuroscience* 10, 748-756.

Williams, P.J., MacVicar, B.A. & Pittman, Q.J. (1990b). Synaptic modulation by dopamine of calcium currents in rat pars intermedia. *Journal of Neuroscience* 10, 757-763.

Williams, P.J., Pittman, Q.J. & MacVicar, B.A. (1991). Ca^{2+}- and voltage-dependent inactivation of Ca^{2+} currents in rat intermediate pituitary. *Brain Research* 564, 12-18.

Wilson, G.G., Baldwin, S., Norman, R.I. & Wray, D. (1991). Possible similarity of structure between different types of calcium channels. *European Journal of Neuroscience Suppl.* 4, 203.

Yaari, Y., Hamon, B. & Lux, H.D. (1987). Development of two types of calcium channels in cultured mammalian hippocampal neurons. *Science* 235, 680-682.

Yakel, J.L. (1992). Inactivation of the Ba^{2+} current in dissociated Helix neurons: voltage dependence and the role of phosphorylation. *Pflugers Archives. European Journal of Physiology* 420, 470-478.

Yamaguchi, K. (1990). Enhancement of the Ca^{2+}-current by serum factor in cultured dorsal root ganglia neurons of the adult guinea pig. *Brain Research* 529, 286-293.

Yanagisawa, M., Kurihara, H., Kimura, S., Tomobe, Y., Kobayaski, M., Mitsui, Y., Yazaki, Y., Goto, K. & Masaki, T. (1988). A novel potent vasoconstrictor peptide produced by vascular endothelial cells. *Nature* 332, 411-415.

Yatani, A., Codima, J., Brown, A.M. & Birnbaumer, L. (1987). Direct activation of mammalian artrical muscarinic potassium channels by GTP and the regulatory protein Gk. *Science* 235, 207-211.

Yawo, H. (1990). Voltage-activated calcium currents in presynaptic nerve terminals of the chicken ciliary ganglion. *Journal of Physiology* 428, 199-213.

Yoshimura, M. & Higashi, H. (1985). 5-hydroxytryptamine mediates inhibitory postsynaptic potentials in rat dorsal raphe neurons. *Neuroscience Letters* 53, 69-74.

Zucker, R.S. & Haydon, P.G. (1988). Membrane potential has no direct role in evoking neurotransmitter release. *Nature* 335, 360-362.